

Copyright
by
Eric A. Wold
2021

**The Dissertation Committee for Eric A. Wold Certifies that this is the approved
version of the following dissertation:**

**Small Molecule Allosteric Modulation of G Protein-Coupled Receptors
and Applications in the Pharmacological Targeting of 5-HT₂ Receptors**

Committee:

Jia Zhou, Ph.D., Supervisor & Chair

Kathryn A. Cunningham, Ph.D.

Shao-Jun Tang, Ph.D.

John A. Allen, Ph.D.

Amy Hauck Newman, Ph.D.

**Small Molecule Allosteric Modulation of G Protein-Coupled Receptors
and Applications in the Pharmacological Targeting of 5-HT₂ Receptors**

by

Eric A. Wold, B.S.

Dissertation

Presented to the Faculty of the Graduate School of

The University of Texas Medical Branch

in Partial Fulfillment

of the Requirements

for the Degree of

Doctor of Philosophy

The University of Texas Medical Branch

April, 2021

Dedication

This dissertation is dedicated to the scientists, advisors, mentors, colleagues, and others of importance in this endeavor who generously gave me opportunities, exemplified scientific thought, encouraged me to pursue this degree, and taught me more than I can describe: Britt Wold, M.Sc., John Eberth, Ph.D., Francisco Robles-Hernandez, Ph.D., Cynthia Brysch, Alexandra Ulmet, Muge Kuyumcu-Martinez, Ph.D., Sunil Verma, Ph.D., Curtis Nutter, Ph.D., Vaibhav Deshmukh, Fernanda Laezza, M.D., Ph.D., Syed Ali, Ph.D., Jim Hsu, MD., PhD., Alexander Shavkunov, Ph.D., Marxa Figueiredo, Ph.D., Joe Shearer, Ph.D., Sam Umbaugh, Ph.D., Sheryl Lichti, Ph.D., Carol Nilsson, M.D., Ph.D., Norelle Wildburger, Ph.D., Mark Emmett, Ph.D., Yuriy Fofanov, Ph.D., George Golovko, Ph.D., Kamil Khanipov, Ph.D., Ekaterina Mostovenko, Ph.D., Gaddiel Galarza-Munoz, Ph.D., Asia Miszkiel, Ph.D., Claudia Soto, Ph.D., Erik Garcia, Ph.D., Dan Felsing, Ph.D., Bob Fox, Sonja Stutz, Konrad Pazdrak, Ph.D., Christina Merritt, Jim Kasper, Ph.D., Monty Pettitt, Ph.D., Omneya Nassar, Ph.D., Emily Davis, Ph.D., Alexis Williams, Ph.D., Zoe Hoffpauir, Ph.D., Noelle Anastasio, Ph.D., Jonathan Hommel, Ph.D., Chris Wild, Ph.D., Zhiqing Liu, Ph.D., Jianping Chen, Ph.D., Ye Ding, Ph.D., Na Ye, Ph.D., Haiying Chen, Pingyuan Wang, Ph.D., Jimin Xu, Ph.D., Yi Li, Ph.D., Yu Xue, Ph.D., Clinton Canal, Ph.D., Thomas Keck, Ph.D., Alexander Sherwood, Ph.D., Chris Cunningham, Ph.D., Jose Barral, M.D., Ph.D., Joan Nichols, Ph.D., David Niesel, Ph.D., Kristen Peek, Ph.D., Daniel Jupiter, Ph.D., John Allen, Ph.D., Shao-Jun Tang, Ph.D., Amy Hauck Newman, Ph.D., Kathryn Cunningham, Ph.D., Jia Zhou, Ph.D., and others that I unintentionally omitted.

Acknowledgements

This work is possible due to the mindful mentoring received from my advisor Jia Zhou, Ph.D. I am grateful to have been supported by the University of Texas Medical Branch Center for Addiction Research Institutional National Research Service Award (T32 DA07287) and by the National Institutes of Health Ruth L. Kirschstein National Research Service Award (F31 DA07287), both grants sponsored by the National Institute on Drug Abuse. I wish to thank the Department of Pharmacology and Toxicology, the Pharmacology and Toxicology Graduate Program, the Center for Addiction Research, the Graduate School of Biomedical Sciences, and all associated personnel who provided unconditional assistance and support.

Small Molecule Allosteric Modulation of G Protein-Coupled Receptors and Applications in the Pharmacological Targeting of 5-HT_{2C} Receptors

Publication No. _____

Eric A. Wold, Ph.D.

The University of Texas Medical Branch, 2021

Supervisor: Jia Zhou, Ph.D.

The discovery of G protein-coupled receptors (GPCRs) and the extensive second messenger systems associated with their activation has ushered in an enormously productive period in drug discovery. The extent to which around one-third of FDA-approved medications target GPCRs. Predictably, small molecule allosteric modulation has emerged in recent years as a new means to control GPCR function with numerous examples nearing FDA approval. This body of work begins with a substantive review of drug discovery efforts in the development of Class A GPCR allosteric modulators as a means to compile successful strategies and take note of the distinct challenges in the field as our group approaches allosteric modulator discovery for the serotonin 5-HT_{2C} receptor (5-HT_{2C}R). From the time of its characterization, the 5-HT_{2C}R has been marked by unique, untapped potential as a drug discovery target for numerous diseases and disorders of the central nervous system. Thus, the second chapter in this work provides a clear rationale for 5-HT_{2C}R allosteric modulator discovery in context of the neurobiological framework wherein the 5-HT_{2C}R plays an integral role in reward-related behaviors and cortical executive functions. With the rationale established, the following sections report our efforts

in the discovery of novel 5-HT_{2C}R positive allosteric modulators (PAMs) from their design and chemical synthesis to the *in vitro* and *in vivo* characterization of these molecules. Additionally, further work describing 5-HT_{2C}R PAM pharmacokinetic properties as suitable for rodent behavioral assays and the structural determinants of 5-HT_{2C}R PAM binding via molecular modeling are discussed. Having discovered allosteric modulators with functionality across the 5-HT_{2R} subfamily and benefiting from the wealth of available structural data for these targets, the final chapter delves into a theoretical mechanism underpinning allosteric modulation of 5-HT_{2R}s. The enhanced activation state (EAS) is thus coined for the first time herein to describe 5-HT_{2R} PAM functionality and is treated with a rigorous theoretical framing comprised of the observed pharmacological, structural, and computational studies that shape our understanding of GPCR dynamics, specifically the activation dynamics of 5-HT_{2R}s. The resultant body of work provides the reader a comprehensive understanding of allosteric modulation and its pharmacological utility in targeting 5-HT_{2R}s.

TABLE OF CONTENTS

List of Tables	x
List of Figures	xii
List of Illustrations	xvi
i	
List of Abbreviations	xvi
ii	
 OVERVIEW AND ANALYSIS OF ALLOSTERIC MODULATION AS A DRUG DISCOVERY APPROACH FOR TARGETING CLASS A G PROTEIN-COUPLED RECEPTORS...21	
Chapter 1. Allosteric Modulation of Class A GPCRs: Targets, Agents, and Emerging Concepts.....	21
1. Introduction.....	22
2. Overview on the Allosteric Modulation of Class A GPCR Drug Targets....	26
3. Recent Advances in the Discovery and Design of Class A GPCR Allosteric Modulators	30
3.1. Aminergic Family Receptors	30
3.2. Lipid Family Receptors.....	53
3.3. Nucleotide Family Receptors.....	69
3.4. Peptide and Protein Family Receptors	81
4. Challenges and Emerging Concepts in Class A GPCR Drug Discovery	91
4.1 Complexities and Nuance Observed in Screening, Optimizing and Advancing Class A GPCR Allosteric Modulators.....	91
4.2 Emerging Strategies for Class A GPCR Small Molecule Allosteric Modulator Discovery and Development.....	93
4.3 New Biology for Class A GPCRs and Implications for Allosteric Modulator Agents.	95
5. Conclusions and Future Directions.....	96

A THERAPEUTIC FOCUS ON THE 5-HT_{2C}R AND APPLYING ALLOSTERIC MODULATION AS A 5-HT_{2C}R DRUG DISCOVERY STRATEGY	99
Chapter 2. Targeting the 5-HT _{2C} Receptor in Biological Context and the Current State of 5-HT _{2C} Receptor Ligand Development	99
1. Introduction to the 5-HT _{2C} R protein structure and function.....	100
2. The 5-HT _{2C} R as a therapeutic target.....	106
3. The current state of 5-HT _{2C} R agonists.....	110
4. Background and rationale for 5-HT _{2C} R allosteric modulators	115
5. The current state of 5-HT _{2C} R positive allosteric modulators	119
6. Conclusion and future directions	125
Chapter 3. Discovery of 4-Phenylpiperidine-2-Carboxamide Analogues as Serotonin 5-HT _{2C} Receptor Positive Allosteric Modulators with Enhanced Drug-Like Properties	127
1. Introduction.....	128
2. Results and Discussion	130
3. Conclusions.....	151
4. Experimental Section.....	152
4.1 Chemistry.....	152
4.2 <i>In silico</i> Molecular Docking	162
4.3 <i>In Vitro</i> Pharmacology	163
4.4 <i>In Vivo</i> Pharmacokinetics and Brain Penetration Analyses	164
Chapter 4. Exploration of sp ² -Rich Scaffolds as Serotonin 5-HT _{2C} Receptor PAMs to Probe Binding Pocket Features and Reduce Chiral Centers.....	169
1. Introduction.....	170
2. Results and Discussion	171
3. Conclusions.....	179
4. Experimental Section.....	180
4.1 Chemistry	180
4.2 <i>In Vitro</i> Pharmacology	184
4.3 <i>In Vivo</i> Pharmacokinetics	186

A DISCUSSION ON MECHANISM AND THEORY IN 5-HT₂R SUBFAMILY ALLOSTERIC MODULATION188

Chapter 5. A Discussion on 5-HT₂R PAM Mechanics and Mode of Action: The Enhanced Activation State.....188

1. Introduction.....189

2. Receptor Activation State Models189

3. Defining the Pathway for Ligand Binding.....191

4. 5-HT_{2A}R and 5-HT_{2C}R PAMs May Stabilize an Enhanced Activation State (EAS)193

5. Dynamic Observations of Receptor Activation States Provide Rationale for an EAS195

6. Evidence for the 5-HT_{2A}R and 5-HT_{2C}R PAM Binding Site and the Functional Relevance of the Extracellular Loop 2197

7. Limitations and Implications of the 5-HT₂R PAM EAS Mechanism200

CONCLUDING REMARKS203

References.....206

Vita 253

List of Tables

Table 1.1 Selected Allosteric Modulators of Class A GPCRs currently in Clinical Trials or Approved for Clinical Use	28
Table 1.2 Allosteric Modulator and Class A GPCR Co-Crystal Structures. ^a	28
Table 2.1 Functional profiling of numerous 5-HT _{2C} R agonists and respective profiles at the 5-HT _{2A} R and 5-HT _{2B} R to show subtype selectivity among 5-HT ₂ Rs.....	113
Table 3.1 Effects of 4-alkylpiperidine-2-carboxamide derivatives (1 nM) on 5-HT-induced Ca _i ²⁺ release in h5-HT _{2C} R-CHO cells	135
Table 3.2 Effects of 4-alkylpiperidine-2-carboxamide derivatives (1 nM) on 5-HT-induced Ca _i ²⁺ release in h5-HT _{2C} R-CHO cells	137
Table 3.3 Effects of active 5-HT _{2C} R PAMs (1 nM) on 5-HT-induced Ca _i ²⁺ release in h5-HT _{2A} R-CHO cells.....	138
Table 3.4 Displacement of radioligand binding by compound 12 (μM) in a broad panel of receptors and transporters	145
Table 3.5 <i>In Vitro</i> Pharmacokinetic Profile and <i>In Silico</i> Toxicity Prediction for Compound 12 ^a	147
Table 3.6 <i>In Vivo</i> Pharmacokinetic Profile and Brain Penetrability of Compound 12 ^a	148
Table 4.1 Functional activity assessments in 5-HT _{2C} R, 5-HT _{2A} R and 5-HT _{2B} R.....	175

Table 4.2 <i>In vitro</i> radioligand binding off-target assessment for compounds 8, 11, 13, 18, 19, and 20	178
Table 4.3 <i>In vivo</i> pharmacokinetic profiling of compound 18	179
Table 5.1 Mutations in the ECL2 alter functional response to 5-HT _{2A} R agonists....	200

List of Figures

Figure 1.1 Signaling Molecule Diversity and Classification for Class A GPCRs....	23
Figure 1.2 Diverse Allosteric Binding Sites Reported across Class A GPCRs	26
Figure 1.3 Representative 5-HT _{2c} R PAMs 1-5	34
Figure 1.4 β_2 AR Co-Crystal Structure with Cmpd-15 (6)	36
Figure 1.5 Representative allosteric modulators of the dopamine D2 and D3 receptors with chemical modifications at selected positions.....	39
Figure 1.6 M ₁ mAChR PAM BQCA (18) and derivatives (19-30) with corresponding SARs	43
Figure 1.7 Representative M ₁ mAChR PAMs with an indole core (red) and SAR (compounds 31-36).....	45
Figure 1.8 Chemically diverse M ₅ mAChR PAMs with key modifications (compounds 37-46)	46
Figure 1.9 Representative M ₅ mAChR PAMs (47-48) and NAMs (49-50)	48
Figure 1.10 M ₄ mAChR PAM derivatives around the 5-amino-thieno[2,3- <i>c</i>]pyridine scaffold and corresponding SAR (51-60)	51
Figure 1.11 M ₂ mAChR-LY2119620 (stick representation, magenta, 61) co-crystal and other representative PAMs.....	53

Figure 1.12 CB ₁ receptor NAMs (63-80) based on the <i>1H</i> -indole-2-carboxamide scaffold and corresponding SAR.....	55
Figure 1.13 CB ₁ receptor NAMs based on the diarylurea scaffold (81-89) and corresponding SAR; additional CB ₁ receptor NAMs (90-92).....	60
Figure 1.14 Representative CB ₁ receptor PAMs (93-94) and 2-phenyl- <i>1H</i> -indole scaffold derivative CB ₁ receptor PAMs (95-98).....	63
Figure 1.15 Representative FFA1 receptor PAMs (99-104) and co-crystal complex of FFA1-MK-8666-AP8.....	67
Figure 1.16 Representative FFA2 receptor PAMs (105-108).....	68
Figure 1.17 Representative FFA3 receptor PAMs (109-111).....	69
Figure 1.18 A ₁ R PAM derivatives designed around the 2-amino-3-benzoyl thiophene scaffold (112-143).....	71
Figure 1.19 Representative A _{2A} R PAMs with centric pyrazine core (144-149).....	76
Figure 1.20 A _{2B} R PAM derivatives on the 1-benzyl-3-ketoindole scaffold side chain (150-156)	77
Figure 1.21 Representative A ₃ R PAMs displaying a ring opening on the <i>1H</i> -imidazo[4,5- <i>c</i>]quinolin-4-amine scaffold (157-158)	78
Figure 1.22 P2Y ₁ receptor allosteric antagonist BPTU (159) and P2Y ₂ receptor allosteric agonists (160-161).....	81

Figure 1.23 Chemical structure of maraviroc (162) with the CCR5-maraviroc co-crystal structure and other allosteric modulators of chemokine receptors	83
Figure 1.24 Chemically diverse allosteric modulators for ORs (171-176).....	90
Figure 1.25 NAMs and PAMs for additional peptide and protein family receptors, as described (181-186)	91
Figure 2.1 The recently solved X-ray crystal structure of the “active-like” state of the 5-HT ₂ CR bound to ergotamine (PDB code: 6BQG) and 5-HT ₂ CR model bound to 5-HT is depicted	101
Figure 2.2 A cross-section of the 5-HT ₂ CR signaling webs initiated by 5-HT binding to the orthosteric site is presented.....	104
Figure 2.3 A schematic of the proposed 5-HT ₂ CR modulation of limbic-corticoaccumbens circuit is represented	106
Figure 2.4 Proposed outcomes mediated by activation of specific members of the 5-HT ₂ R family are depicted.	110
Figure 2.5 Current synthetic 5-HT ₂ CR agonists share similarities in their pharmacophore.....	112
Figure 2.6 A novel pharmacophore for 5-HT ₂ CR agonists is described	114
Figure 2.7 A schematic of potential allosteric modulation of GPCR signal transduction is depicted	117

Figure 2.8 Early reported 5-HT _{2C} R PAMs and the chemical family from which PNU-69176E was derived.....	120
Figure 2.9 A new generation of 5-HT _{2C} R PAMs has emerged.....	122
Figure 3.1 Highlighted compounds resulting from the search for synthetic small molecule 5-HT _{2C} R PAMs	129
Figure 3.2 Medicinal chemistry strategy to achieve optimized 5-HT _{2C} R from PNU-69176E (1)	130
Figure 3.3 The volume, not length, of the undecyl moiety on PNU-69176E (1) and CYD-1-79 (3) may contribute to 5-HT _{2C} R PAM activity.....	131
Scheme 3.1 Synthesis of CYD-1-79 analogues with compact phenyl or cyclohexyl LTs.....	132
Scheme 3.2 Synthesis of CYD-1-79 analogues with phenethyl, ethylcyclohexyl, or substituted phenethyl LTs.....	133
Figure 3.4 Effects of select compounds with shortened lipophilic tail (LT) moieties provide evidence that hydrophobic volume contributes to target engagement.	136
Figure 3.5 Molecular docking illustrates the considerable overlap in ligand poses of six 5-HT _{2C} R PAMs	140
Figure 3.6 Docking site surface mapping illustrates the distinct location of the proposed allosteric site in relation to 5-HT bound to the 5-HT _{2C} R.....	141

Figure 3.7 Docking demonstrates aromatic or aliphatic compact LTs orient towards the hydrophobic pocket between TM2 and TM3 of the 5-HT _{2C} R.....	142
Figure 3.8 Comparison of the allosteric binding site surface map and an independent allosteric binding site prediction program for the 5-HT _{2C} R model.	143
Figure 3.9 Compound 12 dose-dependently augments the stimulus effects of the selective 5-HT _{2C} R agonist WAY163909.....	151
Figure 4.1 Rationale and Strategy.....	170
Scheme 4.1 CYD-1-79 analogues	172
Scheme 4.2 and 4.3 CTW0415 analogues	173
Figure 5.1 Molecular docking studies with the 5-HT _{2A} R	195
Figure 5.2 Lead PAM CTW0415 <i>in vitro</i> functional activity at 5-HT _{2C} R	197
Figure 5.3 Molecular modeling of the allosteric binding site	199

List of Illustrations

Illustration 5.1 Names given to various GPCR binding pockets191

Illustration 5.2 Models for discussion.....193

List of Abbreviations

Abbreviations

GPCRs	G Protein-Coupled Receptors
oGPCRs	Orphan GPCRs
CNS	Central Nervous System
PAM	Positive Allosteric Modulator
NAM	Negative Allosteric Modulator
SALs	Silent Allosteric Ligands
TM	Transmembrane
SAR	Structure-Activity Relationship
5-HT	5-Hydroxytryptamine
5-HT _{2C} R	Serotonin 5-HT _{2C} Receptor
5-HT _{2A} R	Serotonin 5-HT _{2A} Receptor
5-HT _{2B} R	Serotonin 5-HT _{2B} Receptor
5-HT ₆ R	Serotonin 5-HT ₆ Receptor
5-HT _{7A} R	Serotonin 5-HT _{7A} Receptor
IP ₃	Inositol 1,4,5-Triphosphate
SUD	Substance Use Disorder
CHO	Chinese Hamster Ovary
CUD	Cocaine Use Disorder
PK	Pharmacokinetics
ECL	Extracellular Loop

TMH	Transmembrane Helix
PTEN	Phosphatase and Tensin Homolog
ICL	Intracellular Loop
β_2 AR	β_2 -Adrenergic Receptor
cAMP	Cyclic Adenosine Monophosphate
DR	Dopamine Receptors
ADHD	Attention Deficit Hyperactivity Disorder
PLG	Pro-Leu-Gly-NH ₂
HTS	High-Throughput Screen
mACh	Muscarinic Acetylcholine
BQCA	Benzylquinolone Carboxylic Acid
BBB	Blood-Brain Barrier
IP	Inflection Point
tPSA	Topological Polar Surface Area
P-gp	P-glycoprotein
CB receptor	Cannabinoid Receptors
<i>GTPγS</i>	Guanosine 5'-O-[gamma-thio]triphosphate
ERK1/2	Extracellular Signal-Regulated Kinase 1/2
FSK	Forskolin
LAPS	Ligand-Assisted Protein Structure
DSE	Depolarization-Induced Suppression of Excitation
2-AG	2-Arachidonoyl Glycerol
MD	Molecular Dynamics

FFAR	Free Fatty Acid Receptors
ARs	Adenosine Receptors
AEs	Allosteric Enhancers
AM	Allosteric Modulator
UTP	Uridine 5'-Triphosphate
NR4A	Nuclear Receptor 4A
NRCMs	Neonatal Rat Cardiomyocytes
DED	Dry Eye Disease
CCR	Chemokine Receptors
HIV-1	Human Immunodeficiency Virus Type 1
BRET	Bioluminescence Resonance Energy Transfer
SBDD	Structure-Based Drug Discovery
ORs	Opioid Receptors
MOR	μ -opioid Receptor
DOR	δ -opioid Receptors
KOR	κ -opioid Receptor
PAR	Proteinase-Activated Receptors
MCH1R	Melanin-Concentrating Hormone Receptor 1
MBS	Metastable Binding Site
ABS	Allosteric Binding Site
EBP	Extended Binding Pocket
EAS	Enhanced Activation State

**OVERVIEW AND ANALYSIS OF ALLOSTERIC MODULATION AS A DRUG
DISCOVERY APPROACH FOR TARGETING CLASS A G PROTEIN-COUPLED
RECEPTORS**

**Chapter 1. Allosteric Modulation of Class A GPCRs: Targets, Agents,
and Emerging Concepts**

E.A. Wold, J. Chen, K.A. Cunningham, J. Zhou
Published as *J. Med. Chem.* 2019 62 (1), 88-127¹

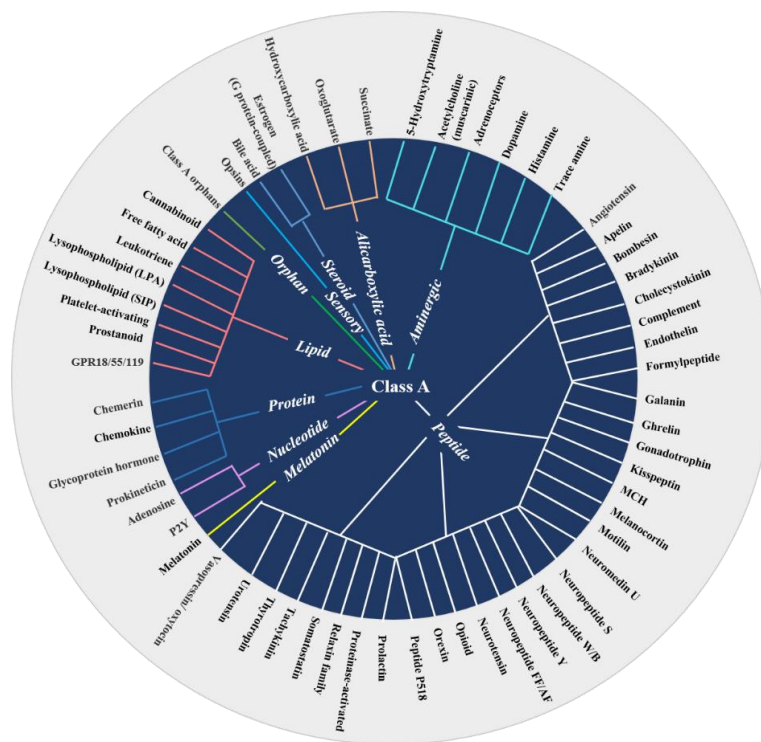
Abstract

G protein-coupled receptors (GPCRs) have been tractable drug targets for decades with over one-third of currently marketed drugs targeting GPCRs. Of these, the Class A GPCR superfamily is highly represented and continued drug discovery for this family of receptors may provide novel therapeutics for a vast range of diseases. GPCR allosteric modulation is an innovative targeting approach that broadens the available small molecule toolbox and is proving to be a viable drug discovery strategy, as evidenced by recent FDA approvals and clinical trials. Numerous Class A GPCR allosteric modulators have been discovered recently and emerging trends, such as the availability of GPCR crystal structures, diverse functional assays and structure-based computational approaches are improving optimization and development. This perspective provides an update on allosterically targeted class A GPCRs and their disease indications, the medicinal chemistry approaches towards novel allosteric modulators and highlights emerging trends and opportunities in the field.

1. INTRODUCTION

G-protein coupled receptors (GPCRs) are seven-transmembrane proteins that have been of high pharmaceutical interest for decades due to their physiological importance and accessibility for small molecule targeting. GPCRs are integral for physiological responses to a variety of stimuli, which span photons, ions, small molecules, macromolecules, peptides and proteins. These diverse stimuli, environmental and endogenous, are in accordance with the vast functions mediated by GPCRs. Aspects of cognition, immune response, and cellular organization, among many others, are regulated by GPCR signaling. The pharmacological modulation of GPCRs provides leverage for the treatment of diseases of the central nervous system (CNS), cancer, viral infections, inflammatory disorders, metabolic disorders, and others. Additionally, the location of GPCRs in the cellular membrane allows unique pharmacological access to these proteins and the effectors and second messenger systems coupled to the receptors allow for efficient drug action. The location, topology, and physicochemical attributes of many GPCR binding pockets have resulted in the discovery of numerous small molecule drugs that have been in clinical use for decades.²

Figure 1.1 Signaling Molecule Diversity and Classification for Class A GPCRs



The inner blue region highlights the diverse endogenous signaling molecules that activate Class A GPCRs. Data retrieved from website <http://www.gpcrdb.org/drugs/drugbrowser>.

GPCRs represent the largest family of druggable proteins in the human genome and unsurprisingly are targeted by more than 30% of marketed drugs in the United States.³ Despite this large percentage, recent studies highlight that a small fraction of the possible druggable GPCRs has been exploited by approved drugs.⁴ Multiple reasons persist for the relatively low number of GPCRs targeted by FDA-approved drugs. Foremost, the biological functions of many potentially druggable GPCRs remain unclear, as seen in the understudied orphan GPCRs (oGPCRs), and new biological complexities remain to be added to established targets.⁵ Another reason is several disease indications with established GPCR targets have not progressed drugs into the clinic when targeted by traditional agonists or antagonists, which bind at highly conserved orthosteric sites and may produce off-target effects.^{6, 7} Undeniably, most of GPCR-targeted FDA-approved drugs bind to orthosteric sites; however, when therapeutic efficacy or safety hinges on distinguishing

between highly homologous receptor subtypes, other modes of modulation, such as allosteric modulation, confer specific advantages.⁸

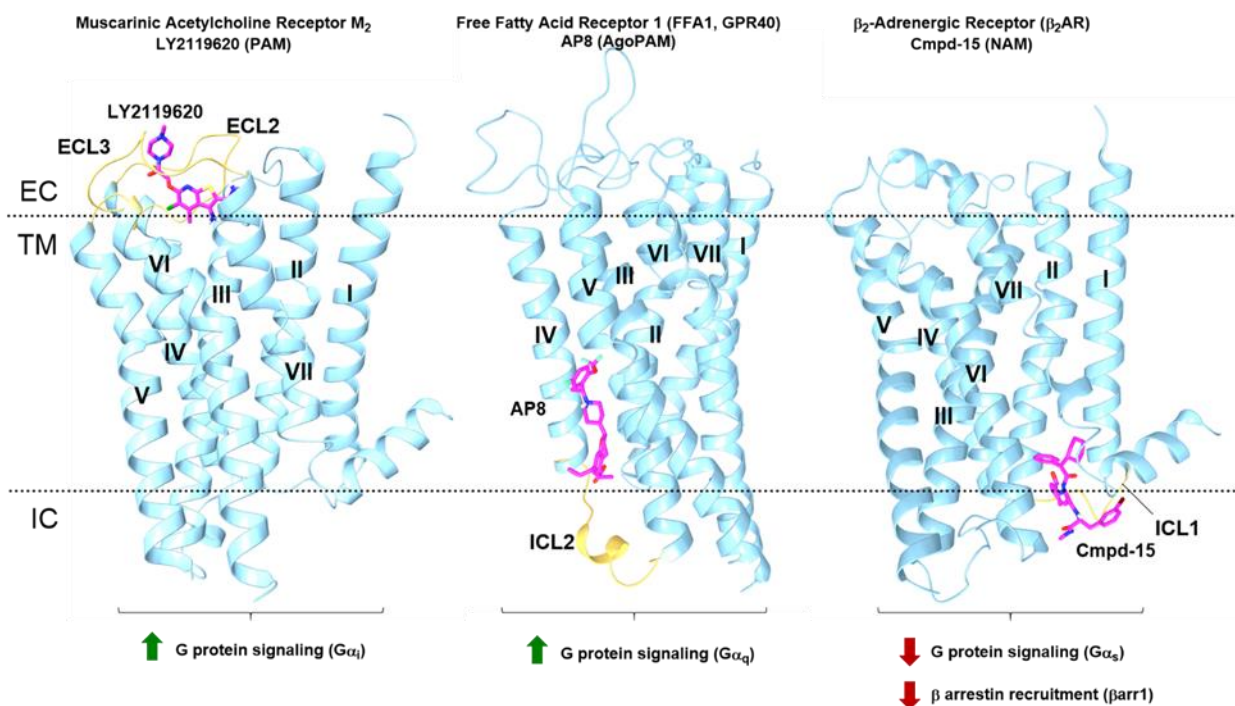
Allosteric modulation of protein function was first described in enzymes and is now understood to be an integral aspect of functionality in other protein types, including GPCRs.⁹ A GPCR allosteric modulator is generally defined as a modulatory ligand that does not occupy the orthosteric binding site and binds to a spatially and topologically distinct (allosteric) site on the receptor. It is now known that endogenous allosteric modulators are ubiquitous among GPCRs, the most apparent being the heterotrimeric G proteins, and many synthetic ligands may exploit these sites.¹⁰ Other examples of allosteric sites seem to be unrelated to endogenous molecules yet display topologically favorable features due to the receptor folding and assembly. Nevertheless, allosteric site residues tend to be less conserved among receptor subtypes and can offer unparalleled subtype specific targeting. Other advantages of allosteric ligands are fundamental to their mode of action, including the ability to fine tune the response to an orthosteric ligand in a time and spatially dependent manner, a feature that holds promise for immune and CNS targets.¹¹ Additionally, allosteric modulators may also confer signaling bias and probe dependence, further contributing to the possibility for remarkably precise pharmacological modulation.¹²

The GPCR superfamily is subdivided into divergent groups (classes) based on homology and function including: Class A (rhodopsin-like receptors), Class B (the secretin family), Class C (metabotropic glutamate receptors), Class D (fungal mating pheromone receptors), Class E (cyclic adenosine monophosphate (cAMP) receptors), and Class F (Frizzled and Smoothed receptors).¹³⁻¹⁵ Class A represents the largest class of GPCRs and contains further classifications for members based on the type of endogenous signaling molecules (**Figure 1.1**). This perspective will focus on recent medicinal chemistry advances for allosteric modulators across a selection of class A GPCRs with diverse signaling molecules, including small molecules, peptides, proteins and lipids. Due to the

size of Class A and the historical importance of many of its members, these receptors make up most of the current receptor drug targets.¹⁶ Likewise, industry and academic programs have been established to discover allosteric modulators of Class A receptors for the treatment of mental health disorders, viral infection, inflammation and other indications.

Mechanistically, allosteric modulators can increase the functional response to an orthosteric agonist, acting as a positive allosteric modulator (PAM), or inhibit the functional response to an orthosteric agonist, acting as a negative allosteric modulator (NAM). There have been reported silent allosteric ligands (SALs), which do not modulate the receptor, but compete with other PAMs or NAMs at the allosteric binding site. Additionally, for many targets included in this perspective, allosteric ligands can be antagonists or agonists with, or without, PAM or NAM activity (e.g., ago-PAMs, allosteric antagonists, etc.). New insights have shown these allosteric alterations can be mediated by various components of the receptor, lipid membrane, orthosteric ligand(s) and effector proteins; ultimately providing a more complete, and complex, view of the potential for allosteric modulation.^{9, 17} These modes of allosteric modulation are conferred via diverse allosteric binding sites that include extracellular regions, the interior and lipid-facing exterior of the transmembrane (TM) helix bundle and intracellular regions. Elegant structural studies have confirmed these interesting binding poses and provide the framework for modulating new targets with notable precision. **Figure 1.2**, containing three GPCR-allosteric modulator co-complex crystal structures, illustrates the concept of allosteric modulators functioning in diverse modes and binding to Class A GPCRs in diverse structural regions. The structural interactions between class A GPCR residues and the corresponding allosteric modulators have been reviewed by Lu and Zhang, also included in the Allosteric Modulators special issue.¹⁸ This perspective will review key concepts for allosteric modulator discovery and optimization, provide a thorough overview of the recent medicinal chemistry efforts for class A GPCR allosteric modulation, and highlight diverse applications of allosteric modulators across the class A GPCR family.

Figure 1.2 Diverse Allosteric Binding Sites Reported across Class A GPCRs



The representative Class A allosteric modulators (stick representation, magenta) are shown bound in the corresponding co-crystal structure at distinct and diverse sites. The M2 mAChR- shows an extracellular (EC) site LY2119620 (left, PDB: 4MQT)¹⁹; FFA1-AP8 co-crystal shows AP8 in the transmembrane (TM) region adjacent to the lipid membrane (center, PDB: 5TZY)²⁰; β_2 AR-Cmpd-15 co-crystal shows an intracellular (IC) binding site (right, PDB: 5X7D)²¹. Bottom: the diverse signaling outcomes on orthosteric agonism by Class A GPCR allosteric modulators.

2. OVERVIEW ON THE ALLOSTERIC MODULATION OF CLASS A GPCR DRUG TARGETS

GPCRs are the most targeted protein class by modern pharmacotherapies due to their innate capability of transducing extracellular signals into wide-ranging cellular responses. In a growing number of molecular and structural studies, activated GPCRs are increasingly appreciated to transduce their signal through structural alterations in the TM domains that not only result in the association of effector heterotrimeric G proteins, but also lead to association of β -arrestins, scaffolding proteins and various kinases.⁵ Due to the known complexities of GPCR signaling and the added intricacy of measuring allosteric

modulation, targeted discovery of allosteric modulators has been enabled only in recent decades by technological improvements in ligand screening assays.²² The most common primary screening assay employed in allosteric modulator discovery is a functional assay in which the effects of allosteric modulators can be observed by alterations to orthosteric agonist or antagonist potency and/or efficacy. An orthosteric agonist or antagonist with known and reproducible activity, along with the potential allosteric ligand, is added to a system in which a functional output can be measured, as in a calcium-mobilization measurement. Since GPCR activity is not a simple on/off mechanism, it is important that the assay be able to measure the magnitude of agonist-induced functional response, as well as the magnitude of functional modulation from an allosteric modulator. The resultant concentration response curve can provide quantitative measures of orthosteric ligand efficacy (E_{\max}) and potency (EC_{50}). When fit to the operational model of allosterism, the unique behavior of the receptor induced by the allosteric ligand can be quantified. The allosteric modulation of orthosteric ligand affinity is denoted as the cooperativity factor (α) and the allosteric modulation of efficacy is described by the value β . These influences may be described by a composite metric of cooperativity denoted by $\log\alpha\beta$. According to this model the intrinsic efficacy of the allosteric ligand can be described by the factor τ_B and the intrinsic efficacy of the orthosteric ligand is described by the value τ_A . Excellent reviews have been published on this model, the contributing factors and the importance of the quantification of allosteric modulator activities.²³⁻²⁵ Binding assays are also commonly employed to understand allosteric modulation and report kinetic inhibition constants (K_i). Throughout the following perspective, these terms will be used to describe the activity of allosteric modulators as reported in the corresponding original manuscript. Additionally, observations should be made regarding the importance of quantitatively characterizing allosteric modulators in multiple dimensions of their effect to thoroughly inform structure-activity relationships (SARs).

Table 1.1 Selected Allosteric Modulators of Class A GPCRs currently in Clinical Trials or Approved for Clinical Use

Family	Target	Name	Indication	Mechanism of Action	Phase
Acetylcholine receptors	M1	VU319	cognitive impairment	PAM	Phase I
Free fatty acid receptors	FFAR1	MK-8666	type 2 diabetes mellitus	partial allosteric agonists	Phase I
Chemokines receptors	CXCR1 CXCR2	Ladarixin (DF2156A)	onset type 1 diabetes	NAM	Phase II
Free fatty acid receptors	FFAR1	TAK-875	type 2 diabetes mellitus	partial allosteric agonists	Phase III
Chemokine receptors	CCR9	Vercirnon	Crohn's disease	NAM	Phase III
Chemokines receptors	CXCR1	Reparixin (DF1681Y)	β -cell transplantation	NAM	Phase III
P2Y receptors	P2Y ₁₂	Ticagrelor	anti-thrombosis	allosteric antagonist	Approved
Chemokine receptors	CCR5	Maraviroc	HIV infection	NAM	Approved
Chemokines receptors	CXCR4	Plerixafor	bone marrow transplantation	NAM	Approved

Data retrieved from a) Cortellis database, <https://www.cortellis.com/intelligence/login.do>; b) Ref.;⁴ c) <http://www.gpcrdb.org/drugs/drugbrowser>; d) <https://www.drugbank.ca>.

Table 1.2 Allosteric Modulator and Class A GPCR Co-Crystal Structures.^a

GPCR	allosteric modulator	mechanism of action	allosteric site distribution	PDB code	Ref.
CCR5	maraviroc	NAM	extracellular side	4MBS	26
CCR2	CCR2-RA-[R]	NAM	intracellular side	5T1A	27
CCR9	vercirnon	allosteric antagonist	intracellular side	5LWE	28
M ₂	LY2119620	PAM	extracellular side	4MQT	19
FFA1 (GPR40)	TAK-875	partial allosteric agonist	extracellular side	4PHU	29
FFA1 (GPR40)	MK-8666	partial allosteric agonist	extracellular side	5TZR	20
FFA1 (GPR40)	MK-8666, AP8	Ago-PAM	intracellular side	5TZY	20

P2Y₁	BPTU	allosteric antagonist	intracellular side	4XNY	30
β₂AR	Cmpd-15PA	NAM	intracellular side	5X7D	21
PAR2	AZ3451	allosteric antagonist	extracellular side	5NDZ	31

^aData as of May 31, 2018.

Traditionally, allosteric modulators have displayed divergent physicochemical properties from those of class A GPCR orthosteric ligands, exemplified by higher lipophilicity, rigidity and typically less affinity for their binding site.³² Due to years of careful optimization and structurally informed design, the development of allosteric modulators has significantly improved in achieving drug-likeness and is now progressing candidates forward in preclinical development and human clinical trials as well as in the market for clinical use (**Table 1.1**). A contributing factor to the optimization of allosteric ligands is the recent availability of ten high resolution crystal structures displaying allosteric binding sites and the corresponding receptor activation states (**Table 1.2**). These structures provide information on binding sites as well as explanation towards differential allosteric modulation of downstream signaling pathways. The latter phenomenon has been termed signaling bias (also functional selectivity) and is characterized by potentiation or inhibition of a selected signaling cascade(s) over other signaling cascades activated by the GPCR.¹² Class A GPCRs translate signaling through association with effector proteins, predominately heterotrimeric G proteins, from whom the receptor class derives its name, and arrestins. Signaling bias, as reported in this perspective, primarily reflects selective or biased modulation of either G protein-mediated signaling or β-arrestin-mediated signaling, although biased receptor interaction with other proteins has been shown as well.^{33, 34} Selectively developing ligands that display a marked signaling bias in accordance with target-specific underlying biology may produce more efficacious drug candidates or may produce candidates with decreased adverse effects. Currently, this trend has been predominantly explored by research groups developing orthosteric ligands for Class A

GPCRs, but it is also a consideration for allosteric ligand development, as shown by selected allosteric modulators in this perspective.

Interest in Class A GPCR allosteric modulators initially grew because of a theoretical improvement in target selectivity, especially among receptor subtypes displaying high degrees of homology in the orthosteric site.³⁵ Since then, subtype selectivity has been shown to be one of many advantages, including the preservation of spacial and temporal dynamics of cell signaling. These benefits are often highlighted in respect to targeting GPCRs within the CNS in which for example, neurotransmitter release and receptor activation are region- and circuit-specific with a high degree of temporal regulation.¹¹ In such a case, an allosteric modulator may preserve these important characteristics and avoid receptor desensitization by relying on endogenous activation events. Additionally, allosteric modulators have a “ceiling effect” whereby the extent of their activity is dictated by the concentration of orthosteric ligand, possibly decreasing overdose concerns. Many of these advantages have been exploited by allosteric modulators targeting receptors in the periphery. For example, the chemokine receptors are an integral component of the immune system and inflammatory response, and one receptor subtype may respond to numerous chemokine ligands (and vice versa) in a receptor-, agonist-, tissue- and time-dependent manner.³⁶⁻³⁸ Thus, allosteric modulation is an attractive strategy for developing precise therapeutics for both the CNS and periphery.

3. RECENT ADVANCES IN THE DISCOVERY AND DESIGN OF CLASS A GPCR ALLOSTERIC MODULATORS

3.1. Aminergic Family Receptors

3.1.1. Serotonin 2C Receptor (5-HT_{2C}R). The serotonin (5-HT) 5-HT_{2C} receptor (5-HT_{2C}R) is a member of the 5-Hydroxytryptamine receptors family, which can activate phospholipase C β (PLC β) via G $\alpha_{q/11}$ to result in production of intracellular inositol 1,4,5-triphosphate (IP₃) and diacylglycerol (DAG) to promote intracellular calcium release

(mobilization).³⁹ Assays described throughout this perspective that relay information on calcium mobilization follow a similar signaling cascade, depending on the activated G protein. The 5-HT₂ subfamily has been of pharmacological interest for decades and is implicated in neurological, psychological and circulatory processes.⁴⁰ It is well known that non-selective antagonists of this subfamily can alleviate symptoms of schizophrenia and anxiety, while non-selective agonists would cause cardiac abnormalities and hallucinations, among other effects. However, selective stimulation of the 5-HT_{2C}R is useful for treating obesity and may be useful for treating substance use disorders (SUD), depression, and other neuropsychological disorders.^{41, 42} Therefore, there remains a need for developing 5-HT_{2C}R targeted ligands that display a high degree of specificity for the 5-HT_{2C}R over the highly homologous 5-HT₂ subtypes 5-HT_{2A}R and 5-HT_{2B}R. As previously mentioned, allosteric modulation holds the potential to differentiate between receptors by targeting less conserved regions and thus provide therapeutic benefit at the 5-HT_{2C}R, while eliminating significant CNS (5-HT_{2A}R) and cardiovascular (5-HT_{2B}R) adverse effects. Two primary groups are engaged in projects aimed at discovering PAMs of the 5-HT_{2C}R.^{43,}
44

PNU-69176E (**1**; **Figure 1.3**) was discovered by Pharmacia (later acquired by Pfizer) via screening of an internal chemical library and is the first reported 5-HT_{2C}R selective positive allosteric modulator.⁴⁵ It was reported that **1** can increase the affinity of 5-HT to the 5-HT_{2C}R low-affinity site with a K_i value 6.4 nM at 20 μ M concentration in human embryonic kidney 293 (HEK293) cell line. Further, **1** displays potentiation in multiple cell lines and potentiates the effects of 5-HT at multiple receptor densities (6 to 45 pmol/mg of protein). Binding selectivity experiments indicate that **1** is a selective 5-HT_{2C}R PAM with no appreciable binding to analogous 5-HT (5-HT_{2A}R, 5-HT_{2B}R, 5-HT₆R and 5-HT_{7A}R) and biologically relevant dopamine receptors (D₂R and D₃R). However, unlike pure PAMs, **1** alone could cause activation of GTP γ S binding, IP₃ release and [³H]-IP₃ accumulation, possibly indicating a stabilization effect of the receptor active state. Both

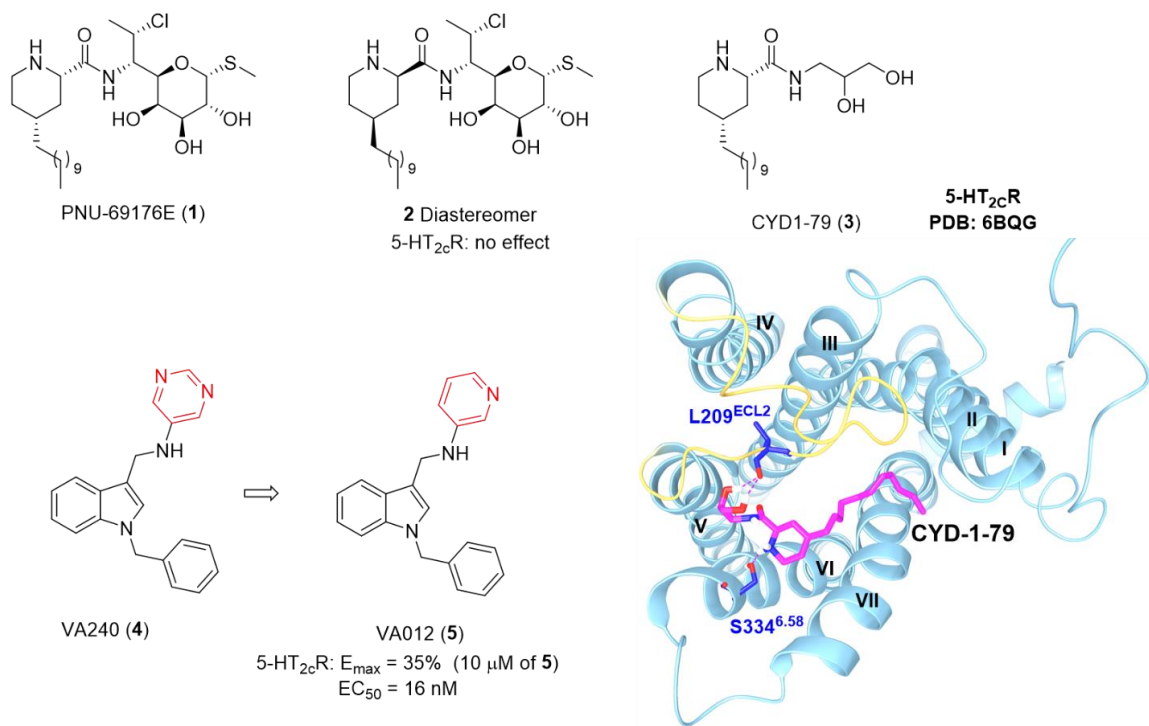
the long alkyl chain and polar moiety (α -D-galactopyranoside) of the chemical structure are reported to be integral to its function and may provide anchoring to the membrane and binding with the allosteric site, respectively. Significantly, its diastereomer **2** (**Figure 1.3**) did not increase 5-HT-evoked intracellular calcium mobilization in 5-HT_{2C}R Chinese hamster ovary (CHO) cells nor did **2** exhibit intrinsic agonist activity.⁴⁶

Recently, our group reported CYD-1-79 (**3**), with a 4-alkylpiperidine-2-carboxamide scaffold, as a selective 5-HT_{2C}R PAM presenting a promising *in vitro* and *in vivo* profile for the treatment of cocaine use disorder (CUD).⁴⁴ Unlike **1**, **3** (**Figure 1.3**) functions as a pure PAM to potentiate 5-HT-evoked calcium mobilization in 5-HT_{2C}R-CHO cells expressing human 5-HT_{2C}R, but exhibits no intrinsic activation of calcium mobilization 5-HT_{2C}R-CHO cells. When investigated in preclinical pharmacokinetic (PK) and rodent efficacy studies, **3** displays measurable blood-brain barrier permeability and significantly suppresses motor impulsivity and cue reactivity assessed as lever presses for cocaine-associated cues in a rodent cocaine self-administration assay. Excitingly, elegant work in the Class A GPCR crystallography field has recently produced a high-resolution crystal structure of the 5-HT_{2C}R capable of enabling molecular docking studies.⁴⁷ Shown in **Figure 1.3**, these studies reveal there is a bridging effect formed by **3** between the extracellular loop (EL) 2 (EL2) and the transmembrane helix (TMH) VI (TMH VI) of the 5-HT_{2C}R via a bidentate, H-bonding interaction. This bridging effect is mediated by a 1,2-diol moiety on **3** to the backbone carbonyl of Leu209^{ECL2} residue of ECL2, and another H-bond between the ionizable *N*-atom of the piperidine ring and the -OH side chain of Ser334^{6.58} of TMH VI (PDB: 6BQG). Significantly, these residues are not conserved in the highly homologous 5-HT_{2A}R or 5-HT_{2B}R, possibly responsible for the selective profile of **3**.⁴⁴

Lopez-Rodriguez and colleagues highlighted 5-HT_{2C}R PAMs as potential anti-obesity therapeutics and recently reported the screening hit VA024 (**4**), featuring an indole scaffold, as a 5-HT_{2C}R PAM.⁴³ In what is only the second reported synthetic small

molecule screening hit for 5-HT_{2C}R PAMs, **4** (**Figure 1.3**) was identified in a Vivia Biotech chemical library via an innovative automated flow cytometry-based screening system, the PharmaFlow platform (previously ExviTech platform).^{43, 48} A minor structural modification of the pyrimidin-5-amine side chain of **4** with pyridine results in VA012 (**5**). Cell studies at a PAM concentration of 10 μM produce a PAM EC₅₀ of 16 nM and a potentiation of the 5-HT E_{max} 35% greater than 5-HT efficacy alone. Further *in vitro* studies indicate **5** does not appreciably bind to important 5-HT₂ family members (5-HT_{2A}R and 5-HT_{2B}R), displays low binding competition against the endogenous agonist (5-HT) and other orthosteric ligands (mesulergine and clozapine) and results in no significant off-target interactions as indicated in a CEREP cellular GPCR panel. Significantly, feeding models in rodents indicate **5** reduces both food intake and body weight gain without causing taste aversion when acutely administered at 2 mg/kg (ip), but evidences of hypolocomotion and anxiety-related behaviors were observed.

Figure 1.3 Representative 5-HT_{2c}R PAMs 1-5



Right: CYD-1-79 (stick representation, magenta, **3**) binding pose from molecular docking on the recently solved 5-HT_{2c}R crystal structure (PDB: 6BQG) interacting with L209^{ECL2} and S334^{6.58}

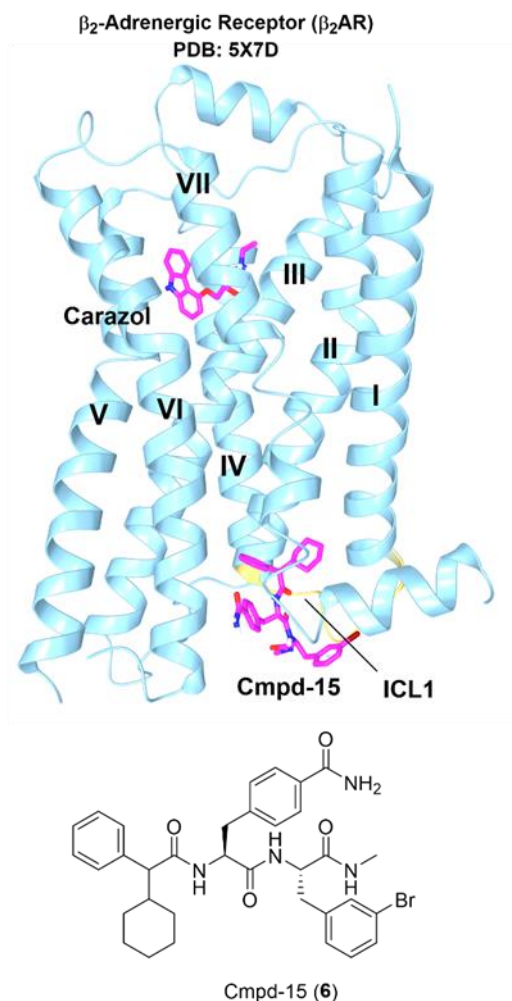
As previously discussed, proteins that interact with Class A GPCRs, such as G proteins, are fundamentally allosteric in their mediation of the receptor structural state and their interference or coordination in allowing other proteins to interact. Structurally, the third intracellular loop and C-terminal tail of the 5-HT_{2c}R, like most other Class A GPCRs, act as scaffolds, molecular levers and protein recruiters with multiple protein binding and phosphorylation sites for mediating receptor function.⁴⁹⁻⁵² Phosphatase and tensin homolog (PTEN) recognizes key residues on the 5-HT_{2c}R intracellular loop III (ICLIII) and mediates 5-HT_{2c}R biological responses. Significantly, this interaction occurs at 5-HT_{2c}R but not at the 5-HT_{2A}R. A fragment of the 5-HT_{2c}R protein, termed 3L4F (third loop, fourth fragment of the human 5-HT_{2c}R), is a peptide derived from the protein interaction site and has been shown to disrupt the 5-HT_{2c}R–PTEN complex and promote 5-HT_{2c}R mediated

downstream signaling, acting as a PAM of 5-HT_{2C}R signaling.⁵³ Subsequent studies revealed that 3L4F-F₁ (Pro280–Arg287), a component of the first eight amino acids of the peptide 3L4F, maintains the efficacy of the full length 3L4F peptide within the picomolar range *in vitro* and also functions as a PAM of 5-HT_{2C}R in rats *in vivo*.⁵³ These examples cover two unique modes for allosterically altering signaling at the 5-HT_{2C}R, where small molecules may bind to the extracellular region of the receptor and stabilize/induce an active state, or peptides and small molecules may bind intracellularly and disrupt protein-protein interactions.

3.1.2. β_2 -Adrenergic Receptor (β_2 AR). The β_2 -adrenergic receptor (β_2 AR) is an aminergic Class A GPCR whose endogenous signaling molecule is adrenaline. The β_2 AR is widely expressed in bronchial smooth muscle, and plays a significant role in cardiovascular and pulmonary physiology.¹⁸ As one of the most highly studied and characterized GPCRs, numerous studies on the β_2 AR represent foundational knowledge on GPCR function, structure and physiological importance for cell signaling.⁵⁴⁻⁵⁹ Therapeutically, β_2 AR agonists represent a large class of drugs used to treat pulmonary disorders and asthma, while β_2 AR antagonists are comprised of selective and non-selective beta-blockers (β -blockers), widely used for the treatment of hypertension, cardiac arrhythmias and other cardiovascular indications. At present, nearly all known β -adrenergic ligands act orthosterically.⁶⁰ Kobilka and colleagues have recently reported the first allosteric β -blocker, or β_2 AR NAM, known as Cmpd-15 (compound-15, **6**) and, significantly, the co-crystal complex with β_2 AR (**Figure 1.4**).^{21, 60} This recently discovered β_2 AR NAM displays low micromolar affinity for β_2 AR and was identified via a DNA-encoded small-molecule library screen comprising 190 million distinct compounds.⁶⁰ SAR studies demonstrate that the formamide group in the para-formamido phenylalanine region and bromine in the meta-bromobenzyl methylbenzamide region are integral for the functional activity of **6** and a dramatic reduction of activity was observed when removing these groups.⁶¹ *In vitro* studies indicate the addition of **6** results in an inhibition of cAMP

production and β -arrestin recruitment. Furthermore, pharmacological studies and the β_2 AR-NAM co-crystal of a polyethylene glycol-carboxylic acid derivative of **6** reveal an intracellular binding site formed by residues from helices I, II, and VI–VIII and the ICL1 of the β_2 AR (PDB code 5X7D).²¹ Only recently have small molecule allosteric sites been identified on the intracellular surface of GPCRs and this finding is significant as these results could extrapolate to additional members of the Class A GPCR family, opening new avenues for allosteric drug discovery.

Figure 1.4 β_2 AR Co-Crystal Structure with Cmpd-15 (**6**)



Top: β_2 AR Co-Crystal Structure with Cmpd-15 (**6**) and agonist carazolol (PDB: 6X7D)²¹;
Bottom: structure of β_2 AR NAM Cmpd-15 (**6**).

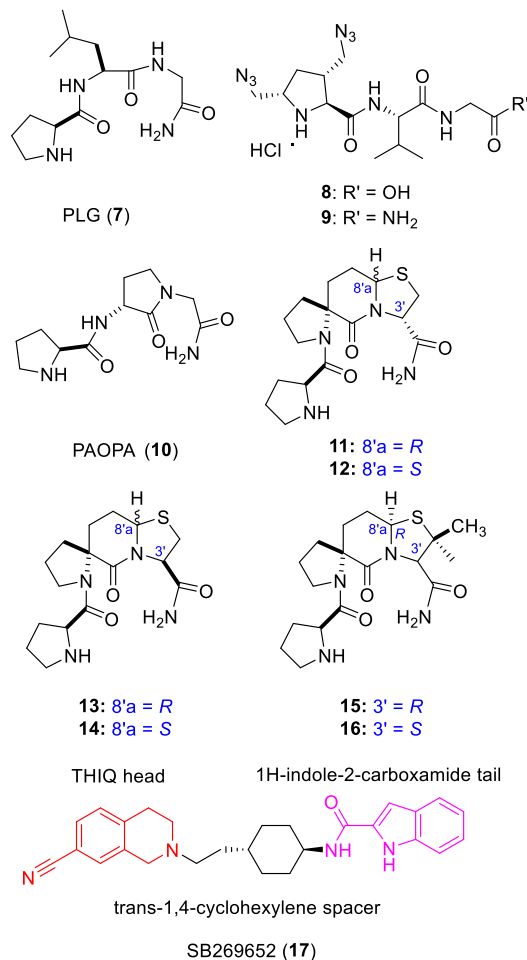
3.1.3. Dopamine Receptors (D_1 , D_2 , D_3). Dopamine receptors represent a therapeutically important subset of Class A GPCRs and exist in two distinct families: 1) D_1 -like family members comprise dopamine D_1 and D_5 receptors, which couple to the $G\alpha_s$ and $G\alpha_{olf}$ G-proteins and stimulate cAMP production, while 2) D_2 -like family members are comprised of D_2 , D_3 and D_4 receptors, which predominantly couple to $G\alpha_{i/o}$ G-proteins and attenuate cAMP production. D_2 -like receptors are widely recognized as the predominant target for the treatment of schizophrenia and Parkinson's disease.^{62,63} However, as a whole, dopamine receptors play a substantial role in numerous neurological and psychological disorders, including also attention deficit hyperactivity disorder (ADHD) and drug and alcohol dependence or SUD.⁶⁴ From a structural perspective of allostery, the evidence of dimerization in dopamine receptors and other GPCRs (homodimers and heterodimers) should not be overlooked, but there is still much to understand about the functional implications of GPCR dimer populations and how these populations might be therapeutically targeted.⁶⁵⁻⁷¹

Due to the therapeutic potential of D_2 -like receptor drugs, several allosteric modulators for D_2 and D_3 have been reported recently (**Figure 1.5**). The neuropeptide Pro-Leu-Gly-NH₂ (PLG, **7**), initially isolated from brain tissue, is an endogenous molecule that has shown potential for pharmacologically treating neurological diseases such as Parkinson's disease and tardive dyskinesia, but the peptide nature of **7** limits its development as a drug. Therefore, the rational design and modification of **7** has led to analogues containing lactam, bicyclic and spiro-bicyclic scaffolds in the search for agents with better PK properties. Subsequent studies show **7** acts as a PAM of the dopamine D_2 and D_4 receptor, and the mode of action for **7** and its peptidomimetics were validated by photoaffinity labeling peptidomimetics.⁷²⁻⁷⁴ Modification of **7** in the L-proline or L-proline and L-leucine residues led to compounds **8-9** displaying similar PAM efficacy, measured by increasing [³H]NPA binding at concentrations between 10⁻¹² and 10⁻⁹ M in human dopamine D_2 receptors.⁷⁵ Improving upon the initial neuropeptide, analogue PAOPA (**10**)

(3(*R*)-[(2(*S*)-pyrrolidinylcarbonyl)amino]-2-oxo-1-pyrrolidineacetamide), a dopamine D₂ receptor selective PAM, is 100–1000-fold more potent than **7** and significantly attenuated schizophrenia-like behavioral phenotypes in preclinical models.⁷⁶⁻⁷⁸ Importantly, **10** displays an improved PK and toxicological profile.

Interestingly, extensive studies with the spiro-bicyclic analogues of **7** have produced both D₂ PAMs and NAMs with minor differences in the stereochemistry of the bridgehead carbon within the same series of peptidomimetics.⁷⁹ Compounds **11** and **13** are D₂ PAMs, while the corresponding diastereoisomeric compounds **12** and **14**, with a difference in the 8'a chiral center, demonstrate D₂ NAM activity in binding experiments with the D₂ receptor agonist NPA and competitive binding with the D₂ PAM.⁸⁰ The molecular conformation is hypothesized to take either a type VI β-turn or polyproline II helix conformation that could place the carboxamide NH₂ pharmacophore in the same topological space as that seen in the type II β-turn, which is vital for the ability to modulate dopamine receptors. Molecular modeling suggests there are two different conformations in the pucker of **14** that may result in divergent effects on the orthosteric site. The modeling results were experimentally tested by incorporating proper chemical substituents to convert the PAM to a NAM. Compounds **15-16** with dimethyl groups in the C2' position of the 5.6.5 bridge were designed to display NAM activity, divergent from the parent compound PAM activity. Indeed, when compared to a control, **15** and **16** demonstrate a NAM profile, which negatively affects the binding of the dopamine receptor agonist NPA to the D₂ receptor and the resultant shift in the EC₅₀ value for [³H] NPA binding to D₂ was 2.7- and 2.8-fold at concentrations of 1 μM and 10 μM, respectively.⁸¹

Figure 1.5 Representative allosteric modulators of the dopamine D₂ and D₃ receptors with chemical modifications at selected positions.



Representative allosteric modulators of the dopamine D₂ and D₃ receptors with chemical modifications at selected positions.

SB269652 (**17**) was found to be a negative allosteric modulator for D₂ and D₃ and the corresponding SAR shows both components of **17** possess influence to some extent on its allosteric activity (**Figure 1.5**).^{82, 83} The THIQ head group is crucial for maintaining allosteric pharmacology, while a “small” substituent in the 7-position is required, and replacement of the alkyl spacer with a linear 1,4-butylene or 1,6-hexylene spacer group conferred an increase in functional affinity. Interestingly, although the tail group is

sensitive to chemical modification, an alternative 7-azaindole tail was reported and demonstrates a 30-fold increase in affinity, while maintaining negative cooperativity with dopamine. Thus, **17** is a current lead compound for developing new dopamine receptor allosteric drugs.⁸⁴ Recently, a benzothiazole scaffold compound was reported as a D₂ PAM, identified via a high-throughput screen (HTS) on 80,000 compounds, and provides another small molecule hit for the development of D₂ PAMs.⁶² Although there are several identified hits coming into the arena for the allosteric modulation of D₂ and D₃, further development to provide mature clinical candidates with improved *in vitro* and *in vivo* properties, along with safer PK profiles is still urgent.

3.1.4. Muscarinic Acetylcholine Receptors (M₁-M₅). Muscarinic acetylcholine (ACh) receptors contain five receptor subtypes (classified as M₁-M₅) and are involved in a wide range of biological processes and diseases, including pain, Alzheimer's disease, schizophrenia, diabetes and obesity.⁸⁵ According to their G-protein coupling preference, there are two major functional classes. The M₁, M₃ and M₅ receptors selectively couple to G-proteins of the G $\alpha_{q/11}$ family, whereas the M₂ and M₄ receptors preferentially activate G $\alpha_{i/o}$ G-proteins. From the perspective of biological distribution, the M₁, M₄ and M₅ receptors are predominantly expressed in the CNS, whereas the M₂ and M₃ receptor subtypes are widely distributed both in the CNS and in peripheral tissues, thus playing an important role in regulating various peripheral and central physiological functions.⁸⁶ As a reference, a recent review by Mohr and colleagues has thoroughly summarized allosteric modulators targeting CNS muscarinic receptors.⁸⁷ Herein, we focus on the recent development of these modulators from a medicinal chemistry perspective, which is mainly reflected in M₁, M₄ and M₅ allosteric modulators.

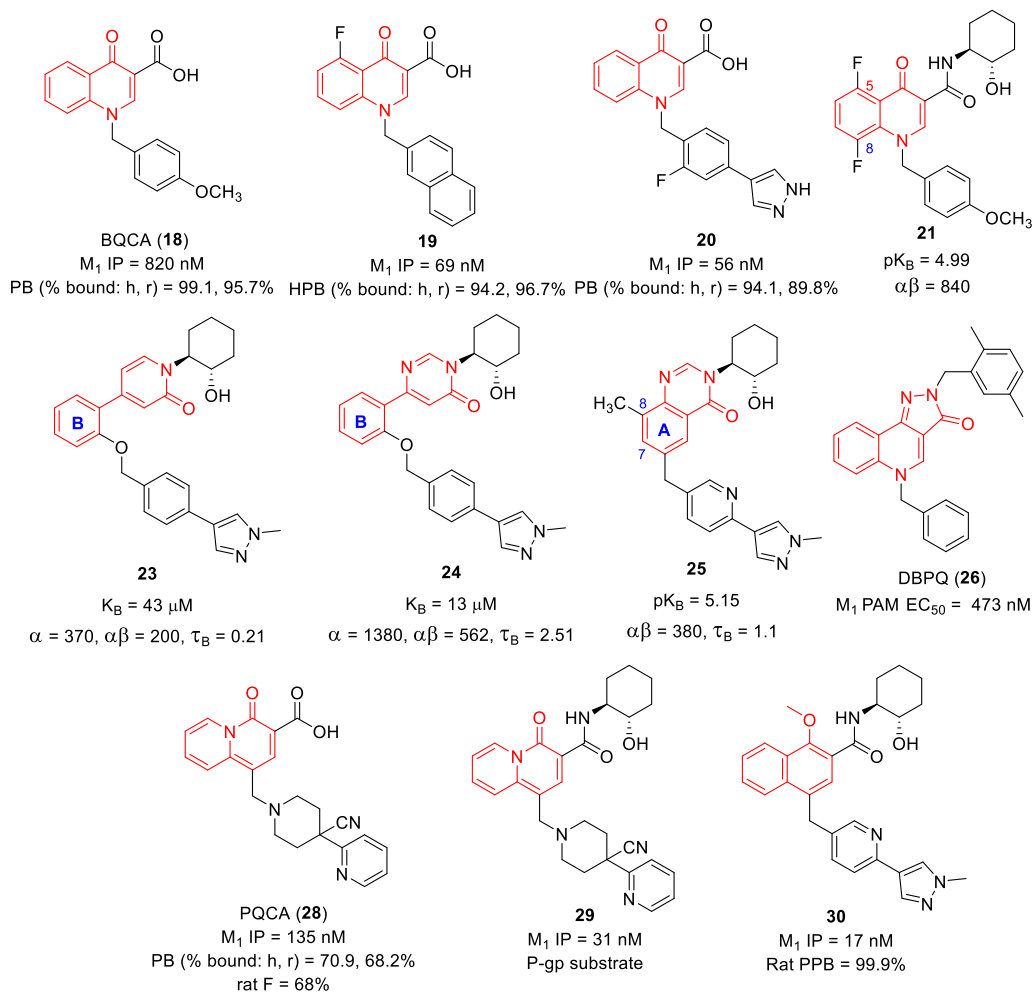
M₁ mAChR. Benzylquinolone carboxylic acid (BQCA, **18**), discovered through HTS efforts at Merck, is a representative scaffold for the development of highly selective M₁ mAChR PAMs, and provides a basis for developing novel therapeutics to counteract the negative cognitive symptoms associated with diseases such as Alzheimer's disease and

schizophrenia (**Figure 1.6**).⁸⁸ According to current ligand classifications, **18** is a PAM which lacks intrinsic activity to induce calcium mobilization at concentrations up to 10 μM , but markedly increases ACh potency 129 fold at 100 μM in human M_1 mAChR expressing CHO cells. Additionally, **18** displays selectivity over the related neuronal M_2 - M_5 mAChR subtypes up to >100-fold and does not modulate signaling at other examined Class A GPCRs. However, **18** presents lackluster PK, resulting in high plasma protein binding and low solubility in its neutral form.

Subsequent SAR-informed optimizations to address these shortcomings were conducted. These studies suggest fluoro-substituents are preferred optimizations for analogues of **18** in terms of M_1 mAChR potency *in vitro*⁸⁹, which was later proven to attribute to increased intrinsic efficacy of these analogues.⁹⁰ Compounds **19-20** were produced based on this principle and displayed an improved inflection point (IP), but maintained high plasma protein binding and poor brain exposure.^{89,91} Amide derivative **21**, with an improved PK profile, produces higher potency binding and functional cooperativity with ACh, bearing cooperativity α and $\log\alpha\beta$ values of 170 and 840 in a calcium mobilization assay, respectively.⁹⁰ Modifications on the benzyl side chain and quinolin-4(*1H*)-one of **18** were examined as a means to further improve affinity, decrease plasma protein binding and address the BBB permeability problem aforementioned. Aryl methyl benzoquinazolinone **22** is a resultant compound with a greater than 50-fold increase in affinity for the M_1 receptor in comparison to **18** ($K_B = 0.3 \mu\text{M}$ for **22** and $15 \mu\text{M}$ for **18**), while retaining similar positive cooperativity and efficacy with ACh.⁹² Mutagenesis studies and molecular modeling, confirm compound **22** occupies the same allosteric binding pocket as **18**. Insights from these studies include key hydrophobic/edge-to-face π - π interactions with residues Tyr-179 in ECL2 and Trp-400^{7,35} in TM7 are critical for the increased affinity and activity of **22**. MK-7622, a mature example in this series, advanced into a Phase II clinical trial in 2013 and was terminated in 2016 for undisclosed reasons.⁹³

For further optimization efforts, modifications were made to the core pharmacophore aryl ring systems. Opening of the aryl A ring of **22** furnishes 4-phenylpyridin-2-one **23**, a structure maintaining intramolecular hydrogen bonding between the carboxylic acid and ketone in **18**.⁹⁴ Compound **23** shows comparable binding affinity to **18** with a K_B value of 43 μM in FlpIN CHO cells, but interestingly improved positive cooperativity with ACh ($\alpha = 370$, $\alpha\beta = 200$), i.e., a significant 370-fold potentiation of ACh affinity, and retained high selectivity for the M_1 mAChR. Further modification of pyridin-2(*1H*)-one to 6-phenylpyrimidin-4-one **24** presents an α value of 1,380, a 4-fold increase in binding cooperativity with ACh, along with an 11-fold increase in intrinsic efficacy ($\tau_B = 2.51$), suggesting further interaction with the allosteric pocket of the M_1 mAChR through the introduction of an additional tertiary nitrogen as a hydrogen bond acceptor. Ring opening of aryl B, replacing the tricyclic benzo[*h*]quinazolin-4(*3H*)-one core with quinazolin-4(*3H*)-one gives compound **25**.⁹⁵ Compound **25** shows improved “drug-likeness” with lower lipophilicity, topological polar surface area (tPSA), molecular weight and also reduces the toxic DNA-chelation concern for polyaromatic heterocycle scaffolds. The methyl group in the 8-position is critical to maintain affinity for the M_1 mAChR compared to **22** with pK_B and $\alpha\beta$ values of 5.15 and 380 for **25** and 5.88 and 370 for **22**, respectively, but lower intrinsic activity ($\tau_B = 1.1$), in radioligand binding experiments using FlpIN CHO cells. Dibenzyl-2*H*-pyrazolo[4,3-*c*]quinolin-3(*5H*)-one (**26**, DBPQ) is another example of a tricyclic scaffold similar to **22**, and was discovered as a hit from a 2012 high-throughput screen of the NIH Molecular Libraries Small Molecule Repository (MLSMR).⁹⁶ Compound **26** exhibits a functional EC_{50} of 473 nM and a depressed ACh maximum response E_{max} of 40% measured by a calcium response assay of the PAM and a submaximal concentration of ACh in a calcium mobilization assay.

Figure 1.6 M₁ mAChR PAM BQCA (**18**) and derivatives (**19-30**) with corresponding SARs



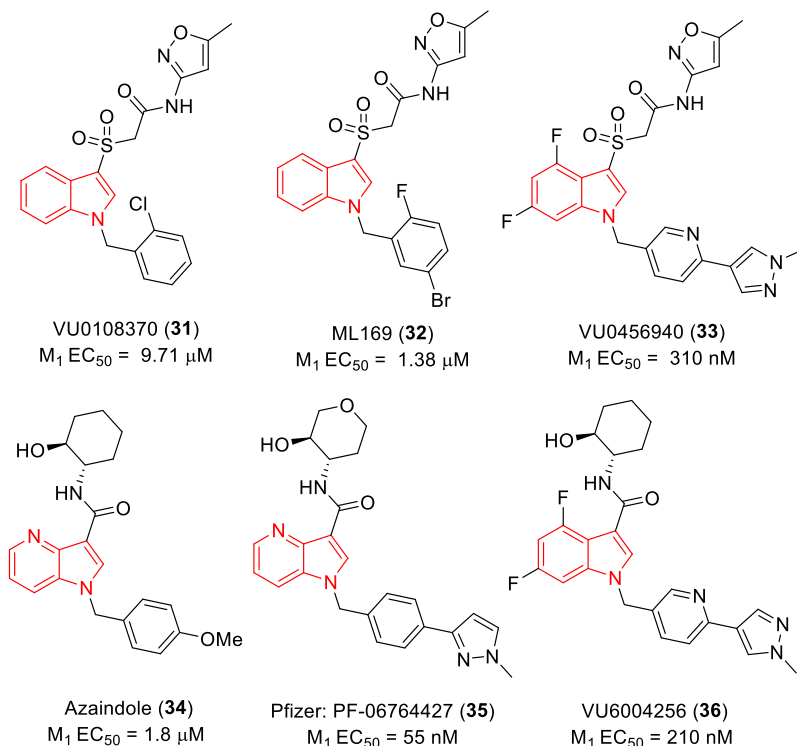
M₁ mAChR PAM BQCA (**18**) and derivatives (**19-30**) with corresponding SARs.

Replacement of the quinolone ring system of **18** with quinolizidinone as an alternate scaffold and exchanging the side benzyl chain with a basic 4-cyanophenyl piperazine linkage led to compound **27**.⁹⁷ Compound **27** shows enhanced CNS exposure with a 13% human free fraction and improved *in vivo* efficacy in a mouse contextual fear conditioning model of memory, while the bioavailability is relatively low, observed as 23% in rats. Noteworthy, this modification limits the liability for efflux by the CNS efflux transporter P-glycoprotein (P-gp). Compound **28** bearing a cyano group at the 4-position

of the piperidine displays increased functional activity (M_1 mAChR IP = 135 nM) in human M_1 mAChR expressing CHO cells determined in the presence of an EC_{20} concentration of ACh by a calcium mobilization readout on a fluorometric imaging plate reader (FLIPR384).⁹⁸ The plasma free fraction value is an acceptable 30% and oral bioavailability is greatly improved to 68% in rats with a 1.7 h half-life. Further modification by replacing the carboxylic acid with cyclic amide substituents to produce **29** significantly improved the potency in functional assays (M_1 mAChR IP = 31 nM); however this led to P-gp efflux liability.⁹⁹ A replacement of the core to methoxynaphthalene led to compound **30** with a M_1 mAChR IP value of 17 nM.¹⁰⁰ Although **30** addressed the P-gp substrate problem, **30** results in high protein binding as observed at 99.9% in rat.

VU0108370 (**31**), a hit discovered via a functional HTS of the NIH's Molecular Libraries Probe Production Centers Network (MLPCN) library, represents a second unique chemotype based on an indole core (**Figure 1.7**).¹⁰¹ Compound **31** shows relatively low potency for ACh at the M_1 mAChR with an EC_{50} value of 9.71 μ M. Structural optimization around **31** afforded ML169 (**32**) as a selective M_1 mAChR PAM MLPCN probe, presenting a moderate yet improved potency (EC_{50} = 1.38 μ M). Difluoro-substitution of the indole core and a pyrazine in the benzyl side chain results in VU0456940 (**33**) and further improves the EC_{50} to 310 nM.¹⁰² Azaindole (**34**) results from the replacement of the quinolone ring of **18** with an azaindole core producing an EC_{50} value of 1.8 μ M.¹⁰³⁻¹⁰⁵ Modification of the substitution on a benzyl with pyrazole furnishes PF-06764427 (**35**) as a highly selective M_1 mAChR PAM and demonstrates excellent cooperativity with a 30-fold potency improvement and favorable *in vivo* efficacy in an amphetamine-stimulated locomotor activity model in rodents.¹⁰⁶ Difluoro-substitution on **35**, resulting in VU6004256 (**36**), improves its safety profile and was reported as lacking severe adverse effects, such as behavioral convulsions and peripheral cholinergic adverse effects in mice, although no improvements to its activity were observed.¹⁰⁷

Figure 1.7 Representative M₁ mAChR PAMs with an indole core (red) and SAR (compounds **31-36**)

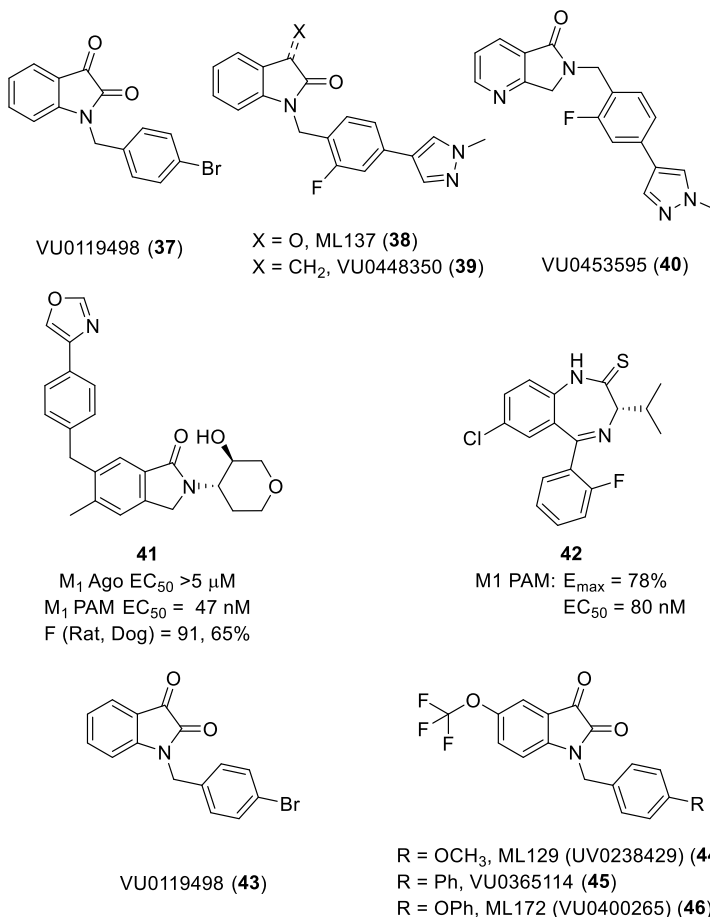


Representative M₁ mAChR PAMs with an indole core (red) and SAR (compounds **31-36**).

A third unique scaffold for M₁ mAChR PAMs consists of an isatin core. VU0119498 (**37**) is a pan-M₁,M₃,M₅-PAM discovered through a HTS campaign and subsequent SAR enabled the rational design of subtype selective PAMs.¹⁰⁸ Chemical optimizations on **37** led to selective M₁ mAChR PAMs ML137 (VU0366369, **38**) and VU0448350 (**39**) with EC₅₀ values of 0.83 μM and 2.4 μM, respectively.^{108, 109} Further modification on this scaffold yields VU0453595 (**40**), a highly selective M₁ mAChR PAM with improved brain exposure in mice after systemic administration.¹¹⁰ Recent modification around isoindolin-1-one produces compound **41**, which displays a significantly improved EC₅₀ value of 47 nM, minimal intrinsic agonist activity and oral bioavailability of 91% in rodents and 65% in canines.¹¹¹ Other work in this arena includes the benzodiazepine derivative **42**, which was recently reported by a team at Roche as a

selective M₁ mAChR PAM with an EC₅₀ value of 80 nM in human M₁ mAChR expressing cells.¹¹² Overall, there are variable improvements in brain exposure and *in vivo* efficacy for selective M₁ mAChR allosteric modulators and development continues for multiple scaffolds presented herein.

Figure 1.8 Chemically diverse M₅ mAChR PAMs with key modifications (compounds 37-46)



Chemically diverse M₅ mAChR PAMs with key modifications (compounds 37-46).

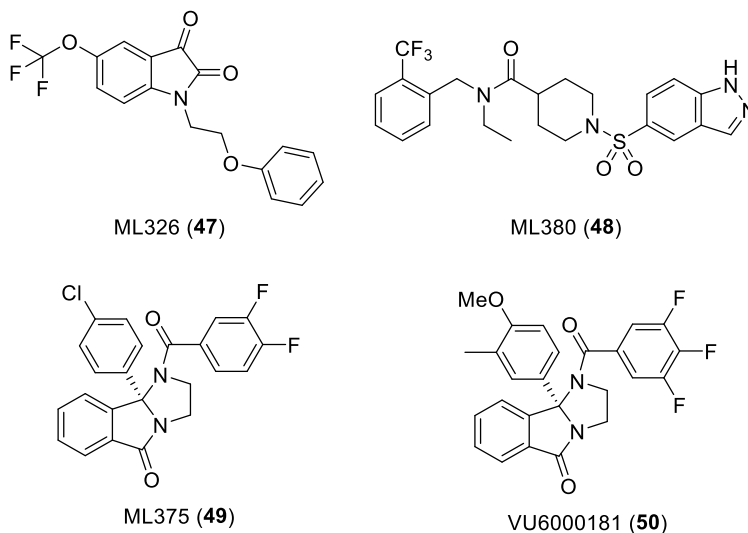
M₅ mAChR. The M₅ mAChR has historically been the least studied receptor of the mAChR family, primarily due to low endogenous expression levels; however there is a current upsurge in interest from drug discovery groups to identify selective PAMs that are efficacious in relevant disease models.¹¹³ Physiological studies indicate the M₅ mAChR is

enriched in the cerebrovascular system and present a potential target for the treatment of numerous CNS disorders including schizophrenia, Alzheimer's disease, ischemia and migraine.¹¹³ As previously highlighted, the small molecule series with an isatin core display PAM activity at the M₅ mAChR in addition to other mAChR subtypes, and thus medicinal chemistry efforts have partly focused on identifying molecular switches to convey subtype specificity in this series. VU0119498 (**43**) is the first reported hit discovered via a HTS and displays micromolar potencies as a pan-PAM for the potentiation of ACh at M₁, M₃ and M₅ mAChR subtypes in cell-based calcium mobilization assays (**Figure 1.8**).¹¹⁴ Subsequent optimization led to the discovery of ML129 (VU0238429, **44**), containing a 5-trifluoromethoxy isatin scaffold, as a selective M₅ mAChR PAM with an EC₅₀ of approximately 1.16 μM.¹¹⁵ Further modifications included substitutions on the benzyl chain where it was shown that VU0365114 (**45**) and ML172 (VU0400265, **46**) could maintain potency, while the addition of a phenoxyethyl substituent in ML326 (**47**) achieved sub-micromolar level potency in a human M₅ mAChR expressing cell line (EC₅₀ = 410 nM, ACh fold-shift = 20, **Figure 1.9**).^{113, 116, 117} However, the suboptimal ionization properties of **47** preclude its utility for *in vivo* assessment due to low CNS exposure.¹¹⁸ ML380 (**48**), a promising and divergent scaffold lacking the common isatin core, was discovered during a HTS of the MLPCN screening deck of ~360,000 compounds against M₁, M₄ and M₅ mAChR subtypes. Compound **48** displayed selective M₅ mAChR PAM activity with submicromolar potency and markedly improved CNS penetration (EC₅₀ = 190 nM, ACh fold-shift = 9.3).¹¹⁸

In regards to NAM discovery, ML375 (**49**) is the first selective M₅ mAChR NAM with sub-micromolar potency and characterization reveals an IC₅₀ of 300 nM at the human M₅ mAChR and an IC₅₀ of 790 nM for rat M₅ mAChR (**Figure 1.9**).¹¹⁹ Compound **49** was also found to exhibit favorable CNS exposure (brain/plasma K_p = 1.8).¹¹⁹ However, high protein binding in both blood and brain tissue (rat f_u = 0.029, rat brain f_u = 0.003) has limited its utility as an *in vivo* tool compound to date.¹²⁰ Through a combination of matrix

libraries and iterative parallel synthesis, optimization of **49** led to VU6000181 (**50**), which maintains potency levels but also retains an unfavorable PK profile.¹²⁰

Figure 1.9 Representative M₅ mAChR PAMs (**47-48**) and NAMs (**49-50**)



Representative M₅ mAChR PAMs (**47-48**) and NAMs (**49-50**)

M₄ mAChR. Interestingly, the analytical specialty chemical thiochrome was one of the first reported selective M₄ mAChR PAMs, but was observed to exhibit low affinity for the receptor.¹²¹ Heightened activity in this arena occurred with the discovery of LY2033298 (**51**) as a benchmark example of selective M₄ mAChR PAMs (**Figure 1.10**).¹²² Compound **51** contains a 5-amino-thieno[2,3-*c*]pyridine scaffold and has a measured K_B value of 200 nM at the allosteric site on the unoccupied human M₄ mAChR.¹²² Chemical modification of **51** on the substitutions in the thieno[2,3-*c*]pyridazine and side chain resulted in the discovery of VU10010 (**52**).¹²³ Compound **52** has a high potency with an EC₅₀ value of 400 nM and elicits a 47-fold leftward shift of an ACh concentration response curve in a calcium-mobilization assay in rat M₄ mAChR expressing cells. Optimization of **52** led to ML108 (**53**) and VU0152099 (**54**), which present nearly equivalent potency while improving CNS exposure as evidenced by peak brain concentrations ranging from 3 to 5

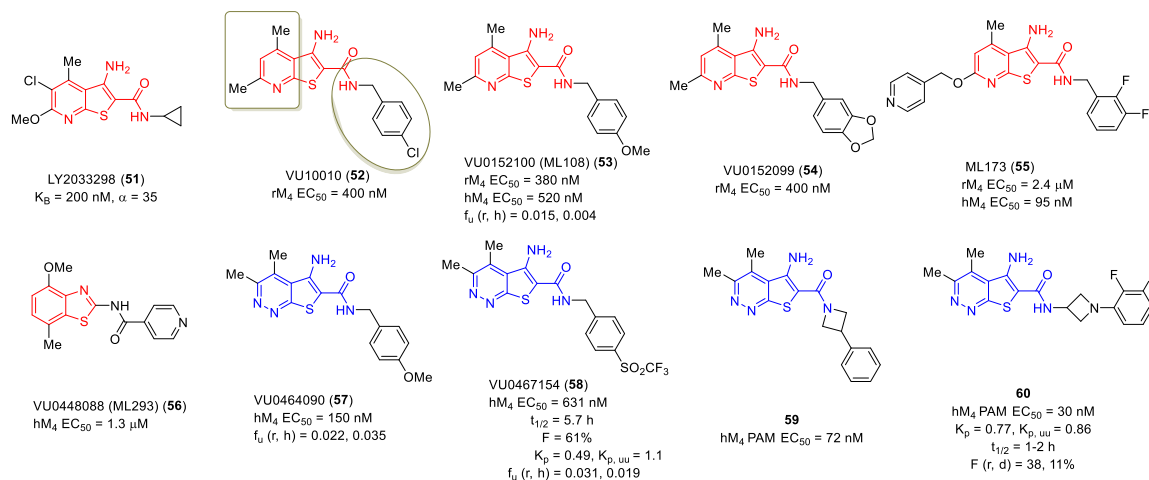
$\mu\text{g/mL}$ after 56.6 mg/kg i.p. administration in rodents.¹²⁴ However, the metabolic stability of this scaffold is poor due to the hydroxylation of the 6-methyl group on the pyridine ring, resulting in less than 10% parent compound remaining after 90 min. Noteworthy, the replacement of the metabolically labile 6-methyl group with an ether linked substituent led to ML173 (**55**) and a significantly improved microsomal stability profile with greater than 90% parent remaining after 90 min, in both rat and human microsomal assays.¹²⁵ Although *in vitro* potency in human M₄ mAChR expressing cells was measured at an EC₅₀ of 95 nM, subsequent preclinical *in vivo* studies demonstrated limited efficacy for **55** in the reversal of amphetamine-induced hyperlocomotion in a rat behavioral model. This result necessitates highlighting an important phenomenon that can be encountered during the preclinical phases of compound optimization: species bias. Additional data indicate that although high potency was observed at the human M₄ mAChR, **55** displays a strong species bias with an EC₅₀ of only 2.4 μM for the rat M₄ mAChR, which leads to exceedingly difficult optimization and ultimately precludes preclinical development of this compound.¹²⁵ In an expert review, Conn, Lindsley, Meiler and Niswender advise identifying and avoiding compounds with an intractable species bias from experience in this series and others.²²

ML293 (**56**) is characterized by a unique scaffold with a benzothiazole core and was developed through an iterative optimization effort at the Vanderbilt Center for Neuroscience Drug Discovery (**Figure 1.10**).¹²⁶ Although **56** displayed low micromolar potency at the human M₄ mAChR, the promising *in vivo* PK properties warrant attention with a lower IV clearance rate (11.5 mL/min/kg) than previous series and excellent brain exposure when orally administered to rats and measured as a brain to plasma ratio (10 mg/kg at 1 h, [Brain] = 10 μM , B:P = 0.85).¹²⁶ The modest potency and half-life (EC₅₀ = 1.3 μM , $t_{1/2}$ = 57 min) necessitates further optimization of this series. Recently reported, modification of the previously described 3-amino-thieno[2,3-*b*]pyridine scaffold (as in **53**) by replacing the pyridine with a pyridazine ring results in VU0464090 (**57**).¹²⁷ Compound

57 displays a 3-fold potency improvement with an EC₅₀ value of 150 nM in human M₄ mAChR expressing cells and a significant 9-fold improvement in free fraction values compared to **53** (f_u rat, human = 0.022, 0.035 for **57** and 0.015, 0.004 for **53**).¹²⁷ This relatively minor chemical modification results in large electronic changes due to the high dielectric constant of the pyridazine ring and likely led to the observed improvement in PK properties. However, the p-methoxybenzyl amide in **57** proved to be metabolically labile via cytochrome P450 (CYP)-mediated oxidative demethylation and alternative amides were explored. Concentrating on sulfur-containing amide moieties, Lindsley and colleagues discovered VU0467154 (**58**) through an iterative optimization campaign.¹²⁷ Although the potency of **58** for human M₄ mAChR is modest with an EC₅₀ value of 631 nM, **58** has proven to be an exemplary rodent M₄ mAChR PAM tool compound, due to its reported minimal off-target interactions, excellent subtype selectivity and good PK profile.^{127, 128} The following optimizations to the 5-amino-thieno[2,3-*c*]pyridazine class of M₄ mAChR PAMs were recently reported and feature an azetidine substituted side chain.¹²⁹ Out of a series of examined cyclic amines, azetidine based linkers in the side chain retained activity. Chemically, compound **59** in this series maintains an amide, however utilization of the azetidine results in a rigid amide lacking H-bonding ability (**Figure 1.10**). Based on the interesting analysis of X-ray crystal structure data, the removal of the amide N-H and the introduction of conformational restraint in the side chain was hypothesized to limit intermolecular interactions between adjacent molecules due to π -stacking and H-bonding, ultimately improving upon the poor solubility of previous derivatives. Indeed, **59** maintains high potency with a human M₄ mAChR EC₅₀ of 72 nM and markedly improved CNS exposure in rat (K_p = 2.6, K_{p,uu} = 2.1).¹²⁹ *In vivo*, **59** was examined in an established rat amphetamine-induced hyperlocomotion assay to determine antipsychotic efficacy and at 30 mg/kg (oral) **59** can attenuate hyperlocomotion by up to 32%. However, the azetidine amide linker in this scaffold is a metabolic weakness with high predicted clearance resulting from both rat and human microsomal preparations (CL_{hep} = 64 (r), 20 (h)

mL/min/kg). Subsequent developments detail a replacement by a 3-aminoazetidine moiety, resulting in VU6000918 (**60**).¹³⁰ Compound **60** is characterized by improved *in vitro* human M₄ mAChR potency (EC₅₀ = 30 nM), a relatively short half-life (1-2 h) and suboptimal oral bioavailability, as measured at 11% in canine (2 mg/kg). At present, this extended series of compounds has demonstrated excellent *in vitro* activity and preferred species selectivity, however achieving an optimal combination of distribution, metabolism and pharmacokinetic (DMPK) properties such as bioavailability, CNS exposure, P-gp efflux liability and metabolic stability has proven to be challenging.

Figure 1.10 M₄ mAChR PAM derivatives around the 5-amino-thieno[2,3-*c*]pyridine scaffold and corresponding SAR (**51-60**)



M₄ mAChR PAM derivatives around the 5-amino-thieno[2,3-*c*]pyridine scaffold and corresponding SAR (**51-60**).

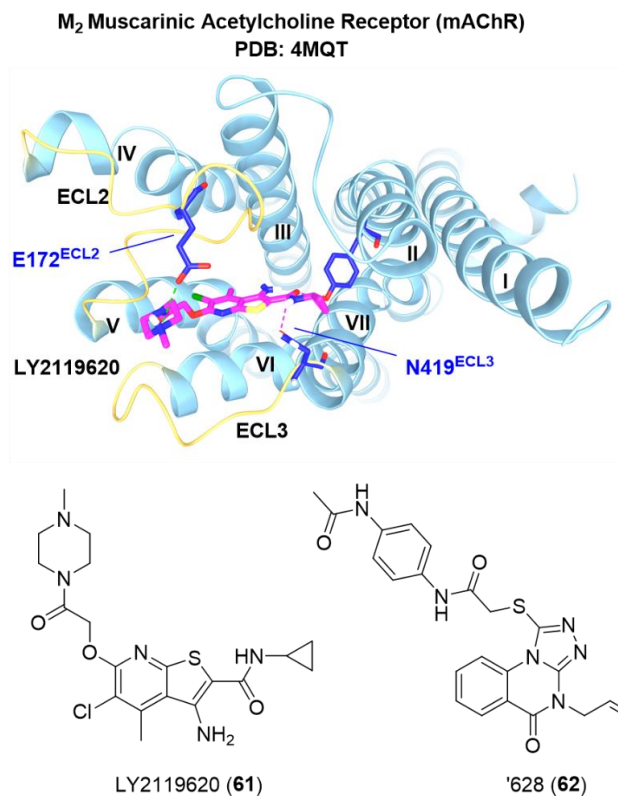
M₂ mAChR. The M₂ mAChR is distributed in both the CNS and periphery and has been predominately studied for its role in regulating parasympathetic cardiac function. In this capacity, the M₂ mAChR modulates potassium channels and its activation leads to the closing of calcium channels, necessary for heart rate reduction.¹³¹ Early examples of M₂ mAChR allosteric modulators, discovered by Mohr and colleagues, include alkane-bisammonio-type ligands.¹³² This chemotype was subjected to subsequent rounds of

chemical modifications, where a switch from negative to positive cooperativity was observed and conjugation to orthosteric ligands resulted in bitopic molecules of interest.¹³³ The importance of the M₂ mAChR lies not in its therapeutic utility as the general consensus is that M₂ mAChR activation leads to undesirable off-target effects for mAChR modulators.¹³⁴ However, from a structural perspective, elegant work on the M₂ mAChR and its PAM LY2119620 (**61**) has enabled major leaps in the understanding of mAChR, and GPCR, allosteric modulation.^{19, 135} Compound **61** is reported as a high-affinity PAM of both the M₄ and M₂ mAChR and it potentiates the activity of agonist iperoxo. The pioneering co-crystal structure of **61** bound to the M₂ mAChR shows **61** occupying a site above the orthosteric iperoxo binding site on the extracellular side of helices II, VI and VII, and forming extensive contacts with ECL2 and ECL3 (PDB: 4MQT, **Figure 1.11**).¹⁹ These contacts include a charge-charge interaction between the piperidine group and residue Glu172 in ECL2, hydrogen bonds between both the amide oxygen and N-H with the side chains of Tyr80^{2,61} and Asn419 in ECL3, and additional hydrophobic interactions with aromatic residues in ECL2. This structural analysis provides insight to one way a PAM can impact agonist binding and resultant receptor activity.

Further contributions from the structure of the M₂ mAChR include a recent discovery effort aimed at finding highly selective PAMs that potentiate binding of non-selective antagonists, whereby the antagonist is essentially turned selective due to PAM induced cooperativity.¹³⁶⁻¹³⁷ These studies utilized extensive molecular libraries for ensemble docking at the M₂ mAChR and realize the potential of allosteric modulators to improve orthosteric ligand selectivity. The resultant compound '628 (**62**) features a unique triazolo-quinazolinone and could enhance binding of the M₂ mAChR antagonist *N*-methyl scopolamine (NMS) with a cooperativity factor (α) of 5.5. Interestingly, **62** can markedly slow the dissociation rate of NMS from the M₂ mAChR by 50-fold. The specific PAM effect of **62** on NMS antagonism was further validated in cell-based functional assays and

the observations translated to membranes from adult rat hypothalamus and to neonatal rat cardiomyocytes.¹³⁷

Figure 1.11 M₂ mAChR-LY2119620 (stick representation, magenta, **61**) co-crystal and other representative PAMs



Top: M₂ mAChR-LY2119620 (stick representation, magenta, **61**) co-crystal extracellular view highlighting interactions with ECL residues E172^{ECL2} and N419^{ECL3} (PDB: 4MQT). Bottom: representative M₂ mAChR PAMs (**61-62**).

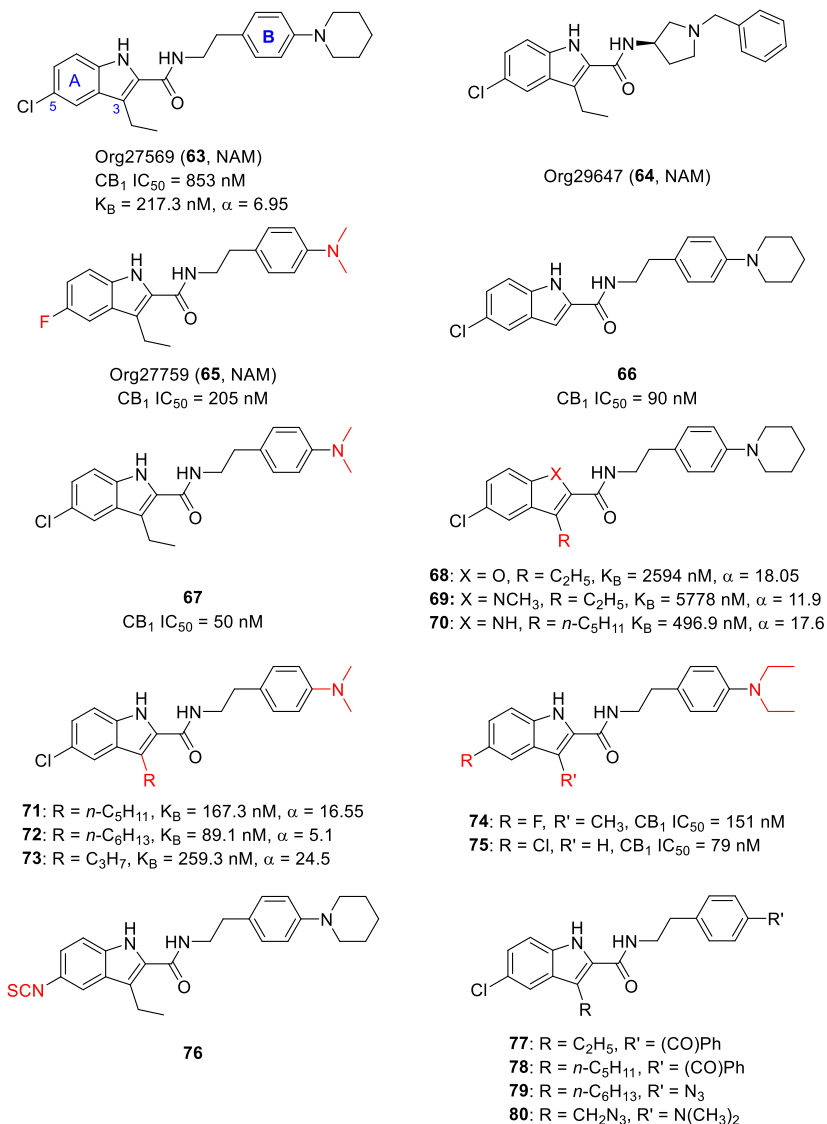
3.2. Lipid Family Receptors

3.2.1. Cannabinoid Receptors (CB₁ and CB₂). The CB₁ receptor and the CB₂ receptor are key mediators of the endocannabinoid system. The cannabinoid CB₁ receptor is widely distributed throughout the CNS and endogenous agonists of the CB₁ receptor include anandamide (AEA) and 2-arachidonylglycerol (2-AG), which regulate many physiological processes related to pain, metabolism, nociception and neurotransmission.¹³⁸

To date, CB₁ receptor orthosteric agonists and antagonists have not realized therapeutic expectations largely due to adverse effects, for example, the orthosteric anti-obesity antagonist rimonabant was withdrawn from the market owing to neuropsychiatric adverse effects.¹³⁹ Alternatively, development of both NAMs and PAMs of the CB₁ receptor has been of high interest in recent years, encompassing structurally distinct synthetic, plant-derived and endogenous allosteric ligands. NAMs of the CB₁ receptor were reported first, mainly comprising two scaffolds that have been extensively characterized: the *1H*-indole-2-carboxamide and the diarylurea analogues. The CB₂ receptor, another important member of the endocannabinoid system, is highly expressed in the periphery, especially in blood cells, and in blood-cell producing organs.¹⁴⁰ Despite recent pharmacological advances in the characterization cannabidiol as an allosteric modulator of the CB₂ receptor¹⁴¹, the therapeutic potential of PAMs and NAMs targeting the CB₂ receptor requires additional investigation, and thus we focus on CB₁ receptor ligand discovery herein.

1H-Indole-2-carboxamide CB₁ receptor NAMs. A major advance was made with the discovery of *1H*-indole-2-carboxamide analogues as CB₁ receptor NAMs. Org27569, Org29647 and Org27759 (**63-65**, **Figure 1.12**) displayed an interesting pharmacological profile by enhancing the affinity yet reducing the efficacy of CB₁ receptor agonists and suggests the existence of an allosteric binding site at the CB₁ receptor. These allosteric ligands have proven to be an excellent series of tool compounds and provide a basis for medicinal chemistry development. When examined in a binding assay, **63-65** augment specific binding of the CB₁ receptor agonist 2-[(1*R*,2*R*,5*R*)-5-hydroxy-2-(3-hydroxypropyl)cyclohexyl]-5-(2-methyloctan-2-yl)phenol [³H]-CP55,940) in membranes from cells expressing the CB₁ receptor. However, in the reported gene assay, the guanosine 5'-*O*-(3-[³⁵S]thio)triphosphate binding assay and the mouse vas deferens assay **63-65** elicit a significant reduction in the E_{max} for CB₁ receptor agonists, showing a resultant CB₁ receptor NAM profile.¹⁴²

Figure 1.12 CB₁ receptor NAMs (**63-80**) based on the *1H*-indole-2-carboxamide scaffold and corresponding SAR



CB₁ receptor NAMs (**63-80**) based on the *1H*-indole-2-carboxamide scaffold and corresponding SAR.

Piscitelli et al. examined a number of 4-substitutions on the phenyl B ring and discovered that piperidinyl or dimethylamino groups at the 4-position of the phenyl ring are preferential for CB₁ receptor NAM activity (**Figure 1.12**).¹⁴³ Compounds **66**, with hydrogen in the C3 position of the indole, and **67**, with a dimethylamino substituent in the 4-position of phenyl, show potent NAM activity with IC₅₀ values of 90 nM and 50 nM,

respectively. The analyses of these compounds also provide evidence that the carboxamide functionality is required and when replaced by an ester, potency is greatly reduced. Lu et al. subsequently conducted a series of SAR studies around the *1H*-indole-2-carboxamide scaffold by measuring two essential parameters: the equilibrium dissociation constant (K_B), which reflects the binding affinity of the allosteric ligand, and the binding cooperativity factor (α), which measures the allosterically induced effects between the orthosteric and allosteric ligands when both are bound to the receptor. These SAR studies report the indole core is essential for the binding affinity (K_B) but not for generating allostery (α) on the orthosteric site, and the C3 substituents of the indole-2-carboxamides significantly impact the cooperativity. Replacing the indole with benzofuran ring (**68**) led to a 3-fold increase in the K_B value (2,594 nM for **68** vs 217.3 nM for **63**) and masking the indole nitrogen with a methyl group as in **69** led to a significant 27-fold decrease. Substitution of the C3 position with a linear *n*-pentyl group, resulting in **70**, displayed a noteworthy cooperativity enhancement ($\alpha = 17.6$), while producing only a moderate binding affinity of 496.9 nM. Additionally, replacing the phenyl B ring piperidinyl substituent in **70** with a dimethylamino moiety yields **71** with improvement to the NAM binding affinity ($K_B = 167.3$ nM) and maintenance of the cooperativity ($\alpha = 16.55$), while functional assays displayed a potent inhibition of GTP γ S binding.^{144, 145} Further investigations modifying the C3 position with variations of the linear alkyl moieties, such as *n*-propyl and *n*-hexyl, yields compounds **72-73**, with **72** displaying the highest allosteric ligand affinity observed ($K_B = 89.1$ nM) and a reduction in cooperativity ($\alpha = 5.1$), while **73** was characterized by modest affinity ($K_B = 217.3$ nM) and a significant enhancement of binding cooperativity ($\alpha = 24.5$).¹⁴⁶ In addition, modification to the substitution on the A ring inform that a 5-halogen substituent is vital to maintain allosteric activity. Functional assays on **72** and **73** demonstrate an interesting effect on CB₁ receptor signaling pathways with a NAM concentration-dependent inhibition of agonist-induced GTP γ S binding, yet they have a PAM effect in a β -arrestin mediated extracellular signal-regulated kinases 1/2 (ERK1/2)

phosphorylation assay. Aside from alkyl chain substituents on the C3 position, less bulky substituents such as methyl and hydrogen on the C3 position and a fluoro or chloro substitution at the C5 position yielded analogues **74-75**, which possess improved CB₁ receptor NAM activity in a calcium-mobilization assay with an IC₅₀ of 151 nM and 79 nM, respectively, which is approximately 5- and 10- fold more potent than the parent compound **71**.¹⁴⁷

Ligand-assisted protein structure (LAPS) is an approach for elucidating structure-function correlates of ligand binding to GPCRs in functionally and physiologically relevant conditions, which is useful for obtaining structural information about the allosteric site since the structures of some receptors are obscure.¹⁴⁸ In this approach, noncovalent, pharmacologically active ligands can be designed and synthesized to accommodate chemically reactive moieties, such as electrophilic groups (e.g., isothiocyanate, benzophenone, etc.) and photoactivatable groups (trifluoromethyl diazirine, aliphatic/aromatic azide, etc.). Thus, upon ligand binding, the reactive group forms a covalent bond at an actionable amino acid residue providing spatial resolution of the allosteric site, in this case. Modification at the 5-position of **63** with the chemically reactive electrophilic group isothiocyanate (NCS) generates CB₁ receptor NAM covalent ligand **76** that retains the affinity-efficacy profile of **63**, but displays reduced inverse agonist activity.¹⁴⁸ Functional assays show a signaling bias toward β -arrestin with an EC₅₀ of 2 nM, an 87-fold difference over cAMP-dependent signaling. To validate the ability of **76** to covalently label human CB₁ receptor time-course experiments were executed, which showed the binding of [³H]-CP55,940 to human CB₁ receptor increases in a time-dependent manner, reaching a maximum by 60 min preincubation time with **76**. Compounds **77-80** are another series of photoactivatable analogues developed by Lu et al. as allosteric modulators for the CB₁ receptor.¹⁴⁹ These compounds preserved the pharmacological properties of **63** negatively modulating the CB₁ receptor agonist CP55,940-induced G protein coupling in a concentration dependent manner with a complete functional inhibition

at 10 μM in their assay system. These results show that the *N*-phenylethyl-*1H*-indole-2-carboxamide scaffold is a potent representative for CB₁ receptor allosteric modulation.

Diarylurea analogues as CB₁ receptor NAMs. A second substantial body of work describes the discovery and interrogation of the diarylurea scaffold as a CB₁ receptor NAM. Numerous studies have now reported chemical leads bearing this scaffold, along with thorough SAR. 1-(4-chlorophenyl)-3-(3-(6-(pyrrolidin-1-yl)pyridine-2-yl)phenyl)urea PSNCBAM-1 (**81**, **Figure 1.13**), discovered via HTS, displays PAM-like positive cooperativity in agonist binding affinity but decreases functional response in cellular assays. As an excellent case for a thorough pharmacological workup, **81** enhanced radioligand [³H]-CP55940 binding levels, but decreased functional responses stimulated by orthosteric agonists in numerous assays, including intracellular calcium mobilization, [³⁵S]GTP- γ -S binding, cAMP accumulation and β -arrestin recruitment.^{150, 151} Interestingly, this profile is similar to *N*-phenylethyl-*1H*-indole-2-carboxamide Org27569 (**63**) with the notable exception of intrinsic efficacy as an agonist in some assays such as ERK1/2 phosphorylation; **81** has not displayed marked agonist activity in similar assays thus far.¹⁵²⁻

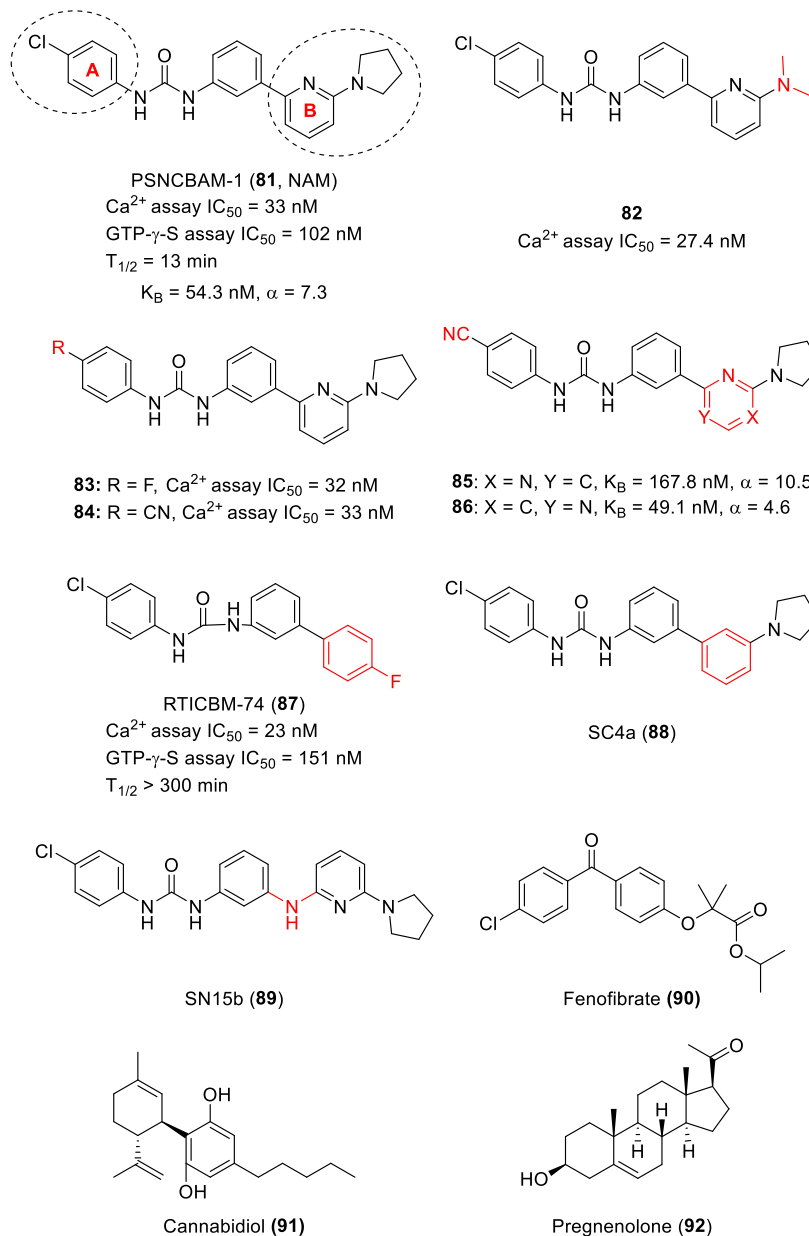
153

Detailed SAR studies on **81** have been reported, firstly focusing on various substitutions on the di-phenyl rings of the urea. Zhang et al. first reported chemical modifications to the 4-chlorophenyl at the A ring and the alkyl substitution at the 6-aminopyridinyl rings of the B ring. The smaller *N,N*-dimethylamino analog **82** displays comparable potency to **81** (27.4 nM vs 32.5 nM), suggesting the pyrrolidinyl ring is not required for this parameter. Further investigation on the A ring uncovered that the key property correspondent to activity was electron density. For example, electronic withdrawing groups at the 4-position provided good potency, with the fluoro (**83**, IC₅₀ = 32 nM) and the cyano analogues (**84**, IC₅₀ = 33 nM). Among them, the cyano analogue possesses much better potency in CB₁ receptor calcium mobilization and radioligand [³H]-CP55940 binding assays with an EC₅₀ of 55.2 nM. Subsequent replacement of the pyridine

ring by a pyrimidine ring, resulting in **85-86** (**Figure 1.13**), presents comparable activity to **81** in binding assays. Functional studies suggest that these compounds now display signaling biased PAM activity, promoting the β -arrestin-1 pathway toward ERK1/2 phosphorylation at 10 μ M without the G_i -mediated signaling activity typically displayed by the agonist CP55940.¹⁵⁴ Further replacing the pyridinyl group with lipophilic aromatic rings (**87-88**) or introducing a spacer (N-H group) between the pyridine ring and the core phenyl (**89**) maintained activity at the CB₁ receptor, and agreed with other work showing the exact properties lent by the pyridinyl and the pyrrolidinyl ring were not necessary for CB₁ receptor activity.^{155, 156} Among this series, RTICBM-74 (**87**) displayed comparable potency to **81** with an IC₅₀ of 23 nM (33 nM for **81**) in a calcium mobilization assay; however, it was not as effective in antagonizing agonist-stimulated [³⁵S]GTP- γ -S binding to mouse CB₁ receptor in mouse cerebellar membranes (**81**, IC₅₀ = 89 nM; **87**, IC₅₀ = 153 nM). A significant metabolic and PK improvement was afforded by the lipophilic phenyl substituent in **87**, as examined in rat liver microsomes showing a more than 22-fold improved half-life ($t_{1/2}$ > 300 min.) and clearance (CL = 4.6 μ L/min/mg). Possibly due to the improved metabolic and PK profile, **87** is more effective than **82** *in vivo* in attenuating the reinstatement of extinguished cocaine-seeking behavior in rats, producing an effect at 10 mg/kg equal to that of 30 mg/kg of **81**.

Finally, some noteworthy additional scaffolds have been reported as CB₁ NAMs recently. Fenofibrate (**90**), a PPAR α agonist, and cannabidiol (**91**), a non-psychoactive phytocannabinoid with therapeutic utility in numerous disorders, have both been shown to act at the CB₁ receptor as NAMs (**Figure 1.13**).^{157, 158} The steroid pregnenolone (**92**) is also reported acting as a NAM of CB₁ receptor-mediated ERK1/2 phosphorylation, devoid of effects on orthosteric agonist binding affinity or cAMP-mediated signaling.¹⁵⁹ Lastly, there have been increased investigations on peptide endocannabinoids (Pepcans) and their ability to allosterically modulate cannabinoid receptor signaling, where some have shown CB₁ receptor NAM activity.¹⁶⁰

Figure 1.13 CB₁ receptor NAMs based on the diarylurea scaffold (**81-89**) and corresponding SAR; additional CB₁ receptor NAMs (**90-92**)



CB₁ receptor NAMs based on the diarylurea scaffold (**81-89**) and corresponding SAR; additional CB₁ receptor NAMs (**90-92**).

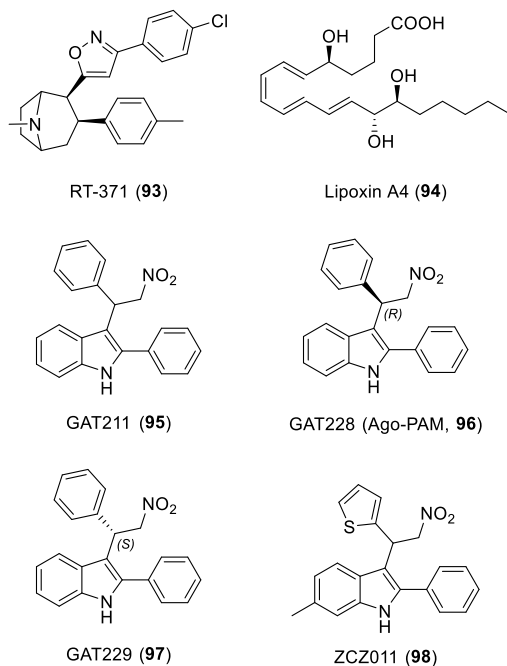
CB₁ receptor PAMs. With a greater understanding of CB₁ receptor biology and the possible therapeutic benefit of agonism, the discovery and development of CB₁ receptor PAMs is a current and evident trend. RTI-371 (**93**), a dopamine transport inhibitor with a

3-phenyltropane backbone, was first found to be a CB₁ receptor PAM via an initial functional assay screen. Compound **93** (**Figure 1.14**) at 10 mmol·L⁻¹ demonstrates potentiation of the efficacy of agonist CP55940 with an E_{max} value of 36% in a human CB₁ receptor cell-based calcium mobilization assay.¹⁶¹ Next, a study found the endogenous anti-inflammatory mediator, lipoxin A4 (**94**), demonstrated allosteric enhancement of CB₁ receptor signaling.¹⁶² Interestingly, this endogenous molecule could enhance the affinity of the assayed ligands to the CB₁ receptor with 100% enhancement of [³H]-CP55940 binding and nearly 30% of [³H]-WIN55212-2 binding, while increasing the potency of AEA in decreasing forskolin (FSK)-induced cAMP levels by 386 times at a concentration of 100 nM in HEK-CB₁ cells. When studied *in vivo* and administered via an intracerebroventricular route (1 pmol/2 μL), **94** could promote neuroprotection against β-amyloid (1-40) (400 pmol/2 μL, i.c.v.)-induced performance deficits in the Morris water maze assay in mice. A novel synthetic small molecule GAT211 (**95**), with a 2-phenyl-1*H*-indole scaffold, was first reported as a CB₁ receptor PAM in a patent filed by Northeastern University and recently Thakur et al. described the synthesis and *in vitro* and *ex vivo* pharmacology of **95** (racemic) and its resolved enantiomers, GAT228 (**96**, *R*) and GAT229 (**97**, *S*).^{160, 163} In membranes taken from CHO cells expressing human CB₁ receptor, **95** enhances the binding of the agonist [³H]-CP55,490 at 100 nM and 1 μM and maintains binding enhancement from 1 nM to 10 μM in *ex vivo* mouse brain membranes, while markedly reducing the binding of the antagonist/inverse agonist [³H]SR141716A from 1 μM to 10 μM in *ex vivo* mouse brain membranes. Compound **95** (1 μM) displays both PAM and intrinsic agonist activity in human CB₁ receptor expressing HEK293A and Neuro2a cells and in mouse brain membranes rich in native CB₁ receptor. However, **95** also exhibits strong PAM activity at a concentration of 1 μM in isolated mouse vas deferens endogenously expressing CB₁ receptor without displaying intrinsic activity. Upon further investigation, the *R*-(+)-enantiomer (**96**) is the contributing factor for the Ago-PAM property of **95**, and displays allosteric agonist activity when tested alone, whereas the *S*-

(-)-enantiomer (**97**) contributes to the PAM activity of **95**, lacking intrinsic efficacy when isolated and tested. This example highlights the importance of interrogating the activities of racemates independently of the racemic allosteric modulator hit and provides evidence that minor stereochemical differences contribute divergent activities. Also, excellently shown in this case, is that the ability to detect allosteric agonism (e.g., ago-PAMs) is dependent on the receptor expression levels in a given cell-type and sensitivity of detection may differ between *in vitro* and *ex vivo* assays. Thus, these factors should be accommodated for in programs screening racemic allosteric modulators in high-expressing cell lines that are not representative of *in vivo* receptor expression levels.

Subsequently, a report on the 2-phenyl-1*H*-indole analogue ZCZ011 (**98**) revealed *in vitro* and *in vivo* evidence of PAM activity. *In vitro*, **98** (**Figure 1.14**) increases the CB₁ receptor agonists [³H]-CP55,940 and [³H]-WIN55212 binding affinity and results in an enhanced functional output of E_{max} value 207% and 225%, respectively (normalized to each agonist functional response at E_{max} 100%). Compound **98** (10 nM) displays enhanced AEA-stimulated signaling via [³⁵S]GTPγS binding with an 40% increase over AEA alone in mouse brain membranes. When additional signaling pathways were investigated, **98** displays a concentration-dependent enhancement of AEA-stimulated β-arrestin recruitment with an E_{max} value of 195% at 1 μM and shows an increase in agonist (AEA and CP55,940) potency by ERK1/2 phosphorylation assays in human CB₁ receptor expressing cells. *In vivo*, **98** (40 mg/kg, i.p.) is brain penetrant and increases the potency of administered orthosteric agonists when examined in cannabimimetic activity behavioral assays in rodents. Therefore, due to broad PAM activity across signaling pathways and multiple agonists, **98** may be useful as a pharmacological tool for mechanistic studies as well as for exploring proof-of-concept studies and potential therapeutic applications of CB₁ receptor PAMs.¹⁶⁴

Figure 1.14 Representative CB₁ receptor PAMs (**93-94**) and 2-phenyl-*1H*-indole scaffold derivative CB₁ receptor PAMs (**95-98**)



Representative CB₁ receptor PAMs (**93-94**) and 2-phenyl-*1H*-indole scaffold derivative CB₁ receptor PAMs (**95-98**).

Straiker and colleagues recently report a physiologically relevant neuronal model of endogenous cannabinoid signaling as an assay to test CB₁ receptor allosteric modulators. In this model, CB₁ receptor ligands are applied to cultured autaptic hippocampal neurons that exhibit depolarization-induced suppression of excitation (DSE), a form of synaptic plasticity that is mediated endogenously by the CB₁ receptor and 2-arachidonoyl glycerol (2-AG).¹⁶⁵⁻¹⁶⁶ The aforementioned NAMs **63**, **81** and Pepcan12 attenuate DSE and do not directly inhibit CB₁ receptors. While NAMs **92** and hemopressin as well as the PAM **94** are without effect in this model. Compounds **95** and **98** each show PAM-like responses in autaptic hippocampal neurons, representing the first PAMs to display efficacy via the 2-AG-utilizing neuronal model system. In context of the above mentioned 2-phenyl-*1H*-indole **95**, further examination of its enantiomers **96** and **97**, shows that the (*S*) enantiomer

97 exhibits pure PAM-like behavior and the (*R*) enantiomer **96** appears to directly activate the CB₁ receptor as an allosteric agonist, which is in accordance with the previous report.¹⁶⁰

Molecular dynamics (MD) simulations of GPCR-ligand binding can provide a unique view into the subtleties of receptor activation and modulation and, importantly, illuminate ligand interactions for complexes that have proven difficult to crystalize thus far. A recent MD study by Tautermann et al. proposes a mechanism of interaction for certain ago-PAMs with two points. First, the agonism may result from the ligand binding to the orthosteric binding site, and the PAM effect is the result of the ligand interacting with an adjunct, deeper binding site in the receptor. Second, the pockets may overlap, resulting in the interaction with residues in both sites simultaneously as one unified pocket and producing the activation and/or modulation effects. Interestingly, this mechanism may explain the observation that Ago-PAM **97** displays competitive binding with CP 55,940 at high concentrations. This interaction mechanism is experimentally validated by showing that multiple binding sites of **98**, another ago-PAM, contribute to its activity; where positive modulation of the orthosteric agonist is observed until the concentration of **98** is increased above its PAM EC₅₀ value and it begins to compete with CP 55,940, owing to its additional affinity for the agonist binding site.¹³⁸

The past decade has seen the identification and characterization of multiple promising compounds as NAMs targeting the CB₁ receptor; however these purported NAMs are beset by moderate efficacy and some CB₁ receptor inverse agonist activity that may hinder their future development. Additionally, *in vivo* studies on CB₁ receptor NAMs are thus far limited and will need to progress towards proof-of-concept studies to show therapeutic utility. As for CB₁ receptor PAMs, the reported small molecules trend towards multifaceted and complicated pharmacology that is sensitive to small molecular modifications, as seen from PAMs of other targets. Additionally, the structural diversity remains relatively small and novel scaffold discovery may open opportunities for CB₁ receptor PAMs with tractable pharmacology. Thus, due to the physiological importance

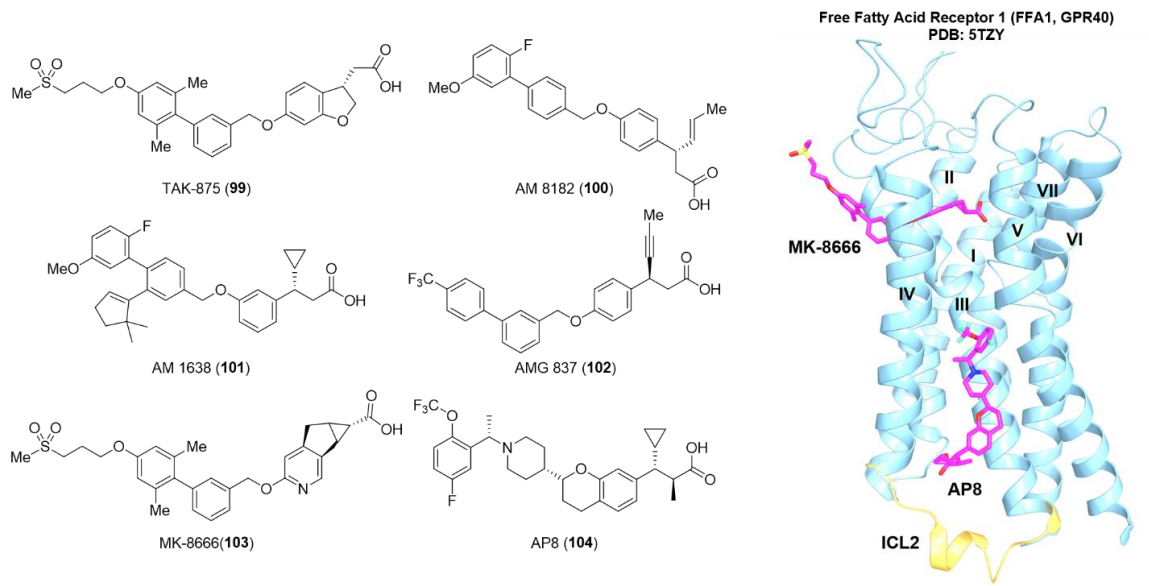
and biological abundance of the CB₁ receptor, innovative medicinal chemistry efforts are necessary to further discovery and development of chemical probes and drug-candidates with improved DMPK characteristics.

3.2.2. Free Fatty Acid Receptors (FFA1-FFA3). Free fatty acid receptors (FFARs) are a recently “deorphanized” family of receptors that are activated by nonesterified, or free, fatty acids (FFAs), which are comprised of a carboxylic acid linked to an aliphatic chain of varying length. The receptors are classified based on the chain length of the endogenous agonist, which are termed short chain fatty acids (SCFAs), medium chain fatty acids (MCFAs) or long chain fatty acids (LCFAs). For example, the FFA1 receptor (also GPR40) and FFA4 receptor (also GPR120) are activated by MCFAs and LCFAs, while the FFA2 (also GPR43) and FFA3 (also GPR41) receptors are activated by SCFAs. The change in name designation, e.g. GPR40 to FFA1, aligns with the discovery of endogenous signaling ligands and deorphanization. As key sensors for dietary and other signaling FFAs, this family of receptors has attracted elevated interest for their role in regulating metabolic and inflammatory processes and has recently been implicated as targets in metabolic disorders and type 2 diabetes. Milligan et al. recently published an extensive review of this receptor family, including FFAR biological importance and druggability.¹⁶⁷

FFA1 Receptor (GPR40). The FFA1 receptor, which has been previously designated GPR40, is predominately expressed in pancreatic β cells and intestinal enteroendocrine cells and has been validated as a potential target for the treatment of type 2 diabetes.¹⁶⁸ Allosteric modulator discovery for this target has produced a rich collection of pharmacologically diverse ligands and elegant structural work has identified multiple allosteric binding sites.^{169, 170} In recent years, numerous full and partial allosteric agonists of FFA1 have been discovered and are described as binding to a select number of distinct allosteric sites, such as TAK 875 (**99**), AM 8182 (**100**), AM 1638 (**101**), AMG 837(**102**), MK8666 (**103**) and AP8 (**104**).¹³² Additionally, recent work in FFAR structural biology and biochemistry describes and validates this multiple-site postulation.^{18, 29-20}

The FFA1 partial agonist TAK-875 (**99**) was discovered as an ago-PAM, binding to a distinct allosteric site and characterized as enhancing the activity of endogenous FFAs.¹⁷¹ Importantly, **99** (**Figure 1.15**) was progressed into Phase III clinical trials for the treatment of type 2 diabetes mellitus but the trial underwent early termination due to toxicity. The co-crystal complex of **99** with FFA1 reveals that the binding site for **99** is formed by helices III-V and the ECL2, and is adjacent to the exterior lipid membrane surface (PDB code 4PHU).²⁹ The allosteric partial agonist MK-8666 (**103**) has recently been approved to advance into a Phase I clinical trial for the treatment of type 2 diabetes mellitus. Interestingly, the co-crystal complex of **103** bound to FFA1 demonstrates a binding site adjacent to the lipid membrane, similar to **99** (PDB code 5TZR).²⁰ Identification of membrane-adjacent binding sites for allosteric modulators is thus far uncommon; however due to the allosteric nature of GPCR interactions with membrane lipids and cholesterol, this site of action may be more common than currently appreciated or may be yet unexploited at additional receptors. A novel ago-PAM, AP8 (**104**), was subsequently discovered and displays a far higher potency for potentiating endogenous FFAs than **99** or **103**.¹⁶⁹ The ternary complex structure of FFA1-**103**-**104** reveals that **104** binds to a lipid-facing pocket formed by helices II-V and ICL2, which is outside the intracellular halves of the TM helical bundle, and this site is completely distinct from the allosteric binding site of **103** (PDB code 5TZY).²⁰ Further validation of the allosteric mechanism and signaling bias of allosteric modulators for FFA1 are still progressing.¹⁷⁰

Figure 1.15 Representative FFA1 receptor PAMs (**99-104**) and co-crystal complex of FFA1-MK-8666-AP8

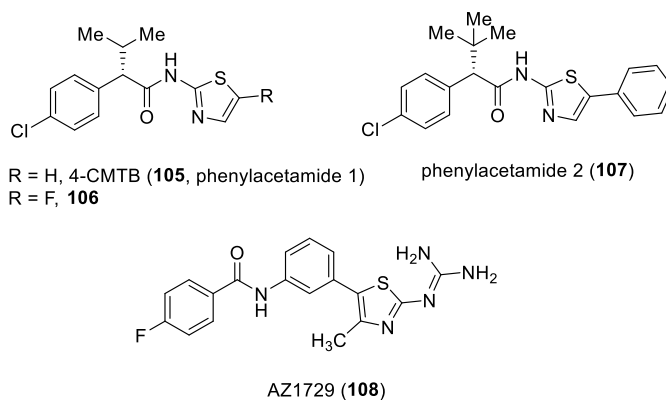


Left: representative FFA1 receptor PAMs (**99-104**); Right: co-crystal complex of FFA1-MK-8666-AP8 showing distinct allosteric sites for both PAMs (PDB: 5TZY).

FFA2 Receptor. FFA2 and FFA3 receptors are predominately expressed in the gut enteroendocrine cells, pancreatic β cells and adipose tissue and have been found expressed in various cancer cells, including breast, colon and liver.¹⁷⁰ The phenylacetamide scaffold series of FFA2 receptor allosteric modulators remain the most studied and characterized allosteric ligands for this target. 4-CMTB (4-chloro- α -(1-methylethyl)-*N*-2-thiazolylbenzeneacetamide, **105**) and its analogue **106** (**Figure 1.16**) were identified via high-throughput screening and represent the first series of synthetic small molecules that display allosteric agonism and PAM-like effects at the FFA2 receptor.^{172, 173} Initial characterization shows that **105** can stimulate signaling via both $G\alpha_{i/o}$ and $G\alpha_{q/11}$ promoted pathways. However, subsequent chemical modifications based on SAR around 4-CMTB results in limited improvements, and poor PK properties in male Sprague-Dawley rats have limited its further development as a preclinical candidate.¹⁷⁴⁻¹⁷⁵ As an alternative,

phenylacetamide **107** was used for *in vivo* proof-of-concept studies to demonstrate an FFA2-mediated reduction in plasma non-esterified fatty acids in wild-type mice.¹⁷⁵ Recently, AZ1729 (**108**) was discovered by introducing a phenyl linkage between the amide and thiazole, and **108** displays an interesting G_i-biased profile as a FFA2 receptor allosteric agonist and can potentiate agonist signaling as a PAM.¹⁷⁶

Figure 1.16 Representative FFA2 receptor PAMs (**105-108**)

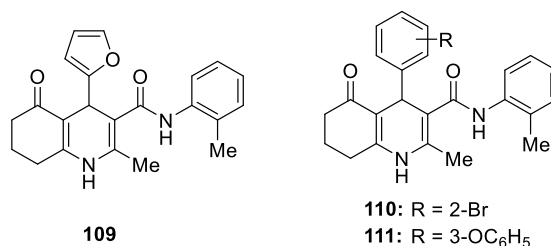


Representative FFA2 receptor PAMs (**105-108**).

FFA3 Receptor. Hexahydroquinolone-3-carboxamides and derivatives thereof are the predominantly reported allosteric FFA3 receptor ligands and derive from a patent by Arena Pharmaceuticals.¹⁷⁷ Compound **109** (**Figure 1.17**) displays intrinsic efficacy as well as orthosteric agonist potentiation as an ago-PAM of the human FFA3 receptor with modest potency and is without activity at the FFA2 receptor.¹⁷⁸ Interestingly, modification of the hexahydroquinolone results in molecular switches that significantly alter the activity profile. For example, when replaced by a 2-bromophenyl group, the modification yields **110** demonstrating a pure PAM profile for the FFA3 receptor without intrinsic agonism, while modification of the phenyl to 3-phenoxy yields **111** demonstrating a FFA3 receptor PAM profile with intrinsic antagonist activity.¹⁷⁸ At present, although FFARs are considered to be an important target for drug discovery and two allosteric ligands have progressed into clinical trials, the overall body of literature remains relatively small,

especially for FFA2-FFA4 receptors. Pharmacological tool compounds characterized by high selectivity for a single FFAR and high potency are needed for further evaluation and validation of mechanisms, binding sites and *in vivo* tolerability. Thus, there remains high value in medicinal chemistry around these receptors and the evaluation of unique allosteric binding sites may provide insight for targeting FFAR family members as well as other GPCRs.

Figure 1.17 Representative FFA3 receptor PAMs (**109-111**)



Representative FFA3 receptor PAMs (**109-111**).

3.3. Nucleotide Family Receptors

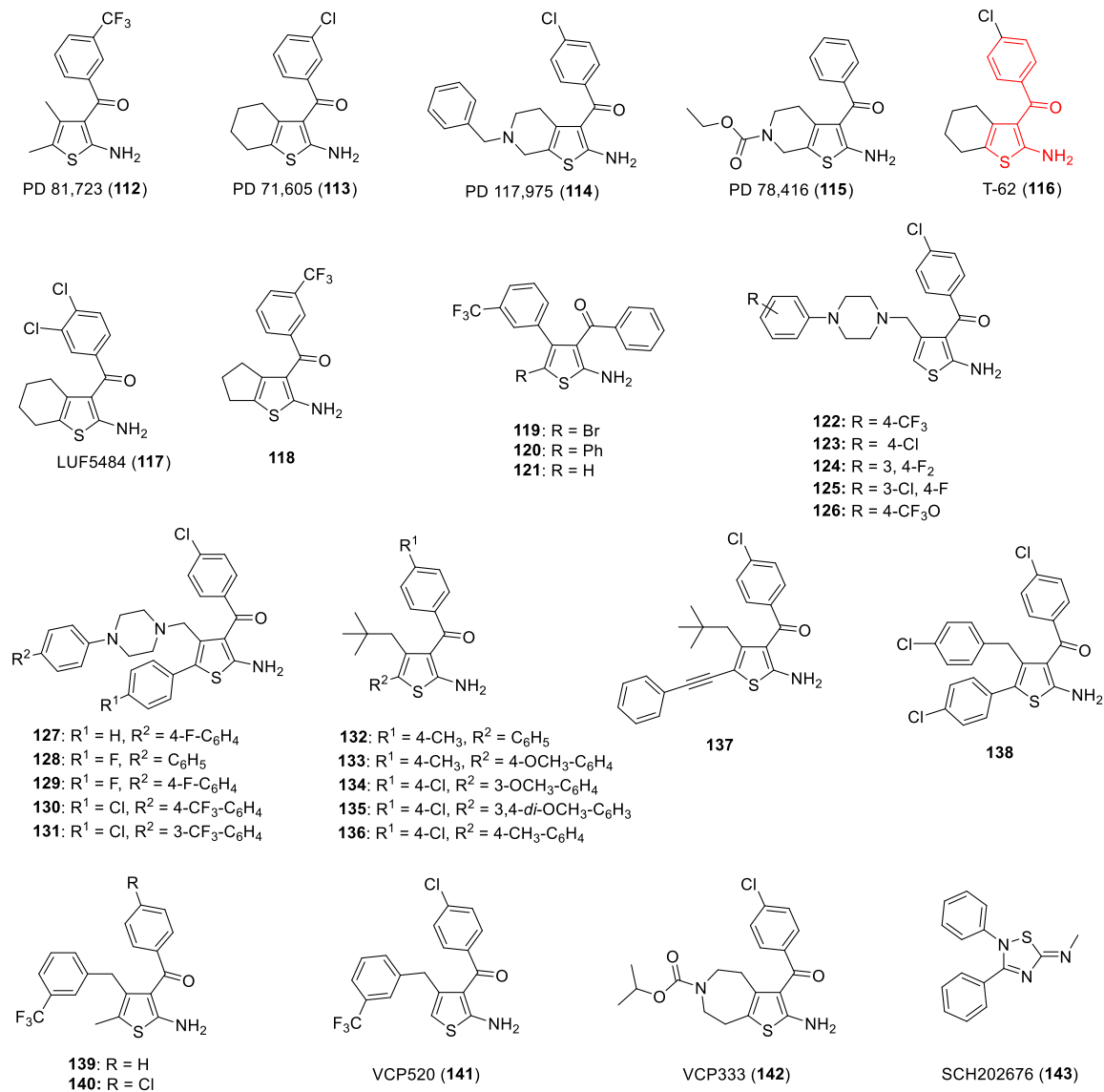
3.3.1. Adenosine Receptors (A_1R - A_3R). Adenosine receptors (ARs), classified as A_1R , $A_{2A}R$, $A_{2B}R$ and A_3R , have been involved in the treatment of diseases that span cardiovascular disease, CNS disorders, inflammatory and allergic disorders and cancer.¹⁷⁹ Historically, both agonists and antagonists have been used to indiscriminately modulate ARs, the most well-known being the endogenous agonist adenosine and the common antagonist caffeine. Recent work has begun to identify subtype selective orthosteric ligands; however allosteric modulation may provide multiple benefits for therapeutically targeting ARs.¹⁸⁰ Allosteric modulators of ARs are increasingly pursued to avoid side effects caused by agonists acting through indiscriminate AR activation, and the propensity for orthosteric agonists to cause receptor desensitization upon prolonged exposure. ARs interact with multiple and divergent second messenger systems, as the A_1R and A_3R reduce

the production of cAMP by coupling to $G\alpha_i$ protein resulting in adenylate cyclase inhibition, while the A_{2A} and A_{2B} subtypes stimulate the production of cAMP via coupling to $G\alpha_s$ or $G\alpha_{olf}$ protein.

A₁R. Evaluation of A₁R allosteric modulators is predominately performed in two *in vitro* functional assays; the first evaluates the inhibitory activity of forskolin-stimulated cAMP accumulation in CHO cells stably expressing the human A₁R, while the second measures phosphorylation of ERK1/2 in the same cell type. Additionally, groups have reported results on A₁R binding parameters (affinity K_D and density B_{max}) and radioligand binding assays that provide association and dissociation kinetics to assess the allosteric modulation of the orthosteric agonist-receptor-G-protein ternary complex. Finally, some observations of antagonist competition binding assays are reported.

Pioneering work by Bruns et al. in 1990 developed a novel series of PAMs (designated allosteric enhancers) known as the “PD” series [PD 81,723 (**112**), PD 71,605 (**113**), PD 117,975 (**114**)] and were characterized by a 2-amino-3-benzoyl thiophene (2A3BT) scaffold, selectively enhancing the binding of *N*⁶-cyclopentyladenosine (CPA) to the A₁R (**Figure 1.18**).¹⁸¹⁻¹⁸³ Analogues of PD 71,605 (**113**) led to the discovery of T-62 (**116**) and LUF 5484 (**117**) with markedly improved potency over **112**.^{181, 184} Among them, **116** (2-amino-4,5,6,7-tetrahydrobenzo[*b*]thiophen-3-yl-(4-chlorophenyl)methanone) was developed by King Pharmaceuticals and advanced into clinical trials for the potential treatment of neuropathic pain associated with hyperalgesia and allodynia.¹⁸³ However, the program was terminated after failure to meet the endpoint for efficacy in Phase IIB.¹⁸⁵⁻¹⁸⁶ The 2-aminothiophene series of PAMs has been recognized as a representative core scaffold for the A₁R, but subsequent observations of intrinsic antagonist activity at high concentrations and moderate efficacy at lower concentrations necessitated further chemical modifications and optimization.¹⁸⁷

Figure 1.18 A₁R PAM derivatives designed around the 2-amino-3-benzoyl thiophene scaffold (**112-143**)



A₁R PAM derivatives designed around the 2-amino-3-benzoyl thiophene scaffold (**112-143**).

The early SAR studies around the 2-amino-3-benzoyl thiophene core generated a preliminary principle that the 2-amino group, 3-benzoyl and the corresponding hydrophobic *para*- and *meta*-substituents on the phenyl in the C3-position are critical to the PAM activity of these analogues.¹⁸⁸ Large hydrophobic groups at the 4-position of the thiophene ring and small substituents (H and CH₃) at the 5-position could improve the

PAM activity, while bulky substituents at the C5-position resulted in allosteric enhancer activity with an apparent intrinsic antagonist profile.¹⁸⁹ The proper combination of these modifications remains a challenging task and requires achieving a high PAM potency with as minimal as possible antagonist activity. Based on this SAR, two functionally divergent binding pockets within the larger allosteric site are proposed, with one interacting with the 2A3BT core and a second possible lipophilic domain to accommodate the C4-/C5-substituents on the thiophene ring.¹⁹⁰⁻¹⁹¹

Subsequently, detailed SAR studies on the 4- and 5-substitution of 2-amino-3-benzoyl thiophene was pursued. Modifying the C4-/C5-substituents with a fused cycloalkyl ring increased lipophilicity and led to **118**, which displays allosteric enhancer and partial agonist characteristics with > 50% intrinsic activity and 98% of the maximum agonist *R*-PIA response at 10 μ M on A₁R-mediated stimulation of ERK1/2 phosphorylation in vitro. However, increasing the ring size from a cyclopentyl moiety gradually to a cycloheptyl substituent in efforts to improve allosteric enhancement results in the loss of activity. Opening the C4/C5 ring furnishes a series of compounds with improved PAM potency. Among the different substitutions on C4/C5, **119** with a bromide in C5 displays higher potency than compound **112** in the kinetic binding assay (2-fold greater affinity than **112** and 3-fold less inhibition of antagonist [³H]-CPX binding).¹⁹² Compound **120** contains a 5-phenyl substituent that increases potency (EC₅₀) 6-fold over **112**, but when no substituent is present in the 5-position (**121**), allosteric enhancement efficacy is improved (77% vs 28%) along with greater antagonist activity compared to **112**.¹⁹³ Additional modifications and SAR provided support for these results and it was concluded that alkyl and aryl groups at the C4-position are favored for allosteric enhancer activity.¹⁹⁴

Romeo and colleagues further modify the C4-substitution to compound **122** (**Figure 1.18**), characterized by aryl piperazine moieties linked to a methylene at the 4-position of the thiophene ring, and evaluate **122** with a cAMP functional assay in human

A₁R expressing CHO cells. A maximal 87% attenuation of cAMP production is observed at 10 μM without antagonist activity, observed by negligible binding inhibition activity to displace the binding of selective agonists to A₁R, A_{2A}R, and A₃R. Saturation binding experiments show **122** produces a A₁R density (B_{max}) shift of [³H]-CCPA binding 7.7-fold to A₁R in CHO cells and enhances the apparent affinity of CCPA approximately 6.3-fold in the A₁R CHO cell membranes by titrating the radioligand [³H]-DPCPX at 10 μM concentration. The number and position of electron-withdrawing or electron-releasing groups on the phenyl attached to the piperazine moiety was determined as highly influential for the overall allosteric enhancement activity. Among them, **123-126** (**Figure 1.18**) possess 4-chloro, 3,4-difluoro, 3-chloro-4-fluoro and 4-trifluoromethoxy derivatives and each has been reported to maintain improved potency in the binding (saturation and competition) and functional cAMP studies.^{189, 195} Subsequently, an aryl substitution at the 5-position was discovered to have a fundamental effect by contributing additively to the allosteric enhancer activity. Compounds **127-131** with a 5-aryl substituent have substantially higher activity than **112** without significantly inhibiting antagonist binding at the A₁R, A₂R or A₃R. Saturation and competition experiments have also shown that this series of 5-aryl-substituted thiophene derivatives were more active than the corresponding 5-unsubstituted analogues with a highest 13.3-fold decreased CCPA K_i value at 10 μM in competition binding experiments (compound **128**).¹⁹⁶ Encouraging results are also reported on **132-136**, which possess a neopentyl and an aryl moiety at the 4- and 5-positions. Moderate to good enhancing activity of cAMP attenuation is observed (up to 64% inhibition at 10 μM) without significant inhibition of antagonist binding across AR subtypes.¹⁹⁷

Further modification around this series obtained compound **137**, characterized by a common 2-amino-3-(pchlorobenzoyl) thiophene core with neopentyl substituent at the C-4 position and benzyl acetylene at the C-5 position of the thiophene ring. Attenuation of cAMP production by **137** shows a 75% inhibition in the presence of 1 pM of orthosteric

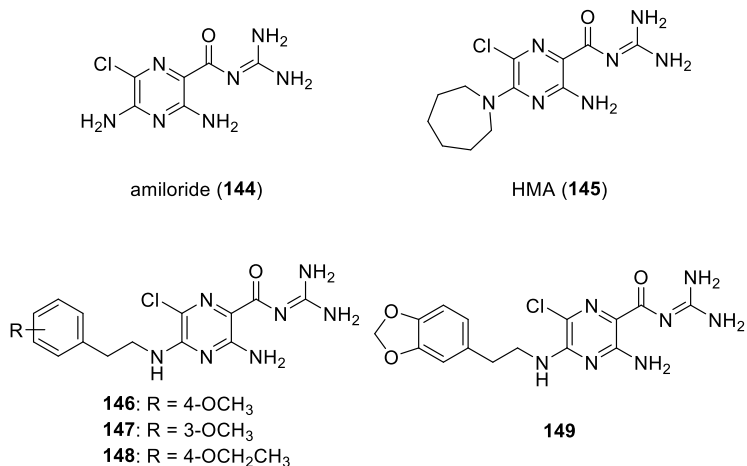
agonist CCPA, which is almost 4-fold greater than the former allosteric enhancer **112** (19%).¹⁸⁸ Interestingly, no change was observed in the affinity (K_D) of CCPA by **137**; however a significant increase was observed for the apparent affinity (K_i) with a 10-fold shift and no evidence of antagonism at AR subtypes. Compound **137** also displayed a slowing of the dissociation rate of the radioagonist [³H]-NECA by 2.1-fold with a corresponding 1.9-fold increase of apparent affinity. Compound **138** with *p*-chlorobenzyl at the C4-position of thiophene and *p*-chlorophenyl substituent at the C5-position showed a 4-fold increase in cAMP production attenuation compared to **112** in a functional assay (84% vs 21%) and delayed the dissociation rate constant of agonist [³H]-NECA by 2.5-fold.¹⁹⁸ No significant binding inhibition was noted for **138** for antagonists of the A₁R, A₂R and A₃R subtypes in competition binding assays. Additionally, significant anti-nociceptive effects were observed in mice at doses of 0.3 and 3 mg/kg of **138**, compared to vehicle-treated mice.

Scammells et al. reported studies interrogating the stimulus bias (i.e., biased signaling, functional selectivity) of their AR molecules, which may provide a strategy to achieve selectivity of signaling at GPCRs associated with ligand directed signaling outcomes manifested as changes in rank orders of potency and or maximal effects relative to a reference (e.g., the endogenous) agonist.¹⁹¹ This highlights how a GPCR bound with both an allosteric modulator and an orthosteric agonist should be viewed as a unique protein state that differs from those promoted by either orthosteric or allosteric agonist alone. Two novel 2A3BT derivatives **139** and **140**, differing by the absence or presence of a halogen atom in the 4-position of the benzoylthiophene ring, induce functionally biased states of the A₁R. In comparison to the orthosteric agonist response from *R*-PIA, **139** alone is biased as an allosteric agonist toward cAMP accumulation over ERK1/2 phosphorylation with a 45-fold bias factor. Compound **139** also allosterically shifted the biased signaling of the agonist *R*-PIA (strongly biased toward the pERK1/2 pathway) towards activation of the two pathways in a nonbiased manner. Conversely, **140** shows minimal bias as an allosteric

agonist (with bias factor 3.5) but demonstrates a pathway-biased allosteric modulation when combined with *R*-PIA. Additionally, they also found that the well-characterized 2A3BT, T62, as well as VCP520 (**141**) and VCP333 (**142**), exhibited stimulus bias toward cAMP inhibition compared to pERK1/2. Finally, SCH-202676 (*N*-(2,3-diphenyl-1,2,4-thiadiazol-5-(2*H*)-ylidene)methanamine, **143**) has also been reported as an allosteric modulator of ARs. **143** could not only selectively slow the agonist dissociation at A₁R but also accelerate agonist dissociation at A₃R and antagonist dissociation at adenosine A_{2A}R at a concentration of 10 μM.¹⁹⁹

A_{2A}R. Amiloride (**144**) and analogue HMA (2,5-(*N,N*-hexamethylene)-amiloride, **145**) are reported to bind to the sodium ion site of adenosine receptors.²⁰⁰⁻²⁰¹ Compounds **146-149** are derivatives of **144** and **145** (**Figure 1.19**) via employing varied 5'-substitutions on amiloride, showing consistent potency as A_{2A}R allosteric antagonists by displacing orthosteric radioligand [³H]-ZM-241,385 from the wild-type human A_{2A}R (59-73%) and displaying even greater potency in the W246A sodium ion site mutant human A_{2A}R (94.6%-100%).²⁰² Docking studies show that these analogues conform to similar binding poses to that of amiloride and HMA observed in previous docking studies, with hydrogen bonding and salt bridge interactions with Asp52^{2.50} and Thr88^{3.36} and occupation of the Trp246^{6.48} position.²⁰³ Noteworthy, the interactions with the Trp246^{6.48} are predicted to be π-π stacking between Trp246^{6.48} and the phenyl group of most analogues, which is not present in **145**. The phenethyl moieties and the substituents attached on the phenyl groups are predicted to reach into a part of the orthosteric binding site surrounded by hydrophobic residues of Phe168^{EL2}, Met177^{5.38}, Leu249^{6.51}, Asn253^{6.55} and Ile274^{7.39}, suggesting that **146-149** can intrude the orthosteric site from the allosteric site and displace orthosteric ligand ZM-241,385 in a direct, competitive manner.

Figure 1.19 Representative A_{2A}R PAMs with centric pyrazine core (**144-149**)

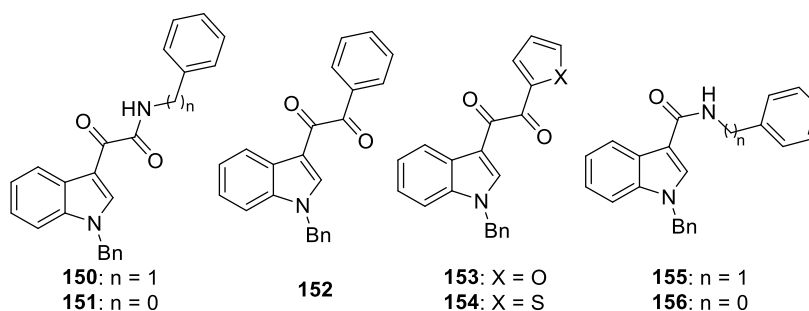


Representative A_{2A}R PAMs with centric pyrazine core (**144-149**).

A_{2B}R. The A_{2B}R is the least characterized subtype in the AR family. Among ARs, the A_{2B}R subtype exhibits low affinity for the endogenous agonist adenosine compared to the A₁R, A_{2A}R and A₃R subtypes and is therefore suggested to be activated when local concentrations of adenosine increase to a large extent following tissue damage. Compounds **150-156**, with small differences in the side chain of the 1-benzyl-3-ketoindole scaffold, are the only reported allosteric modulators for the A_{2B}R (**Figure 1.20**) and have been characterized through binding and functional assays, including cAMP functional assays, dissociation kinetic assays, equilibrium binding assays and [³⁵S]GTPγS binding assays in CHO cells expressing human A₁R, A_{2A}R, A_{2B}R and A₃Rs.²⁰⁴⁻²⁰⁵ The PAMs **150-152** potentiate agonist efficacy but not agonist potency (similar submicromolar potencies at A_{2B}R) with PAM EC₅₀ values between 250 nM and 446 nM. PAM **151** demonstrates a significant reduction in the radioligand [³H]NECA dissociation constant from 0.0162 min⁻¹ to 0.0086 min⁻¹, and increases the efficacy of agonist BAY 60-6583 to stimulate guanine nucleotide exchange with E_{max} values from 155.2% to 175.0% at 1 μM in [³⁵S]GTPγS binding assays. Slight alterations to the side chain are discovered as chemical switches and yield NAMs **153-156** that reduce agonist potency and efficacy. Compound **156**

significantly increases the dissociation rate of [^3H]NECA from $\text{A}_{2\text{B}}\text{R}$ with K_{off} value 0.0481 and results in a pronounced attenuation of the orthosteric ligand BAY 60-6583 mediated stimulation of guanine nucleotide exchange. More work will certainly be done to elucidate the therapeutic potential of the $\text{A}_{2\text{B}}\text{R}$, especially in inflammation and injury, and there remains great potential for further interrogating allosteric modulators of the $\text{A}_{2\text{B}}\text{R}$ through medicinal chemistry. However, these current allosteric modulators comprise both PAMs and NAMs and may provide useful chemical probes to explore the biology and therapeutic potential of $\text{A}_{2\text{B}}\text{R}$ allosteric modulators.

Figure 1.20 $\text{A}_{2\text{B}}\text{R}$ PAM derivatives on the 1-benzyl-3-ketoindole scaffold side chain (150-156)

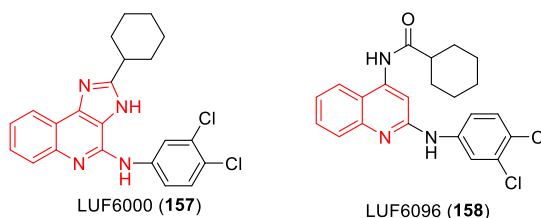


$\text{A}_{2\text{B}}\text{R}$ PAM derivatives on the 1-benzyl-3-ketoindole scaffold side chain (150-156).

A_3R . The A_3R is widely expressed and displays tissue specific regulation regarding cellular energy consumption and energy deficits. Agonists and antagonists have recently been studied and antagonists have been prime candidates for rheumatoid arthritis, glaucoma, psoriasis and hepatocellular carcinoma, as the A_3R is found to be overexpressed in cancer cells.²⁰⁶ Allosteric modulators of the A_3R are a recent development and may provide a unique therapeutic approach towards these disorders and others. Relative to the other members of the AR family, modest numbers of selective allosteric compounds have been reported for the A_3R . The core scaffolds of A_3R allosteric modulators are predominately comprised of *1H*-imidazo[4,5-*c*]quinolin-4-amine and 2,4-disubstituted

quinoline analogues. Reported characterizations of A₃R allosteric ligands are mainly based on the results of radioligand displacement, kinetic dissociation experiments as well as functional (cAMP-based) assays. **LUF6000 (157)** with a *1H*-imidazo[4,5-*c*]quinolin-4-amine scaffold was discovered (**Figure 1.21**) and prioritized for optimization due to significant potentiation of agonist efficacy compared to the former discovered A₃R PAMs. However, like A_{2B}R PAMs, it shows no enhancing effect at 10 μM on agonist potency for human A₃R expressed in CHO cells, observed via cAMP functional readouts.²⁰⁷⁻²⁰⁸ Ring opening around **157** to LUF6096 (**158**), also bearing a 2,4-disubstituted quinoline core, is another example of A₃R PAMs and equally potentiates orthosteric agonist efficacy. Interestingly, **158** also displays allosteric effects on the agonist potency and could produce a shift in the EC₅₀ value of the agonist Cl-IBMECA from 31 nM alone to 9 nM with PAM.²⁰⁹

Figure 1.21 Representative A₃R PAMs displaying a ring opening on the *1H*-imidazo[4,5-*c*]quinolin-4-amine scaffold (**157-158**)



Representative A₃R PAMs displaying a ring opening on the *1H*-imidazo[4,5-*c*]quinolin-4-amine scaffold (**157-158**).

3.3.2. P₂Y Receptors (P₂Y₁ and P₂Y₂ Receptors). Purine and pyrimidine receptors exist in two families: P₁ receptors (adenosine receptors) activated by adenosine, discussed above, and P₂ receptors activated by adenosine 5'-tri- or diphosphate (ATP or ADP) and/or uridine 5'-tri- or diphosphate (UTP or UDP). P₂ receptors are further divided as P₂X and P₂Y receptors, which are ligand gated ion channels and GPCRs, respectively.²¹⁰ The human purinergic GPCRs (P₂Y) are divided into two subfamilies based on their coupling

to specific G-proteins, $G\alpha_{q/11}$ coupled P2Y₁-like receptors and $G\alpha_{i/o}$ coupled P2Y₁₂-like receptors. They are activated by ADP to trigger glutamate release, facilitating thrombus formation and are essential for platelet aggregation and thus considered promising new drug targets.²¹¹

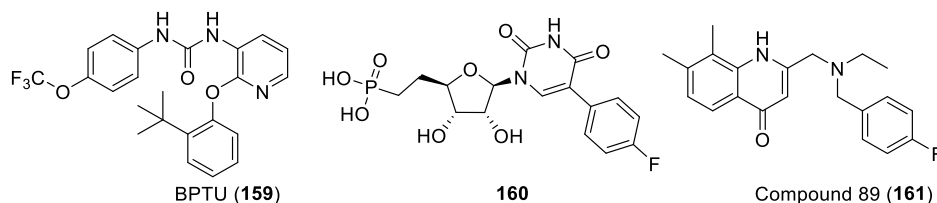
P2Y₁ Receptor. The P2Y₁ receptor is a promising therapeutic target due to its critical role in ADP-induced platelet aggregation and the potential for an improved safety profile over P2Y₁₂ receptor inhibitors regarding bleeding liability.²¹¹ Early efforts in this arena essentially focused on nucleotide derivative orthosteric antagonists. However, the discovery of BPTU (**159**) by Bristol-Myers Squibb (**Figure 1.22**), a hydrophobic diarylurea derivative, as a non-nucleotide allosteric antagonist of the P2Y₁ receptor has provided the foundation for allosteric modulators to be considered as potential therapeutic agents of this receptor.²¹² Thus, there have been recent innovative approaches to design non-nucleotide, diarylurea scaffold allosteric antagonists as antithrombotic agents with improved safety profiles.^{213, 214} As a relatively new target and mode of antagonism, the most extensive characterizations have been performed on **159**, which demonstrates a 68 ± 7% thrombus weight reduction in a rat arterial thrombosis model (10 mg/kg **159**, 10 mg/kg/h rate) with minor effects on overall bleeding in provoked rat bleeding time models. Important structural and pharmacological studies by Jacobson and colleagues have recently begun to illuminate the complex allosteric mechanisms of **159** and its effect on both multiple downstream signaling pathways as well as multiple agonists.^{30, 215} In the recent co-crystal complex, **159** is the first antagonist shown to bind to an allosteric site entirely outside of the helical bundle, not only outside of the orthosteric site. The allosteric binding site of **159** is situated on the outside of the TM domain bundle adjacent to the lipid membrane and engages **159** by mostly hydrophobic and aromatic residues located in the TM helices I-III as well as minor involvement of ECL1. The two nitrogen atoms of the urea group in **159** promote two bidentate hydrogen bonds with the backbone carbonyl of Leu102^{2,55}, which result in the only polar interactions present. The pyridyl group, the

benzene ring of the phenoxy group tethered to pyridine and the *tert*-butyl substituent on the phenoxy group are responsible for forming the main hydrophobic interactions with the P2Y₁ receptor.²¹¹ Insights from the co-crystal complex indicate that this interaction may reasonably stabilize the extracellular helical bundles and restrain the receptor in an inactive state. Thorough pharmacological studies of **159** P2Y₁ receptor allosteric antagonism provide a more nuanced view of its mode of action, including a description of probe dependence and signaling bias.²¹⁵ When provoked by structurally diverse agonists, **159** displayed varying degrees of antagonism across multiple signaling pathways. For example, allosteric antagonism of the agonists 2MeSADP and MRS2365 resulted in decreased potency for ERK1/2 stimulation with no effect on maximal response (E_{\max}); however, in [³⁵S]GTP γ S binding assays and β -arrestin2 recruitment, **159** was able to significantly suppress the respective E_{\max} . Antagonism of the agonist Ap4A resulted in insurmountable suppression of the maximal response across all assays tested. These studies highlight the high level of complexity for allosteric GPCR modulation, but also call to attention the high degree of specificity that can be achieved if probe dependence and signaling bias are therapeutically desired outcomes based upon biological understanding. The FDA approval of ticagrelor (AZD6140), a P2Y₁₂ receptor allosteric antagonist discovered by AstraZeneca, has paved the way for antithrombotic drugs in this class with safer bleeding profiles to emerge as therapeutics.²¹⁶

P2Y₂ Receptor. The P2Y₂ receptor couples primarily to $G\alpha_{q/11}$ to activate PLC- β and has been implicated in diverse physiological processes, including platelet aggregation, immunity, lipid metabolism, gastrointestinal functions and bone homeostasis.²¹⁷ Allosteric agonists for the P2Y₂ receptor have been recently reported.^{210, 218} Of these, **160** is characterized as a partial allosteric agonist and was discovered by the modification of 5'-methylene phosphonate, a derivative of UTP (uridine 5'-triphosphate).²¹⁰ Additionally, compound 89 (**161**), with a novel 4(*IH*)-quinolinone scaffold, is among the first non-nucleotide P2Y₂ receptor allosteric agonists and is selective over closely related subtypes.

Initial characterizations displayed activity in calcium mobilization assays in the 1321N1 human astrocytoma cell line, induction of nuclear receptor 4A (NR4A) in a gene reporter assay and the attenuation of isoproterenol-induced cardiac hypertrophy in neonatal rat cardiomyocytes (NRCMs).²¹⁸ These studies relay **161** (**Figure 1.22**) as a validated chemical tool compound for utilization in further proof-of-concept studies to investigate the therapeutic potential of P2Y₂ receptor allosteric agonists for the treatment of cardiovascular disorders. Interestingly, the P2Y₂ receptor serves as an attractive drug target for Dry Eye Disease (DED) and nucleotide-derived agonists have been approved for the treatment of DED in Japan and Korea.²¹⁹ Further development of **161** and other allosteric agonists may prove advantageous for DED, cardiovascular indications and others.

Figure 1.22 P2Y₁ receptor allosteric antagonist BPTU (**159**) and P2Y₂ receptor allosteric agonists (**160-161**)



P2Y₁ receptor allosteric antagonist BPTU (**159**) and P2Y₂ receptor allosteric agonists (**160-161**).

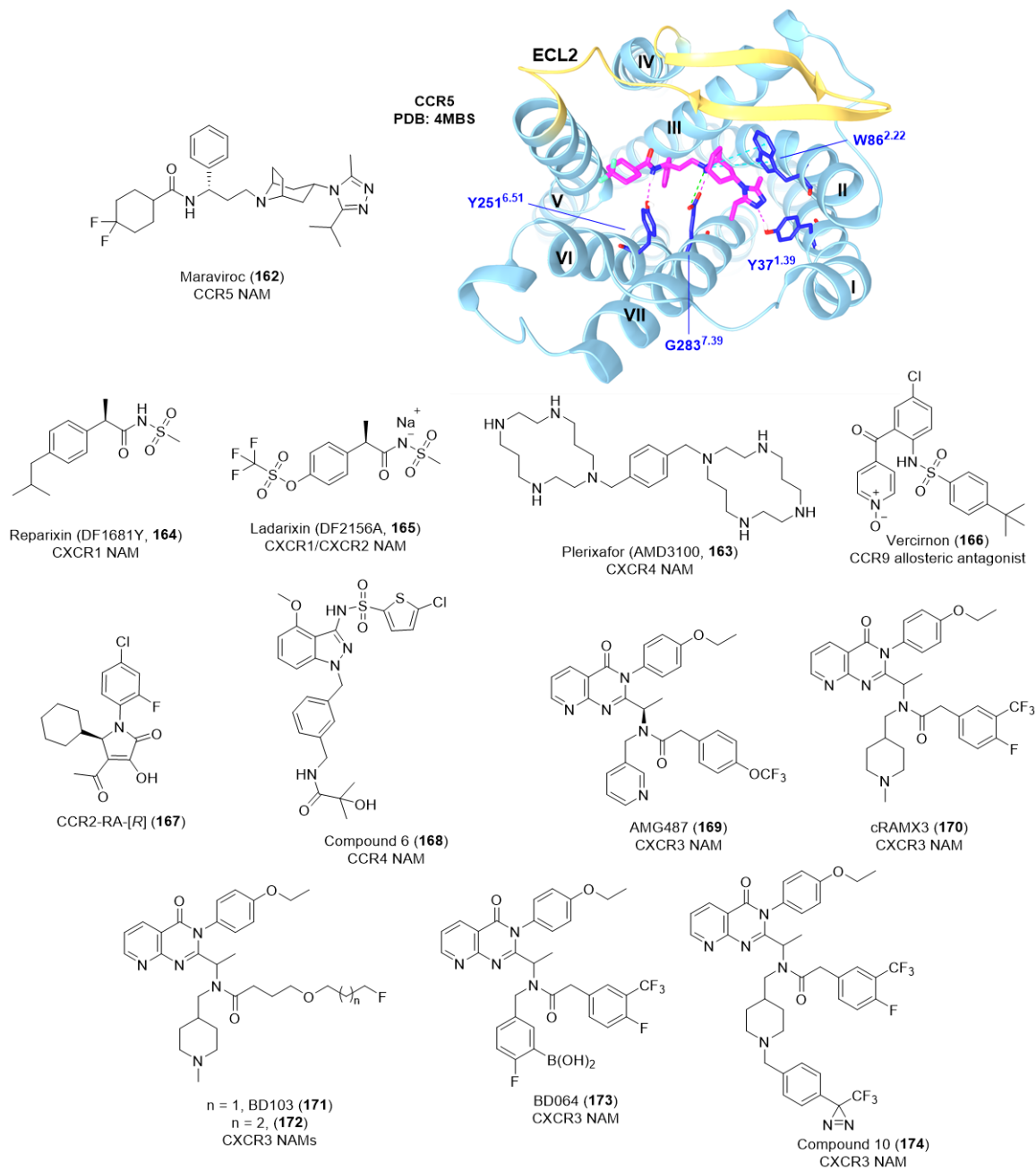
3.4. Peptide and Protein Family Receptors

3.4.1. Chemokine Receptors (CCR5, CCR9, CXCR1, CXCR2, CXCR4).

Chemokine GPCRs contain four families as CCR, CXCR, CX3CR, and XCR based on the relative positioning of conserved cysteine residues in the *N*-terminal domain of their mature ligands. At present, there are roughly 50 chemokines and at least 18 chemokine GPCRs have been identified in humans.²²⁰⁻²²¹ The development of allosteric modulators for chemokine receptors (**Figure 1.23**) represents a profound advance for allosteric modulators of class A GPCRs with marketed drugs (maraviroc, NAM of CCR5; plerixafor, NAM of

CXCR4), clinical candidates (reparixin, NAM of CXCR1; ladarixin, NAM of CXCR1/CXCR2; vercirnon, allosteric antagonist of CCR9) and structural studies of allosteric modulators binding to the receptors in high resolution (for CCR2, CCR5 and CCR9).^{221, 18} Besides synthetic drugs, chemokine receptor allosteric sites have been shown to also bind endogenous mineral cations such as sodium, calcium, zinc and magnesium. These studies included CCR1, CCR4, CCR5 and CCR8, and additional work has shown the metal ion Zn(II) or Cu(II) complex to be an allosteric enhancer of CCL3.²²² Herein, we describe representative allosteric modulators for seven chemokine receptors and the structural and chemical knowledge relating to their discovery.

Figure 1.23 Chemical structure of maraviroc (**162**) with the CCR5-maraviroc co-crystal structure and other allosteric modulators of chemokine receptors



Top: Chemical structure of maraviroc (**162**), an FDA-approved CCR5 NAM with the CCR5-maraviroc co-crystal displaying numerous interactions with residues in the TM bundle (PDB: 4MBS). Bottom: representative allosteric antagonists and NAMs discovered for chemokine receptors (**164-174**).

CCR5. The chemokine receptor CCR5 is widely implicated for its role in the process of human immunodeficiency virus type 1 (HIV-1) infection. Mechanistically, CCR5 forms a co-receptor with the viral envelope glycoprotein gp120, which is required for HIV-1 cell recognition and entry leading to infection.²²³⁻²²⁴ Maraviroc (**162**) is a marketed allosteric drug for anti-HIV (**Figure 1.23**), stabilizing CCR5 in an inactive conformation that blocks CCR5-gp120 interaction by allosterically binding to CCR5.^{225, 226} The co-crystal complex of CCR5 and maraviroc demonstrate that maraviroc occupies an extracellular site of the 7TM helical bundle.²⁶ The protonated nitrogen of the tropane group forms a salt bridge with Glu283^{7,39}. The carboxamide nitrogen and the amine of the triazole group of the ligand form hydrogen bonds with Tyr251^{6,51} and Tyr37^{1,39}, and the phenyl, triazole and cyclohexane ring are responsible for the formation of hydrophobic interaction (PDB code 4MBS). Additionally, CCR5 and the highly homologous CCR2 are promising targets for immunologic and cardiovascular diseases due to their important functions in macrophages, T-lymphocytes and natural killer cells. Chemokine receptors are activated by more than 50 chemokine ligands at specific times and in specific tissues in response to various immunologic or inflammatory events. Thus, probe dependence may be a primary advantage for allosteric modulators of chemokine receptors. In a recent study, Wünsch and colleagues discovered the first probe dependent CCR5 PAM.²⁰⁹ Through an innovative bioluminescence resonance energy transfer (BRET)-cAMP assay, the endogenous agonists CCL4 and CCL5 were screened at CCR2 and CCR5. Chemical modifications and resulting SAR were performed on a 2-benzazapine scaffold showing a sensitive 7-positive where the addition of *p*-tolyl moiety led to a chemical switch towards CCR2 modulation without CCR5 activity. The parent compound displayed PAM activity at CCR5, with no activity at CCR2, and selectively modulated CCL4 versus CCL5.²⁰⁹ Bipyridine and terpyridine, small molecule metal chelators, have also been shown to modulate CCR5 with probe dependency. Biochemical studies indicate that bipyridine and terpyridine are PAMs of CCL3, weakly potentiate CCL4 and compete with CCL5 binding

to CCR5.²¹⁰ CCR5 remains an active target for PAM and NAM discovery and the identification of probe dependent ligands will broaden the biological knowledge of chemokine signaling and the therapeutic relevance.

CXCR1. CXCR1 and CXCR2 are largely expressed on T lymphocytes and natural killer cells, playing a key role in acute and chronic inflammatory conditions.²²¹ Reparixin (**164**) is a non-competitive NAM for CXCR1 (**Figure 1.23**) presenting a selectivity as 400-fold higher efficacy in inhibiting CXCR1 activity versus CXCR2. Compound **164** inhibits the signaling triggered by chemokine CXC ligand 8 (CXCL8) and binds CXCR1 at an allosteric site between TM I, III and VI, and has been advanced into a phase III clinical trial for pancreatic islet auto-transplantation.²²⁷ Ladarixin (DF 2156A, **165**) is the second representative example of this series as a highly potent allosteric inhibitor of CXCR1/CXCR2 with an IC₅₀ value 0.1 nM and has been advanced into clinical trials for type 1 diabetes.²²¹

CXCR4. CXCR4 is expressed by hematopoietic stem cells and progeny, as well as by over 48 different cancers types, and is essential for hematopoietic stem cell colonization of fetal bone marrow during development.²²⁸ Interestingly, Plerixafor (**163**), a NAM of CXCR4 with tetraazacyclotetradecane scaffold (**Figure 1.23**), was initially developed as an anti-HIV drug but has been repurposed and is now marketed for an indication of bone marrow transplantation.²²¹

CCR9. CCR9 is another member of the CC chemokine receptor subfamily implicated in inflammatory bowel disease. Vercirnon (**166**) is a selective allosteric antagonist of CCR9 (**Figure 1.23**) that has entered Phase III clinical trials for the treatment of Crohn's disease.²²⁹ The cocrystal structure of CCR9 with **166** shows that **166** binds to the intracellular side of the CCR9, which is similar to that of CCR2-RA-[R] bound to CCR2. The sulfone group, ketone group and pyridine-*N*-oxide group of **166** could contribute to forming multiple hydrogen bonds with intracellular side of the CCR9. The *tert*-butylphenyl and chlorophenyl group are responsible for the hydrophobic interactions

with the hydrophobic cleft (PDB code 5LWE).²⁸ Allosteric modulation via binding intracellular allosteric sites is still uncommon for class A GPCRs; however this mode of action may have important therapeutic implications, especially for peptide and protein receptors such as chemokine receptors.

CCR2. CCR2 is implicated in numerous inflammatory and neurodegenerative diseases.²³⁰ CCR2-RA-[R] (**167**) is a NAM of CCR2 (**Figure 1.23**) with good selectivity against CCR1 and CCR5, *in vitro* activity characterized by an IC₅₀ of 0.17 μM and also an excellent DMPK profile.¹⁸ The co-crystal structure of CCR2 in a ternary complex with **167** and orthosteric BMS-681 antagonist demonstrates that **167** occupies an intracellular allosteric binding site, as seen in other chemokine receptors. The pyrrolone structure is very important for forming hydrogen bonds between hydroxyl group and Glu310^{8,48} and Lys311^{8,49}, and carbonyl group with the backbone amide of Phe312^{8,50}. The existence of the phenyl group is vital for hydrophobic interactions with various amino residues.²⁷

CCR4. Chemokine receptor 4 (CCR4) is mainly expressed in T helper 2 (Th2) cells and contributes to the pathogenesis of allergic diseases in inflamed tissues. Endogenous agonists chemokine ligand 17 (CCL17) and chemokine ligand 22 (CCL22) are two signaling proteins that bind the orthosteric site of CCR4 and are crucial for recruiting T cells during the inflammatory response upon exposure to allergens.²³¹⁻²³² Interestingly, a functional interrogation of these signaling ligands shows that CCL22 activated CCR4 was able to couple efficiently to β-arrestin and stimulate GTPγS binding, while CCL17 activated CCR4 did not couple to β-arrestin and only partially stimulated GTPγS binding.²³² Thus, the physiological conditions under which some chemokines are released and activate their respective receptors remains an active area of research. The CCR4 has been a target for the discovery of small molecule therapeutics for many due to its central role in pathogenesis such as asthma, atopic dermatitis, cancer and mosquito-borne tropical diseases.²³¹

Indazole sulfonamide series were recently synthesized and examined as human CCR4 antagonists and SAR studies around the C4, C5, C6, C7 and N1, N3 positions were conducted to provide compounds with a better in vivo profile. Among them, **168** with a methoxy-group as C4 substituents, 5-chlorothiophene-2-sulfonamide at N3 and a meta-substituted benzyl group possessing an α -amino-3-[(methylamino)acyl]-group at N1 was the most potent, presenting a pIC₅₀ of 7.4 for CCR4. Compound **168** also demonstrates a good PK profile in three species (rat, dog and human) and was selected for further development.²³¹ Subsequent studies on CCL17- and CCL22-induced responses of human CCR4 expressing T cells suggests there are two additional allosteric sites to which small molecules bind. Compound **168** and its analogues bind to one of them, the intracellular allosteric binding site. Lipophilic heteroarenes possessing basic amino groups have been shown to bind to another site. Additionally, a heteroarylpyrazole arylsulfonamide scaffold was also reported as a potent lead for further development.²³³

CXCR3. The chemokine receptor CXCR3 is mainly activated by γ -inducible chemokines CXCL11, CXCL10 and CXCL9, directing activated T cells to the sites of inflammation and is implicated to play a role in a myriad of inflammatory diseases, such as rheumatoid arthritis, multiple sclerosis, cancer, atherosclerosis and allograft rejection; thus, CXCR3 is viewed as a promising drug target.²³⁴⁻²³⁶ 8-azaquinazolinone derivatives (**169-173**) were characterized as promising allosteric modulators of the chemokine receptor CXCR3 and commonly demonstrate properties of signaling bias and probe-dependence.²³⁶ Among them, **172** can inhibit CXC chemokine 11 (CXCL11)-dependent G protein activation over β -arrestin recruitment with 187-fold selectivity and it inhibits CXCL11-over CXCL10-mediated G protein activation with 12-fold selectivity.²³⁶

Structure-based drug discovery (SBDD) is still in the early phases for receptors such as CXCR3 due to limited structural information and complicated interactions between receptors and chemokine signaling proteins. As an alternative, photoaffinity labeling is an effective biochemical tool to elucidate the binding pocket at the CXCR3 receptor. By this

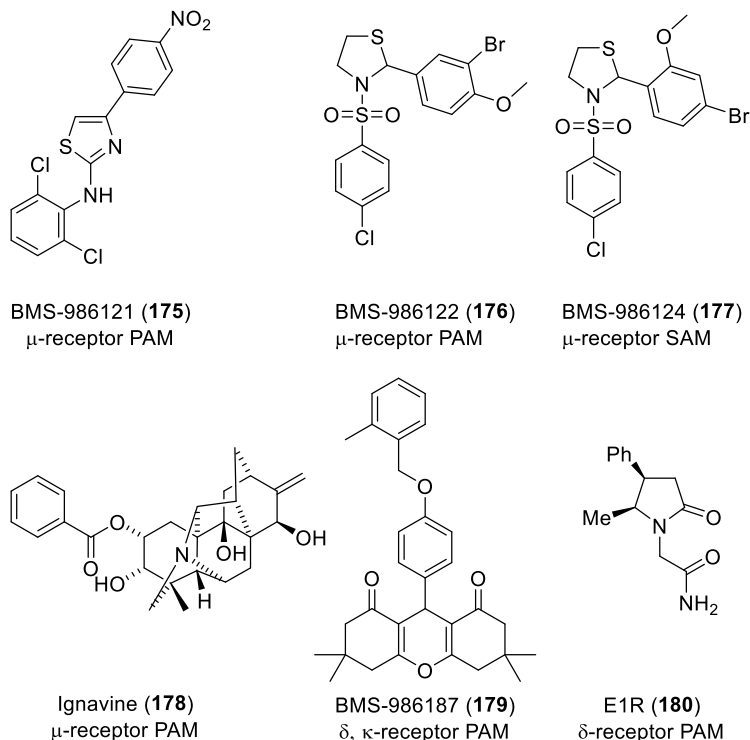
principle, photoactivatable **174** with a nanomolar affinity is synthesized based on the 2,3-disubstituted-8-azaquinazolinone scaffold. Notably, **174** could attenuate radioligand binding by 80% in [³H]-RAMX3 radioligand displacement assay and proved to be a promising chemical tool for further exploration of the allosteric binding site of CXCR3.²³⁵ Aside from photoaffinity labeling, site-directed mutagenesis is another approach to reveal information about ligand-receptor interactions through the mutations of amino acid residues and detection of their influence on modulator binding, signaling and transmission of cooperativity. Compounds **171** and **173** are two biased NAMs and have been shown to exhibit probe-dependent inhibition of CXCR3 signaling. Homology modeling and docking provided direction for site-directed mutagenesis and functional outcomes of the mutations were measured by a BRET-cAMP and β -arrestin recruitment assay. These studies indicated that F131^{3.32}, S304^{7.39} and Y308^{7.43} act as key residues for the compounds to modulate the chemokine response, and notably, mutations of D186^{4.60}, W268^{6.48} and S304^{7.39} led to a G protein–active rather than β -arrestin–inactive conformation.²³⁶

3.4.2. Opioid Receptors (δ -OR, κ -OR, μ -OR). Opioid receptors (ORs), specifically the μ -opioid receptor (MOR), is the therapeutic target for numerous clinically used medications, predominately analgesics. Although MOR activation produces profound analgesia, tolerance develops for opioid drugs and addiction can be severely problematic.²³⁷ Additionally, side effects such as respiratory depression, nausea, constipation and others have highlighted the urgent need for better therapeutic agents targeting the MOR. Allosteric modulators may be suitable in this scenario, as receptor desensitization is less likely and allosteric modulators have a generally safer profile.²³⁸ Both NAMs and PAMs have been explored for opioid receptors, and while most work on allosteric modulation has been directed towards the MOR, a few ligands have been reported as hits for the δ -opioid receptors (DOR).²³⁸

Cannabidiol and salvinorin-A are among the earliest identified NAMs for the MOR and DOR.^{239, 240} Recently, BMS-986121 (**175**) and BMS-986122 (**176**) are reported as the

first series of selective PAMs for the MOR (**Figure 1.24**), identified via a high-throughput screen, presenting a sevenfold leftward shift ($\alpha\beta = 7$) in the potency of endomorphin-I in the β -arrestin assay in U2OS-MOR cells.²⁴¹⁻²⁴² The PAM activity is further characterized by three functional assay as β -arrestin recruitment, inhibition of adenylyl cyclase activity, and G protein activation via [³⁵S]GTP γ S binding. Subsequent chemical SAR study of **176** around the substituents on the side phenyl led to the discovery of BMS-986124 (**177**) as a silent allosteric ligand or SAL.²⁴¹⁻²⁴² Additionally, diterpene alkaloid ignavine (**178**) demonstrates positive modulatory activity for MOR agonists DAMGO, endomorphin-1 and morphine in a cAMP assay with an analgesic effect *in vivo*.²⁴³ BMS-986187 (**179**), with a chemically novel core compared to previous BMS series, was discovered as an effective PAM at the DOR and at the κ -opioid receptor (KOR) rather than the MOR with an approximately 20- to 30-fold higher affinity in the allosteric ternary complex model.²⁴⁴ E1R (**180**), 4,5-disubstituted derivative of piracetam, discovered by Zvejniece and colleagues is revealed as a PAM for the DOR with an *in vitro* profile as increasing agonist binding, enhancing the agonist PRE-084's stimulating effect on electrically stimulated rat vasa deferentia and increasing BK-induced calcium mobilization. Furthermore, **180** (100 mg/kg) alleviated scopolamine-induced cognitive impairment during the PA and Y-maze tests and has no effect on locomotion even dosing up to 100 mg/kg in mice.²⁴⁵ There has been significant interest in light of recent events to discover and develop better opioid receptor therapeutics. Allosteric modulation of ORs holds promise of delivering safer analgesics and other therapeutics to the clinic; however significant optimization and development is still needed.

Figure 1.24 Chemically diverse allosteric modulators for ORs (**171-176**)



Chemically diverse allosteric modulators for ORs (**171-176**).

3.4.3. Other Peptide and Protein Family Receptors

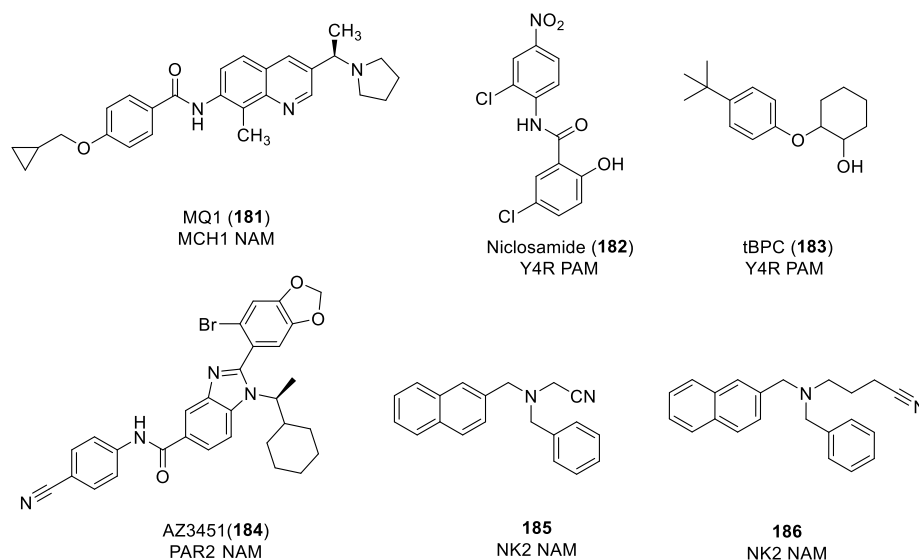
Melanin-Concentrating Hormone Receptor 1 (MCH1R). The MCH1 receptor, an anti-obesity target, is reported to be allosterically inhibited by the small molecule MQ1 (**181**) in multiple signaling pathways for $G\alpha_{i/o}$, $G\alpha_{q/11}$ and β -arrestin. MQ1 has been shown to be a slowly dissociating reversible MCH1 receptor blocker in washout experiments as well as affinity selection-mass spectrometry.²⁴⁶

Neuropeptide Y Receptors (Y1R-Y5R). Niclosamide (**182**) and structurally related compounds are revealed as non-selective small molecule PAM ligands for Y4R versus Y1R, Y2R and Y5R via HTS.²⁴⁷ The small molecule *tert*-butylphenoxy cyclohexanol (tBPC, **183**), a purely efficacy-driven selective Y4R PAM, is reported to potentiate Y4R activation in G-protein signaling and arrestin recruitment experiments.²⁴⁸

Proteinase-Activated Receptors (PAR2). AZ3451 (**184**) is an allosteric antagonist binding to a remote allosteric site of PAR2 and the solved co-crystal structure represents increased success in the structural elucidation for allosteric modulators of Class A GPCRs.³¹

Tachykinin Receptors (NK2). Compound **185** was discovered as a NAM for the NK2 receptor in a FRET-based binding assay and shows a bias for reducing the cAMP-producing conformation rather potentiating the calcium triggering conformation with about 30% decline in the presence of 10 μ M of **185**.²⁴⁹ Modification on **185** to **186** with a butyronitril sidechain presents significantly improved modulatory properties of agonist induced calcium mobilization E_{max} (50% to 68%).²⁵⁰

Figure 1.25 NAMs and PAMs for additional peptide and protein family receptors, as described (**181-186**)



NAMs and PAMs for additional peptide and protein family receptors, as described (**181-186**).

4. CHALLENGES AND EMERGING CONCEPTS IN CLASS A GPCR DRUG DISCOVERY

4.1 Complexities and Nuance Observed in Screening, Optimizing and Advancing Class A GPCR Allosteric Modulators.

The discovery of allosteric modulators for class A GPCRs has been advanced by numerous academic and industry groups over the past decade and has provided a framework for optimization and development of such ligands. This framework includes understanding the multiple facets of allosteric modulator influences on the receptor complex with orthosteric agonists and antagonists, as well as the influence on coupling to effector molecules. As previously suggested, an allosteric modulator-receptor complex can be described as a “new receptor” that results in new or differential biology compared to the native receptor.⁶ Thus, it is important to quantify the allosteric modulator’s effect on the receptor, orthosteric signaling molecule and the downstream effectors. The quantification metrics (cooperativity, intrinsic efficacy, etc.) used throughout hit optimization have been shown to sometimes improve (or decrease) in tandem; however, these measures have often been shown to “uncouple”, such that orthosteric agonist affinity may improve, but there may be no impact on other metrics such as agonist efficacy. Additionally, this trend is observed in which, upon chemical modification, allosteric modulators may acquire intrinsic efficacy as agonists or serve as antagonists. While these outcomes may be advantageous for a particular target, the trend likely will not translate to other orthosteric ligands of the receptor (probe dependence). This can be problematic when the endogenous signaling ligand is not amenable to screening in functional assays (peptides, proteins, etc.) and should be approached with caution. Importantly, GPCRs exist in an ensemble of states and can be stabilized by high-affinity allosteric modulators in a variety of functionally relevant states, such as active states, pathway-specific active states or inactive states.³⁴ The induced receptor conformation may then be more likely to couple with some effectors (e.g., β -arrestins) than others (e.g., G proteins), leading to signaling bias. These complexities may yield therapeutically important results; however, the team must obtain a thorough characterization and SARs of the candidate molecule to effectively move through optimization and development.

Advancing allosteric modulators from *in vitro* to *in vivo* is beset with challenges as well. For instance, dissection of signaling bias in animal models and behavioral paradigms is difficult to achieve and may be highly sensitive to probe dependence, especially if the endogenous signaling agonist could not be used for iterative screening and SAR.²² Additionally, allosteric sites can display a greater divergence between species (e.g., rat vs. human) in comparison to orthosteric sites, complicating interpretations of drug effect across species.¹²⁵ One possible explanation for this observation is that allosteric sites are less homologous due to decreased evolutionary pressure, a feature exploited for subtype selectivity, and may be more pronounced between species. Thus, screening preclinical candidate allosteric modulators at both human and rat GPCRs will help to alleviate this unknown when advancing compounds. Also relevant to *in vivo* characterization, is the presence of “chemical switches” (slight chemical changes that significantly alter or reverse activity) that become apparent during chemical optimization.²⁵¹ Although standard chemical switches are likely to be addressed at an early stage, recent work has highlighted the presence of metabolic chemical switches that lead to major metabolites displaying a different or opposite activity profile.²⁵² Chemical switches may be identified and addressed through early core optimization and the use of the “fluorine walk” to determine scaffold positions amenable to modification, and some success has been reported in the use of halogens or deuterium to dissuade metabolism of some scaffolds.²² Species bias and metabolic switches may complicate preclinical development and should be a key, deciding factor for the abandonment or development of select scaffold.

4.2 Emerging Strategies for Class A GPCR Small Molecule Allosteric Modulator Discovery and Development.

Structure based drug design (SBDD) is emerging in the discovery and optimization of allosteric modulators for class A GPCRs.²⁵³ The growing number of crystal structures

available and the structural studies on allosteric modulator mechanisms are providing the material and insight to engage in SBDD for allosteric modulators.^{254, 255} Importantly, the resolution at allosteric “hot spots”, such as ECLs, has greatly improved in recent reported crystals and is suitable for docking studies or molecular dynamics simulations. From a ligand optimization perspective, these structural studies can be combined with functional assays and site-directed mutagenesis to provide greater clarity on the allosteric mechanism of action at the receptor. Compounds displaying chemical switches may be used in simulations and further inform the structural biology of GPCR activation and signaling enhancement. From a discovery perspective, exciting studies are emerging with de novo allosteric modulators discovered via virtual screening of large libraries. For example, Valant and colleagues recently published the results of an iterative molecular docking and screening project where two subtype selective M₂ mAChR NAMs and one PAM were discovered from the National Cancer Institute (NCI) compound library.²⁵⁶ The success of molecular docking approaches in this example, in which validated and chemically diverse PAMs and NAMs were discovered, is encouraging and this arena is projected to highly important in the future. Considerations of receptor activation state and the ability to predict allosteric modulation by docking to unknown sites remain to be addressed for different members of class A GPCRs.

Another emergent strategy is the utilization of covalent allosteric probes to identify and define the allosteric binding site. Chemically reactive groups can be adapted to allosteric modulators to afford covalent binding to the allosteric site and subsequent peptide mass spectrometry can yield surrounding residues. Followed by site-directed mutagenesis and informed by known structural information, this may be a powerful tool for structurally-informed rational design. This strategy was successfully implemented by Thakur and colleagues to map the CB₁ receptor allosteric binding site.¹⁴⁸ Electrophilic and photoactivatable moieties were added to CB₁ receptor NAMs, which retained their activity and provided useful chemical tool compounds. Of note, the authors engaged in iterative

rational design of numerous covalent derivatives based on previous knowledge of the NAM SAR and discussed modifications that abolished activity. Thus, this powerful strategy may not be suitable for scaffolds prone to chemical switches or shallow SAR.

4.3 New Biology for Class A GPCRs and Implications for Allosteric Modulator Agents.

As studies continue to shed light on the intricate biology of class A GPCRs, new paradigms in drug discovery will emerge. The initial concept of allosteric modulation was developed based on the understanding that allosteric regulation was a ubiquitous and essential element for functional proteins throughout biology.¹⁰ Likewise, biological studies will elucidate new mechanisms for GPCR regulation, expression, function and modulation. There are emerging studies regarding class A GPCR dimerization/oligomerization, subcellular location of GPCRs and temporal regulation of GPCRs that pose interesting paradigms for GPCR modulation. The dimerization, whether homodimers, heterodimers or higher order oligomers, of class A GPCRs has been a thoroughly discussed topic in relation to its biological relevance.²⁵⁷⁻²⁵⁹ A noteworthy reminder, Class C GPCRs are known to form obligatory dimers, thus the discussion is centered on Class A GPCRs.²⁶⁰ A recent review by Gurevich and Gurevich addresses dimerization from a signaling perspective and discusses the stoichiometry observed between class A GPCRs and their effectors: G proteins, β -arrestins and GRKs.²⁶¹ The conclusions state that a single monomeric class A GPCR is sufficient for effector coupling and downstream signaling through multiple pathways, and this is supported by biochemical and functional assays. It is also known that Class A GPCRs do indeed interact as dimers during their “life cycle” and that these interactions may be important regulators for expression, localization and trafficking. Whether or not functional signaling dimers exist, there is evidence for receptor crosstalk that can be modulated, and allosteric modulators can play an important role in regulating

the monomer-dimer equilibrium and may impart therapeutic effects in this manner. Indeed, a recent report shows how the CCR5 receptor allosteric modulator maraviroc (**162**) can influence the dimer population by inducing a third inactive dimer conformation.²⁶² Dimerization of CCR5 is necessary for translocation to the membrane and the dimer induced by **162** may contribute to its efficacy in blocking HIV entry in to the cell. Much more information is needed on these facets of GPCR biology, but novel chemical probes and tool compounds can provide new ways of investigating dimers and the future may hold targeted therapies for such complexes.

Additionally, as Class A GPCR dimers have been visualized in the cell, so have functional intracellular Class A GPCRs. Opioid receptors (ORs) were highlighted in a recent report that identified differential signaling patterns between endogenous peptide-bound ORs at the cell surface and opioid drug-bound ORs in the Golgi membrane within the cell.²⁶³ The authors argue that this “distortion” of typical endogenous peptide activation may drive neuronal toxicity and adverse effects from OR-targeted therapeutics. This effect has been termed location bias for GPCR activation. In a review by Grundmann and Kostenis, the recent consensus on time-encoded GPCR signaling (“temporal bias”) is presented, as are other important kinetic parameters for class A GPCR signaling. As biology has shown signaling bias and probe dependence are emerging as possible therapeutic strategies, the future will likely see dimer equilibrium, location bias and temporal bias become topics of discussion in class A GPCR allosteric modulator drug discovery.

5. CONCLUSIONS AND FUTURE DIRECTIONS

Class A GPCRs hold significant clinical importance and are targeted by a high percentage of currently marketed drugs. Utilizing allosteric modulation to precisely alter the function of these receptors may enable the targeting of GPCRs without marketed drugs and may provide safer drugs for receptors with marketed drugs. The ability to modulate

signaling in a spacial and temporal dependent manner, as well as the potential to therapeutically exploit probe dependence, moves beyond achieving subtype selectivity and towards a remarkably precise therapeutic paradigm. However, the complexities that confer these advantages also must be addressed during allosteric modulator discovery, optimization, development and advancement into preclinical/clinical assessments. Multiple signaling pathways downstream of effectors, such as G proteins and β -arrestins, should be examined to provide informed SAR of the molecule series. Additionally, the endogenous agonist should be assayed, when appropriate, to ensure the translation of the allosteric modulation *in vivo* and avoid unforeseen probe dependence. There are cases, especially in the chemokine receptor family, where probe dependence will be a desirable outcome and should be addressed early in scaffold optimization. Other *in vivo* considerations arise from species bias, which has been observed in mAChR PAMs and NAMs, where activity does not translate from *in vitro* assays employing human mAChRs to rat *in vivo* assays. Thus, early examination of rat and human Class A GPCRs *in vitro* may help avoid this situation. The discovery and development of Class A GPCR allosteric modulators has progressed tremendously in recent years and has provided a framework for overcoming challenges and maturing clinical candidates.

The chemical diversity of Class A GPCR allosteric modulators has grown along with diversity of allosteric binding sites. Allosteric binding sites have been shown to exist in extracellular regions, transmembrane regions and intracellular regions of receptors, all contributing unique mechanisms for modulation. Most ligand interactions with these sites are classified as hydrophobic interactions, while aromatic π - π interactions are also common. Core scaffolds for Class A GPCR allosteric ligands commonly contain a nitrogen amenable to H-bond polar interactions. Drug likeness has improved and is attainable in situations where there are large amounts of SAR to dictate sites available for modification. Chemically successive, iterative ligand design and synthesis should be performed to enable informed SAR and can be aided by strategies such as the “fluorine walk”. Importantly,

emergent structural information may provide information towards chemical modifications that lead to high affinity allosteric ligands and should be utilized where available.

Finally, new biology may direct allosteric modulator discovery towards modes of action other than simple potentiation of activation. As seen in CCR5 dimerization, maraviroc may alter dimer populations to provide antiviral efficacy. Dimer stabilization/destabilization, location bias and temporal bias may become considerations for allosteric mechanism of action. Probe dependence can hinder development; however, it may also be used to selectively potentiate (or diminish) marketed orthosteric drugs. In this way, a promiscuous orthosteric drug can have improved selectivity at its site of action or be altered for a higher affinity at an additional site. Thus, allosteric modulators may improve marketed drugs to provide greater selectivity or if polypharmacology is desired, as in difficult psychiatric conditions, allosteric modulators could enhance activity at other receptors for a given marketed drug that displays moderate affinity for these targets. Allosteric modulation is a fundamental mechanism in biology and exploitation of this paradigm has delivered FDA-approved therapies, multiple drug-candidates in the pipeline and promises to provide more precise and safer small molecule therapeutics in the future.

**A THERAPEUTIC FOCUS ON THE 5-HT_{2C}R AND APPLYING ALLOSTERIC
MODULATION AS A 5-HT_{2C}R DRUG DISCOVERY STRATEGY**

**Chapter 2. Targeting the 5-HT_{2C} Receptor in Biological Context and the
Current State of 5-HT_{2C} Receptor Ligand Development**

E.A. Wold, C.T. Wild, K.A. Cunningham, J. Zhou
Published as *Curr. Top. Med. Chem.* 2019 19 (16), 1381-1398²⁶⁴

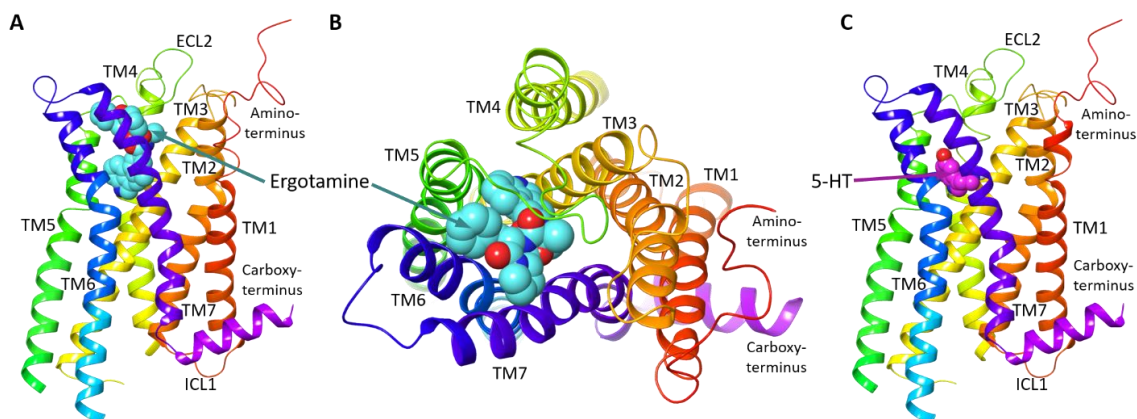
Abstract

The serotonin (5-HT) 5-HT_{2C} receptor (5-HT_{2C}R) is recognized as a critical mediator of disease-related pathways and behaviors based upon actions in the central nervous system (CNS). Since the 5-HT_{2C}R is a class A G protein-coupled receptor (GPCR), drug discovery efforts have traditionally pursued activation of the receptor through synthetic ligands with agonists proposed for treatment of obesity, substance use disorders and impulse control disorders while antagonists may add value in the treatment of anxiety, depression and schizophrenia. The most significant agonist discovery to date is the FDA-approved anti-obesity medication lorcaserin. In recent years, efforts towards developing other mechanisms to enhance receptor function have resulted in the discovery of positive allosteric modulators (PAMs) for the 5-HT_{2C}R, with several molecule series now reported. The biological significance and context for signaling and function of the 5-HT_{2C}R, and the current status of 5-HT_{2C}R agonists and PAMs are discussed in this review.

1. INTRODUCTION TO THE 5-HT_{2C}R PROTEIN STRUCTURE AND FUNCTION

The G protein-coupled receptor (GPCR) super family, a vast group of proteins imbedded in cellular membranes, represents nearly one-third of all therapeutic targets²⁶⁵. Out of the approximately 800 different GPCRs identified in mammals, only 25% have been exploited for therapeutic development and the function of ~200 have yet to be elucidated²⁶⁶. The family of serotonin (5-HT) receptors (5-HT_XRs) are believed to be, from an evolutionary standpoint, among the oldest GPCRs²⁶⁷. There are seven classes of 5-HT_XRs: 5-HT₁R, 5-HT₂R, 5-HT₃R (a ligand-gated ion channel), 5-HT₄R, 5-HT₅R, 5-HT₆R, and 5-HT₇R, which are classified based on sequence homology and functional aspects. The 5-HT_{2C} receptor (5-HT_{2C}R), a receptor subtype in the 5-HT₂R family (5-HT_{2A}R, 5-HT_{2B}R, 5-HT_{2C}R) has been increasingly investigated as a therapeutic target in recent years. Like all other GPCRs, the 5-HT_{2C}R is characterized by seven transmembrane spanning helices (TM I - VII), three extracellular (ECL 1-3) and three intracellular loops (ICL 1-3), an intracellular carboxy-terminus, and an extracellular amino-terminus (**Fig. 2.1**)^{268, 269}. Importantly, the X-ray crystal structure of the 5-HT_{2C}R was recently solved with non-selective 5-HT agonist ergotamine (“active-like” state) or the 5-HT₂R antagonist/inverse agonist ritanserin (inactive state), further allowing a critical review of the receptor’s structural features and conformations for structure-based drug design (PDB: 6BQG)²⁶⁹. Reviewing the 5-HT_{2C}R sequence, there is approximately 80% sequence homology in the TM region between members of the 5-HT₂R family, the region that forms the orthosteric binding site for 5-HT, while the ECL and ICL sequences are known to vary across receptor subtypes²⁷⁰. In addition to the sequence similarity of the orthosteric sites across the 5-HT₂R family that makes the selective chemotype targeting of 5-HT₂Rs difficult, there is the ubiquitous issue that 5-HT binding to all 5-HT₂R, including the 5-HT_{2C}R, results in activation of complex webs of intracellular signaling processes, several of which are inadequately appreciated at present.

Figure 2.1 The recently solved X-ray crystal structure of the “active-like” state of the 5-HT₂CR bound to ergotamine (PDB code: 6BQG) and 5-HT₂CR model bound to 5-HT is depicted



The recently solved X-ray crystal structure of the “active-like” state of the 5-HT₂cR bound to ergotamine (PDB code: 6BQG) and 5-HT₂cR model bound to 5-HT is depicted. (A) The side view of the ergotamine-bound 5-HT₂cR crystal structure with the N- and C-termini, extracellular and intracellular loops, and the transmembrane helices labeled; ECL = extracellular loop, ICL = intracellular loop, TM = transmembrane domain helix, 5-HT (pink space fill representation) at the orthosteric site. (B) Top/extracellular-view of the ergotamine binding site. (C) The side view of a 5-HT₂cR structure model based on the crystal structure with 5-HT docked to the orthosteric site. The 5-HT-bound 5-HT₂cR was generated via induced fit docking protocols on 6BQG using the Schrödinger Drug Discovery Suite.

The canonical G protein-dependent signaling through the 5-HT₂cR is engendered by 5-HT-stimulated coupling to G $\alpha_{q/11}$ to activate the enzyme phospholipase C β (PLC β) mediated hydrolysis of phosphatidylinositol 4,5-biphosphate (PIP₂) to generate the intracellular second messenger inositol-1,4,5-trisphosphate (IP₃), accumulation of the downstream IP₃ metabolite inositol monophosphate (IP₁), and diacylglycerol (DAG) (**Fig. 2.2**). Intracellular calcium (Ca_i²⁺) mobilization, frequently measured with calcium-binding fluorescent dyes, and IP₁ levels, assessed with [³H]-inositol, are well-characterized to be elevated following activation of the 5-HT₂cR (for reviews)^{271, 272}. In fact, the release of Ca_i²⁺ and/or IP₁ are often utilized as a readout in functional cellular assays to measure the extent to which the 5-HT₂cR is activated²⁷³.

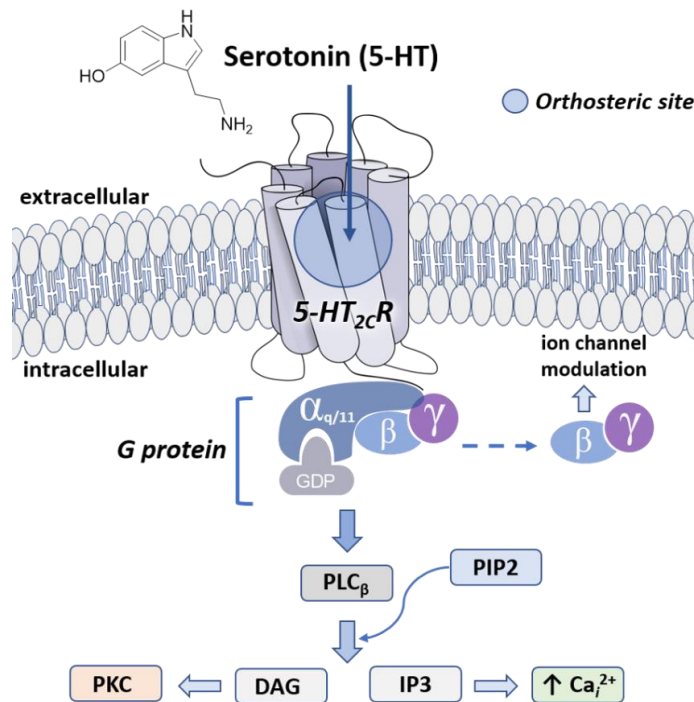
The 5-HT_{2C}R has also been shown to regulate ion channels and transport processes as well activate other downstream effectors, including phospholipase A₂ (PLA₂), phospholipase D (PLD), cyclic nucleotides, and extracellular signal-regulated kinases (ERK_{1/2})^{268, 274}. For instance, stimulation of the 5-HT_{2C}R is thought to activate cytosolic PLA₂ which hydrolyzes arachidonic acid-containing phospholipids to produce free arachidonic acid and a host of its metabolites that are functionally relevant in this signaling web (for review)²⁷⁵. Agonist signaling bias can result in the activation of PLC β over PLA₂, and vice versa, depending on the ligand that binds to the receptor²⁷⁶. Stimulation of the 5-HT_{2C}R leads to activation of protein kinase C (PKC) and downstream stimulation of the mitogen-activated protein kinase cascade resulting in phosphorylation of ERK_{1/2}^{277, 278}. In fact, 5-HT_{2C}R was shown to couple ERK_{1/2} via a PLD- and PKC-dependent pathway possibly through G $\alpha_{12/13}$ proteins²⁷⁸. The PLD and PKC involvement in ERK_{1/2} phosphorylation evoked by 5-HT_{2C}R stimulation was recently validated in a mouse hypothalamic cell line²⁷⁹.

The signaling web for the 5-HT_{2C}R is influenced by the fact that this receptor is the only known GPCR that undergoes RNA editing²⁸⁰. Five closely spaced adenosines within the second intracellular loop of the 5-HT_{2C}R are subject to deamination by Adenosine Deaminases that Act on RNA (ADAR), resulting in an adenosine to inosine substitution which alters the coupling efficiency between the receptor and its G protein and restricts its ability to activate intracellular cascades²⁸¹⁻²⁸⁵. Editing allows the 5-HT_{2C}R to exist in 32 mRNA variants that encode up to 24 predicted proteoforms^{286, 287}. Thus, mRNA editing is fundamentally important to normal 5-HT_{2C}R biological function²⁸⁸. In addition to the increased diversity of signaling afforded by RNA editing of the 5-HT_{2C}R, evidence is accumulating that signaling via the 5-HT_{2C}R is further diversified by the formation of oligomers, in fact the 5-HT_{2C}R appears to function as a homodimer²⁸⁹. Heterodimers are reported to form between the different isoforms of the 5-HT_{2C}R generated by RNA editing²⁹⁰. Likewise, the 5-HT_{2C}R has been reported to heterodimerize with the ghrelin growth

hormone secretagogue receptor 1α , the melatonin MT_2 receptor, and the N-methyl-D-aspartate-gated ion channel subunit $GluN2A$, and most recently with the $5-HT_{2A}R$ and $5-HT_{2B}R$ ²⁹¹⁻²⁹⁶. Intriguingly, the $5-HT_{2A}R:5-HT_{2C}R$ complex did not modify the $G\alpha_{q/11}$ coupling of the receptor subunits, but rather the $5-HT_{2C}R$ exerted dominance when in complex with the $5-HT_{2A}R$, such that only the $5-HT_{2C}R$ coupled with the G protein to generate intracellular signaling; the $5-HT_{2A}R$ signaling is ‘masked’ ²⁹⁵. Thus, the $5-HT_{2A}R:5-HT_{2C}R$ protein complex appears to be a distinct molecular species that contributes to cellular signaling, generating unique properties when co-expressed *in vitro* ²⁹⁵.

The $5-HT_{2C}R$, as for other GPCRs, act via the “receptorsome,” the composition of membrane, cytosolic and accessory proteins through which protein-protein interactions interface GPCR coupling to downstream intracellular signaling cascades to tailor cellular responsiveness. For example, the $5-HT_{2C}R$ interacts with PSD-95/disk large/zonula occludens domain-containing proteins, calmodulin, β -arrestins, and phosphatase and tensin homolog, all of which have been shown to modulate receptor kinetics by varying mechanisms ^{53, 268, 274}. Of relevance, β -arrestins are known to play a key role in desensitization and resensitization processes that regulate the functional activity of $5-HT_{2C}R$, and edited $5-HT_{2C}R$ isoforms have been shown to modify the kinetics of these processes due to divergent magnitudes of association with β -arrestin ²⁹⁷. Agonist-dependent desensitization is associated with $5-HT_{2C}R$ phosphorylation involving G protein receptor kinase₂ (GRK₂), binding of β -arrestin and uncoupling of the receptor from the G protein to result in receptor internalization into endosomes; resensitization and recycling to the plasma membrane occurs with dephosphorylation ^{281, 287}. Thus, there is a rich opportunity to regulate the biological function of the $5-HT_{2C}R$.

Figure 2.2 A cross-section of the 5-HT_{2c}R signaling webs initiated by 5-HT binding to the orthosteric site is presented



Activation of G_{αq/11} promotes phospholipase C_β (PLC_β) mediated hydrolysis of phosphatidylinositol 4,5-bisphosphate (PIP₂) into diacylglycerol (DAG) and inositol-1,4,5-triphosphate (IP₃). IP₃ promotes release of intracellular calcium (Ca_i²⁺) while DAG binds to downstream effector protein kinase C (PKC).

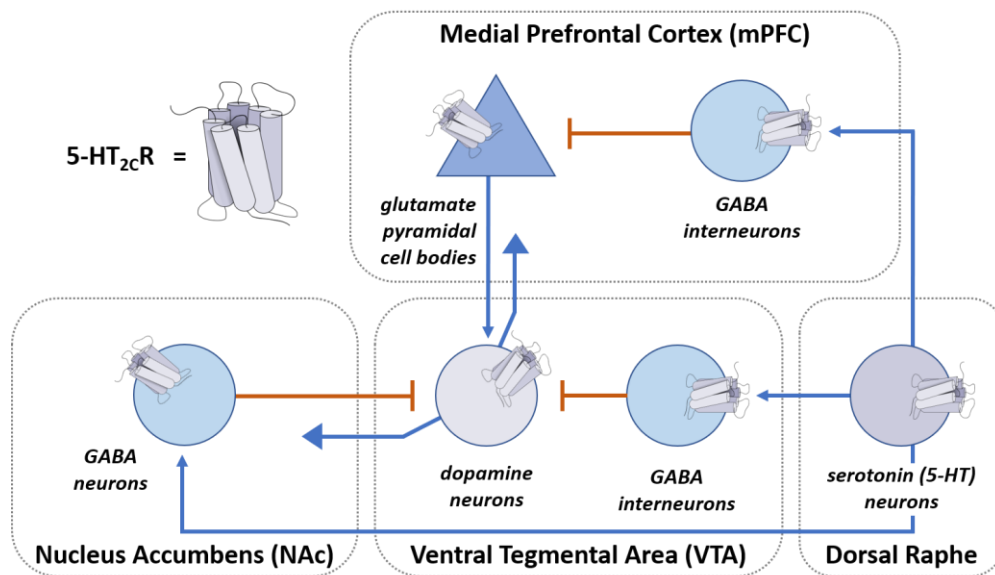
The localization of the family of 5-HT receptors is region- and cell-specific throughout the body, and this is true for the 5-HT_{2c}R, whose expression and function in the central nervous system (CNS) drives its primary, known biology. Serotonergic cell bodies project from the dorsal raphe nuclei in the midbrain to key brain regions associated with the reward pathway (e.g., ventral tegmental area, VTA; nucleus accumbens, NAc) and higher executive function (e.g., prefrontal cortex, PFC)^{298, 299}. Postsynaptic expression of the 5-HT_{2c}R is reported in various neuronal cell types including those that employ acetylcholine, dopamine, and γ -aminobutyric acid (GABA) as neurotransmitters, with a major outcome of 5-HT_{2c}R stimulation defined as modulation of dopamine neuronal function (for review)²⁹⁸. For example, stimulation of the 5-HT_{2c}R in the VTA increases

the firing rate of GABA interneurons, enhances basal GABA release in the VTA in a brain slice preparation, and decreases firing rates of dopaminergic neurons³⁰⁰⁻³⁰². Interestingly, while 5-HT_{2C}R antagonists have been reported to increase dopaminergic neurotransmission and dopamine levels in the NAc, local activation of the NAc 5-HT_{2C}R *in vivo* suppressed potassium-stimulated GABA release³⁰³⁻³⁰⁵. Intriguingly, the 5-HT_{2C}R has also been shown to be expressed on VTA dopamine neurons, including those that project to the NAc^{306,307}. The 5-HT_{2C}R localized to VTA dopamine receptors was recently demonstrated as a key regulator of their physiology as well as binge-like eating behavior in mice³⁰⁸. Thus, the 5-HT_{2C}R controls dopamine neurotransmission within the VTA as well as its target regions in the limbic-corticostriatal circuit, including the NAc and medial prefrontal cortex (mPFC) (**Fig. 2.3**)^{309,310}. These data are but a fraction of research findings that illustrate the nature and complexity of cell- and region-specific roles of this receptor plays in neurobiology.

The interaction between the 5-HT_{2C}R and 5-HT_{2A}R was demonstrated in mPFC and the resulting signaling control *in vivo* is an underappreciated area of research that has recently provided clues to suggest therapeutic modalities for neuropsychiatric disorders^{298, 299, 311}. A review of early work on this topic indicated a likely oppositional relationship between the 5-HT_{2A}R and 5-HT_{2C}R in the control of certain behaviors³¹². However, the relationship is now proving to be more interactive and synergistic in studies that show a combination of a selective 5-HT_{2A}R antagonist and selective 5-HT_{2C}R agonist can work in concert to suppress behaviors associated with substance use disorders (SUDs) in rodents, at doses far below the effective doses needed when administered independently³¹³. This result also suggests a delicate balance of 5-HT_{2R} signaling in healthy individuals that necessitates reliable, selective 5-HT_{2C}R tool compounds for use in probing the mechanisms that underlie chronic psychiatric conditions. The clinical significance of selective 5-HT_{2C}R modulation alone has been recently validated by the approval of the 5-HT_{2C}R agonist lorcaserin (**14, Fig. 2.5**) for the treatment of obesity^{314,315}. Given the notion that 5-HT_{2C}R

can exert inhibitory control over dopaminergic tone in brain regions that drive reward-related behaviors and cortical areas of the brain responsible for higher order executive functions related to acting impulsively and reacting to external cues, the development of 5-HT_{2C}R ligands is a promising approach to treating obesity, SUDs, and other neuropsychiatric conditions³¹⁶⁻³¹⁸. Additionally, improved and functionally diverse 5-HT_{2C}R agonists may enable beneficial combination therapies with 5-HT_{2A}R-acting medications. However, the development of selective small molecule 5-HT_{2C}R agonists remains a challenge and the chemical diversity of known synthetic 5-HT_{2C}R agonists is minimal.

Figure 2.3 A schematic of the proposed 5-HT_{2C}R modulation of limbic-corticoaccumbens circuit is represented



Serotonin (5-HT) neurons originating from the dorsal raphe nuclei innervate GABA interneurons in the medial prefrontal cortex (mPFC), nucleus accumbens (NAc), and the ventral tegmental area (VTA). Inhibitory GABAergic neurons facilitate decreased dopaminergic neuronal firing in the VTA both directly and indirectly. The 5-HT_{2C}R localizes to neurons within each of the nodes in this circuitry.

2. THE 5-HT_{2C}R AS A THERAPEUTIC TARGET

The 5-HT_{2C}R has been targeted for the development of therapeutics for several chronic pathological disorders. Agonists have been suggested for the treatment of obesity, SUDs and impulse control disorders while antagonists may add value in the treatment of anxiety, depression and schizophrenia. In particular, a strong case for the use of a selective 5-HT_{2C}R agonist was made for obesity. The constitutive 5-HT_{2C}R knockout mouse exhibited hypophagia and increased body mass in the context of both insulin resistance and late-onset obesity, while weight gain as well as a greater relative risk of metabolic dysfunction and diabetes develops with the chronic treatment of atypical antipsychotics with 5-HT_{2C}R antagonist properties (e.g., olanzapine) in humans and animals³¹⁹⁻³²². Selective 5-HT_{2C}R agonists have been consistently demonstrated to suppress food intake^{319, 323-325}, in fact, the selective 5-HT_{2C}R agonist WAY163909 dose-dependently decreased food intake in normal Sprague–Dawley rats, obese Zucker rats and mice with diet-induced obesity³²⁶. Investigations of 5-HT involvement in the mechanisms underlying satiety have focused predominantly on neural loci in the hypothalamus and midbrain/hindbrain circuits which synchronize energy balance and glucose homeostasis in concert with peripheral systems (for reviews)^{327, 328}. Based upon these findings, lorcaserin (Belviq®) was approved by the U.S. Federal Drug Administration (FDA) as the first-in-class 5-HT_{2C}R agonist marketed for weight reduction in patients with a body-to-mass (BMI) index of >30 or with a BMI >27 comorbid with type-2 diabetes, hypertension or dyslipidemia^{314, 329}.

Extensive preclinical studies have also demonstrated the role of the 5-HT_{2C}R in the rewarding and incentive-salience value of cocaine, other psychostimulants, ethanol and, most recently, opioids as well as factors involved in relapse vulnerability during recovery from SUDs^{237, 298, 311, 330, 331}. For example, employing the self-administration assay, the preclinical model with the best validity for human drug-taking, systemic administration of a selective 5-HT_{2C}R agonist suppressed cocaine intake and the resurgence of drug-seeking evoked by pretreatment with cocaine or exposure to cocaine-associated cues [i.e., drug-taking environment, and the discrete cues associated with previous cocaine delivery (e.g.,

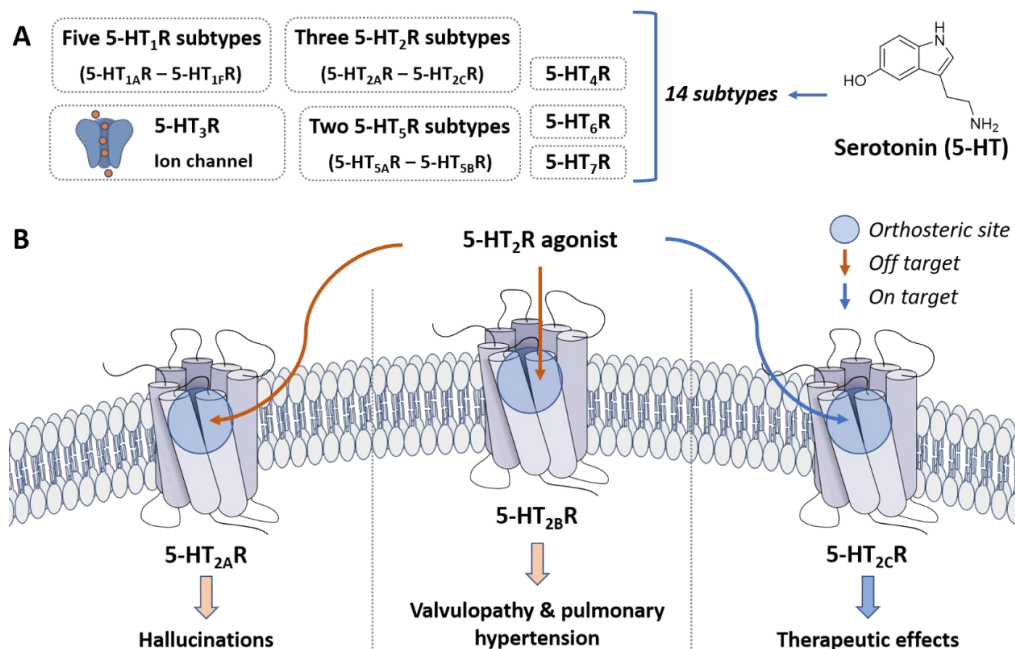
lights, tones)]³³²⁻³³⁴. These effects of the 5-HT_{2C}R agonist were reversed by a selective 5-HT_{2C}R antagonist. Conversely, pretreatment with a selective 5-HT_{2C}R antagonist enhanced self-administration of low doses of cocaine and cocaine-evoked reinstatement of drug-seeking, while the selective 5-HT_{2C}R antagonist SB242084 is self-administered in primates³³⁵⁻³³⁸. In humans, lorcaserin improved smoking cessation rates and significantly decreased corticolimbic activation elicited by palatable food cue exposure, further supporting the role of the 5-HT_{2C}R in as a common mediator of reward and cue-associated events across abused drugs and palatable food^{339, 340}. The added value of lorcaserin to suppress the rewarding effects of cocaine and other abused drugs imputes a further dimension of likely therapeutic utility^{299, 311, 313}, and lorcaserin is currently in clinical trials for cocaine use disorder (CUD) and other SUDs (clinicaltrials.gov; accessed May 6, 2019).

Serotonin is one of the primary regulators of behavioral inhibition, a fundamental aspect of impulse control. Impulsivity, a predisposition toward rapid unplanned reactions to stimuli without regard to the negative consequences contributes to initial drug use and is perpetrated by continued use of the abused drug (for reviews)^{341, 342}. Intriguingly, individuals with poor impulse control may be more vulnerable to drug-associated stimuli, and less capable of engaging processes that override heightened attentional bias for cues^{343, 344}. The role of the 5-HT_{2C}R in these interlocked behavioral phenotypes has been demonstrated in that selective 5-HT_{2C}R agonists consistently reduced and the 5-HT_{2C}R antagonist SB242084 enhanced motor impulsivity, while mice with a constitutive loss of the 5-HT_{2C}R exhibit elevated motor impulsivity^{53, 333, 345-347}. The status of 5-HT_{2C}R function in the mPFC appears to be a contributor to the vulnerability of impulsive rats to cocaine reward and sensitivity to cue-associated relapse vulnerability, which is interwoven with vulnerability to endogenous factors (e.g., craving, stress, withdrawal), all of which can serve as immediate antecedents to relapse^{311, 348}. Relapse is a major hurdle for the successful treatment of chronic SUD and a pharmacotherapy that can improve inhibitory control would represent a first-in-class drug for those sufferers^{349, 350}. Thus, the 5-HT_{2C}R

is a potential therapeutic target at the intersection of disinhibited behaviors that contribute to obesity and SUD. Given that obesity is at epidemic levels in the U.S. while drug overdoses and SUDs continue to drive unprecedented mortality and morbidity rates, targeting the 5-HT_{2C}R is an attractive and urgent approach towards the development of a neuropharmacotherapy to treat these intractable public health concerns.

Selective targeting of the 5-HT_{2C}R remains a challenge for medicinal chemists primarily due to the fourteen 5-HT receptor subtypes distributed throughout the body in various cell types and tissues and that each receptor accommodates 5-HT at a conserved orthosteric binding site. It is well established that, when only comparing the 5-HT₂R subtypes (5-HT_{2A}R, 5-HT_{2B}R, and 5-HT_{2C}R), receptor subtype selectivity is a major determining factor with regard to the scale of potential therapeutic utility (**Fig. 2.4**). With the understanding that 5-HT_{2A}R or 5-HT_{2B}R agonists are expected to evoke hallucinations or cardiac valvulopathy, respectively, the need for 5-HT_{2C}R orthosteric agonists that lack demonstrable efficacy at 5-HT_{2A}R and 5-HT_{2B}R sharpened^{351,352}. For example, the potent 5-HT releaser fenfluramine was approved and marketed in the U.S. as an appetite suppressant in combination with the norepinephrine releaser phentermine (Fen-Phen) in 1983. A proportion of patients treated with fenfluramine developed pulmonary hypertension and valvular heart disease, resulting in its withdrawal from the market in 1997 and subsequent legal damages exceeding \$10 billion U.S.³⁵³. Activation of the 5-HT_{2B}R on heart valves by the fenfluramine metabolite norfenfluramine is the primary pathogenic mechanism³⁵². An additional example of this scale in clinical utility stems from concern over lorcaserin which has a low potential for abuse but could lead to positive subjective effects at supratherapeutic doses, based upon its action as a partial agonist at the 5-HT_{2A}R which is responsible for hallucinogenic actions³⁵⁴. The FDA deliberations led to a Schedule IV classification for lorcaserin under the Controlled Substances Act. Thus, the therapeutic utility of lorcaserin (**14; Fig. 2.5**) in the general population is limited by concern of side effects^{354,355}.

Figure 2.4 Proposed outcomes mediated by activation of specific members of the 5-HT₂R family are depicted.



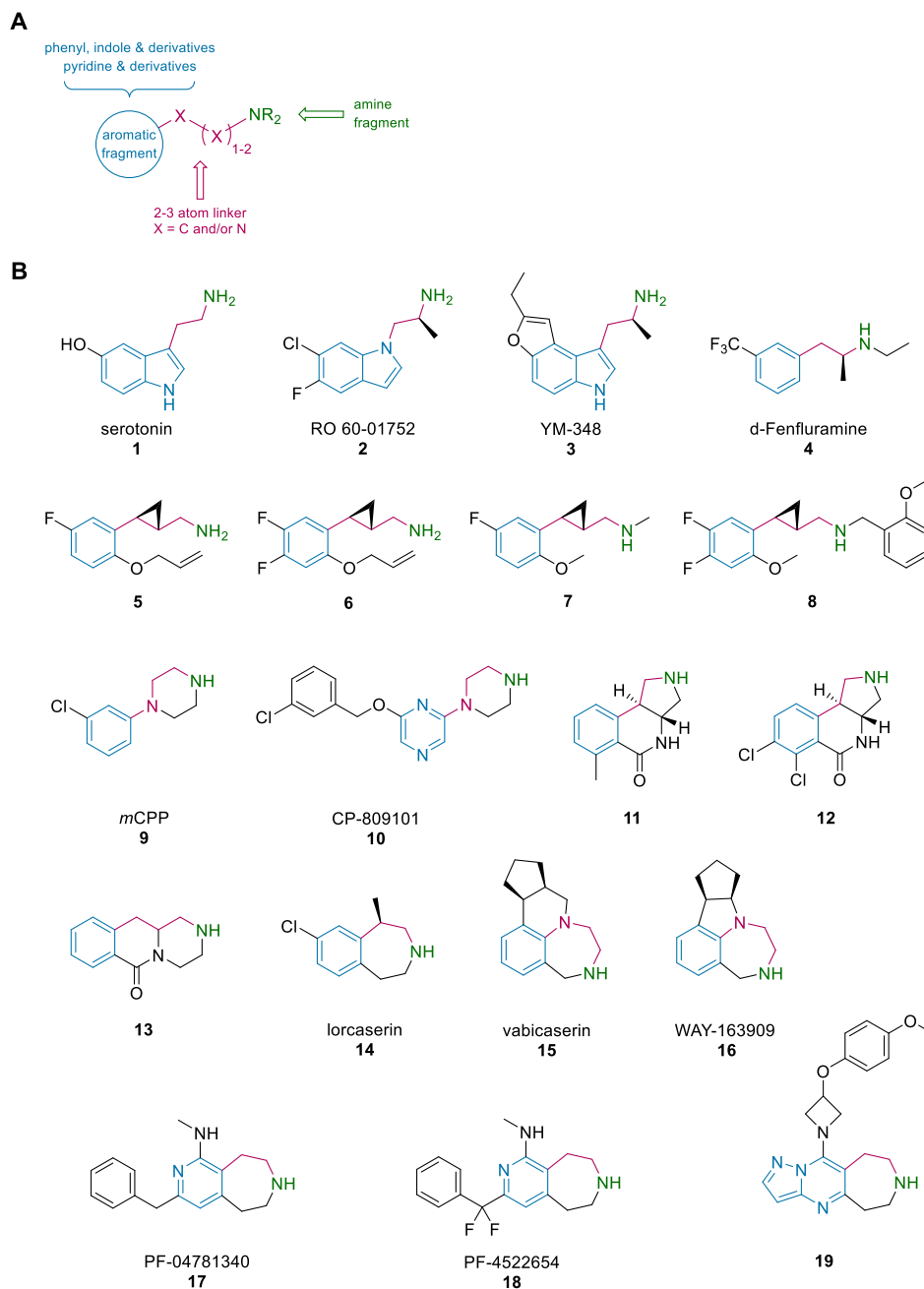
(A) The 5-HT receptor family is comprised of 13 GPCRs and one ligand-gated ion channel (divided into seven subtype categories). Each receptor is activated by endogenous 5-HT. Therefore, the orthosteric site is highly conserved across receptor subtypes. (B) Agonist-mediated activation of 5-HT_{2A}R accounts for the hallucinogenic actions of such abused drugs as *d*-lysergic acid diethylamide. Agonist-mediated activation of 5-HT_{2B}R can lead to pulmonary hypertension and valvular heart disease. Agonist-mediated activation of 5-HT_{2C}R represents an attractive therapeutic approach to treat obesity, substance use disorders and impulse control disorders. However, the high sequence homology at the orthosteric sites of these receptors present challenges to selectively target the 5-HT_{2C}R.

3. THE CURRENT STATE OF 5-HT_{2C}R AGONISTS

Targeting the 5-HT_{2C}R for therapeutic purposes has led to the discovery of many ligands that vary in activity and selectivity yet, in a general sense, come from very similar chemotypes. A brief structural survey of the most selective 5-HT_{2C}R agonists highlights the lack of chemical diversity, which in turn leads to a limited selection of tool compounds (Fig. 2.5). Coupled with the reality that the 5-HT₂R subtype orthosteric sites share high homology, agonists that lack diverse scaffolds are historically unlikely to overcome the subtype selectivity challenge. Virtually all compounds shown (Fig. 2.5) rely on the

phenethylamine moiety or a derivative thereof. More accurately, each of the indicated agonists require a general scaffold that incorporates an aromatic ring attached to an ionizable nitrogen via a two-three atom linker, usually carbon (**Fig. 2.5**). While many examples of 5-HT_{2C}R agonists from the aforementioned chemotypes are known, most do not demonstrate an acceptable functional selectivity for the 5-HT_{2C}R over the 5-HT_{2A}R and 5-HT_{2B}R (**Table 2.1**). Though several compounds show promise, even the most selective compounds are similar to **14**, while the most selective compound listed herein, CP-809101 (**10**), has been shown to produce genotoxic effects³⁵⁶. As observed in early work on 5-HT_{2C}R agonist discovery, novel scaffolds that deviate from the traditional chemotype and can selectively target the 5-HT_{2C}R are difficult to discover and further exploration of chemical space may yield therapeutically important scaffolds.

Figure 2.5 Current synthetic 5-HT_{2C}R agonists share similarities in their pharmacophore



(A) The general chemical scheme describing structural requirements for 5-HT_{2C}R agonists is presented. (B) Selected 5-HT_{2C}R agonists are organized based on chemotype. Blue indicates the common aromatic fragment, green indicates the requisite ionizable amine, and magenta highlights the linker.

Table 2.1 Functional profiling of numerous 5-HT_{2C}R agonists and respective profiles at the 5-HT_{2A}R and 5-HT_{2B}R to show subtype selectivity among 5-HT₂Rs.

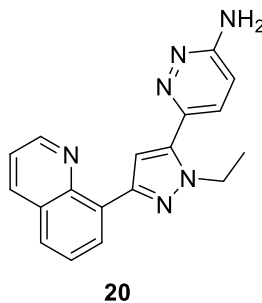
Compound	5-HT _{2C} R		5-HT _{2A} R		5-HT _{2B} R		2A/2C ratio	2B/2C ratio	Ref.
	EC ₅₀ (nM)	E _{max} (%)	EC ₅₀ (nM)	E _{max} (%)	EC ₅₀ (nM)	E _{max} (%)			
5-HT (1)	3.48	100	14.04	100	20 ± 2.8	100	4.03	5.75	357
RO 60-0175 (2)	52 ± 3	88 ± 20	400 ± 20	91 ± 5	2.4 ± 1	130 ± 30	7.69	0.05	358
YM-348 (3)	1.0 ± 0.2	76 ± 1	93 ± 10	97 ± 2	3.2 ± 3	110 ± 10	93.0	3.2	359
<i>d</i> -fenfluramine (4)	300 ± 29	90 ± 9	720 ± 77	80 ± 4	23 ± 4	100 ± 10	2.4	0.08	360
5	4.2	87	374	56	NE	NE	89.0	-	361
6	8.7	97 ± 1	491	21 ± 0	1745	35 ± 7	57.1	200.6	362
7	7.65	71	6.57	79	7.05	54	0.86	0.92	363
8	7.63	92	NE	NE	6.86	63	-	0.90	326
<i>m</i> CPP (9)	120 ± 10	63 ± 3	150 ± 20	18 ± 2	93 ± 50	21 ± 9	1.25	0.78	359
CP-809101 (10)	0.11	93	153	67	65.3	57	1391	593.6	364
11	1.1 ± 0.4	90	127 ± 82	100	94 ± 68	50	115.5	85.5	365
12	3.3 ± 1.8	90	128 ± 44	100	414 ± 468	130	38.8	125.5	365
13	36	100	707	100	>10000	-	19.6	>277.8	366
lorcaserin (14)	9 ± 0.5	100	168 ± 11	75	943 ± 90	100	18.7	104.8	314
vabicaserin (15)	8	100	1650	- ^a	>10,000	80	206.3	0.19	367
WAY-163909 (16)	8 ± 3	90 ± 6	NE	NE	185 ± 105	40 ± 3	-	23.1	326
PF-04781340 (17)	9	99	-	-	1484	69	-	164	368
PF-4522654 (18)	16	58	NE	NE	>10000	<10	-	>625	369
19	95	76	2634	21	503	31	27.7	5.3	370
20	5 ± 3	-	635 ± 862	-	48 ± 41	-	127	9.6	371

^aFunctional output indicated antagonist activity; Values with error represent the mean ± SD; For 5-HT_{2A}R and 5-HT_{2B}R, large reported errors indicate inconsistent results from compounds showing no effect and intermittent positive effects; No effect (NE); Not applicable or not tested (-).

Within the past few years, there has been renewed attention on the 5-HT_{2C}R and innovative drug discovery strategies have been employed to probe the chemical space for

5-HT_{2C}R agents and also to uncover unique functional characteristics of the 5-HT_{2C}R. Towards novel chemotype discovery, Wacker and co-workers at Bristol-Myers Squibb reported a series of analogues lacking a basic amine interaction at the active site Asp 134 residue, which is a requisite interaction for traditional 5-HT_{2C}R synthetic agonists and 5-HT³⁷¹. Noteworthy contributions from this work included the screening of ligands in cells expressing the edited (VNV) isoform of the 5-HT_{2C}R containing a residue mutation, replacing the active site Asp 134 residue with Ala (D134A). This mutant allowed the subsequent screening of agonist hits, found via traditional compound library screening techniques, to selectively identify and optimize atypical agonists. Compound **20** was obtained after rounds of optimization to a non-basic heterocyclic amide agonist hit and was administered orally to rats, displaying a reduction in food intake that could be reversed via a 5-HT_{2C}R antagonist (**Fig. 2.6**). Additionally, Wacker and co-workers reported that the initial hit compounds were discovered during a search for 5-HT_{2C}R positive allosteric modulators, further demonstrating the increased interest in diverse approaches for potentiating 5-HT_{2C}R signaling.

Figure 2.6 A novel pharmacophore for 5-HT_{2C}R agonists is described



Compound **20** is the result of an intentional screening and optimization study which sought to discover non-traditional 5-HT_{2C}R ligands, as defined by an aromatic ring joined to an amine fragment by a short aliphatic linker.

A phenomenon in GPCR signaling known as signaling bias or functional selectivity is evident under conditions in which an agonist displays divergent levels of activation through the multiple signaling pathways linked to receptor activation. Functional

selectivity is well-characterized for the 5-HT_{2C}R^{287,363}. For example, compounds **7** and **8** reported by Kozikowski and colleagues display preferential activation through the G α_q -mediated signaling pathway (**Fig. 2.5**)³⁶³. Significantly, incorporation of the *N*-benzyl moiety that differentiates **8** from **7** leads to a complete loss of function at the 5-HT_{2B}R, while retaining efficacy for the 5-HT_{2C}R. This compound (**8**) suppressed amphetamine-induced hyperactivity in rodents, consistent with the efficacy of other 5-HT_{2C}R agonists³⁶³. Additionally, a recent manuscript by Booth and coworkers provides a further investigation into 5-HT_{2C}R desensitization after agonist activation, which is understood to be mediated to some extent by the β -arrestin signaling pathway³⁷². Multiple agonists were tested in a PLC β -activation desensitization assay, including 5-HT (**1**), **14** and *m*-chlorophenylpiperazine (*m*CPP) (**9**) (**Fig. 2.5**). The magnitude of 5-HT_{2C}R-mediated PLC β activation correlated with desensitization in their assay. Furthermore, the selection of agonists was assessed in a β -arrestin recruitment assay, where a correlation between desensitization and β -arrestin recruitment was observed. Expanded chemical space, functional selectivity, and 5-HT_{2C}R desensitization are concepts that, when incorporated into ligand discovery, will greatly aid in the development of novel 5-HT_{2C}R agonists with improved selectivity and functional profiles. However, there continues to be a lack of subtype selective, novel chemotypes that display significant clinical potential, which is evidenced by a recent surge of interest in targeting spatially distinct, allosteric binding sites.

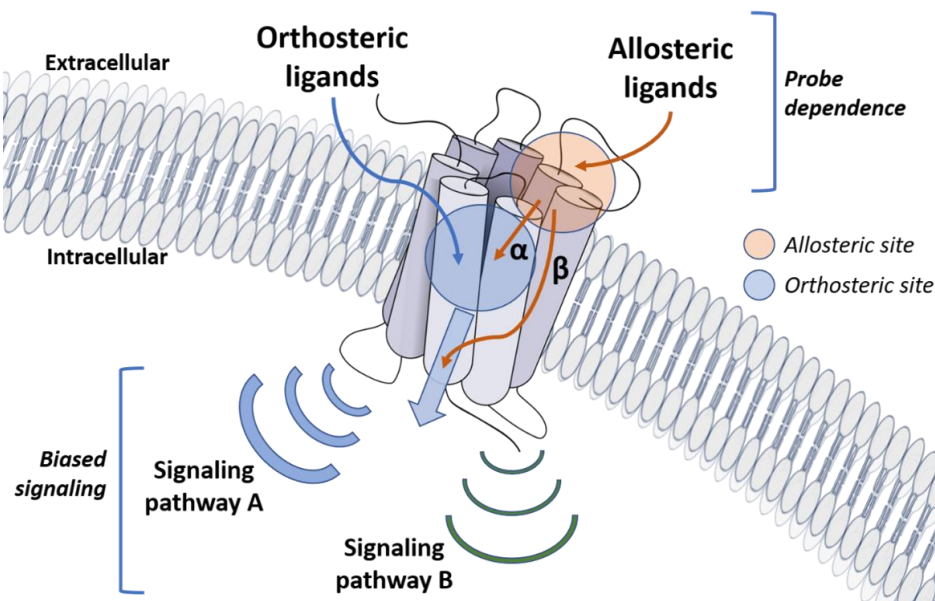
4. BACKGROUND AND RATIONALE FOR 5-HT_{2C}R ALLOSTERIC MODULATORS

Agonists and antagonists targeted to GPCRs that are traditionally designed to bind to a receptor orthosteric site, which has co-evolved with an endogenous ligand for a given receptor. However, in many cases, endogenous signaling ligands activate multiple receptors that are classified in a family. To accommodate the same signaling ligand, the orthosteric site is highly conserved among GPCR family members, which may modulate diverse physiological functions in distinct tissues. Exemplary GPCR families include the

metabotropic glutamate receptors (mGluRs) and 5-HT_XRs which are comprised of eight and 14 receptor subtypes respectively^{330, 373}. Thus, targeting the orthosteric site of the 5-HT_{2C}R among closely related subtypes, 5-HT_{2A}R and 5-HT_{2B}R, has remained a challenge for medicinal chemists.

One strategy that has emerged over the past decade for the selective modulation of GPCRs is the identification and targeting of allosteric sites, which are defined as ligand binding sites that are spatially distinct from an orthosteric site³⁷⁴. In many cases, allosteric sites have proven to be less conserved than the respective receptor orthosteric sites, leading to improved ligand selectivity across subtypes^{85, 375-377}. Thus, allosteric modulation provides an opportunity to specifically target receptors that belong to a subfamily of similar GPCRs, potentially minimizing off-target effects, a significant advantage over typical agonists that at the endogenous ligand binding pocket. Additionally, most GPCR-targeted neurotherapeutic regimens result in chronic exposure of the receptor to orthosteric ligands, differing from the temporal control of endogenous ligands, which has been shown to alter 5-HT_{2C}R trafficking kinetics due to internalization and desensitization and resensitization processes^{372, 378}. An allosteric modulator may minimize the aforementioned detrimental effects of synthetic agonists by maintaining the natural spatial and temporal signaling characteristics that are key features of neuronal circuitry¹¹. Additionally, the fine-tuning of GPCR may be afforded by allosteric ligand structural modifications that result in separate control of orthosteric ligand affinity or efficacy³⁷⁹.

Figure 2.7 A schematic of potential allosteric modulation of GPCR signal transduction is depicted



The allosteric ligand binds to a site (orange circle) that is distinctly different than the orthosteric site (blue circle) which accommodates the orthosteric ligand. Actual binding site locations are generally dictated by the specific GPCR family member. Allosteric modulators can modulate binding affinity (α) and/or efficacy (β) of orthosteric ligands in a positive (PAM) or negative manner (NAM), or may simply occupy the site as a neutral allosteric ligand (NAL). The nature of the modulation is determined by several features of signaling including the orthosteric ligand employed (i.e., probe dependence) as well as the ligand-dependent selectivity for certain downstream transduction mechanisms within a given cell (i.e., biased signaling).

Theoretically, small molecule allosteric modulators of the 5-HT_{2C}R can promote a conformational change in the receptor or stabilize certain conformational populations of the receptor that produce several possible outcomes when coupled with agonist (e.g., 5-HT) binding: (i) positive allosteric modulators (PAMs) increase the binding affinity and/or efficacy of orthosteric ligands, (ii) negative allosteric modulators (NAMs) decrease binding affinity and/or efficacy of the orthosteric ligand, and (iii) neutral allosteric ligands (NALs) bind to the allosteric site without actuating a change in orthosteric ligand binding or efficacy³⁸⁰⁻³⁸². Another important, yet understudied aspect of 5-HT_{2C}R allosteric modulation is the potential leveraging of biased signaling (i.e., promotion of one signaling pathway over another at the same receptor) or probe dependence (differing signaling

outcomes based on the identity of the orthosteric ligand) on 5-HT_{2C}R function, which may be exploited as a novel modality toward the treatment of complex neuropsychiatric disorders (**Fig. 2.7**)³⁸³. Importantly, from a structural biology perspective, rapid progress is being made in the analysis of structural determinants for allosteric modulator function at well-studied GPCRs and a X-ray crystal structure of the 5-HT_{2C}R is now available that is amenable to allosteric modulator docking and modelling^{269, 384}. From the pharmacology and medicinal chemistry perspectives, key concepts with regard to GPCR allosteric modulator discovery and development have been extensively analyzed and reported, with a major focus on mGluR and muscarinic receptor allosteric modulators^{385, 386}. These insights on how to approach the development of GPCR allosteric modulators lay the groundwork for the exploration of allosteric modulation at other GPCRs, including efforts to develop allosteric modulators for the 5-HT_{2C}R³⁸⁷.

Certain distinctive challenges exist in the development of GPCR allosteric modulators, which are applicable to the 5-HT_{2C}R (see reviews)^{85, 377, 388}. For instance, less-conserved allosteric sites across a subfamily of receptors (e.g., 5-HT₂Rs) that are a result of decreased evolutionary pressure at these sites might lead to residue or structural differences in the allosteric site of the 5-HT_{2C}R between species. Additionally, most drug discovery initiatives in this arena ascribe pharmacological profiles to discovered compounds based upon screening in cells expressing the human unedited (INI) 5-HT_{2C}R, however, this is not the most abundant isoform localized in brain and the importance of the diversity of signaling afforded by RNA editing of the 5-HT_{2C}R is left out of the equation of developing new ligands in this chemical space. The potential of probe dependence of novel 5-HT_{2C}R allosteric modulators necessitates careful selection of orthosteric ligands for assays in which the endogenous ligand 5-HT is a preferred choice. However, efforts to selectively potentiate the FDA-approved anti-obesity medication and 5-HT_{2C}R agonist **14** at the 5-HT_{2C}R over other 5-HT₂Rs should preferentially employ **14** in cell-based screening assays. Further, allosteric modulator design may suffer from a featureless or “flat”

structure-activity relationship (SAR) if only binding affinity or efficacy are considered without appreciation of other parameters such as the cooperativity between the affinity and efficacy of the allosteric and orthosteric ligands. Elegant work has been accomplished to aid in the quantification of allosteric effects through the development of the “operational model of allostery”, which may be employed to aid analysis of SAR and appropriately define allosteric modulator mechanism³⁷⁵. Given that 5-HT_{2C}R agonists interact at the conserved orthosteric site of the receptor and, in general, 5-HT_{2C}R agonists are of similar chemotypes, PAMs targeting a topologically distinct site may be ideal for the discovery of selective small molecules with expanded clinical utility.

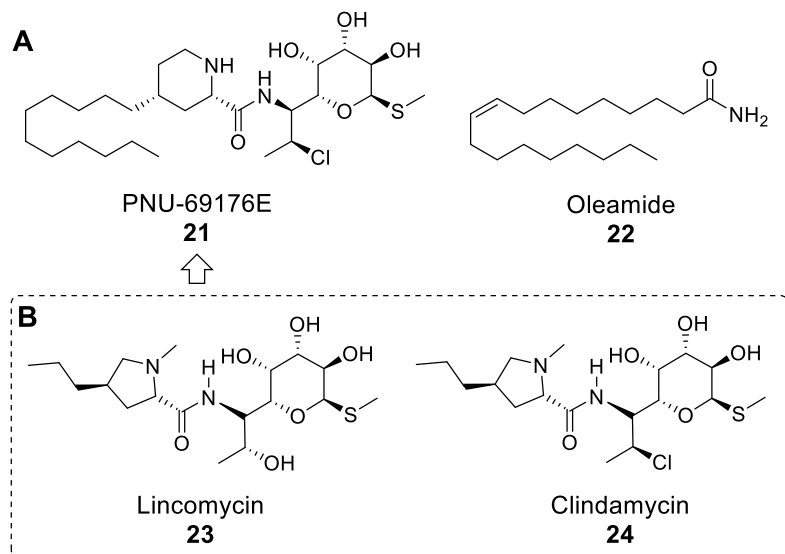
5. THE CURRENT STATE OF 5-HT_{2C}R POSITIVE ALLOSTERIC MODULATORS

The design of allosteric modulators for GPCRs is a relatively recent endeavor and interest in designing allosteric modulators for numerous, diverse GPCRs is increasing (see reviews)^{1, 85, 374}. Very few examples of allosteric modulators of 5-HT_XR are known. Provided with consistent evidence that activation of the 5-HT_{2C}R will afford therapeutic benefits, it is presumed that 5-HT_{2C}R PAMs will engender therapeutic benefits alongside the intrinsic advantages of allosteric modulation.

The discovery of PNU-69176E (**21**) as the first known subtype-selective 5-HT_{2C}R PAM was the result of an early, undescribed screening of a chemical library by Pharmacia (now Pfizer) in 1999 (**Fig. 2.8**)⁴⁵. Structurally, **21** is an analogue of the natural product antibiotic lincomycin (**23**) and a derivative of the clinically available clindamycin (**24**) (**Fig. 2.8**)³⁸⁹. As such, **21** was likely the product of an antibiotic medicinal chemistry campaign. The compound consists of three readily identifiable fragments. At the core is a piperidinyll carboxamide displaying a 2,4-*cis* geometry. A distinct polar head (PH) moiety comprised of an α -D-galactopyranoside and an undecyl lipophilic tail (LT) contribute to the stereochemistry- and sp³-rich (tetrahedral) framework, a significant departure from known 5-HT_{2C}R activators and small molecule therapeutics in general⁴⁶. The natural

product-like framework can allow for a more robust exploration of the chemical space in three-dimensions versus the typical sp^2 -rich (planar) carbon frameworks commonly employed in medicinal chemistry as a result of the current state of metal-mediated coupling chemistry. However, the calculated physicochemical parameters of **21** are less than ideal according to Lipinski's Rule of Five [e.g., total polar surface area (TPSA) = 111.04, ClogP = 4.90, molecular weight (MW) = 537.21, hydrogen bond donors (HBD) = 5].

Figure 2.8 Early reported 5-HT_{2C}R PAMs and the chemical family from which PNU-69176E was derived



(A) The earliest reported small molecules with allosteric modulatory activity at the 5-HT_{2C}R are PNU-69176E (**21**) and oleamide (**22**). (B) PNU-69176E is an analogue of the natural product antibiotic lincomycin (**23**) and a derivative of the clinically available antibiotic clindamycin (**24**).

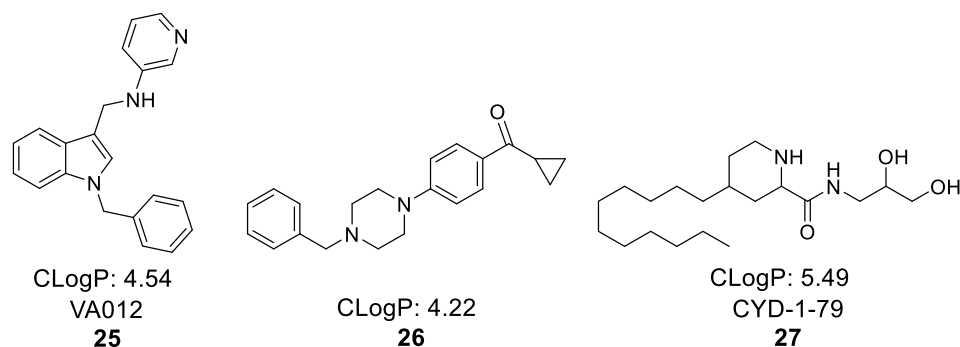
Our team validated 5-HT_{2C}R PAM activity for compound **21** via in-house synthesis and pharmacological characterization in a cell-based assay used to measure Ca_i^{2+} release as a result of 5-HT_{2C}R activation⁴⁶. Compound **21** potentiated Ca_i^{2+} release evoked by 5-HT [0.3 nM, a concentration that induced ~20% of maximal Ca_i^{2+} release (EC₂₀)] in cells stably expressing physiological levels of the unedited (INI), human isoform of the 5-HT_{2C}R. Subsequently, **21** or its diastereomer were added to provide titration curves used to elucidate the extent to which **21** potentiated Ca_i^{2+} release in the presence of 5-HT⁴⁶. We

found that **21** enhanced 5-HT-induced Ca_i^{2+} release over a range of concentrations. On the other hand, the diastereomer did not potentiate 5-HT_{2C}R-mediated signaling under the same conditions, indicating a stereochemical requirement for the PAM activity. Consistent with PAM activity, **21** did not display intrinsic activity as a 5-HT_{2C}R agonist. Furthermore, the **21** did not alter Ca_i^{2+} release in cells stably expressing the highly homologous human 5-HT_{2A}R, underscoring that this scaffold-type can allow for subtype selective targeting of 5-HT₂Rs.

An additional compound that was characterized in earlier work as an allosteric modulator of the 5-HT_{2C}R was oleamide (**22**), the primary amide of oleic acid (**Fig. 2.9**). Structurally, oleamide contains a primary amide and a long hydrophobic tail that contains 17 carbons and a *cis*-double bond at the 9-position. Compound **22** was discovered to exist in the cerebrospinal fluid of sleep-deprived cats and has been shown to modulate sleep in rats³⁸⁷. Evidence of its *de novo* synthesis from rat brain microsomes has been reported³⁹⁰⁻³⁹². This naturally occurring compound has been reported to exhibit a complex pharmacological profile interacting with systems including cannabinoid receptors and various 5-HT_XRs^{393, 394}. Initial investigations illustrated that **22** positively modulated 5-HT-induced 5-HT_{2A}R- and 5-HT_{2C}R-mediated chloride currents in *Xenopus* oocytes³⁹⁵. A follow-up study demonstrated that **22** may act as an allosteric modulator at the 5-HT_{2A}R by increasing 5-HT-induced potentiation of phosphoinositide hydrolysis *in vitro* while no effect was observed in the absence of 5-HT. Additionally, in the same study, **22** acted as a NAM at the 5-HT₇R, leading to a decreased production of cyclic adenosine monophosphate (cAMP) in the presence of 5-HT. However, in the absence of 5-HT, **22** displayed partial agonist activity and promoted cAMP production via an allosteric site³⁹⁶. An analysis of **22** and related compounds was conducted to establish ligand subtype selectivity with respect to the 5-HT_{2A}R versus the 5-HT_{1A}R. Compound **22** displayed no selectivity and potentiated signaling through both receptor subtypes in the presence of 5-HT³⁹⁴. In addition to functional modulation of the 5-HT₇R, **22** induced a robust increase in 5-HT binding affinity

to the 5-HT₇R orthosteric site³⁹⁷. Behavioral pharmacological studies in rodents agree with the *in vitro* observations^{392, 393, 398}. Given the complex pharmacology of **22**, further investigation into the optimization of this compound as a potential therapeutic is warranted.

Figure 2.9 A new generation of 5-HT_{2C}R PAMs has emerged



The lead compounds from recent 5-HT_{2C}R PAM discovery projects include VA012 (**25**), **26**, and CYD-1-79 (**27**) respectively. The CLogPs are reported to demonstrate that elevated lipophilicity is common among these newly discovered 5-HT_{2C}R PAMs.

Recently, three groups have embarked on drug discovery campaigns to identify 5-HT_{2C}R PAMs and as a result there are three new synthetic 5-HT_{2C}R lead PAMs that display interesting scaffold diversity (**Fig. 2.9**). In a trend seen among other GPCR allosteric modulators, these compounds are characterized as generally lipophilic, with each displaying a CLogP greater than 4, as calculated by the BioByte algorithm via ChemDraw Professional. While lipophilic small molecules are understood to engender an enhanced ability to pass through the hydrophobic cell phospholipid bilayer and passively diffuse into the CNS, additional pharmacodynamic obstacles are faced when compounds are highly lipophilic³⁹⁹. Thus, these 5-HT_{2C}R PAMs represent the beginning stages of drug discovery in this space.

López-Rodríguez and colleagues reported the first of the recent synthetic 5-HT_{2C}R PAMs, VA012 (**25**), in a manuscript published in 2017 (**Fig. 2.9**)⁴³. The team from Vivia Biotech implemented a proprietary high-throughput screening method based on whole-cell

flow cytometry, termed ExviTech, in which ~1,600 small molecules from an in-house library were screened against the 5-HT_{2C}R at 10 μM concentration in HeLa cells stably expressing physiological levels of the human 5-HT_{2C}R. In the same manner, hits from the 5-HT_{2C}R-based assay were counter-screened at the 5-HT_{2A}R and 5-HT_{2B}R. Hit compound activity was validated via a functional cell-based assay designed to measure IP₁ levels, a well-known component of the Gα_q signaling cascade. The reported compounds are characterized by a common 1-benzyl-1*H*-indole scaffold with various cyclic and heterocyclic moieties substituted at the 3 position. The necessity of an aromatic moiety at the indole 1 position was probed by substituting a cyclopropane ring in this position, which resulted in loss of PAM activity. The project yielded **25**, which was subsequently evaluated for off-target effects showing no effects in a GPCR panel and brain penetration showing a brain-plasma ratio of 3.8 after 120 min at 10 mg/kg in rodents. In an *in vitro* IP₁-based functional assay, **25** potentiated a 5-HT-induced functional response in a concentration-dependent manner at the 5-HT_{2C}R and did not display significant 5-HT binding inhibition at 10 μM, as tested in an *in vitro* competition binding assay. *In vivo*, **25** reduced food intake and body weight gain in a rodent feeding model without producing CNS-related malaise or resulting in taste aversion to **25**. These results support the assertion that 5-HT_{2C}R PAMs may hold therapeutic potential for obesity.

Our group reported a different strategy towards identifying novel 5-HT_{2C}R PAMs in 2019³⁸¹. Following on our work characterizing **21**, we sought to deconstruct this hit into a simplified pharmacophore in which a piperidine core was flanked by an undecyl carbon chain at the 4 position and a simplified alcohol connected by an amide linker at the 2 position⁴⁶. Our primary goal was to improve the drug-likeness of **21**, which was already shown to be subtype selective, by replacing the complex α-D-galactopyranoside with a simplified fragment that retained activity to investigate the therapeutic potential of 5-HT_{2C}R PAMs *in vivo*. The resulting lead compound, CYD-1-79 (**27**), was discovered by substituting a propanediol moiety in place of the α-D-galactopyranoside, which engendered

a more drug-like profile and improved synthetic scale-up feasibility. Compound **27** was confirmed to be an *in vivo* rodent model candidate following *in vitro* pharmacological evaluation, off-target panel screening, and pharmacokinetic/pharmacodynamic profiling (**Fig. 2.9**).

Specifically, **27** enhanced *in vitro* 5-HT_{2C}R functional response to 5-HT in a concentration-dependent manner and was inactive in a similar assay at the 5-HT_{2A}R. A radioligand competition binding assay was used to profile off-target interactions and resulted in no significant binding inhibition at any 5-HT_XR family member. Compound **27** was assessed in a battery of rat behavioral assays following an *in vivo* rat pharmacokinetic evaluation that showed reasonable oral bioavailability ($F\% = 39.1$) and half-life ($T_{1/2} = 5.82 \pm 0.37$ h). We found that **27** suppressed motor activity in the presence of exogenous 5-HT_{2C}R stimulation with the selective 5-HT_{2C}R agonist **16**. In rats trained to discriminate the 5-HT_{2C}R agonist **16** from saline, compound **27** partially substituted for **16** and synergized with a low dose of **16** to substitute fully for the stimulus effects of **16**. Given that the drug discrimination assay has face validity for modeling the subjective effects of drugs that penetrate the blood-brain barrier and has been employed to establish allosteric modulator effects on the interoceptive effects of receptor-selective agonists, these data support the contention that **27** is a 5-HT_{2C}R PAM⁴⁰⁰⁻⁴⁰². Lastly, in a cocaine self-administration model in rats, **27** suppressed cocaine-seeking provoked by exposure to the cocaine-taking environment and cocaine-associated cues. The sensitivity to cocaine-associated cues increases the risk of craving and relapse during abstinence, thus, these findings suggest that **27** may provide value as a therapeutic strategy to extend recovery in CUD.

The latest 5-HT_{2C}R PAM in this trio is **26** which was reported by Yadav and colleagues in 2019 (**Fig. 2.9**)⁴⁰³. This work identifies a phenyl cyclopropyl-linked *N*-heterocycle pharmacophore as producing multiple derivatives with PAM activity at the 5-HT_{2C}R and one compound (**26**) with additional NAM activity at the 5-HT_{2B}R. Robust SAR

studies were reported for their scaffold of interest, however the origin of this pharmacophore and the rationale for designing *N*-heterocycle compounds as potential 5-HT_{2C}R PAMs was not fully disclosed. Interestingly, using an *in vitro* luciferase-based assay, **27** was shown to enhance 5-HT-mediated functional response at the 5-HT_{2C}R up to 139% E_{max}, while additionally reducing 5-HT potency at the 5-HT_{2B}R with no effect on 5-HT E_{max} at the 5-HT_{2B}R. In agreement with its *in vitro* characterization as a 5-HT_{2C}R PAM, **26** decreased food intake with approximately equivalent efficacy as lorcaserin in Sprague Dawley rats. Thus, this report provides additional *in vivo* evidence that 5-HT_{2C}R PAMs may prove to be therapeutically important molecules for obesity and additional optimization should proceed.

6. CONCLUSION AND FUTURE DIRECTIONS

The 5-HT_{2C}R is an important clinical target for obesity and several chronic pathological disorders³⁸², and will certainly continue to be actively pursued for therapeutic development as well as further study of the complex neurobiology that is coordinated through the 5-HT_{2C}R. One such aspect that requires further study is the signaling and trafficking mechanisms of class A GPCRs in their oligomeric forms. Specifically for the 5-HT_{2C}R, it is important to understand the functional implications of homodimerization (two 5-HT_{2C}R proteins) or heterodimerization (one 5-HT_{2C}R protein interacting with, for example, one 5-HT_{2A}R protein), which is only beginning to be unraveled by a few research groups^{292, 293, 404}. As new biological information is available, medicinal chemists will be enabled to strategically design new compounds to modulate oligomerization or biased signaling, which may lead to future breakthrough therapies. The 5-HT_{2C}R PAMs reported to date share an interesting characteristic in that significant increases in 5-HT efficacy (E_{max}), but not potency, at the 5-HT_{2C}R are observed *in vitro*. Observations such as this will direct structural biology studies in the future to investigate conformational shifts responsible for efficacy increases and solving the structure of a PAM-agonist-5-HT_{2C}R co-

complex will provide valuable information towards this goal. It is conceivable that a structure such as this will be available in the coming years due to recent successes in solving 5-HT_{2C}R active and inactive state crystal structures²⁶⁹. Additionally, the discovery of 5-HT_{2C}R PAMs that enhance 5-HT potency will enable the investigation of similar or contrasting *in vivo* effects compared to 5-HT_{2C}R PAMs that enhance 5-HT efficacy alone. In light of the complex modulatory role for the 5-HT_{2C}R in neurobiological processes, a diverse array of ligand modulation modalities should improve our understanding of the specific ligand profiles needed to pursue clinical endpoints.

As an important therapeutic target for diverse neurological and psychiatric disorders, medicinal chemists should pursue diverse mechanisms of receptor engagement at the 5-HT_{2C}R and groups have begun to rise to this challenging task. For agonist discovery, expansion of available pharmacophores is critically important and significant work towards this goal was recently reported by Wacker and co-workers at Bristol-Myers Squibb utilizing an orthosteric-site mutant version of the 5-HT_{2C}R. Additionally, further investigation into the complexity of 5-HT_{2C}R signaling and oligomerization, as studied recently by Cunningham and colleagues³⁷² will help guide future compound design. In conclusion, there has been considerable recent progress in targeting the 5-HT_{2C}R, as shown by the FDA-approved agonist **14**, yet significant gaps in understanding 5-HT_{2C}R biology remain as do pharmacophore challenges for medicinal chemists in moving towards safer, more efficacious clinical therapies targeting the 5-HT_{2C}R.

Chapter 3. Discovery of 4-Phenylpiperidine-2-Carboxamide Analogues as Serotonin 5-HT_{2C} Receptor Positive Allosteric Modulators with Enhanced Drug-Like Properties

E.A. Wold, E.J. Garcia, C.T Wild, J.M. Miszkiel, C.A. Soto, J. Chen, K. Pazdrak, R.G. Fox, N.C. Anastasio, K.A. Cunningham, J. Zhou
Published as *J. Med. Chem.* 2020 63 (14), 7529-7544⁴⁰⁵

Abstract

Targeting the serotonin (5-HT) 5-HT_{2C} receptor (5-HT_{2C}R) allosteric site to potentiate endogenous 5-HT tone may provide novel therapeutics to alleviate the impact of costly, chronic diseases such as obesity and substance use disorders. Expanding upon our recently described 5-HT_{2C}R positive allosteric modulators (PAMs) based on the 4-alkylpiperidine-2-carboxamide scaffold, we optimized the undecyl moiety at the 4-position with variations of cyclohexyl- or phenyl-containing fragments to reduce rotatable bonds and lipophilicity. Compound **12** (CTW0415) was discovered as a 5-HT_{2C}R PAM with improved pharmacokinetics and reduced off-target interactions relative to our previous series of molecules. The *in vivo* efficacy of compound **12** to potentiate the effects of a selective 5-HT_{2C}R agonist was established in a drug discrimination assay. Thus, **12** is reported as a 5-HT_{2C}R PAM with characteristics suitable for *in vivo* pharmacological studies to further probe the biological and behavioral mechanisms of allosteric modulation of a receptor important in several chronic diseases.

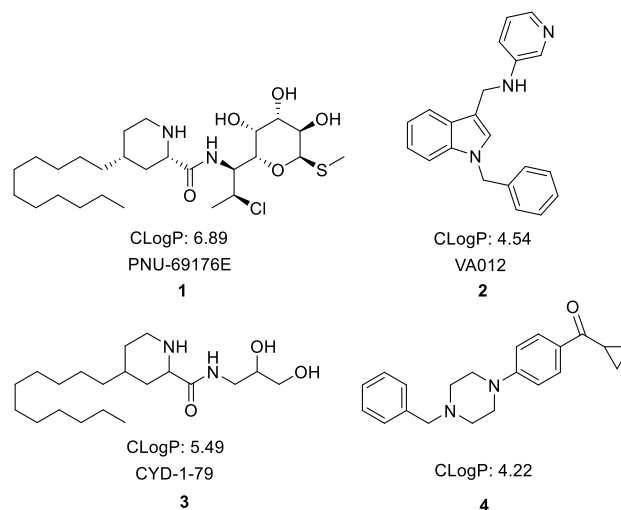
1. INTRODUCTION

Neuropsychiatric and metabolic disorders currently encompass exceedingly costly and intractable diseases both in the U.S. and worldwide. Indeed, obesity and substance use disorders (SUDs) can manifest as chronic conditions that dramatically reduce life expectancy. The serotonin (5-HT) 5-HT_{2C} receptor (5-HT_{2C}R) is a central nervous system (CNS) G protein-coupled receptor (GPCR) that modulates key disease-related neurological pathways and behaviors.⁴⁰⁶ For example, 5-HT_{2C}R agonists suppress food intake and increase satiety in humans and animals,^{319, 324-326, 407} and preclinical studies indicate a major role for the 5-HT_{2C}R in modulating the rewarding and incentive-salience value of psychostimulants (e.g., cocaine), ethanol, and opioids as well as behavioral factors predictive of relapse during recovery from SUDs.^{237, 298, 311, 330, 331} In human studies, the 5-HT_{2C}R agonist lorcaserin improved tobacco smoking cessation rates, while also decreasing corticolimbic activation evoked by presentation of palatable food cues, thus implicating the 5-HT_{2C}R as a potential drug target to treat disorders characterized by reward and cue-associated events.^{339, 340} Therefore, the 5-HT_{2C}R is a promising therapeutic target at the intersection of disinhibited behaviors that contribute to obesity and SUDs, and a pharmacotherapy that could aid in the successful treatment of SUDs would represent a first-in-class drug.^{349, 350}

Selective targeting of the 5-HT_{2C}R remains challenging since each of the 13 5-HT GPCR subtypes accommodates 5-HT at a conserved orthosteric binding site. Among the 5-HT_{2R} subtypes (5-HT_{2AR}, 5-HT_{2BR}, and 5-HT_{2CR}), 5-HT_{2C}R selectivity is necessary to avoid the potential for hallucinations or cardiac valvulopathy that may occur from 5-HT_{2AR} or 5-HT_{2BR} stimulation, respectively.^{351, 352} One possible strategy to achieve selective 5-HT_{2C}R modulation is the rational design of positive allosteric modulators (PAMs).²⁶⁶ By targeting a binding site that is spatially distinct from the conserved 5-HT orthosteric site, divergent residues or topological surfaces may be exploited to achieve 5-

HT_{2c}R selectivity while enhancing the functional response to 5-HT.³⁸³ This strategy has been employed for numerous class A GPCRs¹ and specifically for the discovery of 5-HT_{2c}R PAMs by our group and others (**Figure 3.1**).^{43, 45, 46, 381, 403}

Figure 3.1 Highlighted compounds resulting from the search for synthetic small molecule 5-HT_{2c}R PAMs

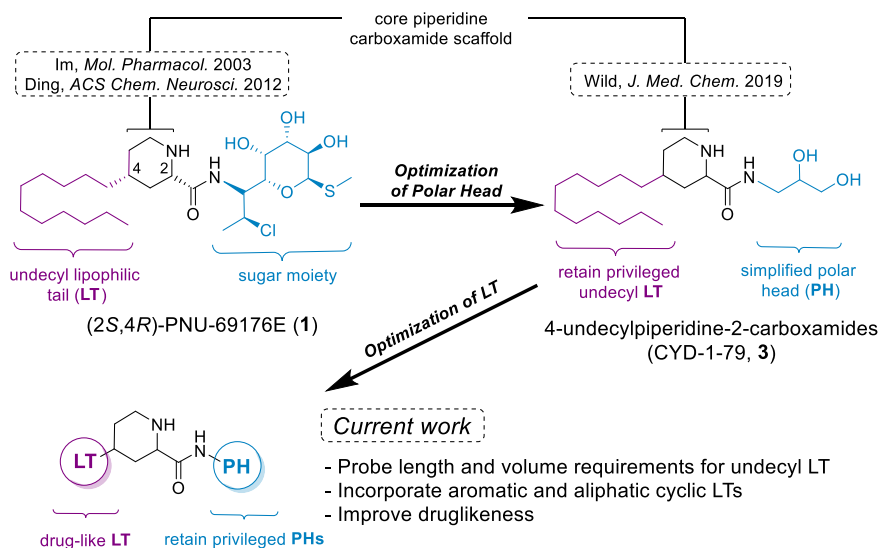


Highlighted compounds resulting from the search for synthetic small molecule 5-HT_{2c}R PAMs. Highlighted here are lead compounds from the published 5-HT_{2c}R PAM drug discovery campaigns. The ClogP, calculated in ChemDraw 18.0, for each compound displays a trend in high lipophilicity.

Our previously described 5-HT_{2c}R PAMs were obtained by an iterative exploration and optimization process beginning with the initial 5-HT_{2c}R PAM small molecule PNU-69176E (**1**). The first priority in this process was the simplification of the α -D-galactopyranoside fragment, termed the polar head (PH), to provide a more drug-like compound for *in vitro* and *in vivo* proof of concept studies (**Figure 3.2**). From this effort, CYD-1-79 (**3**) was obtained and characterized as a selective 5-HT_{2c}R PAM (**Figure 3.1**).³⁸¹ The PH moiety of **3** was modified to retain 5-HT_{2c}R PAM activity while engendering decreased molecular weight and complexity. Next, changes to the undecyl substituent at the 4-position of the piperidine, which is termed the lipophilic tail (LT), were

probed as an option for further improvements. In the current study, we chemically modified the LT position with shorter, compact fragments to reduce lipophilicity while maintaining 5-HT_{2C}R PAM activity (**Figure 3.2**). Additionally, we rationalized that the compact LT substituents would reduce the number of rotatable bonds and improve the drug-likeness of the 4-alkylpiperidine-2-carboxamide scaffold, which was further demonstrated by the calculated physicochemical properties for the synthesized test compounds herein. Importantly, modifying the undecyl LT position with compact, cyclic moieties – providing increased structural rigidity – yielded small molecules that are advantageous for computational molecular modeling and docking studies to ultimately illuminate features of the 5-HT_{2C}R PAM binding site.

Figure 3.2 Medicinal chemistry strategy to achieve optimized 5-HT_{2C}R from PNU-69176E (**1**)

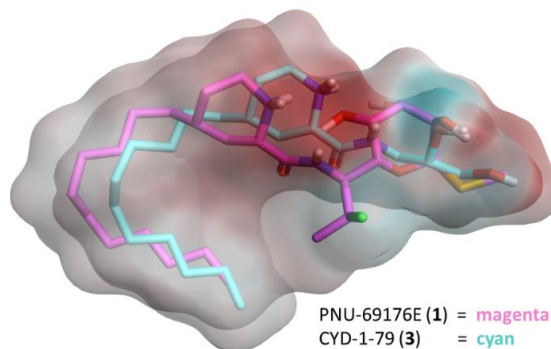


Medicinal chemistry strategy to achieve optimized 5-HT_{2C}R PAMs from PNU-69176E (**1**). A lincomycin derivative, PNU-69176E (**1**), was the first synthetic small molecule reported to allosterically modulate the 5-HT_{2C}R. Subsequent work has focused on chemical modifications of the polar head (PH) and the lipophilic tail (LT) to engender drug-like properties.

2. RESULTS AND DISCUSSION

Chemistry. Allosteric modulation of the 5-HT_{2C}R is a new endeavor with a small number of probe compounds identified in recent years.^{43, 381, 403} Our chemical approach is focused on the optimization of our previously reported compound **3**. Elevation of intracellular calcium (Ca_i²⁺) release is a key downstream impact of 5-HT_{2C}R activation which is oft utilized as a readout in functional cellular assays.²⁷³ Compound **3** was shown to enhance Ca_i²⁺ release ~23% above the maximal effect of 5-HT alone in Chinese hamster ovary (CHO) cells stably transfected with human (h)5-HT_{2C}R. In the absence of 5-HT, **3** had no effect on Ca_i²⁺ release, indicating the PAM nature of this compound. Compound **3** also exhibited *in vivo* efficacy to decrease locomotor activity and suppress cocaine-seeking during abstinence from cocaine self-administration in rats; **3** potentiated the substitution of low doses of the 5-HT_{2C}R agonist WAY163909 in a drug discrimination assay.³⁸¹ Therefore, the 1,2-diol moiety in the PH position of **3** was considered a privileged fragment and was retained. Additional PH fragments were employed in the following chemical series based upon their previously observed activity or inactivity as a basis of comparison.

Figure 3.3 The volume, not length, of the undecyl moiety on PNU-69176E (**1**) and CYD-1-79 (**3**) may contribute to 5-HT_{2C}R PAM activity

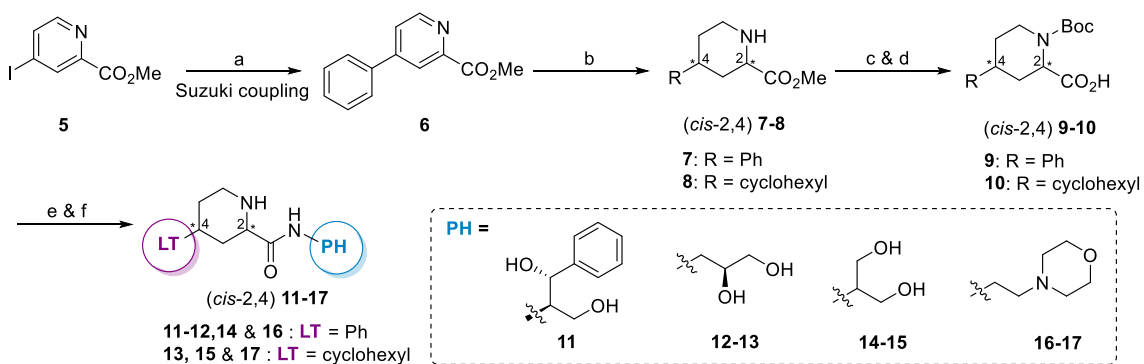


The volume, not length, of the undecyl moiety on PNU-69176E (**1**) and CYD-1-79 (**3**) may contribute to 5-HT_{2C}R PAM activity. Compounds **1** and **3** favor similar minimized conformations which leads to overlapping hydroxyl moieties in the PH and to a folded substructure for the undecyl LT. The preferred, contracted substructure for the undecyl LT suggests that hydrophobic volume is important.

Initial structure-activity relationship (SAR) studies of compound **1** showed that shorter alkyl chains (methyl to *n*-methyl groups) as LTs failed to exert positive allosteric

modulatory actions at the 5-HT_{2C}R⁴⁵, however we reasoned that the volume of the LT, not the length, may play a role in compound activity. This hypothesis was based partially upon *in silico* ligand minimization and electrostatic complementarity experiments comparing compound **1** with compound **3** (**Figure 3.3**). First, the modeling shows how the replacement of the α -D-galactopyranoside PH fragment with the simplified 1,2-diol fragment found in **3** retains key hydroxyl group orientations and thus potentially conserve H-bond partners and interaction distances. Second, the minimized alignment of the undecyl LT fragments are shown in a conformation that suggests an exploitation of a hydrophobic binding pocket due to lipophilic volume. Thus, we designed new small molecules to incorporate shorter LTs with aromatic and aliphatic rings able to provide a comparable volume to the longer alkyl chain counterparts. Crucially, these new analogues reduce the overall number of rotatable bonds and engender enhanced drug-like properties and development potential.

Scheme 3.1 Synthesis of CYD-1-79 analogues with compact phenyl or cyclohexyl LTs

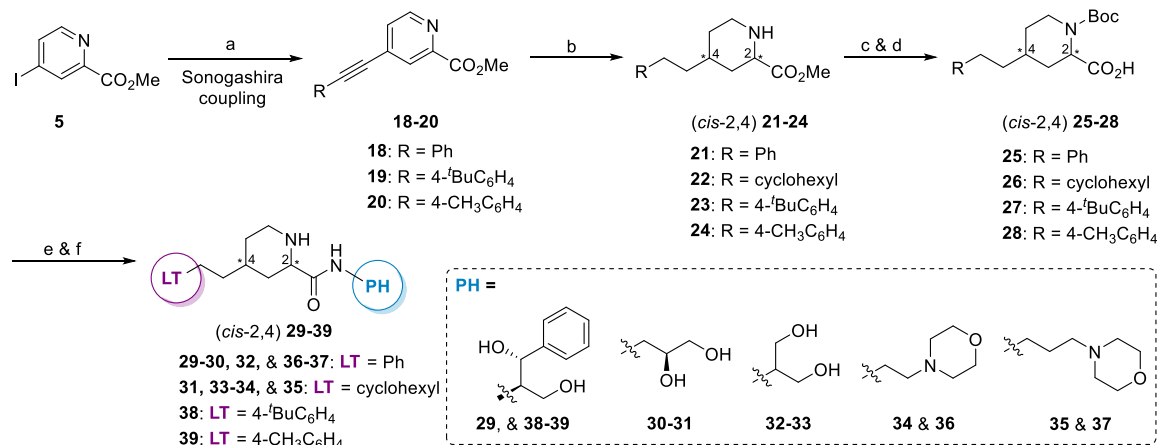


Reagents and conditions: a) phenylboronic acid, Pd(PPh₃)₄, Na₂CO₃, EtOH/H₂O/PhMe = 2:1:1, reflux. b) H₂, PtO₂, HCl/MeOH/H₂O, rt, 16 h. c) (Boc)₂O, Et₃N, MeOH, rt, 16 h. d) LiOH, THF/H₂O (v/v = 2:1), rt, 48 h. e) amino alcohols, HBTU, DIPEA, DMF, rt, 16 h. f) TFA, CH₂Cl₂, rt.

Similar to our previously established synthetic route, a six-step protocol from **5** affords the target compounds.^{46, 381} The iodinated ester of picolinic acid (**5**) underwent Suzuki (**Scheme 3.1**) or Sonogashira coupling (**Scheme 3.2**) to provide incorporation of various LTs that included aromatic rings (e.g., phenyl, phenethyl, 4'-methylphenethyl, and

4'-*t*-butylphenethyl fragments). Metal-catalyzed hydrogenation, Boc-protection, and hydrolysis readily provided the (*cis*-2,4)-piperidyl carboxylic acids **9-10** and **25-28**. As a result of the metal-catalyzed reduction conditions, the pyridine ring was consistently reduced, whereas the aromatic LTs either did not undergo hydrogenation or were fully reduced into separable products. Therefore, isolable aliphatic versions of the aromatic LTs were obtained, and upon HBTU-mediated coupling to suitable amines and N-Boc deprotection, target compounds **11-17** and **29-39** were obtained. All isomers with the 2-amino-1-phenyl-1,3-propanediol PH were separable, consistent with our previous report.³⁸¹ All other compounds were an inseparable mixture of isomers and were tested as such (Schemes 3.1 & 3.2).

Scheme 3.2 Synthesis of CYD-1-79 analogues with phenethyl, ethylcyclohexyl, or substituted phenethyl LTs



Reagents and conditions: a) Phenylacetylenes, CuI, Pd(PPh₃)₂Cl₂, Et₃N, rt, 12 h. b) H₂, PtO₂, HCl/MeOH/H₂O, rt, 16 h. c) (Boc)₂O, Et₃N, MeOH, rt, 16 h. d) LiOH, THF/H₂O (v/v = 2:1), rt, 48 h. e) amino alcohols, HBTU, DIPEA, DMF, rt, 16 h. f) TFA, CH₂Cl₂, rt.

Compound Screening *In Vitro*. A highly characterized intracellular pathway of the 5-HT_{2C}R is the activation of phospholipase C β via G $\alpha_{q/11}$ proteins leading to the production of inositol-1,4,5-trisphosphate and diacylglycerol, resulting in increased Ca_i²⁺ release from intracellular stores.²⁶⁴ Therefore, the functional characterization of these synthetic compounds was determined using a fluorescence-based, *in vitro* Ca_i²⁺ release

assay to measure activation of the 5-HT_{2C}R signaling pathway. The Ca_i²⁺ release assay was conducted in Chinese hamster ovary (CHO) cells stably transfected with the human 5-HT_{2C}R (unedited INI isoform; h5-HT_{2C}R-CHO cells). The maximum 5-HT-induced Ca_i²⁺ release (E_{\max}) was measured and normalized to 100% response. All test compounds were assessed in 4-6 biological replicates, each conducted in technical triplicates and results are shown relative to the E_{\max} of 5-HT alone. Compound **1** increased 5-HT-evoked release in titration studies and evoked a leftward shift of the 5-HT-evoked Ca_i²⁺ response curve.⁴⁶ Therefore, the initial compound screen was conducted at 1 nM to determine the extent to which compounds enhanced Ca_i²⁺ release elicited by increasing concentrations of 5-HT in h5-HT_{2C}R-CHO cells. The h5-HT_{2C}R-CHO cells were pretreated for 15 min with each test compound to determine intrinsic agonist activity in each assay. None of the compounds tested exhibited intrinsic activity to induce Ca_i²⁺ release in h5-HT_{2C}R-CHO cells in the absence of 5-HT. The assessment of compounds tested in the Ca_i²⁺ release assay in h5-HT_{2C}R-CHO cells is summarized in **Table 3.1** and **Table 3.2**, and all concentration response curve shift plots are in this manuscript's supplemental figures.

Of the 22 compounds tested, several displayed 5-HT_{2C}R PAM activity comparable to the previously reported **3** which displayed an approximate 23% increase in the E_{\max} for 5-HT-induced Ca_i²⁺ release in h5-HT_{2C}R-CHO cells.³⁸¹ Compounds **(2S,4R)-11** and **(2R,4S)-11** included a phenyl ring as the LT and incorporated a (1*S*,2*S*)-2-amino-1-phenyl-1,3-propanediol PH (**Table 3.1**). In our previous report, when combined with an undecyl LT, the (1*S*,2*S*)-2-amino-1-phenyl-1,3-propanediol PH displayed negative allosteric modulatory (NAM) activity in (2*S*,4*R*) conformation.³⁸¹ However, **(2S,4R)-11** showed no activity while **(2R,4S)-11** displayed modest allosteric activity in the Ca_i²⁺ assay. Intriguingly, both **12** and **13**, which incorporate an isomer [(*S*)-1,2-diol] of the same 1,2-diol moiety PH as compound **3**, displayed 5-HT-evoked E_{\max} values of 127.4 ± 8.79% (p<0.05; **Figure 3.4A**) and 117.9 ± 4.71% (p<0.05), respectively, close to the activity seen for **3** (123.2 ± 4.1%, p<0.05).³⁸¹ This outcome was observed even though the new

analogues possess a phenyl ring and a cyclohexyl ring as the LT (**12** and **13**, respectively), which is an extreme departure from the eleven-carbon tail in our previously reported compounds. These findings provide additional confirmation that the 1,2-diol moiety is a privileged fragment. The 1,3-propanediol as a PH did promote PAM activity when coupled with a phenyl LT (**14**, $118.8 \pm 2.92\%$, $p < 0.05$; **Figure 3.4B**). The same PH with a cyclohexyl LT (**15**) and the retention of the phenyl or cyclohexyl LT with incorporation of a morpholino with a two-carbon spacer (**16** and **17**, respectively) did not result in positive allosteric effects.

Table 3.1 Effects of 4-alkylpiperidine-2-carboxamide derivatives (1 nM) on 5-HT-induced Ca_i^{2+} release in h5-HT_{2C}R-CHO cells

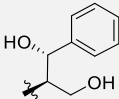
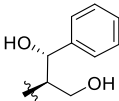
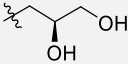
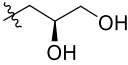
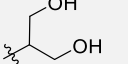
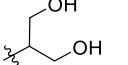
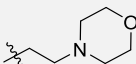
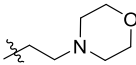
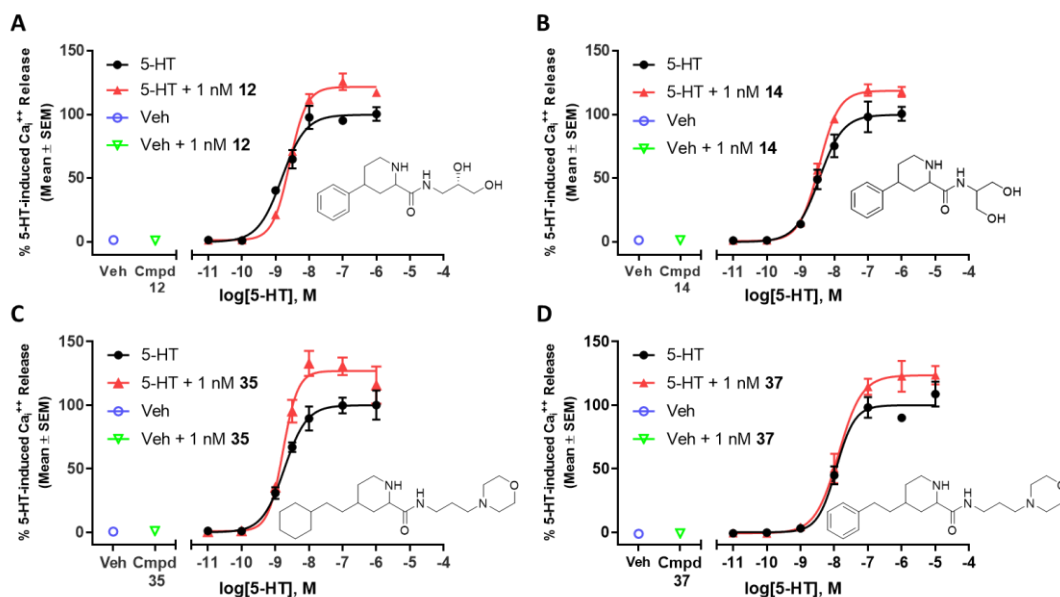
Compound Number	LT	PH	<i>E</i> _{max} RFU (% 5-HT) ^a
(2 <i>S</i> ,4 <i>R</i>)- 11			102.9 ± 7.67
(2 <i>R</i> ,4 <i>S</i>)- 11			$118.2 \pm 2.39^*$
12			$127.4 \pm 8.79^*$
13			$117.9 \pm 4.71^*$
14			$118.8 \pm 2.92^*$
15			119.1 ± 10.20
16			113.6 ± 7.72
17			121.4 ± 12.16

Figure 3.4 Effects of select compounds with shortened lipophilic tail (LT) moieties provide evidence that hydrophobic volume contributes to target engagement.

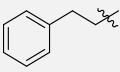
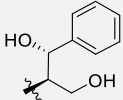
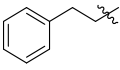
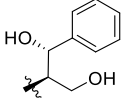
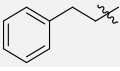
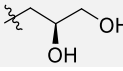
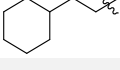
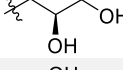
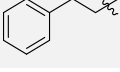
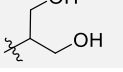
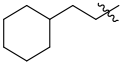
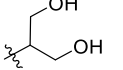
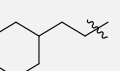
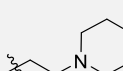
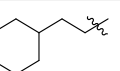
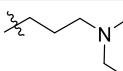
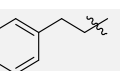
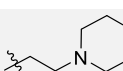
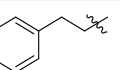
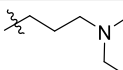
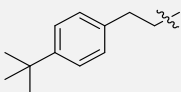
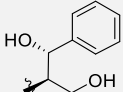
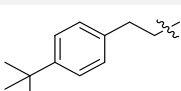
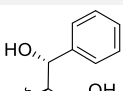
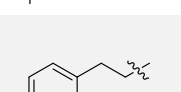
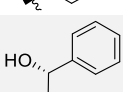


Effects of select compounds with shortened lipophilic tail (LT) moieties provide evidence that hydrophobic volume contributes to target engagement. Data are plotted for compounds **12** (A), **14** (B), **35** (C), and **37** (D). The effects of these compounds on 5-HT-induced Ca_i^{2+} release in h5-HT_{2c}R-CHO cells are shown in the absence (black) and presence of the test compound (red) against the concentration-response curve for 5-HT. The assessment of vehicle (HBSS, blue circle), or vehicle with test compound (green triangle) is also illustrated.

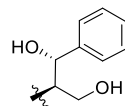
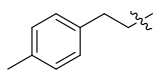
Utilization of the PHs while incorporating either phenethyl or ethylcyclohexyl LTs resulted in a series of molecules with a range of activity (~94% - ~117%) dependent upon the type of PH incorporated (Table 3.2). Positive allosteric effects were not seen with the 1,2-diol and 1,3-diol PHs with either aforementioned LT (compounds **30** – **33**). For both the ethylcyclohexyl and phenethyl LT, the two-carbon spaced morpholino as the PH did not produce PAM effects (**34**, **36**). However, the addition of the morpholino with a three-carbon spacer did produce PAM effects, suggesting there is a length requirement for morpholino fragment compounds (**35**, $118.2 \pm 3.61\%$, $p < 0.05$; Figure 3.4C; **37**, $117.9 \pm 5.90\%$, $p < 0.05$; Figure 3.4D). An increase in the length and volume of the LT via the inclusion of a *t*-butyl or methyl in the 4-position of the phenethyl LT did not lead to active compounds (**38** – **39**), an interesting finding given previous suggestions that LT length is

a critical component of PAM activity for this chemotype.⁴⁵ These data reinforce the notion that a diol moiety PH, specifically an (*S*)-1,2-diol fragment, is an important structural element in 5-HT_{2C}R PAMs (compounds **3** and **12**) and that the 5-HT_{2C}R PAM pharmacophore is accepting of compact, cyclic LTs.

Table 3.2 Effects of 4-alkylpiperidine-2-carboxamide derivatives (1 nM) on 5-HT-induced Ca_i²⁺ release in h5-HT_{2C}R-CHO cells

Compound Number	LT	PH	E _{max} RFU (%5-HT) ^a
(2 <i>S</i> ,4 <i>R</i>)-29			109.8 ± 2.29*
(2 <i>R</i> ,4 <i>S</i>)-29			108.7 ± 7.91
30			108.5 ± 7.41
31			109.7 ± 8.42
32			101.0 ± 5.26
33			106.4 ± 6.75
34			110.2 ± 6.68
35			118.2 ± 3.61*
36			94.2 ± 2.48
37			117.9 ± 5.90*
(2 <i>S</i> ,4 <i>R</i>)-38			114.7 ± 10.10
(2 <i>R</i> ,4 <i>S</i>)-38			106.7 ± 10.25
(2 <i>R</i> ,4 <i>S</i>)-39			98.9 ± 4.15

(2*S*,4*R*)-**39**



99.3 ± 2.15

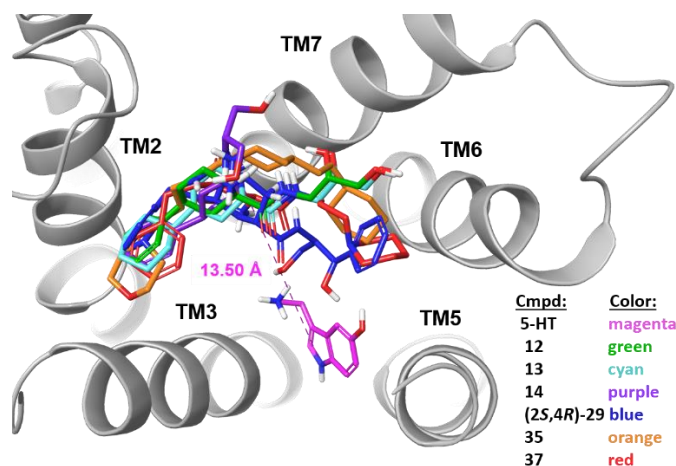
Compared to **3**, *in vitro* characterization of **12** displayed a similar increase in the E_{\max} of 5-HT-induced Ca_i^{2+} release in the absence of a leftward shift in the EC_{50} , indicating that **12** improved the efficacy of 5-HT without a change in potency for 5-HT at the 5-HT_{2C}R. Compound **12** was counter-screened in h5-HT_{2A}R-CHO cells and no alteration in the E_{\max} or EC_{50} of 5-HT-induced Ca_i^{2+} release was observed (**Table 3.3**). Likewise, the additional compounds [(**2*R*,4*S***)-**11**, **13**, **14**, **29**, **35**, **37**] that were validated *in vitro* as 5-HT_{2C}R PAMs did not significantly alter the E_{\max} or EC_{50} of 5-HT-induced Ca_i^{2+} release in h5-HT_{2A}R-CHO cells. Thus, the herein identified 5-HT_{2C}R PAMs exhibit selectivity against 5-HT_{2A}R *in vitro*.

Table 3.3 Effects of active 5-HT_{2C}R PAMs (1 nM) on 5-HT-induced Ca_i^{2+} release in h5-HT_{2A}R-CHO cells

Compound Number	LT	PH	E_{\max} RFU (%5-HT) ^a
(2<i>R</i>,4<i>S</i>)- 11			102.6 ± 2.81
12			103.4 ± 5.79
13			97.8 ± 2.44
14			99.3 ± 1.58
29			103.9 ± 2.22
35			97.2 ± 4.64
37			97.9 ± 1.99

Molecular Modeling and Docking of 5-HT_{2C}R PAMs. The narrow range of the elevated E_{\max} values resulting from our 5-HT_{2C}R PAMs suggests a conserved positive allosteric modulatory mechanism, likely originating from binding to a shared allosteric binding site. To probe possible binding sites the Schrödinger Drug Discovery Suite was used for modeling the 5-HT_{2C}R and for docking the 5-HT_{2C}R PAM molecules. This effort utilized the recently reported 5-HT_{2C}R X-ray crystal structure in complex with the orthosteric agonist ergotamine (PDB: 6BQG).²⁶⁹ Ergotamine is larger than the 5-HT_{2C}R endogenous agonist 5-HT and ergotamine interacts with numerous 5-HT_{2C}R residues throughout the transmembrane domains (TM) and extracellular loop 2 (ECL2). In this context, PAM docking protocols are improved due to the stabilization and resultant enhanced atomic resolution in the outer regions of the TM as well as the ECL2. However, to obtain a docking model that is representative of the 5-HT_{2C}R conformation encountered by 5-HT_{2C}R PAMs *in vitro* and *in vivo*, the Schrodinger Induced Fit Docking (IFD) utility was used to replace ergotamine with 5-HT and allow ligand-induced conformational flexibility. Briefly, the X-ray crystal structure of ergotamine-5-HT_{2C}R (PDB: 6BQG) was preprocessed and optimized with the Schrödinger Protein Preparation Wizard using default settings and each ligand (5-HT and 5-HT_{2C}R PAMs) was prepared with the LigPrep tool to generate 3D conformations for docking. Serotonin was docked to the 5-HT_{2C}R orthosteric site via IFD with a Glide grid centered on the ergotamine indole N atom and default values for sidechain and residue flexibility. The resultant 5-HT-5-HT_{2C}R complex model (**Figure 3.5**) was checked against published site-directed mutagenesis studies to assess 5-HT orientation accuracy and was subsequently used for the remaining ligand docking.⁴⁰⁸

Figure 3.5 Molecular docking illustrates the considerable overlap in ligand poses of six 5-HT_{2C}R PAMs

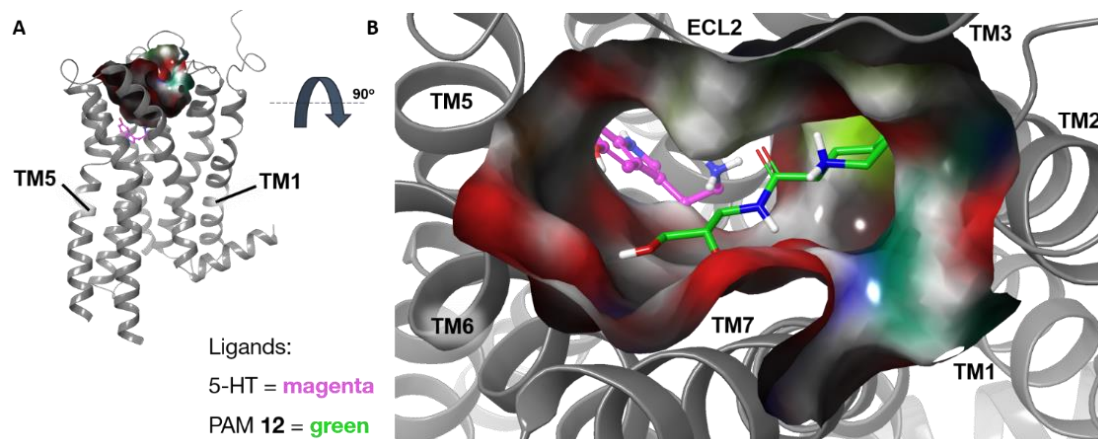


Molecular docking illustrates the considerable overlap in ligand poses of six 5-HT_{2C}R PAMs. Six small molecules with a 5-HT_{2C}R PAM profile are represented in different colors along with the endogenous agonist 5-HT. A representative pose for each 5-HT_{2C}R PAM was selected rationally from a top-scoring, enriched cluster docked to the 5-HT_{2C}R X-ray crystal structure (PDB: 6BQG). A measurement from the 5-HT (magenta) indole N atom to the piperidine core N atom of compound **12** was found to be 13.5 Å (illustrated by the dashed line).

Selected compounds that displayed *in vitro* 5-HT_{2C}R PAM functional activity were docked to the 5-HT-5-HT_{2C}R complex model using Glide XP precision and IFD without designated exclusion parameters, as the model contained a 5-HT molecule to block the interaction of PAMs with the orthosteric binding site. Scoring functions (GScore) and biological and chemical rationales were used for ligand pose clustering and selection. The result upon docking six PAMs [**12**, **13**, **14**, (**2S,4R**)-**29**, **35**, **37**] to the 5-HT-5-HT_{2C}R model is a striking display of conformational agreement at a spatially distinct allosteric site (**Figure 3.5**). The distance between the 5-HT indole N-atom and the piperidine ring N-atom from the core of **12** is 13.5 Å. Surface mapping using electrostatics and polarity was used for further docking site characterization with **12**, which shows that the allosteric site is positioned near extracellular-facing regions of the 5-HT_{2C}R (**Figure 3.6A**). Additionally, the PAM orientation reaches across the transmembrane bundle from a lipophilic pocket between TM2 and TM3 towards polar residues located in TM6 and TM7 (**Figure 3.6B**). Interestingly, the lipophilic and polar surfaces of the docking site correspond to the LT and

PH moieties that have been featured in all active 5-HT_{2C}R PAMs throughout our discovery and optimization efforts.

Figure 3.6 Docking site surface mapping illustrates the distinct location of the proposed allosteric site in relation to 5-HT bound to the 5-HT_{2C}R.

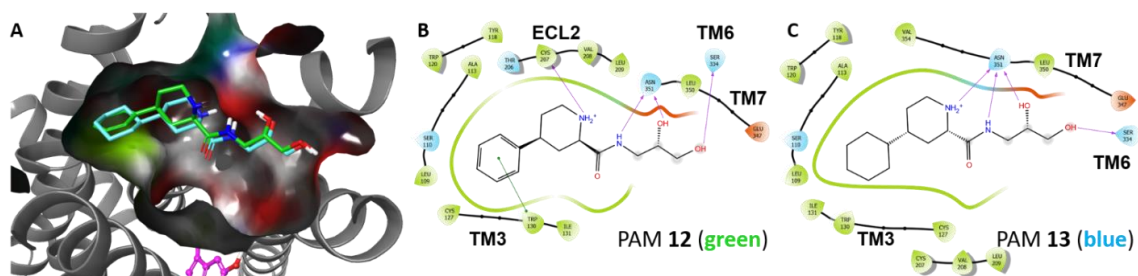


Docking site surface mapping illustrates the distinct location of the proposed allosteric site in relation to 5-HT bound to the 5-HT_{2C}R. (A) The side profile view of 5-HT_{2C}R with the protein surface illustrated around the allosteric docking site in the transmembrane helical bundle. 5-HT (magenta) can be seen below the surface illustration. (B) Docking pose of **12** (green) is shown bridging the helical bundle at a site distinct from 5-HT. (5-HT_{2C}R PDB: 6BQG)

The depth of the lipophilic pocket between TM2 and TM3 drew our attention and likely provides a volume for anchoring the PAM LT. A comparison of docking poses of the 4-phenyl substituted **12** and the 4-cyclohexyl substituted **13** (Figure 3.7A) reveals an aromatic, π - π stacking interaction between **12** and TRP130 located in TM3 (Figure 3.7B), which is not present with the non-aromatic **13** and may prove to be an important feature of the lipophilic pocket. Of note, when viewing compounds **35** and **37** (Figure 3.5), which contain a less polar morpholine PH and differ by an ethylcyclohexyl or phenethyl respectively, the presence of an aromatic interaction between TRP130 and **37** may result in the phenethyl preferentially occupying the lipophilic pocket. Contrarily, **35** is unable to form an aromatic interaction with TRP130 in the lipophilic pocket and results in a flipped pose in which the morpholine occupies the lipophilic pocket. Consistent with our previous docking results for **3**,³⁸¹ compound **12** forms contacts with SER334 in TM6 and a residue

in the ECL2 (**Figure 3.7B**). Reducing the length and rotatable bond number in the LT of **12** may have allowed for an optimized binding orientation with the number of molecular contacts increasing accordingly compared to **3**. **Figure 3.7B** shows the interaction diagram for **12** and includes an aromatic interaction with TRP130 (TM3), an H-bond interaction between the ionizable N atom of the piperidine ring and CYS207 (ECL2), H-bond interactions between the amide NH, 1,2-diol hydroxy group and ASN351 (TM7), and an H-bond interaction between the remaining 1,2-diol hydroxy group and SER334 (TM6). The 4-cyclohexyl substituted **13** (**Figure 3.7C**) lacks the π - π stacking ability of **12** while retaining activity; thus, suggesting the aromatic interaction is not a major contributor to functional activity. Additionally, the piperidine core configuration of **12** (*2R,4S*) as docked is notably different than that of **13** (*2S,4R*), and, among 5-HT_{2C}R PAMs that returned rational poses, there was no consensus for the preferred conformation. Thus, these findings suggest that the piperidine core may not be critical for binding or functional activity once the PH and LT are in favorable positions.

Figure 3.7 Docking demonstrates aromatic or aliphatic compact LTs orient towards the hydrophobic pocket between TM2 and TM3 of the 5-HT_{2C}R.

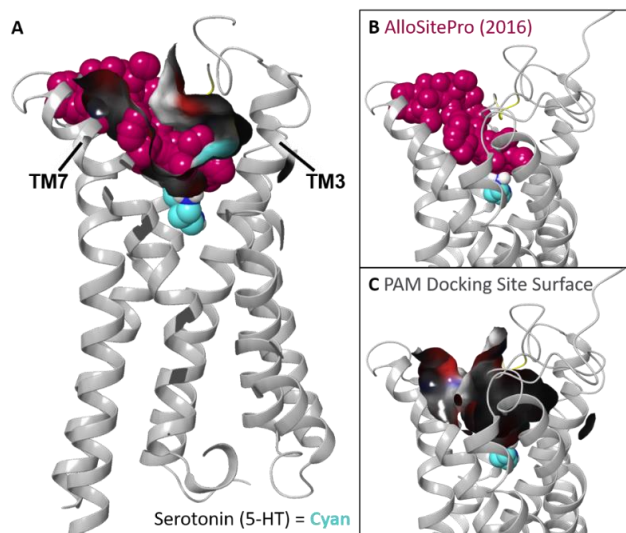


Docking demonstrates aromatic or aliphatic compact LTs orient towards the hydrophobic pocket between TM2 and TM3 of the 5-HT_{2C}R. **(A)** This view features a cutaway of the surface illustration to show how the phenyl and cyclohexyl LTs of **12** (green) and **13** (blue) occupy a hydrophobic pocket within the transmembrane helical bundle. **(B)** Predicted interactions formed by docking **12** including a possible aromatic interaction with TRP130 in the hydrophobic pocket. **(C)** Predicted interactions formed by docking **13**. (5-HT_{2C}R PDB: 6BQG)

Following the prediction of a conserved allosteric docking site via the Schrodinger Drug Discovery Suite, an additional *in silico* methodology was employed to predict

possible allosteric binding sites on the 5-HT_{2C}R without *a priori* PAM structural information. AlloSitePro is a computational tool featuring a support vector machine (SVM) decision engine based on topological and physicochemical properties of the binding pocket.⁴⁰⁹ Thus, this methodology provides a ligand-independent allosteric site prediction, whereas by definition, docking provides a ligand-dependent allosteric site prediction. The web-based AlloSitePro was initiated using the ergotamine-5-HT_{2C}R complex X-ray crystal structure (PDB: 6BQG). The coordinates for predicted allosteric binding site volumes were translated into magenta-colored sphere representation and superimposed on the molecular docking model (**Figure 3.8A-B**). When viewed simultaneously, the allosteric docking site surface map and the allosteric site prediction coordinates are highly convergent, providing further support for the described, putative 5-HT_{2C}R allosteric site (**Figure 3.8A**).

Figure 3.8 Comparison of the allosteric binding site surface map and an independent allosteric binding site prediction program for the 5-HT_{2C}R model.



Comparison of the allosteric binding site surface map and an independent allosteric binding site prediction program for the 5-HT_{2C}R model. **(A)** Composite model displaying docking site protein surface and predicted allosteric site volume (magenta balls) seen via cutaway to visualize the overlap between the models. **(B)** The volume (magenta) determined to be a probable binding pocket capable of accommodating an allosteric modulator. **(C)** From the same angle as panel B, the docking site protein surface is displayed. (5-HT_{2C}R PDB: 6BQG)

***In Vitro* Assessment of Off-target Effects of Compound 12.** To evaluate off-target interactions for a panel of biologically relevant GPCRs and monoamine transporters, **12** was submitted to the National Institute of Mental Health (NIMH) Psychoactive Drug Screening Program (PDSP). At the assessed PAM concentration of 10 μ M, none of the receptor targets returned inhibition greater than 50%, a level considered above assay noise and indicative of test ligand interaction (**Table 3.4**). This result improves upon our previously reported compound **3**, (10 μ M) which exhibited marked inhibition of radioligand binding interactions at the dopamine transporter (DAT; 66.3%), dopamine D3 receptor (71.7%), and α 2A and α 2B receptors (85.1% and 80.7%, respectively).³⁸¹ Interestingly, **12** maintains the same 1,2-propanediol moiety in the PH position as **3**, differing only the LT position by replacing the undecyl moiety with a phenyl substituent. The undecyl to phenyl change results in a more compact, aromatic ligand, which could be expected to increase promiscuity among monoamine GPCRs. However, it is likely that the removal of the undecyl moiety reduces nonspecific lipophilic interactions, while the replacement with a phenyl group allows further site-specific interactions to occur, as suggested by molecular modeling. Thus, the selectivity profile of **12** against numerous GPCR orthosteric sites and the comparative analysis vs. **3** provides evidence that the functional allosteric site occupied by **12** is not an evolutionarily residual binding pocket from another orthosteric site. From a development perspective the selectivity profile strongly supports the advancement of **12** towards *in vitro* pharmacokinetic (PK) evaluation and *in vivo* rodent behavioral characterization.

Table 3.4 Displacement of radioligand binding by compound 12 (μM) in a broad panel of receptors and transporters

Receptor / transporter	Radioligand	% inhibition (10 μM) ^a	K _i (μM) ^b
5-HT _{1A}	[³ H]-8-OH-DPAT	28.4	NT
5-HT _{1B}	[³ H]-GR125743	12.3	NT
5-HT _{1D}	[³ H]-GR125743	15.3	NT
5-HT _{1E}	[³ H]-5-HT	6.3	NT
5-HT _{2A}	[³ H]-Ketanserin	-4.3	NT
5-HT _{2B}	[³ H]-LSD	-7.2	NT
5-HT _{2C}	[³ H]-Mesulergine	26.9	NT
5-HT ₃	[³ H]-LY278584	22.3	NT
5-HT _{5A}	[³ H]-LSD	-4.3	NT
5-HT ₆	[³ H]-LSD	2.5	NT
5-HT ₇	[³ H]-LSD	2.2	NT
D ₁	[³ H]-SCH23390	9.7	NT
D ₂	[³ H]- <i>N</i> -Methylspiperone	7.5	NT
D ₃	[³ H]- <i>N</i> -Methylspiperone	19.4	NT
D ₄	[³ H]- <i>N</i> -Methylspiperone	-9.3	NT
D ₅	[³ H]-SCH23390	9.4	NT
DAT	[³ H]-WIN35428	40.8	NT
SERT	[³ H]-Citalopram	47.5	NT
NET	[³ H]-Nisoxetine	74.4	2.5
α 1A	[³ H]-Prazosin	-16.2	NT
α 1B	[³ H]-Prazosin	-11.0	NT
α 1D	[³ H]-Prazosin	-4.8	NT
α 2A	[³ H]-Rauwolscine	-7.6	NT
α 2B	[³ H]-Rauwolscine	14.5	NT
α 2C	[³ H]-Rauwolscine	-1.8	NT
β 1	[¹²⁵ I]-Pindolol	-7.7	NT
β 2	[³ H]-CGP12177	-15.9	NT
β 3	[³ H]-CGP12177	-11.2	NT
CB ₁	-	-	NT
CB ₂	[³ H]-CP55940	30.6	NT
δ OR	[³ H]-DADLE	-6.1	NT
κ OR	[³ H]-U69593	13.4	NT
μ OR	[³ H]-DAMGO	23.3	NT
GABA _A	[³ H]-Muscimol	7.0	NT

^a The percent (%) inhibition at multiple targets was tested at 10 μM of compound 12. Inhibition results > 50% are considered to be a reliable indication that the test compound displaced the radioligand at the target binding site. ^b For inhibition results > 50%, a K_i value was obtained via a non-linear regression analysis of radioligand competition isotherms. K_i values were calculated from best fit IC₅₀ values using the Cheng-Prusoff equation. NT = not tested, The average K_i from repeated experiments was determined for NET.

***In Vitro* and *In Vivo* Pharmacokinetic (PK) Profiling and *In Silico* Toxicological Profiling.** The PK profile of **12** was assessed to determine whether this compound maintained favorable drug-like properties for utility as an *in vivo* probe. Additionally, *in silico* toxicological prediction scoring was used as a cautionary guide before *in vivo* rat behavioral assessments were made. Initially, **12** was subject to a battery of *in vitro* PK assessments, which returned an excellent profile (**Table 3.5**). In rat liver microsomal fractions spiked with NADPH, clearance (CL_{int}) was $< 9.6 \mu\text{L}/\text{min mg}$ and the half-life ($t_{1/2}$) was > 240 min. Rat plasma protein binding studies displayed a free (unbound) fraction of 66% for **12**. Compound **12** was highly soluble in physiologically relevant conditions and did not display meaningful inhibition of any cytochrome P450 enzyme tested. In an efflux substrate assay utilizing a semi-permeable membrane of Madin-Darby Canine Kidney (MDCK) cells expressing the P-glycoprotein (P-gp) efflux protein and the multidrug resistance mutation 1 (MDR1) gene (MDCK-MDR1), compound **12** exhibited a tolerable efflux ratio of 30.9. *In silico* toxicity profiling was performed using the ProTox-II web-based prediction tool and **12** was predicted to belong to a low toxicity class with a high degree of safety predicted for the doses utilized for *in vivo* assessments (below).⁴¹⁰ We also calculated the CNS multiparameter optimization (MPO) value for compound **12** to be 4.7. CNS MPO values range from 0 to 6 with the higher MPO scores predicted to be more desirable for CNS-penetrant medication candidates.⁴¹¹ Lastly, the *in vivo* PK profile of **12** was obtained in male Sprague-Dawley rats (**Table 3.6**) and was observed as overall favorable and in line with our *in vitro* observations (**Table 3.5**). Specifically, 10 mg/kg of **12** administered iv ($t_{1/2} = 1.25 \pm 0.02$ h) or 20 mg/kg administered po ($t_{1/2}=4.4 \pm 0.5$ h) resulted in appropriate blood plasma concentrations (**Table 3.6**). The brain concentrations of **12** administered at 10 mg/kg iv were 96.4 ± 7.2 ng/g at 15 min and 94.0 ± 1.3 ng/g at 1 hr. The brain-to-plasma ratios at 10 mg/kg iv were 0.07 ± 0.0012 (15 min) and 0.11 ± 0.0056 (1 hr). Brain-to-plasma concentration ratios >0.04 are consistent with CNS

penetration.⁴¹² These cumulative findings suggested that compound **12** would have adequate target exposure for *in vivo* rat behavioral assessments.

Table 3.5 *In Vitro* Pharmacokinetic Profile and *In Silico* Toxicity Prediction for Compound **12**^a

Compound 12			
<i>In Vitro</i> Pharmacokinetics		<i>In Silico</i> Toxicity (ProTox-II)	
Rat Liver Microsomal Clearance (NADPH)	CL _{int} = <9.6 μL/min mg t _{1/2} = >240 min	Predicted LD ₅₀	3990 mg/kg
Rat Plasma Protein Binding	Fu _{plasma} = 66%	Toxicity Class 1-6 (1 = high, 6 = low)	5
CYP3A4 Inhibition	0.0% (10 μM)	Prediction Accuracy	69.26%
CYP2C9 Inhibition	0.0% (10 μM)	Organ Toxicity (probability)	Inactive (0.83)
CYP2D6 Inhibition	1.9% (10 μM)	Carcinogenicity (probability)	Inactive (0.71)
CYP2C19 Inhibition	0.0% (10 μM)	Immunotoxicity (probability)	Inactive (0.99)
CYP1A2 Inhibition	11.8% (10 μM)	Mutagenicity (probability)	Inactive (0.66)
Kinetic Solubility (PBS; pH 7.4)	>100 μM (2 hr)	Cytotoxicity (probability)	Inactive (0.76)
MDCK-MDR1 Permeability	P _{app} ^{A→B} = 0.04 • 10 ⁻⁶ cm/s	Aryl hydrocarbon Receptor (probability)	Inactive (0.96)
	P _{app} ^{B→A} = 1.3 • 10 ⁻⁶ cm/s	Estrogen Receptor Alpha (probability)	Inactive (0.90)
	Efflux ratio = 30.9	Androgen Receptor (probability)	Inactive (0.95)

^a*In vitro* PK included assessment of 10 μM of compound **12** in liver microsomal clearance performed under NADPH-dependent conditions and cytochrome P450 enzymatic inhibition assays performed and represented as percent inhibition. The P-gp efflux substrate experiment employed Madin-Darby Canine Kidney (MDCK) cells expressing multidrug resistance mutation 1 (MDR1) gene. *In silico* toxicity prediction profile shown along with statistical probabilities (more information at http://tox.charite.de/protox_II/).

Table 3.6 *In Vivo* Pharmacokinetic Profile and Brain Penetrability of Compound 12^a

Pharmacokinetic profile of 12							
Dose (mg/kg)	T _{1/2} (h)	T _{max} (h)	CL (L h ⁻¹ kg ⁻¹)	V _{ss} (L/kg)	C _{max} (ng/mL)	AUC _{0-inf} (ng·h·mL ⁻¹)	F (%)
10, iv	1.25 ± 0.02	<i>b</i>	3.28 ± 0.2	5.4 ± 0.3	2408.6 ± 216.8	3065.6 ± 184.7	<i>b</i>
20, po	4.4 ± 0.5	1.3 ± 0.34	10.89 ± 3.5	70.6 ± 23.7	411.3 ± 105.7	2244.7 ± 667.8	36.3 ± 11

Brain penetration analysis of 12				
Dose (mg/kg)	Time (h)	Brain conc. (ng/g)	Plasma conc. (ng/mL)	Brain:Plasma Ratio
10, iv	0.25	96.4 ± 7.2	1486.5 ± 89.6	0.07 ± 0.0012
10, iv	1.0	94.0 ± 1.3	892.1 ± 39.1	0.11 ± 0.0056

^aValues are the average of results (± SEM) from male Sprague-Dawley rats (n = 3/treatment group). Vehicle, 10% DMSO:90% 2-hydroxypropyl-β-cyclodextrin (HP-β-CD). T_{1/2}, half-life; T_{max}, time of maximum concentration; CL, plasma clearance; V_{ss}, volume of distribution; C_{max}, maximum concentration; AUC_{0-inf}, area under the plasma concentration–time curve; F, oral bioavailability; Time, hours after dose for brain collection; Brain conc., averaged concentration of **12** in tissue sample. ^bNot determined.

Effects of Compound 12 in a WAY163909 vs. Saline Drug Discrimination

Assay. The drug discrimination assay is a powerful *in vivo* tool with face validity for determining the interoceptive (subjective) effects of novel compounds as well as for establishing their mechanisms of action in humans and animals.^{381, 413-422} This assay has been employed to reliably characterize the neuropharmacological profile of 5-HT_{2C}R agonists (e.g., *m*-chlorophenylpiperazine, Ro 60-0175, WAY163909) as well as GPCR allosteric modulators.^{381, 414, 417-421} In the present series of studies, we trained rats (n=13) to discriminate the selective 5-HT_{2C}R agonist WAY163909 [0.75 mg/kg, intraperitoneal (ip); 15 min pretreatment] from an equivalent volume (1 ml/kg) of saline (0.9% NaCl) in a two-lever drug discrimination protocol under a fixed ratio 20 (FR 20) schedule of water reinforcement.³⁸¹ Two pharmacological manipulations were performed during test sessions. In substitution tests, animals were tested for lever selection after the administration of various doses of the training drug WAY163909 or compound **12**. In combination tests, animals were administered **12** (0.5-2 mg/kg) with a dose of

WAY163909 (0.5 mg/kg) that produced ~50% WAY163909-appropriate responding when given alone. We also assessed the ability of the selective 5-HT_{2C}R antagonist SB242084 to block the substitution of compound 12 *plus* a low dose of WAY163909.⁴²³

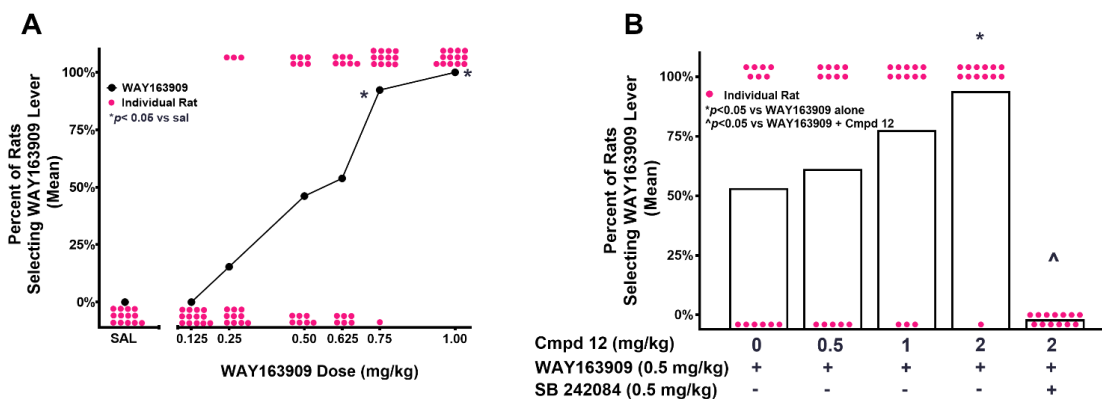
All rats acquired the WAY163909 vs. saline discrimination to criterion. The mean number of sessions required to meet the acquisition criterion (defined as 10 consecutive sessions with $\geq 80\%$ of stimulus-appropriate responding) for the WAY163909 vs. saline discrimination was 57 training sessions (range: 39-68). Substitution of a test drug for the training stimulus is typically a quantal rather than continuous function of stimulus similarity in the two-choice drug discrimination assay.^{381, 413-421} Thus, intermediate doses of WAY163909 evoke responding confined to one lever. Full substitution was defined as $\geq 80\%$ of rats selecting the WAY163909-appropriate lever. Partial substitution was defined as $\geq 40\%$ and $< 80\%$ drug-appropriate responding. As can be seen in **Figure 3.9A**, 0% of rats (0/13 rats) chose the WAY163909-associated lever when administered saline or 0.125 mg/kg, while 92% (12/13 rats) and 100% (13/13) of rats chose the WAY163909-associated lever at the training dose (0.75 mg/kg) and 1.0 mg/kg of WAY163909, respectively (vs. saline, $p < 0.05$). Intermediate doses of WAY163909 (0.25-0.625 mg/kg) resulted in a graded, quantal increase in the number of rats selecting the WAY163909-associated lever. The response rate (responses/min) observed following saline administration was significantly higher than following injection of 0.75 mg/kg ($t_{12} = 2.22$, $p < 0.05$) and 1.0 mg/kg of WAY163909 ($t_{12} = 3.74$, $p < 0.05$). The response rates analyzed for remaining doses of WAY163909 tested (0.125, 0.25, 0.50, 0.625, 1.0 mg/kg, ip) did not differ relative to 0.75 mg/kg of WAY163909 (n.s.). Here, 0.5 and 0.625 mg/kg doses of WAY163909 resulted in 46% and 54% of rats selecting the WAY163909-appropriate lever. Log-probit analyses indicate that the dose of WAY163909 predicted to result in 50% drug-associated responses (ED₅₀) is 0.51 mg/kg, in agreement with our previous study (0.53 mg/kg).³⁸¹

Compound **12** did not exhibit intrinsic activity as a 5-HT_{2C}R agonist *in vitro* (**Figure 3.4A**). This result shaped the hypothesis that **12** would fail to substitute in the

WAY163909 vs. saline discrimination. As expected from *in vitro* analyses, **12** (0.5 - 5 mg/kg), administered ip 30 min prior to testing, evoked saline-lever responding with no change in response rates. The observed lack of substitution supports the premise that **12** and the full 5-HT_{2C}R agonist WAY163909 have dissociable discriminative stimulus effects.

We next tested the hypothesis that **12** would enhance the discriminative stimulus effects of a subthreshold dose of WAY163909 (0.5 mg/kg). To test this hypothesis, rats were pretreated with **12** (0, 0.5, 1 or 2 mg/kg) 15 min before WAY163909 (0.5 mg/kg), followed 15 min later by placement in the chambers. **Figure 3.9B** demonstrates that ~53% of rats (7/13 rats) selected the drug-associated lever following WAY163909 (0.5 mg/kg). Pretreatment with 1 or 2 mg/kg of **12 plus** WAY163909 (0.5 mg/kg) evoked ~77% (10/13 rats) and ~92% (12/13 rats) of rats selecting the WAY163909 lever, respectively, suggesting a synergistic substitution for the training drug (**Figure 3.9B**). The selective 5-HT_{2C}R antagonist SB242084 completely reversed the substitution of **12** (2 mg/kg) *plus* WAY163909 (0.5 mg/kg) in 13/13 rats. In summary, **12** did not evoke intrinsic 5-HT_{2C}R agonist actions, but potentiated a behavioral marker associated with 5-HT_{2C}R agonist-mediated signaling *in vivo*.

Figure 3.9 Compound 12 dose-dependently augments the stimulus effects of the selective 5-HT_{2C}R agonist WAY163909



Compound 12 dose-dependently augments the stimulus effects of the selective 5-HT_{2C}R agonist WAY163909. **(A)** The dose-response relationship for WAY163909 is shown (n = 13 rats). Filled **magenta circles** denote the rats that chose either the saline- or WAY163909-associated lever for each condition/dose. Closed **black circles** denote the mean percentage of rats selecting the WAY163909-associated lever (Y-axis) [**p* < 0.05 vs. saline (SAL)]. **(B)** Compound (**Cmpd**) 12 (0-2 mg/kg) or WAY163909 (0.5 mg/kg) was administered alone or combination as illustrated, with or without pretreatment with SB242084 (0.5 mg/kg). Open bars illustrate the mean percentage of rats selecting the WAY163909-associated lever during combination tests (Y-axis) [**p* < 0.05 vs. WAY163909 (0.5 mg/kg) alone; $\wedge p$ < 0.05 vs. combination of compound **12** plus WAY163909 following pretreatment with SB242084 (0.5 mg/kg)]. The details of the statistical analyses are found in the Methods section.

3. CONCLUSIONS

A series of structurally optimized analogues was rationally designed and synthesized based on the scaffold of our previously reported 5-HT_{2C}R PAM CYD-1-79 (**3**), bearing privileged diol PH moieties. Specifically, the reported investigation focused on the replacement of the undecyl LT moiety with hydrocarbon fragments (cyclic in nature) with a decreased length while approximately maintaining a similar molecular volume to maintain activity and improve drug-likeness. Compound **12** (CTW0415) displayed significant PAM activity at the 5-HT_{2C}R using a fluorescence-based, 5-HT-evoked Ca_i²⁺ release assay and was shown to be inactive as an agonist or allosteric modulator at the 5-HT_{2A}R. An additional six compounds were characterized as 5-HT_{2C}R PAMs, enriching our

computational molecular modelling studies by providing an interesting array of chemical diversity. The molecular modelling and docking studies provide compelling support for a unique, spatially distinct 5-HT_{2C}R allosteric binding site that bridges a hydrophobic pocket between the TM2 and TM3 helices to polar contacts on the TM6 and TM7 helices. One aspect to consider regarding the location of the suggested allosteric site is the evidence of metastable binding sites within transmembrane helical bundles that can briefly accommodate orthosteric ligands.⁴²⁴⁻⁴²⁶ The transient nature of these binding pockets may provide a site or a portion of a binding site for specific allosteric modulators to exert negative or positive effects. Future computational and pharmacological experiments are needed to address these ideas.

Compound **12** was ultimately chosen for progression towards *in vivo* behavioral studies due to superior physicochemical properties, an appropriate MPO value, highly selective off-target profile, and promising pharmacokinetics. Moreover, the structure of **12** lends itself to additional medicinal chemistry efforts as the compound is well within the boundaries of Lipinski's Rule of Five. Compound **12** dose-dependently potentiated the stimulus effects of the 5-HT_{2C}R agonist WAY163909. Importantly, this effect was completely blocked by the 5-HT_{2C}R antagonist SB242084, supporting the critical involvement in the synergism between **12** and a selective 5-HT_{2C}R agonist *in vivo*. Taken together, **12** is an ideal compound for further optimization as a 5-HT_{2C}R PAM and the continued development of this class of molecules may be aided by the structural presentation of a putative 5-HT_{2C}R allosteric binding site.

4. EXPERIMENTAL SECTION

4.1 Chemistry

General. All commercially available starting materials and solvents were reagent grade and used without further purification. Reactions were performed under a nitrogen atmosphere in dry glassware with magnetic stirring. Preparative column chromatography

was performed using silica gel 60, particle size 0.063-0.200 mm (70-230 mesh, flash). Analytical TLC was carried out employing silica gel 60 F254 plates (Merck, Darmstadt). Visualization of the developed chromatograms was performed with detection by UV (254 nm). NMR spectra were recorded on a Bruker-600 (^1H , 600 MHz; ^{13}C , 150 MHz) spectrometer or Bruker-300 (^1H , 300 MHz; ^{13}C , 75 MHz). ^1H and ^{13}C NMR spectra were recorded with TMS as an internal reference. Chemical shifts were expressed in ppm, and J values were given in Hz. High-resolution mass spectra (HRMS) were obtained from Thermo Fisher LTQ Orbitrap Elite mass spectrometer. Parameters include the following: Nano ESI spray voltage was 1.8 kV; Capillary temperature was 275 °C and the resolution was 60,000; Ionization was achieved by positive mode. Melting points were measured on a Thermo Scientific Electrothermal Digital Melting Point Apparatus and uncorrected. The purity of final compounds was determined by analytical HPLC using a Shimadzu HPLC system (model: CBM-20A LC-20AD SPD-20A UV/VIS). HPLC analysis conditions: Waters μ Bondapak C18 (300 \times 3.9 mm); flow rate 0.5 mL/min; UV detection at 270 and 254 nm; linear gradient from 10% acetonitrile in water to 100% acetonitrile in water in 20 min followed by 30 min of the last-named solvent (0.1% TFA was added into both acetonitrile and water). All biologically evaluated compounds have been characterized with ^1H NMR, ^{13}C NMR, HRMS, and HPLC analyses to ensure a purity of > 95%.

General procedure for the synthesis of 11-17. To a solution of **9** or **10** (0.18 mmol) and amino alcohols (0.18 mmol) in 4 mL of DMF was added HBTU (0.23 mmol) and DIPEA (0.45 mmol). The resulting mixture was stirred at room temperature for 16 h. The DMF was removed under vacuum to give a brown oily residue, which was partitioned between CH_2Cl_2 (50 mL) and 10% citric aqueous solution (10 mL). The organic layer was separated and washed with saturated aqueous NaHCO_3 (10 mL). After drying over anhydrous Na_2SO_4 , the solvent was removed under vacuum to give an oily residue. This residue was purified with a silica gel column (5% MeOH in CH_2Cl_2) and afforded the corresponding Boc-protected amide. The amide (0.13 mmol) was dissolved in CH_2Cl_2 (1

mL), followed by the addition of TFA (250 μ L). The resulting mixture was stirred at room temperature. After 2 h, TLC showed that the starting material had disappeared. The solvent was removed under vacuum to give an oily residue. The residue was partitioned between CH_2Cl_2 (30 mL) and saturated NaHCO_3 aqueous solution (10 mL). The organic layer was dried over anhydrous Na_2SO_4 , filtered, and concentrated to give an oily residue. This residue was purified with a silica gel column (eluting with 10% MeOH in CH_2Cl_2), affording compound **11-17**.

(2*S*,4*S*)-*N*-((1*S*,2*S*)-1,3-Dihydroxy-1-phenylpropan-2-yl)-4-phenylpiperidine-2-carboxamide ((2*S*,4*S*)-11) and (2*S*,4*R*)-*N*-((1*S*,2*S*)-1,3-dihydroxy-1-phenylpropan-2-yl)-4-phenylpiperidine-2-carboxamide ((2*S*,4*R*)-11): Compounds (2*R*,4*S*)-11 (36 mg, 40%) and (2*S*,4*R*)-11 (38 mg, 43%) were prepared from **9** (2 steps), respectively. These two isomers could be separated by preparative TLC as colorless amorphous gel. Compound (2*R*,4*S*)-11: ^1H NMR (600 MHz, CDCl_3) δ 7.42 (m, 2H), 7.30 (m, 4H), 7.22 (m, 2H), 7.12 (d, 2H, $J = 7.2$ Hz), 5.06 (d, 1H, $J = 4.2$ Hz), 4.12 (m, 1H), 3.80 (m, 1H), 3.72 (m, 1H), 3.25 (dd, 1H, $J = 3.0$ Hz, 12.0 Hz), 3.10 (d, 1H, $J = 12.0$ Hz), 2.65 (m, 1H), 2.55 (m, 1H), 1.95 (d, 1H, $J = 12.6$ Hz), 1.75 (d, 1H, $J = 12.6$ Hz), 1.75 (m, 1H), 1.28 (q, 1H, $J = 12.6$ Hz). ^{13}C NMR (150 MHz, CDCl_3): δ 174.5, 145.2, 141.4, 128.4, 128.3 (2C), 127.7, 126.7 (2C), 126.4, 126.1 (2C), 125.9, 73.1, 62.9, 61.0, 56.5, 45.7, 42.0, 37.1, 32.9. HRMS Calcd for $\text{C}_{21}\text{H}_{26}\text{N}_2\text{O}_3$: $[\text{M} + \text{H}]^+$ 355.2016; found 355.2022. Compound (2*S*,4*R*)-11: ^1H NMR (600 MHz, CDCl_3) δ 7.56 (d, 1H, $J = 7.8$ Hz), 7.26 (m, 4H), 7.17 (m, 3H), 7.09 (t, 1H, $J = 7.2$ Hz), 7.04 (d, 1H, $J = 7.8$ Hz), 4.96 (d, 1H, $J = 1.8$ Hz), 4.63 (br s, 3H), 4.12 (m, 1H), 3.77 (m, 1H), 3.69 (m, 1H), 3.38 (d, 1H, $J = 12.0$ Hz), 3.06 (d, 1H, $J = 10.8$ Hz), 2.59 (m, 1H), 2.54 (m, 1H), 1.87 (d, 1H, $J = 10.8$ Hz), 1.70 (d, 1H, $J = 10.8$ Hz), 1.44 (m, 1H), 1.27 (q, 1H, $J = 13.2$ Hz). ^{13}C NMR (150 MHz, CDCl_3): δ 173.2, 144.6, 141.5, 128.5 (2C), 128.2 (2C), 127.5, 126.6 (3C), 125.8 (2C), 72.8, 62.8, 59.8, 56.5, 44.9, 41.3, 36.7, 32.1. HRMS Calcd for $\text{C}_{21}\text{H}_{26}\text{N}_2\text{O}_3$: $[\text{M} + \text{H}]^+$ 355.2016; found 355.2019.

(2,4-cis)-N-((S)-2,3-Dihydroxypropyl)-4-phenylpiperidine-2-carboxamide

(12): Compound **12** (20 mg, 91%), a diastereomeric mixture, was prepared from **9** (2 steps) as mixture whitish wax. ¹H-NMR (300 MHz, CDCl₃ : CD₃OD) δ 7.43 – 7.23 (m, 2H), 7.22 – 7.12 (m, 3H), 3.77 – 3.61 (m, 1H), 3.57 – 3.40 (m, 2H), 3.40 – 3.07 (m, 8H), 2.92 – 2.58 (m, 2H), 2.28 – 2.06 (m, 1H), 1.92 – 1.75 (m, 1H), 1.68 – 1.40 (m, 2H). ¹³C NMR (75 MHz, CDCl₃ : CD₃OD) δ 175.0, 174.9, 145.2, 128.5, 126.6, 126.4, 70.6, 70.5, 63.6, 63.5, 60.5, 45.8, 45.7, 42.19, 42.15, 41.8, 41.7, 37.5, 37.4, 33.07, 33.05. HRMS (ESI) calcd for C₁₅H₂₂N₂O₃ [M + H]⁺ 279.1703; found 279.1696.

((2,4-cis)-4-Cyclohexyl-N-((S)-2,3-dihydroxypropyl)piperidine-2-

carboxamide (13): Compound **13** (20 mg, 80%), a diastereomeric mixture, was prepared from **10** (2 steps) as a whitish wax. ¹H-NMR (300 MHz, CDCl₃ : CH₃OD) δ 3.80 – 3.48 (m, 5H), 3.42 (d, *J* = 5.3 Hz, 2H), 3.38 – 3.22 (m, 1H), 3.16 (dd, *J* = 13.7, 6.7 Hz, 1H), 3.07 (d, *J* = 11.3 Hz, 1H), 2.53 (t, *J* = 11.3 Hz, 1H), 1.90 (d, *J* = 12.0 Hz, 1H), 1.81 – 1.49 (m, 6H), 1.42 – 0.72 (m, 10H). ¹³C NMR (75 MHz, CDCl₃ : CD₃OD) δ 175.55, 70.48, 63.47, 60.56, 45.71, 42.81, 41.70, 41.40, 33.79, 29.80, 29.30, 26.54, 26.44. HRMS (ESI) calcd for C₁₅H₂₈N₂O₂ [M + H]⁺ 285.2173; found 258.2169.

(2,4-cis)-N-(1,3-Dihydroxypropan-2-yl)-4-phenylpiperidine-2-carboxamide

(14): Compound **14** (20 mg, 55.6%), a diastereomeric mixture, was prepared from **9** (2 steps) as mixture whitish wax. ¹H-NMR (300 MHz, CDCl₃ : CH₃OD) δ 7.31 – 7.24 (m, 2H), 7.23 – 7.13 (m, 3H), 3.91 – 3.79 (m, 1H), 3.76 – 3.57 (m, 4H), 3.52 – 3.29 (m, 5H), 3.25 (d, *J* = 12.7 Hz, 2H), 2.74 (m, 2H), 2.15 (d, *J* = 12.8 Hz, 1H), 1.84 (d, *J* = 12.8 Hz, 1H), 1.71 – 1.43 (m, 2H). ¹³C NMR (75 MHz, CDCl₃ : CD₃OD) δ 173.89, 145.17, 128.53, 126.65, 126.48, 61.80, 61.74, 60.48, 52.32, 45.63, 42.06, 37.25, 32.86. HRMS (ESI) calcd for C₁₅H₂₂N₂O₃ [M + H]⁺ 279.1703; found 279.1700.

(2,4-cis)-4-Cyclohexyl-N-(1,3-dihydroxypropan-2-yl)piperidine-2-

carboxamide (15): Compound **15** (5 mg, 36%), a diastereomeric mixture, was prepared from **10** (2 steps) as a whitish wax. ¹H-NMR (300 MHz, CDCl₃ : CH₃OD) δ 3.88 – 3.78

(m, 1H), 3.70 – 3.60 (m, 4H), 3.41 – 3.29 (m, 1H), 3.21 (d, $J = 12.5$ Hz, 1H), 2.69 (t, $J = 12.2$ Hz, 1H), 2.02 (d, $J = 13.0$ Hz, 1H), 1.76 – 1.64 (m, 4H), 1.62 (d, $J = 12.1$ Hz, 1H), 1.36 – 1.25 (m, 1H), 1.25 – 1.13 (m, 5H), 1.13 – 1.03 (m, 2H), 0.98 – 0.86 (m, 2H). ^{13}C NMR (75 MHz, CDCl_3 : CD_3OD) δ 172.82, 61.79, 60.02, 52.59, 45.12, 42.57, 40.71, 32.69, 29.76, 28.01, 26.50, 26.42. HRMS (ESI) calcd for $\text{C}_{15}\text{H}_{28}\text{N}_2\text{O}_3$ $[\text{M} + \text{H}]^+$ 285.2173; found 285.2169.

(2,4-*cis*)-*N*-(2-Morpholinoethyl)-4-phenylpiperidine-2-carboxamide (16):

Compound **16** (29 mg, 76%), a diastereomeric mixture, was prepared from **9** (2 steps) as mixture whitish wax. ^1H -NMR (300 MHz, CDCl_3 : CD_3OD) δ 7.39 – 6.87 (m, 5H), 4.01 – 3.72 (m, 7H), 3.75 – 3.44 (m, 5H), 3.29 (d, $J = 10.9$ Hz, 1H), 2.99 – 2.53 (m, 2H), 2.15 (d, $J = 11.9$ Hz, 1H), 1.86 (d, $J = 11.7$ Hz, 1H), 1.64 (dt, $J = 24.8, 12.5$ Hz, 2H). ^{13}C NMR (75 MHz, CDCl_3) δ 172.46, 144.44, 128.56, 126.64, 126.55, 61.36, 59.73, 52.63, 41.40, 36.42, 31.62. HRMS (ESI) calcd for $\text{C}_{18}\text{H}_{27}\text{N}_3\text{O}_2$ $[\text{M} + \text{H}]^+$ 318.2176; found 318.2190.

(2,4-*cis*)-4-Cyclohexyl-*N*-(2-morpholinoethyl)piperidine-2-carboxamide (17):

Compound **17** (13 mg, 81%), a diastereomeric mixture, was prepared from **10** (2 steps) as a whitish wax. ^1H -NMR (300 MHz, CDCl_3) δ 6.94 (s, 1H), 3.75 – 3.68 (m, 4H), 3.37 (q, $J = 6.0$ Hz, 2H), 3.16 (dd, $J = 11.4, 2.7$ Hz, 2H), 2.65 (td, $J = 12.0, 2.6$ Hz, 1H), 2.48 (dd, $J = 11.8, 5.6$ Hz, 6H), 2.08 (dd, $J = 12.6, 2.0$ Hz, 1H), 1.92 (s, 1H), 1.81 – 1.54 (m, 6H), 1.31 – 0.78 (m, 9H). ^{13}C NMR (75 MHz, CDCl_3) δ 174.49, 166.62, 66.96, 61.24, 57.29, 53.43, 46.26, 42.96, 41.62, 35.42, 34.27, 30.05, 29.87, 29.60, 26.70, 26.61. HRMS (ESI) calcd for $\text{C}_{18}\text{H}_{33}\text{N}_3\text{O}_2$ $[\text{M} + \text{H}]^+$ 324.2646; found 324.2642.

(2*S*,4*R*)-*N*-((1*R*,2*R*)-1,3-Dihydroxy-1-phenylpropan-2-yl)-4-phenethylpiperidine-2-carboxamide ((2*S*,4*R*)-29) and (2*R*,4*S*)-*N*-((1*R*,2*R*)-1,3-dihydroxy-1-phenylpropan-2-yl)-4-phenethylpiperidine-2-carboxamide ((2*R*,4*S*)-29):

Compounds (2*S*,4*R*)-29 (45 mg, 35%) and (2*R*,4*S*)-29 (50 mg, 39%) were prepared from **25** (2 steps), respectively, by a procedure similar to that used to prepare compound **11**. These two isomers could be separated by preparative TLC as colorless amorphous gels.

Compound (2*S*,4*R*)-29: ¹H NMR (600 MHz, CDCl₃) δ 7.54 (br s, 1H), 7.39 (d, 2H, *J* = 7.2 Hz), 7.32 (m, 2H), 7.26 (m, 3H), 7.17 (m, 3H), 4.91 (d, 1H), 4.12 (dd, 1H, *J* = 5.4 Hz), 3.64 (dd, 1H, *J* = 5.4 Hz), 3.51 (dd, 1H, *J* = 5.4 Hz), 3.48 (m, 1H), 3.25 (m, 1H), 2.76 (m, 1H), 2.63 (t, 2H, *J* = 7.8 Hz), 2.08 (d, 1H, *J* = 12.6 Hz), 1.85 (d, 1H, *J* = 13.8 Hz), 1.26 (m, 1H), 1.16 (q, 1H, *J* = 12.6 Hz). ¹³C NMR (150 MHz, CDCl₃): δ 171.6, 141.8, 141.5, 128.2, 128.1 (3C), 127.5, 126.1 (2C), 125.7, 72.1, 61.4, 58.9, 57.0, 48.0, 44.1, 38.0, 34.7, 34.2, 32.4, 29.6. HRMS Calcd for C₂₃H₃₀N₂O₃: [M + H]⁺ 383.2329; found 383.2332. Compound (2*R*,4*S*)-29: ¹H NMR (600 MHz, CDCl₃) δ 7.74 (br s, 1H), 7.32 (d, 2H, *J* = 7.8 Hz), 7.24 (m, 4H), 7.14 (m, 4H), 5.04 (br s, 2H), 4.97 (s, 1H), 4.12 (s, 1H), 3.77 (m, 1H), 3.70 (m, 1H), 3.38 (s, 2H), 3.34 (m, 1H), 3.02 (d, 1H, *J* = 9.6 Hz), 2.50 (m, 3H), 1.72 (d, 1H, *J* = 10.2 Hz), 1.61 (d, 1H, *J* = 10.2 Hz), 1.39 (m, 2H), 1.01 (m, 1H), 0.81 (m, 1H). ¹³C NMR (150 MHz, CDCl₃): δ 172.2, 142.0, 141.6, 128.4 (2C), 128.2 (2C), 127.4, 125.9 (3C), 72.6, 62.7, 59.1, 56.6, 50.4, 44.2, 38.2, 35.1, 34.3, 32.5, 30.2. HRMS Calcd for C₂₃H₃₀N₂O₃: [M + H]⁺ 383.2329; found 383.2334.

(2,4-*cis*)-*N*-((*S*)-2,3-Dihydroxypropyl)-4-phenethylpiperidine-2-carboxamide

(30): Compound **30** (20.0 mg, 55.4%), a diastereomeric mixture, was prepared from **25** (2 steps) by a procedure similar to that used to prepare compound **11**, as a white solid. mp 103.2-104.3 °C; ¹H-NMR (300 MHz, CDCl₃ : CD₃OD) δ 7.41 – 7.31 (m, 1H), 7.31 – 7.23 (m, 2H), 7.22 – 7.10 (m, 3H), 3.80 – 3.71 (m, 1H), 3.62 – 3.46 (m, 2H), 3.45 – 3.27 (m, 3H), 3.22 (dd, 2H, *J* = 11.6, 2.7 Hz), 3.18 – 3.09 (m, 1H), 2.62 (t, 3H, *J* = 8.0 Hz), 2.10 (d, 1H, *J* = 13.2 Hz), 1.73 (d, 1H, *J* = 13.3 Hz), 1.56 (q, 2H, *J* = 7.6, 7.2 Hz), 1.50 – 1.39 (m, 1H), 1.26 (s, 1H), 1.17 – 0.96 (m, 2H) ¹³C NMR (75 MHz, CDCl₃) δ 175.5, 166.6, 142.3, 128.4, 128.3, 125.8, 70.9, 63.8, 63.7, 60.5, 45.6, 42.0, 38.7, 36.7, 35.5, 35.4, 32.7, 32.4. HRMS (ESI) calcd for C₁₇H₂₆N₂O₃ [M + H]⁺ 307.2016; found 307.2009

(2,4-*cis*)-4-(2-Cyclohexylethyl)-*N*-((*S*)-2,3-dihydroxypropyl)piperidine-2-

carboxamide (31): Compound **31** (44 mg, 94%), a diastereomeric mixture, was prepared from **26** (2 steps) by a procedure similar to that used to prepare compound **11**, as a whitish

wax. $^1\text{H-NMR}$ (300 MHz, CDCl_3) δ 7.44 (s, 1H), 3.90 – 3.66 (m, 4H), 3.62 – 3.42 (m, 2H), 3.44 – 3.30 (m, 2H), 3.30 – 3.17 (m, 1H), 3.13 (d, 1H, $J = 12.0$ Hz), 2.63 (t, 1H, $J = 12.1$ Hz), 2.02 (d, 1H, $J = 12.5$ Hz), 1.68 (d, 6H, $J = 11.4$ Hz), 1.37 (bs, 1H), 1.30 – 1.08 (m, 8H), 1.00 (t, 2H, $J = 12.3$ Hz), 0.94 – 0.77 (m, 2H). $^{13}\text{C NMR}$ (75 MHz, CDCl_3) δ 175.3, 70.9, 70.8, 63.8, 63.7, 60.5, 45.6, 42.0, 37.8, 36.8, 36.2, 36.1, 34.2, 33.4, 32.5, 26.7, 26.4. HRMS (ESI) calcd for $\text{C}_{17}\text{H}_{32}\text{N}_2\text{O}_3$ $[\text{M} + \text{H}]^+$ 313.2486; found 313.2486.

(2,4-*cis*)-*N*-(1,3-Dihydroxypropan-2-yl)-4-phenethylpiperidine-2-

carboxamide (32): Compound **32** (27 mg, 99%), a diastereomeric mixture, was prepared from **25** (2 steps) by a procedure similar to that used to prepare compound **11**, as a white wax-like material. $^1\text{H-NMR}$ (300 MHz, CDCl_3 : CD_3OD) δ 7.24 – 7.15 (m, 2H), 7.13 – 7.04 (m, 3H), 3.99 (s, 7H), 3.88 – 3.76 (m, 1H), 3.37 (d, 1H, $J = 10.5$ Hz), 3.18 (d, 1H, $J = 11.7$ Hz), 2.82 – 2.61 (m, 1H), 2.60 – 2.50 (m, 2H), 2.04 (d, 1H, $J = 12.6$ Hz), 1.75 (d, 1H, $J = 12.6$ Hz), 1.66 – 1.37 (m, 3H), 1.33 – 0.97 (m, 3H). $^{13}\text{C NMR}$ (75 MHz, CDCl_3 : CD_3OD) δ . 172.1, 141.9, 128.3, 128.1, 125.7, 61.2, 59.3, 52.7, 44.5, 38.2, 35.0, 34.5, 32.4, 30.3. HRMS (ESI) calcd for $\text{C}_{17}\text{H}_{26}\text{N}_2\text{O}_3$ $[\text{M} + \text{H}]^+$ 307.2016; found 307.2012.

(2,4-*cis*)-4-(2-Cyclohexylethyl)-*N*-(1,3-dihydroxypropan-2-yl)piperidine-2-

carboxamide (33): Compound **33** (20.7 mg, 76.6%), a diastereomeric mixture, was prepared from **26** (2 steps) by a procedure similar to that used to prepare compound **11**, as a whitish solid. mp 145.2-150.0 °C. $^1\text{H-NMR}$ (300 MHz, CDCl_3 : CD_3OD) δ . 3.86 (t, 1H, $J = 4.8$ Hz), 3.80 – 3.57 (m, 4H), 3.48 – 3.33 (m, 1H), 3.23 – 3.06 (m, 2H), 2.70 – 2.54 (m, 1H), 2.00 (d, 1H, $J = 13.1$), 1.75 – 1.60 (m, 6H), 1.38 (bs, 2OH), 1.33 – 1.06 (m, 9H), 1.09 – 0.96 (m, 2H), 0.95 – 0.75 (m, 3H). $^{13}\text{C NMR}$ (75 MHz, CDCl_3 : CD_3OD) δ 174.4, 61.8, 61.7, 60.4, 52.2, 45.5, 37.7, 36.5, 36.0, 34.1, 34.0, 33.3, 32.3, 26.6, 26.3. HRMS (ESI) calcd for $\text{C}_{17}\text{H}_{32}\text{N}_2\text{O}_3$ $[\text{M} + \text{H}]^+$ 313.2486; found 313.2487.

(2,4-*cis*)-4-(2-Cyclohexylethyl)-*N*-(2-morpholinoethyl)piperidine-2-

carboxamide (34): Compound **34** (43 mg, 93%), a diastereomeric mixture, was prepared from **26** (2 steps) by a procedure similar to that used to prepare compound **11**, as a

yellowish solid. mp 45.0-47.1 °C; ¹H-NMR (300 MHz, CDCl₃) δ 6.93 (t, 1H, *J* = 5.5 Hz), 3.80 – 3.59 (m, 4H), 3.35 (dtd, 2H, *J* = 6.7, 5.6, 5.0, 1.2 Hz), 3.14 (tt, 2H, *J* = 11.9, 2.4 Hz), 2.77 – 2.56 (m, 1H), 2.56 – 2.37 (m, 6H), 2.18 – 2.03 (m, 1H), 1.95 (d, 1H, *J* = 9.0 Hz), 1.82 – 1.58 (m, 6H), 1.40 – 1.30 (m, 1H), 1.34 – 1.08 (m, 8H), 1.08 – 0.96 (m, 1H), 0.96 – 0.74 (m, 3H). ¹³C NMR (75 MHz, CDCl₃ : CD₃OD) δ 174.3, 67.0, 57.3, 53.4, 46.0, 37.8, 37.2, 36.3, 35.4, 34.2, 33.4, 32.8, 26.7, 26.4. HRMS (ESI) calcd for C₂₀H₃₇N₃O₂ [M + H]⁺ 352.2959; found 352.2952.

(2,4-*cis*)-4-(2-Cyclohexylethyl)-N-(3-morpholinopropyl)piperidine-2-carboxamide (35): Compound **35** (33 mg, 99%), a diastereomeric mixture, was prepared from **26** (2 steps) by a procedure similar to that used to prepare compound **11**, as a white wax-like solid. ¹H-NMR (300 MHz, CDCl₃) δ 7.51 (t, 1H, *J* = 5.5 Hz), 3.74 (td, 4H, *J* = 4.4, 1.5 Hz), 3.33 (m, 2H), 3.13 (m, 2H), 2.66 (td, 1H, *J* = 12.1, 2.7 Hz), 2.43 (m, 6H), 2.09 (dq, 1H, *J* = 12.8, 2.7 Hz), 1.81 (s, 1H), 1.67 (m, 8H), 1.35 (m, 1H), 1.19 (m, 8H), 1.03 (m, 1H), 0.86 (m, 3H). ¹³C NMR (75 MHz, CDCl₃) δ. HRMS (ESI) calcd for C₂₁H₃₉N₃O₂ [M + H]⁺ 366.3115; found 366.3112.

(2,4-*cis*)-N-(2-morpholinoethyl)-4-phenethylpiperidine-2-carboxamide (36): Compound **36** (45 mg, 96%), a diastereomeric mixture, was prepared from **25** (2 steps) by a procedure similar to that used to prepare compound **11**, as a yellowish solid. mp 156.6-157.9 °C; ¹H-NMR (300 MHz, CDCl₃) δ 7.31 – 7.24 (m, 2H), 7.12 – 7.13 (m, 3H), 6.94 (t, 1H, *J* = 5.6 Hz), 3.71 (t, 4H, *J* = 3.0 Hz), 3.36 (q, 2H, *J* = 6.0 Hz), 3.23 – 3.08 (m, 2H), 2.72 – 2.59 (m, 3H), 2.53 – 2.39 (m, 6H), 2.17 (dq, 1H, *J* = 12.7, 2.8 Hz), 1.73 (dt, 1H, *J* = 12.8, 2.8 Hz), 1.64 – 1.52 (m, 2H), 1.51 – 1.39 (m, 1H), 1.25 (bs, 1H), 1.18 – 1.04 (m, 1H), 1.03 – 0.91 (m, 1H). ¹³C NMR (75 MHz, CDCl₃) δ 174.2, 166.7, 142.5, 128.3, 128.3, 125.7, 67.0, 60.8, 57.3, 53.4, 45.9, 38.9, 35.6, 35.4, 32.8, 32.6. HRMS (ESI) calcd for C₂₀H₃₁N₃O₂ [M + H]⁺ 346.2489; found 346.2482.

(2,4-*cis*)-N-(3-morpholinopropyl)-4-phenethylpiperidine-2-carboxamide (37): Compound **37** (25 mg, 99%), a diastereomeric mixture, was prepared from **25** (2 steps) by

a procedure similar to that used to prepare compound **11**, as a white solid. mp 59.8-61.5 °C; ¹H-NMR (300 MHz, CDCl₃) δ 7.53 (t, 1H, J = 5.2 Hz), 7.27 (m, 2H), 7.17 (m, 3H), 3.74 (dt, 4H, J = 4.4, 1.5 Hz), 3.34 (m, 2H), 3.14 (m, 2H), 2.64 (m, 3H), 2.43 (m, 6H), 2.18 (dq, 1H, J = 12.6, 2.8 Hz), 1.69 (m, 4H), 1.56 (m, 2H), 1.46 (m, 1H), 1.09 (ddd, 1H, J = 15, 12, 3 Hz), 0.96 (q, 1H, J = 12 Hz). ¹³C NMR (75 MHz, CDCl₃) δ 174.2, 142.4, 128.3, 128.2, 125.7, 66.9, 61.0, 57.7, 53.8, 45.9, 38.9, 38.6, 37.1, 35.7, 32.8, 32.6, 25.4. HRMS (ESI) calcd for C₂₁H₃₃N₃O₂ [M + H]⁺ 360.2646; found 360.2638.

(2*S*,4*R*)-4-(4-(*tert*-Butyl)phenethyl)-*N*-((1*R*,2*R*)-1,3-dihydroxy-1-phenylpropan-2-yl)piperidine-2-carboxamide ((2*S*,4*R*)-38) and (2*R*,4*S*)-4-(4-(*tert*-butyl)phenethyl)-*N*-((1*R*,2*R*)-1,3-dihydroxy-1-phenylpropan-2-yl)piperidine-2-carboxamide ((2*R*,4*S*)-38): Compounds (2*S*,4*R*)-38 (40 mg, 28%) and (2*R*,4*S*)-38 (50 mg, 36%) were prepared from 27 (2 steps), respectively, by a procedure similar to that used to prepare compound 11. These two isomers could be separated by preparative TLC as colorless amorphous gels. Compound (2*S*,4*R*)-38: ¹H NMR (600 MHz, CDCl₃ + CD₃OD) δ 7.46 (br s, 1H), 7.39 (d, 2H, J = 7.2 Hz), 7.31 (m, 4H), 7.24 (t, 1H, J = 7.2 Hz), 7.10 (d, 1H, J = 8.4 Hz), 4.96 (d, 1H, J = 4.8 Hz), 4.09 (q, 1H, J = 5.4 Hz), 3.68 (m, 1H), 3.57 (m, 1H), 3.21 (dd, 1H, J = 3.0 Hz, 12.0 Hz), 3.12 (m, 1H), 2.63 (m, 1H), 2.57 (t, 2H, J = 7.8 Hz), 1.91 (d, 1H, J = 13.2 Hz), 1.76 (d, 1H, J = 12.6 Hz), 1.54 (m, 2H), 1.46 (m, 1H), 1.30 (s, 9H), 1.12 (qd, 1H, J = 3.6 Hz, 12.0 Hz), 0.91 (q, 1H, J = 12.6 Hz). ¹³C NMR (150 MHz, CDCl₃ + CD₃OD): δ 174.0, 148.5, 141.6, 139.0, 128.1 (2C), 127.8 (2C), 127.4, 126.0, 125.9, 125.1 (2C), 72.0, 61.8, 59.9, 56.6, 44.9, 38.5, 35.8, 34.9, 34.2, 31.9, 31.3, 31.1 (3C). HRMS Calcd for C₂₇H₃₈N₂O₃: [M + H]⁺ 439.2950; found 439.2957. Compound (2*R*,4*S*)-38: ¹H NMR (600 MHz, CDCl₃ + CD₃OD) δ 7.68 (br s, 1H), 7.38 (d, 2H, J = 7.8 Hz), 7.31 (m, 4H), 7.22 (t, 1H, J = 7.2 Hz), 7.11 (d, 2H, J = 8.4 Hz), 4.99 (d, 1H, J = 4.2 Hz), 4.11 (m, 1H), 3.75 (m, 1H), 3.66 (m, 1H), 3.47 (dd, 1H, J = 2.4 Hz, 12.6 Hz), 3.20 (d, 1H, J = 11.4 Hz), 2.72 (m, 1H), 2.56 (m, 2H), 1.87 (d, 1H, J = 13.2 Hz), 1.78 (d, 1H, J = 13.8 Hz), 1.52 (m, 3H), 1.31 (s, 9H), 1.18 (m, 1H), 0.96 (q, 1H, J = 12.0 Hz). ¹³C NMR (150 MHz,

CDCl₃+CD₃OD): δ 171.7, 148.7, 141.5, 138.8, 128.1 (2C), 127.8 (2C), 127.4, 125.9 (2C), 125.2 (2C), 72.4, 62.3, 59.0, 56.6, 44.2, 38.2, 34.8, 34.2, 31.9, 31.3 (4C), 30.1. HRMS Calcd for C₂₇H₃₈N₂O₃: [M + H]⁺ 439.2950; found 439.2955.

(2*R*,4*S*)-*N*-((1*S*,2*S*)-1,3-Dihydroxy-1-phenylpropan-2-yl)-4-(4-methylphenethyl)piperidine-2-carboxamide ((2*R*,4*S*)-39) and (2*S*,4*R*)-*N*-((1*S*,2*S*)-1,3-dihydroxy-1-phenylpropan-2-yl)-4-(4-methylphenethyl)piperidine-2-carboxamide ((2*S*,4*R*)-39): Compounds (2*R*,4*S*)-39 (50 mg, 34%) and (2*S*,4*R*)-39 (53 mg, 37%) were prepared from 28 (2 steps), respectively, by a procedure similar to that used to prepare compound 11. These two isomers could be separated by preparative TLC as colorless amorphous gels. Compound (2*R*,4*S*)-39: ¹H NMR (600 MHz, CDCl₃ + CD₃OD) δ 7.46 (br s, 1H), 7.39 (d, 2H, *J* = 7.8 Hz), 7.31 (t, 2H, *J* = 7.8 Hz), 7.25 (t, 1H, *J* = 7.2 Hz), 7.09 (d, 2H, *J* = 8.4 Hz), 7.05 (d, 2H, *J* = 7.8 Hz), 4.97 (d, 1H, *J* = 4.2 Hz), 4.08 (d, 1H, *J* = 4.8 Hz), 3.69 (m, 1H), 3.58 (m, 1H), 3.15 (dd, 1H, *J* = 3.0 Hz, 12.0 Hz), 3.11 (m, 1H), 2.60 (m, 1H), 2.55 (t, 2H, *J* = 7.8 Hz), 2.31 (s, 3H), 1.86 (d, 1H, *J* = 13.2 Hz), 1.73 (d, 1H, *J* = 13.2 Hz), 1.50 (m, 2H), 1.42 (m, 1H), 1.09 (dq, 1H, *J* = 4.2 Hz, 12.6 Hz), 0.86 (q, 1H, *J* = 12.0 Hz). ¹³C NMR (150 MHz, CDCl₃ + CD₃OD): δ 174.3, 141.6, 139.1, 135.1, 128.9 (2C), 128.1 (2C), 128.0 (2C), 127.4, 126.0 (2C), 72.0, 61.9, 60.0, 56.5, 45.0, 38.6, 36.0, 35.0, 32.0, 31.5, 20.6. HRMS Calcd for C₂₄H₃₂N₂O₃: [M + H]⁺ 397.2486; found 397.2490. Compound (2*S*,4*R*)-39: ¹H NMR (600 MHz, CDCl₃) δ 7.45 (d, 1H, *J* = 8.4 Hz), 7.35 (d, 2H, *J* = 7.2 Hz), 7.25 (m, 2H), 7.18 (t, 1H, *J* = 7.2 Hz), 7.08 (d, 1H, *J* = 7.8 Hz), 7.02 (d, 1H, *J* = 8.4 Hz), 5.02 (d, 1H, *J* = 3.0 Hz), 4.65 (br s, 3H), 4.10 (m, 1H), 3.78 (m, 1H), 3.71 (m, 1H), 3.13 (d, 1H, *J* = 13.8 Hz), 2.94 (d, 1H, *J* = 12.0 Hz), 2.48 (t, 2H, *J* = 7.8 Hz), 2.41 (m, 1H), 2.31 (s, 3H), 1.74 (d, 1H, *J* = 12.0 Hz), 1.59 (d, 1H, *J* = 12.0 Hz), 1.39 (m, 2H), 1.31 (m, 1H), 0.90 (m, 1H), 0.78 (q, 1H, *J* = 12.6 Hz). ¹³C NMR (150 MHz, CDCl₃): δ 173.5, 141.8, 139.1, 135.2, 129.1 (3C), 128.1 (3C), 127.4, 125.9 (2C), 72.7, 62.9, 59.8, 56.4, 44.7, 38.7, 36.1, 34.8, 32.1, 31.5, 21.0. HRMS Calcd for C₂₄H₃₂N₂O₃: [M + H]⁺ 397.2486; found 397.2487.

4.2 *In silico* Molecular Docking

Molecular modeling and ligand docking were performed in the Maestro (11.9) workspace using modules (LigPrep, Protein Preparation Wizard, Induced Fit Docking, and Glide) in the Small Molecule Drug Discovery Suite (2019-1, Schrödinger, LLC, New York, NY, 2017). The crystal structure of ergotamine-5-HT_{2C}R (PDB Code: 6BQG) was fetched from RCSB PDB bank and was preprocessed and optimized with Schrödinger Protein Preparation Wizard using default settings. All ligands (5-HT and 5-HT_{2C}R PAMs) were created with Maestro 2D-sketcher and prepared with LigPrep to generate suitable 3D conformations for docking. Induced Fit Docking was used to dock 5-HT and replace ergotamine. For this initial model generation, a grid was applied via Glide on the ergotamine-5-HT_{2C}R structure centering on the indole N atom of ergotamine, as a representation of the orthosteric binding site. A new 5-HT-bound 5-HT_{2C}R model was generated in this manner, allowing default flexibility and movement of amino acid residues surrounding the orthosteric site, now accommodating 5-HT. The 5-HT-bound 5-HT_{2C}R model was exported as a single protein structure (both 5-HT and protein), and subsequently used for docking of the 5-HT_{2C}R PAMs. No exclusion volumes were necessary to apply due to the presence of 5-HT in the orthosteric site. Compound **12** was pharmacologically validated as a 5-HT_{2C}R PAM, thus **12** was docked to the model using the Induced Fit Docking protocol, allowing default residue flexibility. A rationally selected docking pose for **12** was used as a center for a new grid. This grid was applied for the standard docking of remaining ligands, conducted with Glide XP mode. All docked results were viewed in Maestro for visualization and clustering. Scoring functions (GScore) and biological and chemical rationale were used for ligand pose selection. For all ligands that were pharmacologically tested as a mixture of two isomers, both isomers were docked and analyzed. Visualization aids such as the protein surface predictions around the docking site were performed in the Maestro workspace.

4.3 *In Vitro* Pharmacology

Intracellular Calcium (Ca_i^{2+}) Release Assay in h5-HT₂R-CHO Cells. Chinese hamster ovary (CHO) cells stably transfected with the human unedited (INI) h5-HT_{2C}R (h5-HT_{2C}R-CHO cells) or the human h5-HT_{2A}R (h5-HT_{2A}R-CHO cells) were the generous gift from Drs. Kelly A. Berg and William P. Clarke (University of Texas Health Science Center, San Antonio). Cells were grown at 37°C, 5% CO₂, and 85% relative humidity environment in GlutaMax-MEM medium (Invitrogen, Carlsbad, CA) containing 5% fetal bovine serum (Atlanta Biologicals, Atlanta, GA) and 100 µg/mL hygromycin (Mediatech, Manassas, VA) and were passaged when they reached 80% confluency. The Ca_i^{2+} release assay was performed according to our recent publications.³⁸¹ Briefly, cells (150 µL; passages 6-16 (FlexStation 3; Molecular Devices) or 30,000 cells/well (FLIPR^{TETRA}; Molecular Devices) in black-wall 96-well culture plates with optically clear flat bottoms. To ensure even plating of cells, the source reservoir was frequently agitated or triturated, and plates were maintained on a rotary shaker at low speed for 20 min after plating and returned to the incubator overnight. Approximately 24 h after plating, the medium was replaced with serum-free (SF) GlutaMax-MEM medium supplemented with 20 nM to 100 µM putrescine (Sigma-Aldrich, St. Louis, MO), 20 nM to 100 µM progesterone (Sigma-Aldrich), and 1:100 ITS (1000 mg/L human recombinant insulin, 550 mg/L human recombinant transferrin, 0.67 mg/L selenious acid; Corning Inc., Corning, NY) (SF+ medium). Following a 3 h incubation, SF+ medium was replaced with 40 µL of Hank's balanced saline solution (HBSS; without CaCl₂ or MgCl₂, pH 7.4) plus 40 µL of Calcium 4 dye solution (FLIPR No-wash kit, Molecular Devices, Sunnyvale CA, catalog no R8142) supplemented with 2.5 mM of water-soluble probenecid (Sigma-Aldrich) to inhibit extracellular transport of the dye. Plates were incubated with dye solution for 60 min at 37°C, 15 min at room temperature in the dark. Drug dilutions were prepared at 5x final concentration in 1x HBSS; delivery of compound (20 µL/well) was followed 15 min later

by 5-HT (10 pM to 10 μ M; 25 μ L/well). A baseline was established for each well before addition of the test compound and again before addition of 5-HT. The fluorescence read following the addition of 5-HT was used to assess allosteric modulation of 5-HT-evoked Ca_i^{2+} release. Fluorescence was measured using a FlexStation 3 (Molecular Devices) or FLIPR^{TETRA} (130 gain, 60% intensity, 0.3 s exposure). For the FlexStation 3, a 17 s baseline was established before addition of compounds following which fluorescence was recorded every 1.7 s for a total 240 s. Maximum peak height was determined by the SoftMax software (Pro 5.4.5) for each well. For the FLIPR^{TETRA}, a 10 s baseline was established before addition of compounds following which fluorescence was recorded every 1 s for 120 s following compound or for 360 s following 5-HT. Maximum peak height was determined by ScreenWorks 4.0 software for each well. After the final readings, cells were fixed in 2% paraformaldehyde (Sigma) overnight. The maximum 5-HT-induced Ca_i^{2+} release (E_{max}) in the presence of test compound was determined using 4-parameter nonlinear regression analysis (GraphPad Prism 7.04) and calculated from 4-6 biological replicates, each conducted in technical triplicates. The E_{max} for the test compound plus 5-HT was normalized to the E_{max} for 5-HT alone. Subsequent *post hoc* comparisons between means for E_{max} were made using Welch's unpaired *t* test (GraphPad Prism). All statistical analyses were conducted with an experiment-wise error rate of $\alpha = 0.05$. All treatment assignments were blinded to investigators who performed *in vitro* assays and endpoint statistical analyses.

4.4 *In Vivo* Pharmacokinetics and Brain Penetration Analyses

Male Sprague–Dawley rats ($n = 3$ /treatment group; Charles River Laboratories) weighing 200–250 g at the beginning of the experiment were housed three per cage in a pathogen-free, temperature (20–26°C) and humidity-controlled (40–70%) environment with a 12 h light-dark cycle and ad libitum access to food and filtered water. Rats were randomly assigned to treatment groups. Vehicle [10% DMSO:90% HP- β -CD] or

compound **12** dissolved in vehicle was administered to rats intravenously (iv) at 10 mg/kg or *per os* (po) at 20 mg/kg. Blood samples (0.3 mL) were collected from the retro-orbital sinus vein before dosing and at 0.08, 0.25, 0.5, 1.0, 2.0, 4.0, 8.0, and 24 h postdosing for iv administration and 0.25, 0.5, 1.0, 2.0, 4.0, 8.0, and 24 h postdosing for po administration. Blood samples were placed in heparinized tubes and centrifuged at 12,000g for 5 min at 4°C. Brain samples were collected at 0.25 and 1 h postdosing. All samples were stored at -20°C. The concentration of **12** in each sample was analyzed by Sundia MediTech Co., Ltd. The study and the related standard operating procedures (SOPs) were reviewed and approved by Sundia Institutional Animal Care and Use Committee. The Sundia animal facility is approved with yearly inspection by the Shanghai Laboratory Animal Management Committee.

The pharmacokinetic parameters of compound **12** were calculated according to a noncompartmental model using WinNonlin 8.1 (Pharsight Corporation, ver 5.3, Mountain View, CA, USA). The peak concentration (C_{\max}) and time of peak concentration (T_{\max}) were directly obtained from the plasma concentration–time plot. The elimination rate constant (λ) was obtained by the least-squares fitted terminal log–linear portion of the slope of the plasma concentration–time profile. The elimination half-life ($t_{1/2}$) was evaluated according to $0.693/\lambda$. The area under the plasma concentration–time curve from 0 to time t (AUC_{0-t}) was evaluated using the linear trapezoidal rule and further extrapolated to infinity (AUC_{0-inf}) according to the following equation: $AUC_{0-inf} = AUC_{0-t} + C_{\text{last}}/\lambda$. The pharmacokinetic parameters and brain concentrations are presented as mean \pm S.E.M. in Table 6. All treatment assignments were blinded to investigators who performed pharmacokinetic assays and endpoint statistical analyses.

Effects of Compound 12 in a WAY163909 vs. Saline Drug Discrimination Assay. **Drugs:** WAY163909 [(7b-R,10a-R)-1,2,3,4,8,9,10,10a-octahydro-7bH-cyclopenta[*b*][1,4] diazepino[6,7,1*hi*]indole] was a gift from Pfizer, Inc. (New York, NY) and was dissolved in 0.9% NaCl (vehicle employed for comparison to WAY163909).

SB242084 [6-chloro-5-methyl-1-[[2-(2-methylpyrid-3-yloxy)pyrid-5-yl]carbamoyl]indoline dihydrochloride; Sigma Chemical Co., St. Louis, MO, USA] was dissolved in saline containing 10 mmol/L citric acid (Sigma Chemical Co.) and 8% 2-hydroxypropyl- β -cyclodextrin (Trappsol Hydroxypropyl Beta Cyclodextrin, pharmaceutical grade, Cyclodextrin Technologies Development Inc., High Springs, FL, USA) with the final pH of the solution adjusted to 5.6. SB242084, WAY163909, and compound **12** were injected intraperitoneally (ip) at a volume of 1 mL/kg.

Animals: Male Sprague–Dawley rats (n = 13; Envigo) weighing 300–325 g (~ 60 days of age) at the beginning of the experiment were housed two per cage in a temperature (21–23°C) and humidity-controlled (45–50%) environment; lighting was maintained under a 12h light–dark cycle (0700–1900 h). Rats were maintained at 80–90% of their free-feeding weights by restricting access to water. Rats received water during daily training sessions (5–6 mL/rat/session), several hours after training (20 min), and over the weekend (36 h). Experiments were conducted during the light phase of the light–dark cycle (between 0900 and 1200 h) and were carried out in accordance with the National Institutes of Health Guide for the Care and Use of Laboratory Animals (2011) and with the approval of the Institutional Animal Care and Use Committee at University of Texas Medical Branch.

Drug Discrimination Procedures: Full experimental details of the procedures and analyses have been previously described.^{381, 413, 420, 427} Briefly, standard two-lever, water-reinforced drug discrimination procedures were used (Med Associates, St. Albans, USA). Each chamber was equipped with a water-filled dispenser mounted equidistantly between two retractable response levers on the wall and housed in a light- and sound-proof cubicle. Illumination came from a 28V house light; ventilation and masking noise were provided by a ventilation fan. A computer with Med-PC IV software was used to run programs and record all experimental events.

Rats were trained to discriminate an injection of WAY163909 (0.75 mg/kg; 1.0 mL/kg, ip) from saline (1.0 mL/kg, ip) administered 15 min before start of training sessions. Daily sessions lasted 15 min and were conducted Monday through Friday. During the phase of errorless training, only the stimulus-appropriate (drug or saline) lever was present. Training began under a fixed ratio 1 (FR1) schedule of water reinforcement, and the FR requirement was incremented until all animals were responding reliably under an FR20 schedule for each experimental condition. Left and right levers were counterbalanced across rats for WAY163909/saline assignments. During this phase of training, WAY163909 and saline were administered randomly with the restriction that neither condition prevailed for more than three consecutive sessions. After responding stabilized, both levers were introduced simultaneously during 15 min training sessions. The rats were required to respond on the stimulus-appropriate (correct) lever to obtain water reinforcement. There were no programmed consequences for responding on the incorrect lever. This phase of training continued until the performance of all rats attained criterion (defined as mean accuracies of at least 80% stimulus-appropriate responding for ten consecutive sessions).

Test sessions were initiated and conducted once or twice per week; with training sessions completed on intervening days. Rats were required to maintain accuracies >80% correct for saline and WAY163909 maintenance sessions, which immediately preceded all tests. During test sessions, animals were placed in the chambers and, upon completion of 20 responses on either lever, a single water reinforcer was delivered, and the house lights were turned off. The rat was removed from the chamber and returned to the colony. The test sessions were terminated after 15 min if the rats did not complete 20 responses on either lever; only data from rats that completed the test were included in data analysis. In substitution tests, rats were administered compound **12** (0.5, 1.0, 2.0, 5.0 mg/kg, ip) 30 min before the start of the test. WAY163909 (0.125, 0.25, 0.5, 0.625, 0.75, or 1.0 mg/kg, ip), or saline was administered 15 min prior to the start of the test. In combination tests, rats

were tested for lever selection following administration of compound **12** (0, 0.5, 1.0, or 2.0 mg/kg, ip) or vehicle 30 min and WAY163909 (0.5 mg/kg ip) or saline 15 min before start of the test. In combination tests, SB242084 (0.5 mg/kg) was administered 15 min before administration of WAY163909. The dose of WAY163909 (0.5 mg/kg, ip) employed evoked ~50% drug-appropriate responding. Full substitution was defined as $\geq 80\%$ of rats selecting the WAY163909-appropriate lever. Partial substitution was defined as $\geq 40\%$ and $< 80\%$ drug-appropriate responding.

Statistical Analyses: All treatment assignments were blinded to investigators who performed *in vivo* assays and endpoint statistical analyses. Rat performance in training and test sessions was expressed as the average percentage of rats selecting the WAY163909-associated lever because responding is typically a quantal rather than continuous function of stimulus similarity in the two-choice drug discrimination assay.^{381, 413-421} Thus, intermediate doses of the training drug or substitution test responses are typically confined to one lever. During test sessions, the lever selection is defined by the initial FR20 schedule completion at which point the test terminates and the animal is removed from the chamber without delivery of a reinforcer. Logistic regression analyses were used to determine the effects of increasing doses of WAY163909, compound **12**, or combination treatments on the probability that rats responded on the WAY163909-associated lever (binary response variable). The response rate (responses per minute) was calculated as the total number of responses emitted before completion of the first FR 20 divided by the number of minutes taken to complete the first ratio. Response rates were analyzed using one-way ANOVA with Dunnett's correction for comparisons to vehicle or control groups. Log-probit analyses were used to estimate the dose of WAY163909 predicted to elicit 50% WAY163909-associated lever responses (ED_{50}). All statistical significance was set at an experimenter-wise error rate of $\alpha = 0.05$.

Chapter 4. Exploration of sp^2 -Rich Scaffolds as Serotonin 5-HT_{2C} Receptor PAMs to Probe Binding Pocket Features and Reduce Chiral Centers

E.A. Wold

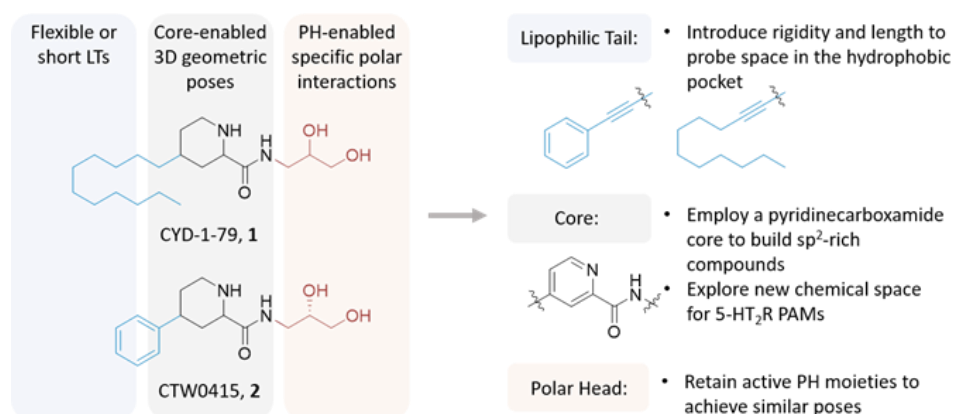
Abstract

A common feature shared by previously designed 5-HT_{2C}R PAMs that originated from the hit compound PNU-69176E is the piperidinecarboxamide core of the scaffold. The analogues that followed have retained the piperidinecarboxamide core and thus have retained the saturated ring geometry, commonly referred to as three-dimensional compared to planar ring systems. The goal of this work is three-fold. First, the core will be replaced by an unsaturated, planar pyridine ring to probe binding pocket accommodations of sp^2 -rich analogues. Second, increased rigidity will be introduced to the lipophilic tail moiety to explore binding pocket depth and volume constraints, as the moiety can no longer collapse into a minimal volume. Third, increased synthesis efficiency is prioritized, considering large-quantity scale-up will be required as the drug discovery campaign matures. Thus, we aimed to synthesize a collection of non-chiral-core, sp^2 -rich compounds that feature a pyridinecarboxamide core and are designed around activity data and structural modeling generated by earlier discovery efforts, namely lead molecules CYD-1-79 and CTW0415. To this end we achieved substituted pyridine-2-carboxamide 5-HT_{2R} PAMs that increased synthetic feasibility and potentiated 5-HT signaling at 5-HT_{2Rs} in calcium-based functional assays. Future derivatives building on this work will need to overcome sub-optimal DMPK properties, as well as the apparent pan-5-HT_{2R} promiscuity introduced by aromatic ring systems, as described herein.

1. INTRODUCTION

As highlighted in previous chapters, the 5-HT_{2C}R is an important drug target for multiple human conditions including substance use disorders (SUDs) and obesity.²⁶⁴ Our previous work towards discovering novel 5-HT_{2C}R PAMs has achieved the lead compounds **1** and **2** (**Fig. 4.1**).^{381, 405} These molecules are designed around a piperidinecarboxamide core, flanked by lipophilic tail (LT) and polar head (PH) moieties. This design endows these compounds with interesting, three-dimensional (3D) geometry originating from the chiral carbon atoms in the piperidine ring. However, it is unknown if this feature is preferable or required for 5-HT_{2C}R PAM activity, and the resultant design can lead to difficulties in isomer separation. Additionally, the LT moieties seen in our previous discovery efforts are typically flexible and discerning structure-activity relationship (SAR) from flexible moieties characterized by non-specific protein interactions can prove difficult. The study conducted herein sought to introduce new geometry to the molecules and rigidly extend the LT to gain insights into the 5-HT_{2C}R PAM binding pocket. An important aspect of this endeavor was to retain the PH moieties previously found to be present in active 5-HT_{2C}R PAMs, as this fragment provides specific interactions with key residues in the PAM binding site.

Figure 4.1 Rationale and Strategy



An additional goal of this study was to eliminate the chiral carbon atoms in the piperidinecarboxamide core of our current 5-HT_{2C}R PAMs, replacing it with a pyridinecarboxamide core, and thereby simultaneously reducing the number of steps in compound synthesis. The current lead compounds **1** and **2** shown in **Figure 4.1** clearly display the aliphatic piperidine ring. To achieve this structural moiety a metal-catalyzed hydrogenation reaction is required, which is followed by protection of the secondary amine of the piperidine ring. Derivatives can then be achieved by conjugating various amino moieties to the core. This procedure necessarily produces two substituted chiral carbon atoms in the piperidine ring and results in enantiomeric products. Separation of the enantiomers is often prohibitive at such an early stage in a drug discovery campaign, but when successful the pharmacological characterization can produce valuable structure-activity relationship data.

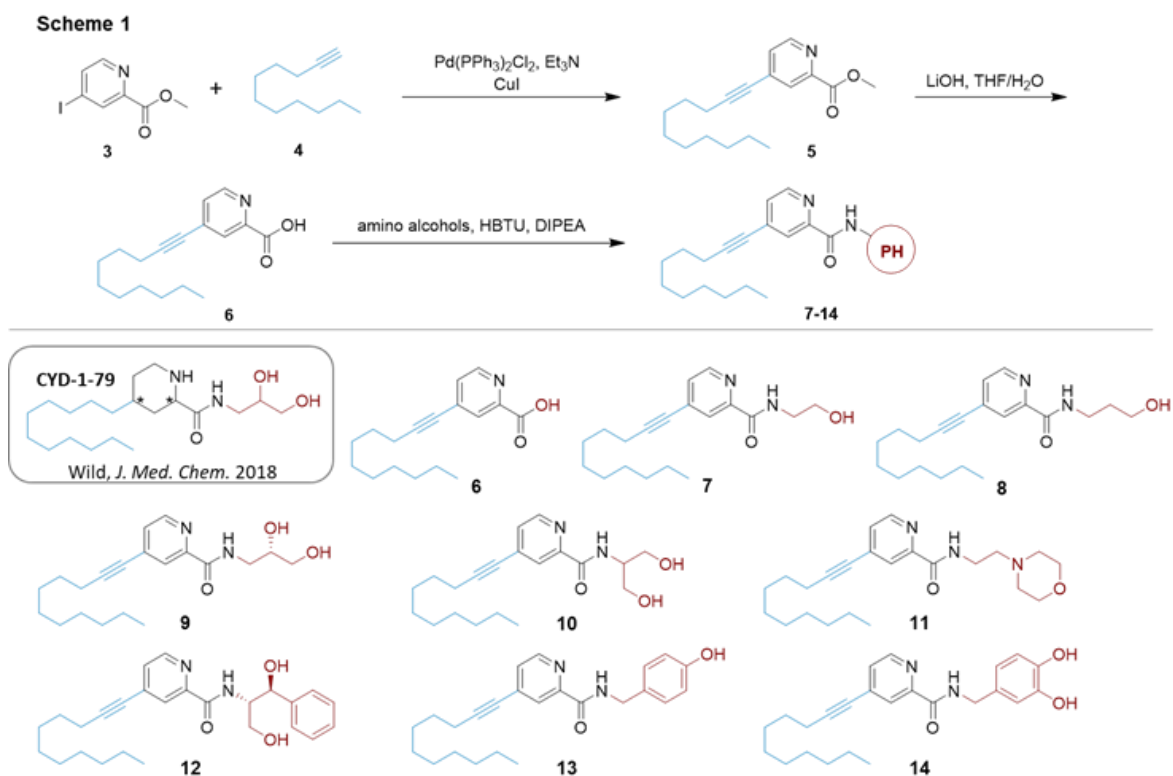
Described herein is a series of pyridinecarboxamide core compounds that were assessed for activity at the 5-HT_{2C}R and followed by select screening at the 5-HT_{2A}R and 5-HT_{2B}R to determine subtype selectivity. We performed a calculation to predict central nervous system (CNS) exposure that returns a value known as the CNS-MPO score.⁴¹¹ This score weights different physicochemical properties of a small molecule and produces a value between zero and six, where the closer a score is to six the higher probability it will obtain CNS exposure. This was followed by an off-target assessment at nearly 50 biologically relevant receptors and transporters to determine selectivity across many targets specifically in the CNS.⁴²⁸ Finally, we subjected the most promising 5-HT_{2C}R PAM to *in vivo* pharmacokinetic (PK) analysis to determine suitability for *in vivo* rodent behavioral assays.

2. RESULTS AND DISCUSSION

Chemistry. Reviewing our previously established synthetic protocol, the synthetic route was modified to achieve final products after a three-step synthesis, compared to the

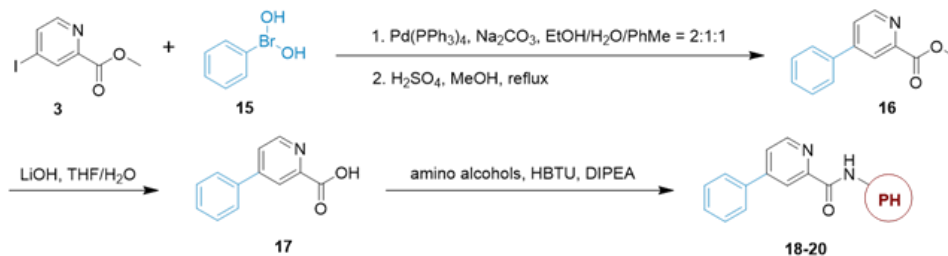
previous six-step protocol.^{46, 381, 405} The starting material was the iodinated ester of picolinic acid, which underwent Sonogashira (**Schemes 4.1 and 4.3**) or Suzuki (**Scheme 4.2**) coupling to lipophilic tail (LT) moieties (e.g., undec-1-yn-1-yl, phenyl, and phenylethynyl fragments). Hydrolysis of the ester provided the pyridinyl carboxylic acids **6**, **17**, and **23**. The application of *N,N,N',N'*-tetramethyl-*O*-(1*H*-benzotriazol-1-yl)uronium hexafluorophosphate (HBTU)-mediated coupling to selected amines achieved the target compounds **7-14**, **18-20**, and **24-26**. Due to the intrinsic characteristics of the pyridinecarboxamide scaffold, we avoided the challenge of inseparable isomer mixtures as seen in previous 5-HT_{2C}R PAM syntheses.^{381, 405}

Scheme 4.1 CYD-1-79 analogues

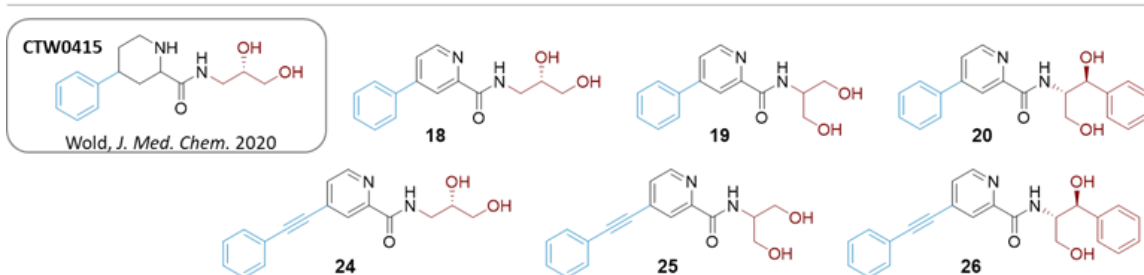
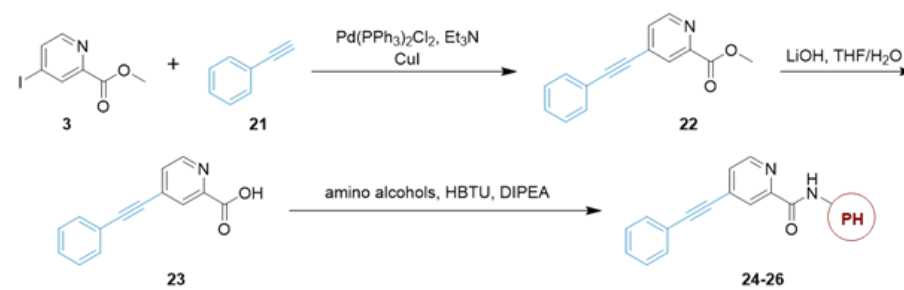


Scheme 4.2 and 4.3 CTW0415 analogues

Scheme 2



Scheme 3



Compound screening *in vitro*. Following receptor activation, the 5-HT₂R_s initiate an intracellular signaling cascade beginning with the coupling, nucleotide exchange and dissociation of the G_{αβγ} heterotrimer. G_{αq} proceeds to stimulate phospholipase C β (PLC β), which results in the production of inositol-1,4,5-triphosphate (IP₃), diacylglycerol (DAG) and the eventual efflux of Ca_i²⁺ from intracellular stores. This cascade of events is generally referred to as the canonical signaling pathway for GPCRs and has been characterized extensively. Thus, employing a calcium-sensitive fluorescent sensor to a cell-based functional screening system enables the measurement of 5-HT₂R activation by correlating receptor activity to fluorescent response in a tightly controlled environment. This principle was used to measure the *in vitro* Ca_i²⁺ release upon 5-HT₂R activation, providing a

functional characterization of the newly synthesized compounds. The compounds were screened for activity at the 5-HT_{2C}R, and selected compounds were screened at the 5-HT_{2A}R and 5-HT_{2B}R. The maximum efficacy (E_{\max}) of 5-HT-induced Ca_i^{2+} release was measured, and compound screening activity data is reported as a percent of the normalized 5-HT response (100%). Each compound was screened in a minimum of four biological replicates conducted in technical triplicate. The E_{\max} of each test compound was determined via a concentration-response curve of increasing concentrations of 5-HT in the presence of 1 nM test compound. Intrinsic agonist activity was monitored via a 15 min. pre-incubation of the test compounds, and none are reported to possess agonist activities at 1 nM test concentrations. The results of compound screening in 5-HT_{2C}R, 5-HT_{2A}R and 5-HT_{2B}R expressing cells are shown in **Table 4.1**.

Several compounds are reported as PAMs at the 5-HT_{2C}R, however the resultant structure-activity relationship (SAR) analysis is notably divergent from other series of 5-HT_{2C}R PAMs we have synthesized. Compound **9** displayed no activity at the 5-HT_{2C}R compared the piperidinecarboxamide **1** (~23% E_{\max} increase) on which the aromatic design was based, indicating an incompatible pose was induced by the saturated design. While surprisingly, **8** was found to potentiate 5-HT-induced Ca_i^{2+} release at the 5-HT_{2C}R with an E_{\max} of $119.4 \pm 7.4\%$ ($p < 0.05$). Additionally, the piperidinecarboxamide analogue of **10** was previously found to show activity, while **10** is inactive. The morpholine-containing compound **11** displayed 5-HT_{2C}R activity with an E_{\max} of $128.0 \pm 9.9\%$ ($p < 0.05$). For the remaining undec-1-yn-1-yl LT derivatives, only **13** displayed 5-HT_{2C}R activity with an E_{\max} of $121.8 \pm 8.0\%$ ($p < 0.05$), and interestingly showed activity at the 5-HT_{2A}R ($E_{\max} = 117.9 \pm 4.3\%$; $p < 0.05$), being the only compound from this design to show activity at both the 5-HT_{2C}R and 5-HT_{2A}R. Thus, **13** is reported herein as a dual 5-HT_{2C}R and 5-HT_{2A}R PAM; however, results for the 5-HT_{2B}R were not determined. These results prove difficult to interpret in comparison to the SAR generated by the undecyl derivatives from which **1** was derived.³⁸¹

Table 4.1 Functional activity assessments in 5-HT_{2C}R, 5-HT_{2A}R and 5-HT_{2B}R

Functional Screening		5-HT _{2C} R		5-HT _{2A} R	5-HT _{2B} R	
Cmpd	Compound Structure	5-HT E _{max} % (SEM)	5-HT+Cmpd LogEC ₅₀ (SEM)	5-HT E _{max} % (SEM)	5-HT E _{max} % (SEM)	CNS- MPO
6		111.2 (8.1) P=0.224	-8.34 (0.09) p=0.295	n.d.	n.d.	n.d.
7		120.6 (14.9) p=0.218	-8.16 (0.159) p=0.658	n.d.	n.d.	n.d.
8		119.4 (7.4)* p=0.046	-8.37 (0.15) p=0.882	103.2 (4.9) p=0.5403	n.d.	3.9
9		100.5 (9.5) p=0.962	-8.58 (0.137) p=0.695	n.d.	n.d.	n.d.
10		116.9 (11.4) p=0.213	-8.19 (0.172) p=0.982	n.d.	n.d.	n.d.
11		128.0 (9.9)* p=0.025	-8.45 (0.13) p=0.870	104.9 (2.9) p=0.2394	n.d.	3.9
12		105.6 (5.7) p=0.400	-8.25 (0.090) p=0.356	n.d.	n.d.	n.d.
13		121.8 (8.0)* p=0.042	-8.34 (0.154) p=0.755	117.9 (4.3)* p=0.0251	n.d.	3.4
14		121.0 (11.6) p=0.1440	-8.41 (0.14) p=0.677	n.d.	n.d.	n.d.
18		120.3 (5.9)* p=0.014	-8.35 (0.07) p=0.514	105.8 (6.9) p=0.4579	115 (9.7) p=0.1832	5.2
19		123.0 (5.0)* p=0.003	-8.39 (0.11) p=0.443	n.d.	117.7 (4.6)* p=0.0312	5.2
20		118.0 (7.0)* p=0.042	-8.24 (0.12) p=0.230	95.85 (4.4) p=0.4181	126.2 (8.3)* p=0.0341	5.0

24		113.4 (9.3) p=0.244	-8.44 (0.04) p=0.611	n.d.	n.d.	n.d.
25		114.0 (8.0) p=0.155	-8.45 (0.11) p=0.935	n.d.	n.d.	n.d.
26		97.6 (2.3) p=0.358	-8.19 (0.07) p=0.013	n.d.	n.d.	n.d.

To further probe 5-HT_{2C}R accommodation of the pyridinecarboxamide core, three compounds were synthesized based on 5-HT_{2C}R lead PAM **2**. It was established that the 1,3-propanediol PH acted as a privileged fragment and thus **18** was produced.⁴⁰⁵ Compound **18** displayed 5-HT_{2C}R PAM activity with an E_{max} of 120.3 ± 5.9% (p < 0.05), consistent with our findings for **2** (E_{max} of 127.4 ± 8.8%). Lengthening of the LT by incorporating a phenylethynyl LT abolished 5-HT_{2C}R activity. This effect was reproducible for compounds **19** and **20**, where the phenylethynyl derivatives, **25** and **26** respectively, consequently abolished 5-HT_{2C}R activity. Of note, the smaller phenyl LT-based 5-HT_{2C}R PAMs gained the apparent ability to also interact with the 5-HT_{2B}R. Functional potentiation at the 5-HT_{2B}R was observed for **19** (E_{max} = 117.7 ± 4.6%; p < 0.05) and **20** (E_{max} = 126.2 ± 8.3%; p < 0.05), while radioligand binding studies (**Table 4.2**) show significant binding inhibition of the radioligand at the 5-HT_{2B}R for compound **18**, potential inhibition at the 5-HT_{2B}R for **19**, and potential inhibition at the 5-HT_{2C}R and 5-HT_{2B}R for **20**. These cross-5-HT₂R interactions were particularly interesting since the productive functional activity and binding inhibition were correlated and both assays showed no interactions at the 5-HT_{2A}R for **18**, **19** and **20**. Thus, **19** and **20** are reported herein as dual 5-HT_{2C}R and 5-HT_{2B}R PAMs at 1 nM concentrations and the pyridinecarboxamide core appears to provide selectivity against the 5-HT_{2A}R. Referencing our previously reported radioligand binding data for compound **2**, which showed no displacement at any 5-HTRs, these data suggest that the aromatic core introduction

broadens activity to the 5-HT_{2B}R (and potentially the 5-HT_{1A}R and 5-HT_{1B}R), while remaining selective against the 5-HT_{2A}R.

The previously discussed undec-1-yn-1-yl LT 5-HT_{2C}R PAMs **8**, **11** and **13** displayed notable radioligand displacement across the panel of screened receptors and transporters (**Table 4.2**). Compound **11** significantly inhibited radioligand binding at the 5-HT_{2C}R, 5-HT_{2A}R and 5-HT_{2B}R, and had appreciable effects at six other targets. This data, along with poor CNS-MPO scores (**Table 4.1**), and poor DMPK attributes for **13**, ultimately precludes these compounds from being useful *in vivo* tool compounds in their present configuration. However, the phenyl LT derivative **18** appeared to be the most selective 5-HT_{2C}R PAM (showing no activity at the 5-HT_{2A}R or 5-HT_{2B}R) and having calculated a promising CNS-MPO score, we proceeded to assess the *in vitro* and *in vivo* DMPK parameters for **18**.

***In vivo* PK profiling of compound 18.** Briefly, the *in vivo* PK profile of 18 was assessed both intravenously (IV, 10 mg/kg) and orally (PO, 20 mg/kg) in male Sprague Dawley rats (**Table 4.3**). Although the free fraction (F) of $48.79 \pm 11.96\%$ after oral dosing was promising, the half-life ($T_{1/2}$) was sub-optimal for both IV and PO. Additionally, the clearance and associated parameters were poor for **18**. This result may be expected for small molecular weight, aromatic compounds, however if the half-life is taken into consideration **18** may be suitable for *in vivo* rodent behavioral assays given its clean off-target profile and good CNS-MPO score.

Table 4.3 *In vivo* pharmacokinetic profiling of compound **18**

<i>In vivo pharmacokinetic profile of 18</i>							
Dose (mg/kg)	$T_{1/2}$ (h)	T_{max} (h)	CL ($L h^{-1} kg^{-1}$)	V_{ss} (L/kg)	C_{max} (ng/mL)	AUC _{0-inf} (ng·h/mL)	F (%)
10 IV	0.66 ± 0.05	n.a.	2.02 ± 0.13	1.92 ± 0.26	10267.9 ± 1143.2	4971.6 ± 316.6	n.a.
20 PO	0.97 ± 0.29	0.50 ± 0.00	4.31 ± 1.20	6.34 ± 3.75	3967.8 ± 957.1	4857.2 ± 1187.0	48.79 ± 11.96

3. CONCLUSIONS

A series of rationally designed and synthesized analogues containing a pyridinecarboxamide core were obtained and pharmacologically characterized. The initial goal of probing the 5-HT_{2C}R binding pocket with analogues characterized by increased rigidity and planar geometry was achieved. However, an additional and important observation was made regarding the importance of a saturated piperidinecarboxamide core for 5-HT_{2R} subtype selectivity. The analogues herein displayed interesting activities across 5-HT_{2R}s, including the dual 5-HT_{2C}R and 5-HT_{2A}R PAM **13** and the dual 5-HT_{2C}R and 5-HT_{2B}R PAMs **19** and **20**. Further structural work can be performed based on these observations to provide more information about 5-HT_{2R} subtype selectivity. Finally,

compound **18** was discovered as a 5-HT_{2C}R selective PAM with an excellent off-target profile and an adequate *in vivo* PK profile for use as an *in vivo* tool compound.

4. EXPERIMENTAL SECTION

4.1 Chemistry

General. All commercially available starting materials and solvents were reagent grade and used without further purification. Reactions were performed under a nitrogen atmosphere in dry glassware with magnetic stirring. Preparative column chromatography was performed using silica gel 60, particle size 0.063-0.200 mm (70-230 mesh, flash). Analytical TLC was carried out employing silica gel 60 F254 plates (Merck, Darmstadt). Visualization of the developed chromatograms was performed with detection by UV (254 nm). NMR spectra were recorded on a Bruker-600 (¹H, 600 MHz; ¹³C, 150 MHz) spectrometer or Bruker-300 (¹H, 300 MHz; ¹³C, 75 MHz). ¹H and ¹³C NMR spectra were recorded with TMS as an internal reference. Chemical shifts were expressed in ppm, and *J* values were given in Hz. High-resolution mass spectra (HRMS) were obtained from Thermo Fisher LTQ Orbitrap Elite mass spectrometer. Parameters include the following: Nano ESI spray voltage was 1.8 kV; Capillary temperature was 275 °C and the resolution was 60,000; Ionization was achieved by positive mode. Melting points were measured on a Thermo Scientific Electrothermal Digital Melting Point Apparatus and uncorrected. The purity of final compounds was determined by analytical HPLC using a Shimadzu HPLC system (model: CBM-20A LC-20AD SPD-20A UV/VIS). HPLC analysis conditions: Waters μBondapak C18 (300 × 3.9 mm); flow rate 0.5 mL/min; UV detection at 270 and 254 nm; linear gradient from 10% acetonitrile in water to 100% acetonitrile in water in 20 min followed by 30 min of the last-named solvent (0.1% TFA was added into both acetonitrile and water). All biologically evaluated compounds have been characterized with ¹H NMR, ¹³C NMR, HRMS, and HPLC analyses to ensure a purity of > 95%.

General procedure for the synthesis of 6-14. To a solution of **6**, **17**, or **23** (0.18 mmol) and amino alcohols (0.18 mmol) in 4 mL of DMF was added HBTU (0.23 mmol) and DIPEA (0.45 mmol). The resulting mixture was stirred at room temperature for 16 h. The DMF was removed under vacuum to give a brown oily residue, which was partitioned between CH₂Cl₂ (50 mL) and 10% citric aqueous solution (10 mL). The organic layer was separated and washed with saturated aqueous NaHCO₃ (10 mL). After drying over anhydrous Na₂SO₄, the solvent was removed under vacuum to give an oily residue. This residue was purified with a silica gel column (eluting with 10% MeOH in CH₂Cl₂), affording compounds **7-14**, **18-20**, and **24-26**.

4-(Undec-1-yn-1-yl)picolinic acid (6). ¹H-NMR (300 MHz, CDCl₃) δ 8.24 (s, 1H), 7.88 (s, 1H), 7.12 – 6.84 (m, 1H), 2.32 (t, *J* = 7.1 Hz, 2H), 1.54 (t, *J* = 7.3 Hz, 2H), 1.27 (q, *J* = 4.5 Hz, 12H), 0.97 – 0.77 (m, 3H). ¹³C-NMR (75 MHz, CDCl₃) δ 171.07, 152.94, 147.79, 133.43, 127.01, 126.65, 96.24, 78.38, 31.88, 29.50, 29.33, 29.18, 29.02, 28.47, 22.68, 19.50, 14.10.

N-(2-Hydroxyethyl)-4-(undec-1-yn-1-yl)picolinamide (7). ¹H-NMR (300 MHz, CDCl₃) δ 8.50 – 8.42 (m, 1H), 8.11 – 8.04 (m, 1H), 7.36 (dt, *J* = 4.8, 1.4 Hz, 1H), 3.75 (dd, *J* = 7.2, 3.6 Hz, 2H), 3.58 (td, *J* = 5.6, 2.9 Hz, 2H), 2.42 (td, *J* = 7.0, 2.6 Hz, 2H), 1.59 (tt, *J* = 6.9, 3.4 Hz, 2H), 1.42 (t, *J* = 7.3 Hz, 2H), 1.36 – 1.16 (m, 10H), 0.85 (td, *J* = 6.7, 2.8 Hz, 3H). ¹³C-NMR (75 MHz, CDCl₃) δ 164.99, 149.45, 148.00, 134.17, 128.19, 124.46, 97.66, 77.94, 61.19, 41.95, 31.78, 29.37, 29.19, 29.03, 28.83, 28.22, 22.57, 19.40, 13.96.

N-(3-Hydroxypropyl)-4-(undec-1-yn-1-yl)picolinamide (8). ¹H-NMR (300 MHz, CDCl₃) δ 8.49 (dd, *J* = 5.0, 0.9 Hz, 1H), 8.29 (s, 1H), 8.19 (dd, *J* = 1.6, 0.9 Hz, 1H), 7.41 (dd, *J* = 5.0, 1.6 Hz, 1H), 3.70 (dt, *J* = 12.3, 6.1 Hz, 4H), 2.48 (t, *J* = 7.0 Hz, 2H), 1.85 (p, *J* = 5.9 Hz, 2H), 1.66 (p, *J* = 6.9 Hz, 2H), 1.49 (t, *J* = 7.4 Hz, 2H), 1.43 – 1.26 (m, 10H), 1.02 – 0.87 (m, 3H). ¹³C-NMR (75 MHz, CDCl₃) δ 165.25, 149.45, 147.95, 134.18, 128.11, 124.66, 97.61, 78.09, 59.00, 35.82, 32.55, 31.85, 29.45, 29.27, 29.11, 28.90, 28.31, 22.65, 19.50, 14.08.

(S)-N-(2,3-Dihydroxypropyl)-4-(undec-1-yn-1-yl)picolinamide (9). ¹H-NMR (300 MHz, CDCl₃) δ 8.46 (dd, *J* = 5.1, 0.9 Hz, 1H), 8.09 (dd, *J* = 1.7, 0.8 Hz, 1H), 7.39 (dd, *J* = 5.0, 1.6 Hz, 1H), 3.85 (p, *J* = 5.2 Hz, 1H), 3.70 – 3.46 (m, 4H), 2.44 (t, *J* = 7.0 Hz, 2H), 1.71 – 1.54 (m, 2H), 1.44 (t, *J* = 7.4 Hz, 2H), 1.39 – 1.20 (m, 10H), 0.94 – 0.82 (m, 3H). ¹³C-NMR (75 MHz, CDCl₃) δ 165.48, 149.19, 148.09, 134.22, 128.31, 124.57, 97.77, 70.79, 63.55, 41.93, 31.80, 29.40, 29.22, 29.17, 29.05, 28.86, 28.24, 22.60, 19.44, 14.01

N-(1,3-Dihydroxypropan-2-yl)-4-(undec-1-yn-1-yl)picolinamide (10). ¹H-NMR (300 MHz, CDCl₃) δ 8.42 (dd, *J* = 5.0, 1.5 Hz, 1H), 8.02 (q, *J* = 1.3 Hz, 1H), 7.38 – 7.28 (m, 1H), 4.04 (p, *J* = 5.2 Hz, 1H), 3.89 – 3.71 (m, 4H), 2.39 (td, *J* = 7.1, 1.5 Hz, 2H), 1.64 – 1.50 (m, 2H), 1.47 – 1.33 (m, 2H), 1.24 (d, *J* = 6.4 Hz, 10H), 0.82 (dt, *J* = 7.0, 3.3 Hz, 3H). ¹³C-NMR (75 MHz, CDCl₃) δ 164.67, 149.33, 148.04, 134.16, 128.25, 124.41, 97.67, 77.87, 61.31, 52.49, 31.74, 29.33, 29.15, 28.99, 28.79, 28.17, 22.53, 19.35, 13.90.

N-(2-Morpholinoethyl)-4-(undec-1-yn-1-yl)picolinamide (11). ¹H-NMR (300 MHz, CDCl₃) δ 8.51 (dd, *J* = 5.0, 0.9 Hz, 1H), 8.33 (s, 1H), 8.18 (dd, *J* = 1.7, 0.8 Hz, 1H), 7.39 (dd, *J* = 5.0, 1.6 Hz, 1H), 3.84 – 3.71 (m, 4H), 3.63 (q, *J* = 6.1 Hz, 2H), 2.65 (t, *J* = 6.3 Hz, 2H), 2.56 (dd, *J* = 5.6, 3.7 Hz, 4H), 2.47 (d, *J* = 7.1 Hz, 2H), 1.71 – 1.58 (m, 2H), 1.48 (t, *J* = 7.4 Hz, 2H), 1.33 (dq, *J* = 7.2, 3.9 Hz, 10H), 1.01 – 0.85 (m, 3H). ¹³C-NMR (75 MHz, CDCl₃) δ 164.06, 150.01, 147.98, 133.96, 127.87, 124.51, 97.31, 78.18, 66.98, 57.32, 53.48, 36.01, 31.85, 29.45, 29.26, 29.11, 28.90, 28.32, 22.65, 19.50, 14.08.

N-((1S,2S)-1,3-Dihydroxy-1-phenylpropan-2-yl)-4-(undec-1-yn-1-yl)picolinamide (12). ¹H-NMR (300 MHz, CDCl₃) δ 8.70 (d, *J* = 8.4 Hz, 1H), 8.46 (dd, *J* = 5.0, 0.9 Hz, 1H), 8.14 – 8.02 (m, 1H), 7.49 – 7.42 (m, 2H), 7.40 – 7.25 (m, 3H), 5.20 (t, *J* = 3.5 Hz, 1H), 4.34 (dq, *J* = 8.9, 4.6 Hz, 1H), 4.09 (s, 1H), 4.03 – 3.83 (m, 2H), 3.59 (s, 1H), 2.49 (t, *J* = 7.1 Hz, 2H), 1.75 – 1.61 (m, 2H), 1.58 – 1.45 (m, 32H), 1.42 – 1.27 (m, 10H), 1.01 – 0.90 (m, 3H). ¹³C-NMR (75 MHz, CDCl₃) δ 164.82, 149.36, 148.03, 141.19, 134.04, 128.42, 128.12, 127.79, 126.13, 124.62, 97.55, 78.08, 73.93, 63.49, 56.92, 31.87, 29.47, 29.29, 29.13, 28.93, 28.32, 22.68, 19.52, 14.12.

***N*-(4-Hydroxybenzyl)-4-(undec-1-yn-1-yl)picolinamide (13).** ¹H-NMR (300 MHz, CDCl₃) δ 8.47 (dd, *J* = 5.0, 0.9 Hz, 1H), 8.36 (t, *J* = 6.1 Hz, 1H), 8.22 (dd, *J* = 1.6, 0.9 Hz, 1H), 7.40 (dd, *J* = 5.0, 1.6 Hz, 1H), 7.26 – 7.16 (m, 2H), 6.89 – 6.78 (m, 2H), 4.61 (d, *J* = 6.0 Hz, 2H), 2.48 (t, *J* = 7.0 Hz, 2H), 1.66 (p, *J* = 6.9 Hz, 2H), 1.49 (t, *J* = 7.4 Hz, 2H), 1.43 – 1.24 (m, 10H), 0.98 – 0.86 (m, 3H). ¹³C-NMR (75 MHz, CDCl₃) δ 164.03, 155.64, 149.66, 147.91, 134.24, 129.56, 129.24, 128.14, 124.73, 115.66, 97.68, 78.11, 43.16, 31.86, 29.45, 29.27, 29.11, 28.91, 28.31, 22.66, 19.52, 14.09.

***N*-(3,4-Dihydroxybenzyl)-4-(undec-1-yn-1-yl)picolinamide (14).** ¹H-NMR (300 MHz, CDCl₃) δ 8.49 – 8.40 (m, 1H), 8.16 (dd, *J* = 1.6, 0.8 Hz, 1H), 7.39 (dd, *J* = 5.0, 1.6 Hz, 1H), 6.89 (d, *J* = 2.0 Hz, 1H), 6.84 (d, *J* = 8.1 Hz, 1H), 6.75 (dd, *J* = 8.1, 1.9 Hz, 1H), 4.54 (d, *J* = 6.1 Hz, 2H), 2.48 (t, *J* = 7.1 Hz, 2H), 1.67 (p, *J* = 7.0 Hz, 2H), 1.48 (t, *J* = 7.4 Hz, 2H), 1.33 (q, *J* = 5.0 Hz, 10H), 1.01 – 0.85 (m, 3H). ¹³C-NMR (75 MHz, CDCl₃) δ 164.31, 149.29, 147.98, 144.27, 143.87, 134.28, 129.93, 128.28, 124.68, 119.97, 115.26, 114.85, 97.83, 78.04, 43.35, 31.85, 29.44, 29.27, 29.10, 28.93, 28.30, 22.65, 19.53, 14.08.

(*S*)-*N*-(2,3-Dihydroxypropyl)-4-phenylpicolinamide (18). ¹³C-NMR (75 MHz, CDCl₃) δ 166.13, 150.01, 149.77, 148.77, 137.17, 129.58, 129.23, 127.07, 124.10, 120.27, 71.33, 63.76, 42.24. ¹H-NMR (300 MHz, CDCl₃) δ 8.56 (d, *J* = 5.1 Hz, 1H), 8.40 (t, *J* = 1.6 Hz, 1H), 7.71 – 7.60 (m, 3H), 7.55 – 7.42 (m, 3H), 3.96 (m, 1H), 3.76 – 3.57 (m, 4H).

***N*-(1,3-Dihydroxypropan-2-yl)-4-phenylpicolinamide (19).** ¹H-NMR (300 MHz, CDCl₃) δ 8.64 (d, *J* = 7.8 Hz, 1H), 8.54 (d, *J* = 5.1 Hz, 1H), 8.37 (s, 1H), 7.70 – 7.61 (m, 2H), 7.60 – 7.56 (m, 1H), 7.53 – 7.43 (m, 2H), 4.21 (dq, *J* = 9.2, 4.6 Hz, 1H), 4.04 – 3.88 (m, 4H). ¹³C-NMR (75 MHz, CDCl₃) δ 165.21, 150.06, 149.92, 148.71, 137.18, 129.53, 129.20, 127.05, 123.96, 120.18, 63.17, 52.93.

***N*-((1*S*,2*S*)-1,3-Dihydroxy-1-phenylpropan-2-yl)-4-phenylpicolinamide (20).** ¹H-NMR (300 MHz, CDCl₃) δ 8.76 (d, *J* = 8.3 Hz, 1H), 8.53 (ddt, *J* = 5.1, 1.9, 0.8 Hz, 1H), 8.32 (s, 1H), 7.68 – 7.53 (m, 3H), 7.51 – 7.41 (m, 5H), 7.34 – 7.22 (m, 2H), 5.18 (d, *J* = 4.3 Hz, 1H), 4.34 (dq, *J* = 8.9, 4.6 Hz, 1H), 4.04 – 3.83 (m, 2H). ¹³C-NMR (75 MHz,

CDCl₃) δ 165.27, 150.00, 149.83, 148.71, 141.23, 137.25, 129.49, 129.19, 128.46, 127.83, 127.06, 126.17, 123.89, 120.21, 74.12, 63.62, 57.08.

(S)-N-(2,3-Dihydroxypropyl)-4-(phenylethynyl)picolinamide (24). ¹H-NMR (300 MHz, CDCl₃) δ 8.60 (dd, *J* = 5.0, 0.9 Hz, 1H), 8.49 (s, 1H), 8.34 (dd, *J* = 1.6, 0.9 Hz, 1H), 7.68 – 7.60 (m, 2H), 7.58 (dd, *J* = 5.0, 1.6 Hz, 1H), 7.53 – 7.43 (m, 3H), 3.98 (p, *J* = 5.0 Hz, 1H), 3.84 – 3.59 (m, 4H). ¹³C-NMR (75 MHz, CDCl₃) δ 165.69, 149.33, 148.26, 133.36, 132.01, 129.49, 128.55, 128.01, 124.48, 121.79, 95.45, 86.15, 71.35, 63.67, 42.22.

N-(1,3-Dihydroxypropan-2-yl)-4-(phenylethynyl)picolinamide (25). ¹H-NMR (300 MHz, CDCl₃) δ 8.54 (ddd, *J* = 5.0, 1.7, 0.8 Hz, 1H), 8.22 (ddd, *J* = 2.4, 1.5, 0.8 Hz, 1H), 7.63 – 7.48 (m, 3H), 7.40 (qt, *J* = 4.8, 2.3 Hz, 3H), 4.22 – 3.99 (m, 1H), 3.88 (ddd, *J* = 11.3, 4.5, 2.3 Hz, 2H), 3.79 (ddd, *J* = 11.4, 5.4, 2.3 Hz, 2H), 3.27 (s, 2H). ¹³C-NMR (75 MHz, CDCl₃) δ 164.53, 149.62, 148.23, 133.26, 131.92, 129.44, 128.48, 127.92, 124.25, 121.69, 95.31, 86.06, 61.59, 52.59.

N-((1S,2S)-1,3-Dihydroxy-1-phenylpropan-2-yl)-4-(phenylethynyl)picolinamide (26). ¹H-NMR (300 MHz, CDCl₃) δ 8.55 (dd, *J* = 5.0, 0.8 Hz, 1H), 8.12 (dd, *J* = 1.6, 0.9 Hz, 1H), 7.61 – 7.53 (m, 2H), 7.50 (dd, *J* = 5.0, 1.7 Hz, 1H), 7.47 – 7.36 (m, 5H), 7.36 – 7.19 (m, 3H), 5.15 (d, *J* = 3.6 Hz, 1H), 4.32 – 4.21 (m, 1H), 3.83 (qd, *J* = 11.2, 5.4 Hz, 2H). ¹³C-NMR (75 MHz, CDCl₃) δ 164.56, 149.51, 148.26, 141.47, 133.13, 131.91, 129.40, 128.47, 128.23, 127.82, 127.50, 125.97, 124.19, 121.73, 95.18, 86.10, 72.46, 62.50, 56.70.

4.2 *In Vitro* Pharmacology

Intracellular Calcium (Ca²⁺) Release Assay in h5-HT₂R-CHO Cells. Chinese hamster ovary (CHO) cells stably transfected with the human unedited (INI) h5-HT₂cR (h5-HT₂cR-CHO cells) or the human h5-HT₂aR (h5-HT₂aR-CHO cells) were the generous gift from Drs. Kelly A. Berg and William P. Clarke (University of Texas Health Science Center, San Antonio). Cells were grown at 37°C, 5% CO₂, and 85% relative humidity

environment in GlutaMax-MEM medium (Invitrogen, Carlsbad, CA) containing 5% fetal bovine serum (Atlanta Biologicals, Atlanta, GA) and 100 $\mu\text{g}/\text{mL}$ hygromycin (Mediatech, Manassas, VA) and were passaged when they reached 80% confluency. The Ca_i^{2+} release assay was performed according to our recent publications.³⁸¹ Briefly, cells (150 μL ; passages 6-16 (FlexStation 3; Molecular Devices) or 30,000 cells/well (FLIPR^{TETRA}; Molecular Devices) in black-wall 96-well culture plates with optically clear flat bottoms. To ensure even plating of cells, the source reservoir was frequently agitated or triturated, and plates were maintained on a rotary shaker at low speed for 20 min after plating and returned to the incubator overnight. Approximately 24 h after plating, the medium was replaced with serum-free (SF) GlutaMax-MEM medium supplemented with 20 nM to 100 μM putrescine (Sigma-Aldrich, St. Louis, MO), 20 nM to 100 μM progesterone (Sigma-Aldrich), and 1:100 ITS (1000 mg/L human recombinant insulin, 550 mg/L human recombinant transferrin, 0.67 mg/L selenious acid; Corning Inc., Corning, NY) (SF+ medium). Following a 3 h incubation, SF+ medium was replaced with 40 μL of Hank's balanced saline solution (HBSS; without CaCl_2 or MgCl_2 , pH 7.4) plus 40 μL of Calcium 4 dye solution (FLIPR No-wash kit, Molecular Devices, Sunnyvale CA, catalog no R8142) supplemented with 2.5 mM of water-soluble probenecid (Sigma-Aldrich) to inhibit extracellular transport of the dye. Plates were incubated with dye solution for 60 min at 37°C, 15 min at room temperature in the dark. Drug dilutions were prepared at 5x final concentration in 1x HBSS; delivery of compound (20 $\mu\text{L}/\text{well}$) was followed 15 min later by 5-HT (10 pM to 10 μM ; 25 $\mu\text{L}/\text{well}$). A baseline was established for each well before addition of the test compound and again before addition of 5-HT. The fluorescence read following the addition of 5-HT was used to assess allosteric modulation of 5-HT-evoked Ca_i^{2+} release. Fluorescence was measured using a FlexStation 3 (Molecular Devices) or FLIPR^{TETRA} (130 gain, 60% intensity, 0.3 s exposure). For the FlexStation 3, a 17 s baseline was established before addition of compounds following which fluorescence was recorded every 1.7 s for a total 240 s. Maximum peak height was determined by the SoftMax

software (Pro 5.4.5) for each well. For the FLIPR^{TETRA}, a 10 s baseline was established before addition of compounds following which fluorescence was recorded every 1 s for 120 s following compound or for 360 s following 5-HT. Maximum peak height was determined by ScreenWorks 4.0 software for each well. After the final readings, cells were fixed in 2% paraformaldehyde (Sigma) overnight. The maximum 5-HT-induced Ca_i^{2+} release (E_{max}) in the presence of test compound was determined using 4-parameter nonlinear regression analysis (GraphPad Prism 7.04) and calculated from 4-6 biological replicates, each conducted in technical triplicates. The E_{max} for the test compound plus 5-HT was normalized to the E_{max} for 5-HT alone. Subsequent *post hoc* comparisons between means for E_{max} were made using Welch's unpaired *t* test (GraphPad Prism). All statistical analyses were conducted with an experiment-wise error rate of $\alpha = 0.05$. All treatment assignments were blinded to investigators who performed *in vitro* assays and endpoint statistical analyses. Similar procedures were followed for *in vitro* pharmacological screening in 5-HT_{2A}R and 5-HT_{2B}R expressing cells.

4.3 *In Vivo* Pharmacokinetics

Male Sprague–Dawley rats ($n = 3$ /treatment group; Charles River Laboratories) weighing 200–250 g at the beginning of the experiment were housed three per cage in a pathogen-free, temperature (20–26°C) and humidity-controlled (40–70%) environment with a 12 h light-dark cycle and ad libitum access to food and filtered water. Rats were randomly assigned to treatment groups. Vehicle [10% DMSO:90% HP- β -CD] or compound **18** dissolved in vehicle was administered to rats intravenously (iv) at 10 mg/kg or *per os* (po) at 20 mg/kg. Blood samples (0.3 mL) were collected from the retro-orbital sinus vein before dosing and at 0.08, 0.25, 0.5, 1.0, 2.0, 4.0, 8.0, and 24 h postdosing for iv administration and 0.25, 0.5, 1.0, 2.0, 4.0, 8.0, and 24 h postdosing for po administration. Blood samples were placed in heparinized tubes and centrifuged at 12,000g for 5 min at 4°C. All samples were stored at –20°C. The concentration of **18** in each sample was

analyzed by Sundia MediTech Co., Ltd. The study and the related standard operating procedures (SOPs) were reviewed and approved by Sundia Institutional Animal Care and Use Committee. The Sundia animal facility is approved with yearly inspection by the Shanghai Laboratory Animal Management Committee.

The pharmacokinetic parameters of compound **18** were calculated according to a noncompartmental model using WinNonlin 8.1 (Pharsight Corporation, ver 5.3, Mountain View, CA, USA). The peak concentration (C_{\max}) and time of peak concentration (T_{\max}) were directly obtained from the plasma concentration–time plot. The elimination rate constant (λ) was obtained by the least-squares fitted terminal log–linear portion of the slope of the plasma concentration–time profile. The elimination half-life ($t_{1/2}$) was evaluated according to $0.693/\lambda$. The area under the plasma concentration–time curve from 0 to time t (AUC_{0-t}) was evaluated using the linear trapezoidal rule and further extrapolated to infinity ($AUC_{0-\infty}$) according to the following equation: $AUC_{0-\infty} = AUC_{0-t} + C_{\text{last}}/\lambda$. The pharmacokinetic parameters are presented as mean \pm S.E.M. in Table 6. All treatment assignments were blinded to investigators who performed pharmacokinetic assays and endpoint statistical analyses.

**A DISCUSSION ON MECHANISM AND THEORY IN 5-HT₂R SUBFAMILY
ALLOSTERIC MODULATION**

**Chapter 5. A Discussion on 5-HT₂R PAM Mechanics and Mode of
Action: The Enhanced Activation State**

E.A. Wold

Abstract

As described at length in the preceding chapters, small molecule allosteric modulators of G protein-coupled receptors (GPCRs) provide a unique approach to therapeutically engage a protein class that is the target for one-third of all FDA-approved medications. The intrinsic benefit of allosteric modulation, described as fine-tuning receptor response, also introduces layers of complexity that can be magnified by the biological system of interest and unexpected allosteric networks within the targeted GPCR. The following discussion will draw heavily from recent discoveries in GPCR activation dynamics and apply these insights towards understanding allosteric modulation of the 5-HT_{2A}R and 5-HT_{2C}R. Molecular modeling and pharmacological characterizations performed by our team are used to construct a rationale for the basis of 5-HT_{2A}R and 5-HT_{2C}R positive allosteric modulator (PAM) design and function. Specifically, the enhanced activation state (EAS) is proposed as a potential mechanism for the observation that 5-HT_{2A}R and 5-HT_{2C}R PAMs significantly increase 5-HT-induced G protein activation efficacy, while significant 5-HT potency shifts are not observed. This framework can provide compelling rationale for the application of 5-HT_{2A}R and 5-HT_{2C}R PAMs in psychiatric and neurological disease, where 5-HT concentrations are dynamic and responsive to a variety of cognitive processes.

1. INTRODUCTION

G protein-coupled receptors (GPCRs) present excellent drug targets due to their typical membrane localization and second messenger systems that enable expansive modulation of cellular systems. As such, nearly one-third of marketed drugs act on GPCRs and this popularity has remained steady in new drug discovery campaigns.²⁶⁵ Functionally, GPCRs are primarily responsible for signal transduction across the cellular membrane and are ubiquitously expressed throughout the body. Signals recognized by GPCRs include photons, ions, small molecules, peptides and proteins. The recognition step implies a conformational change in the GPCR protein structure that promotes the activation of intracellular second messenger system proteins. This section will primarily focus on how the recognition step translates into G protein activation, and specifically how allosteric modulators of 5-HT₂Rs could enhance this process.

2. RECEPTOR ACTIVATION STATE MODELS

Early work on GPCR activation dynamics envisioned a two-state model where a receptor exists in an inactive state (R) and an activated state (R*⁴²⁹). The R to R* transition was understood to be mediated by the binding of an agonist and associated allosteric effects that enabled coupling of the G protein heterotrimer complex. Further work expanded on this concept to provide the cubic ternary complex model, which defines additional states including the pre-coupling of the G protein complex to the receptor prior to ligand binding.^{430, 431} The application of X-ray crystallography and cryoelectron microscopy (cryo-EM) to elucidate GPCR structures has enabled the visualization of these conformational states, including agonist, antagonist and G protein complexed receptors within the 5-HT₂R subfamily, most structures having been solved within only the past few years.^{269, 432-436} Importantly, it was becoming clear that receptor functional states are comprised of populations of conformers within an energy landscape that is dependent on the precise ligand examined in complex. This feature was examined by the Roth group in

the 5-HT_{2B}R, where they compared the structures of ergotamine and lysergic acid diethylamide (LSD), both considered agonists, but adopting different conformations of the active state.^{433, 436} Additionally, much work has been accomplished on the functional consequences of active state conformers and their capacity to bias signaling outputs, typically focusing on the canonical G protein or non-canonical β -arrestin pathways.⁴³⁷⁻⁴³⁹ Biased signaling can be viewed as shifting the efficiency of coupling and activation between various downstream signaling partners and the receptor, as a consequence of conformational alterations. However, the addition of allosteric modulators increases this complexity even further by introducing an allosteric ligand that can influence any number of steps in the aforementioned process. The addition of allosteric modulators to the ternary complex model sought to provide a means to quantify the influence of allosteric modulators on the orthosteric ligand's affinity, the receptor's coupling efficacy, or both.⁴⁴⁰⁻⁴⁴² By combining structural and pharmacological evidence with concepts of receptor state models this chapter seeks to explain the allosteric mechanism of action for our newly discovered 5-HT_{2C}R and 5-HT_{2A}R PAMs.

Illustration 5.1 Names given to various GPCR binding pockets

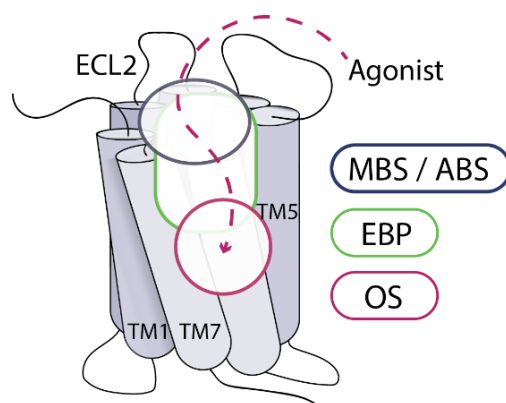


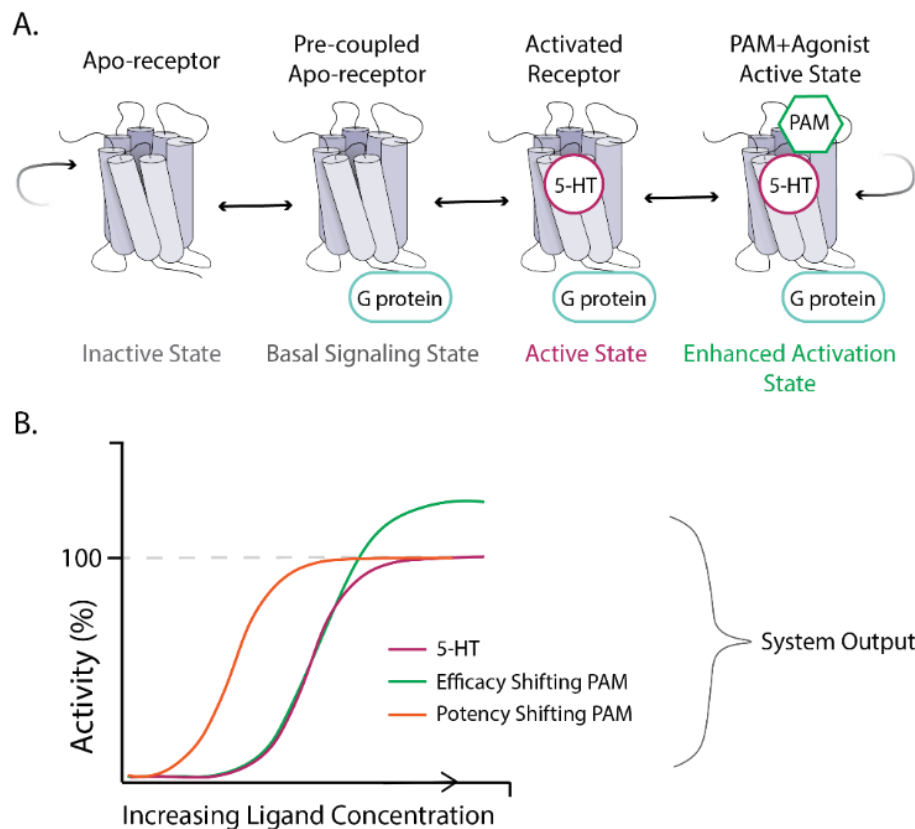
Illustration of the names given to various binding pockets within the transmembrane bundle (TM) of a GPCR. The pathway taken to reach the orthosteric site (OS) by a typical endogenous ligand is denoted by the dashed line with arrow. The most extracellular pocket is the metastable binding site (MBS) and is also known as an allosteric binding site (ABS). The region between, and often occupied by large ligands is the extended binding pocket (EBP). Extracellular loop 2 (ECL2), TM1, TM5 and TM7 are noted.

3. DEFINING THE PATHWAY FOR LIGAND BINDING

Before further discussion, some definitions are necessary to establish. The 5-HT_{2R} heptahelical bundle contains the orthosteric site (OS) wherein the endogenous agonist 5-HT binds to activate the receptor (**III. 5.1**). The metastable binding site (MBS), as relevant to this work, has been described as a transient, low-affinity ligand-recognition site that is located further towards extracellular space from the OS.^{424, 425} An earlier term for this site was the “extracellular vestibule” coined by Dror, et. al in a seminal MD simulation paper on the β_2 -adrenergic receptor in 2011.⁴²⁶ Additionally, many researchers in the field have discussed an extended binding pocket (EBP) when describing the binding pose of a notably larger ligand compared to the endogenous or reference agonist.²⁶⁹ Typically, a described EBP is nearer to the OS than is a MBS, but it is unclear if there is a boundary; MBS and EBP are not mutually exclusive and there is reason to suggest they are describing the same region of the receptor. The allosteric binding site (ABS) as it relates to GPCRs is a ligand

binding site that is spatially distinct from the OS and precludes overlap.³⁸³ Thus, the ABS can exist in the MBS or rather anywhere else on the receptor other than the OS, as has previously been discussed at length for class A GPCR allosteric modulators.¹ Finally, of importance is properly describing the difference in information provided by functional assays in comparison to conformational observations, such as NMR, MD simulations and X-ray crystal structures. In essence these studies are complementary and support one another, but typical functional assays (e.g., cell-based, 5-HT_{2C}R-Gq-mediated calcium efflux fluorescence assay) provide as an output a summation of the system comprised of numerous functional units and conformational observations focus on a single functional unit (e.g., 5-HT_{2C}R ergotamine-bound active state X-ray crystal structure) or smaller groups of units (**III. 5.2**). This clarification is supremely important when discussing the relative abundance of different conformational states in a given condition and how states may become over-represented if conditions change (e.g., the addition of a PAM).

Illustration 5.2 Models for discussion



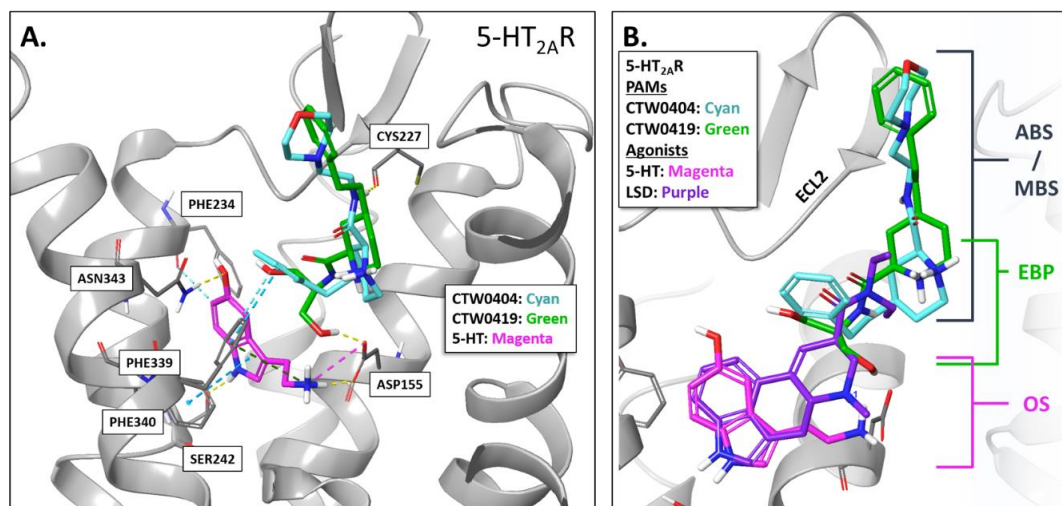
Illustrated models for discussion. (A) The states that may exist during 5-HT₂R activation and PAM potentiation. Some states with a receptor population are certainly omitted here. (B) An illustrated example of a concentration response curve with possible curve shifts in the presence of a PAM.

4. 5-HT_{2A}R AND 5-HT_{2C}R PAMs MAY STABILIZE AN ENHANCED ACTIVATION STATE (EAS)

The theoretical assertion of this work is that 5-HT_{2A}R and 5-HT_{2C}R PAMs can stabilize an enhanced activation state (EAS) of the 5-HT-bound active state (III. 5.2A). The need to propose this theory lies in the observation that thus far 5-HT_{2A}R and 5-HT_{2C}R PAMs increase signaling efficacy for the canonical G_q pathway, while the potency of 5-HT-mediated G_q activation is unchanged (III. 5.2B). Most GPCR PAMs have an appreciable effect on the agonist potency. To describe this phenomenon, two lines of GPCR-specific work will be evaluated. First, numerous studies have applied inherently

dynamic observations of GPCRs to elucidate the conformational ensembles responsible for the static, representative states resolved by X-ray crystallography and cryo-EM, such as isotopic labeling for one- and two-dimensional nuclear magnetic resonance (NMR) spectroscopy of GPCRs in micelles and membrane systems, computational molecular dynamics (MD) simulations, single-molecule fluorescence spectroscopy and electron paramagnetic resonance spectroscopy. The focus here is that there are apparent high-probability conformers and low-probability conformers situated along an energy gradient, which can be altered by allosteric networks within the receptor upon ligand binding and/or second messenger coupling. Central to the EAS theory of 5-HT_{2A}R and 5-HT_{2C}R PAM activity is the evidence for multiple active state conformers, which differ in signaling efficacy and energetic favorability, and have been recently described in remarkable detail for the adenosine A_{2A} receptor (A_{2A}R) GPCR.⁴⁴³ The second line of work presented herein is the mounting evidence that the GPCR metastable binding site (MBS) and extracellular loop 2 (ECL2) plays an important role in contributing to the overall functional state of this class of receptors. Studies with the 5-HT₂Rs, mu and kappa opioid receptors (MOR and KOR), A_{2A}R, β_2 -adrenergic receptor, ghrelin receptor and others have shown diverse mechanisms by which small molecule and peptide ligands can interact with the MBS and ECL2 an impart conformational changes of functional significance.^{424-426, 432, 434, 436, 443-445} The relevance of these studies for our 5-HT_{2A}R and 5-HT_{2C}R PAMs can be seen from our molecular modeling and ligand docking work (**Fig. 5.1**).

Figure 5.1 Molecular docking studies with the 5-HT_{2A}R



Docking images of the 5-HT_{2A}R (PDB: 6WGT) in the presence of PAMs (CTW0404, CTW0419), 5-HT, and LSD. (A) The ECL2 residue CYS227 can be seen forming an H-bond with CTW0404 in this view. (B) A docking image showing the various spaces that ligands can occupy. Of note is the overlap between PAMs and LSD in the extended binding pocket (EBP).

5. DYNAMIC OBSERVATIONS OF RECEPTOR ACTIVATION STATES PROVIDE RATIONALE FOR AN EAS

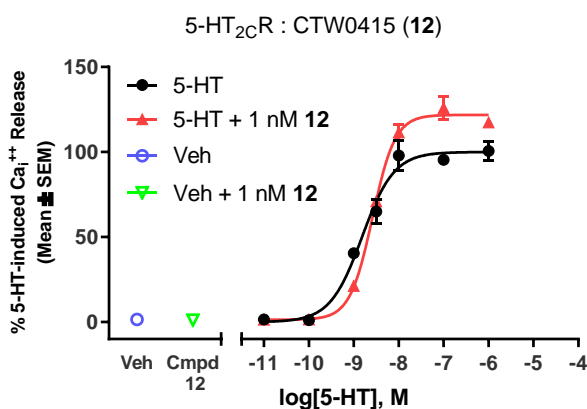
G protein-coupled receptor function is inherently mediated by allosteric networks that have evolved with the protein structure and its surroundings. Embedded in a lipid membrane, GPCRs are sensitive to the molecular composition of the membrane, cholesterol concentrations, metal ions, protein-protein interactions (e.g., Gq coupling), and other factors that ultimately produce a functional response to a ligand. Thus, GPCRs are highly dynamic proteins that adopt a staggering array of poses within an ensemble and elucidating the functionally or therapeutically relevant conformation is a considerable challenge. Huang, et. al approached this challenge with an elegant application of fluorine isotopic labeling of the A_{2A}R observed by NMR spectroscopy.⁴⁴³ They reported notable conformational shifts when the receptor was coupled to the heterotrimeric G protein

(G_Sαβγ) and additional shifts in the observed conformational ensemble after GDP release. This clear G protein allosteric influence was present in conditions of apo-receptor and inverse agonist, partial agonist or full agonist binding. The resultant landscape for A_{2A}R activation provided evidence for unique sub-populations of conformers for each ligand tested, finding at least three predominant active state conformers that varied depending on ligand. Thus, various ligands and second messenger coupling alter the receptor conformational equilibria and nucleotide exchange kinetics (i.e., efficacy). Peters, et. al recently published a computational study on the 5-HT_{2B}R activation pathway with the agonist LSD and antagonist lisuride.⁴⁴⁶ Employing enhanced sampling MD simulations they were able to calculate the free energy landscape and predict the conformer distribution in agonist- or antagonist-bound forms, while comparing to the theoretical free energy minimum conformations. Of importance to this chapter, they found that LSD promoted two distinct conformer populations in the active ensemble and that these populations were distant from the free energy minimum, indicating that there is feasibility for numerous active-like conformers and that some may have improved energetics and stability.

If one considers a system wherein 5-HT and a 5-HT_{2A}R or 5-HT_{2C}R PAM are able to occupy and stabilize a unique conformation, first there is the assumption that 5-HT could alone occupy a similar conformation, but it would be in low abundance due to less favorable energetics. For EC₅₀ concentrations of 5-HT and non-saturating concentrations of a PAM, the probability of stabilizing a distinctly low-abundance conformation would be minimal. Thus, the apparent potency of the system could remain similar for 5-HT and 5-HT+PAM conditions until 5-HT neared saturation (i.e., curve plateau). Additionally, at the level of a single functional unit (i.e., receptor), if 5-HT and the PAM are considered a single ligand for this example, the high-efficacy, low-probability 5-HT+PAM receptor conformation would have a measurable K_d , which can be calculated as the K_{off}/K_{on} . Due to this ratio, there can be alterations of a similar magnitude in the rates for K_{on} and K_{off} for 5-HT+PAM that will achieve a K_d value similar to that of 5-HT alone. For example, a K_d

value of 100 nM can be derived from a K_{on} of $10^5 \text{ M}^{-1} \text{ S}^{-1}$ and K_{off} of 10^{-2} S^{-1} and also from a K_{on} of $10^2 \text{ M}^{-1} \text{ S}^{-1}$ and K_{off} of 10^{-5} S^{-1} , a dramatic kinetic difference. It is certainly unlikely that the kinetics alone lend the apparent PAM effect seen in our assays (**Fig. 5.2**); however, in addition to receptor conformation energetics, and thus probabilities, there seems to be a reasonable argument to be made.

Figure 5.2 Lead PAM CTW0415 *in vitro* functional activity at 5-HT_{2C}R



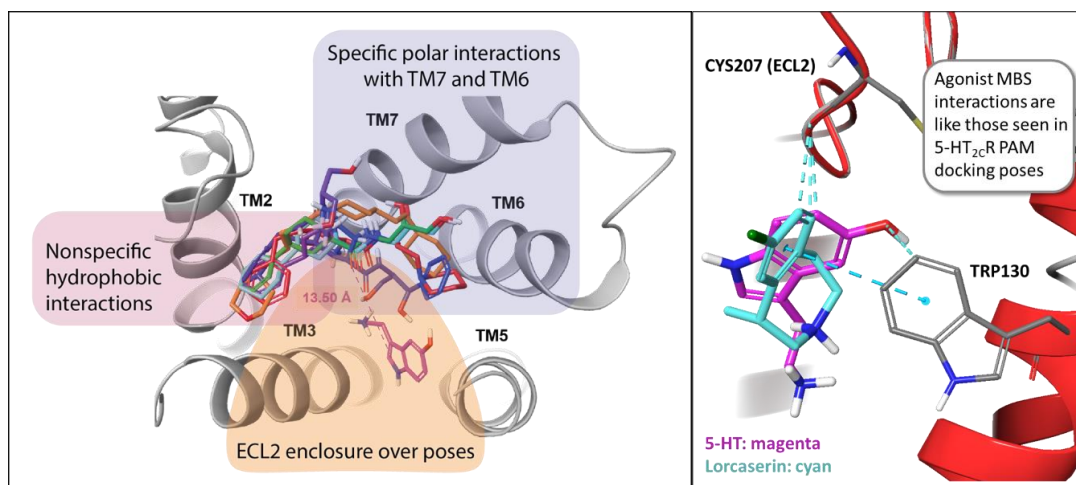
Experimental functional data from Wold, et al., *J. Med. Chem.* 2020, 63, 14, 7529-7544. This plotted data shows the efficacy increase (E_{max}) from 1 nM of the 5-HT_{2C}R PAM CTW0415 (Chapter 3, compound 12). Additionally, the lack of intrinsic agonist activity is displayed (Veh + 1 nM 12).

6. EVIDENCE FOR THE 5-HT_{2A}R AND 5-HT_{2C}R PAM BINDING SITE AND THE FUNCTIONAL RELEVANCE OF THE EXTRACELLULAR LOOP 2

In recent years, high-quality cryo-EM and X-ray crystal structures of the 5-HT_{2A}R and 5-HT_{2C}R have been solved in complex with numerous agonists and antagonists.^{269, 432, 435, 436} Importantly, the agonists have ranged in size from 25CN-NBOH (MW = 312.4 g/mol) and LSD (MW = 323.4 g/mol) to ergotamine (MW = 581.7 g/mol), allowing occupancy and stabilization of the OS and EBP. We first employed the ergotamine-5-HT_{2C}R complex structure (PDB: 6BQG) to model a 5-HT-bound 5-HT_{2C}R active

conformation and run PAM docking experiments.^{269, 381, 405} We found a notable convergence of 5-HT_{2C}R PAM docking poses interacting with ECL2, TM6 and TM7 in the putative ABS (**Fig. 5.3A**).⁴⁰⁵ The existence of a ligand binding site in this area has precedent if one recalls the Dror, et. al paper where the authors describe the “extracellular vestibule” as being a hydrophobic surface-rich location enclosed by ECL2, ECL3, TM5, TM6 and TM7.⁴²⁶ Additionally, the authors describe this site as a transient pocket for agonist recognition along the path towards the high-affinity OS. The lipophilic characteristics of our 5-HT_{2C}R PAMs brought even more attention to the “extracellular vestibule” (i.e., MBS) concept and thus a computational experiment was performed with an apo-5-HT_{2C}R model for time-sensitive, dynamic docking of 5-HT and the 5-HT_{2C}R agonist lorcaserin. We found evidence of a similar path towards the high-affinity OS, where 5-HT interacts with residues on the ECL2, TM7 and TM2 in its extracellular-most pose, and lorcaserin followed suit with a similar set of poses (**Fig. 5.3B**). Thus, the putative ABS may have evolved as a low-affinity MBS for 5-HT recognition and receptor entry. Metastable binding sites have recently been targeted in drug discovery campaigns to improve receptor subtype selectivity and increase receptor functionality.^{424, 425}

Figure 5.3 Molecular modeling of the allosteric binding site



(A) Docking poses of 5-HT_{2c}R PAMs and the illustrated regions of importance. (B) Agonists 5-HT and lorcaserin occupy a metastable binding site and interact with the same or similar residues that are engaged by 5-HT_{2c}R PAM docking.

Functionally, the ECL2 in many GPCRs plays an important role in ligand binding, constitutive activity and functional selectivity.^{436, 444, 445} The recent Huang, et al. paper on the A_{2A}R provided an illuminating study on one possible mechanism for ECL2 influence.⁴⁴³ As previously mentioned, the authors noted substantial conformational shifts when the receptor was allowed to pre-couple with the heterotrimeric G protein. To understand this effect further, a computational study was performed using rigidity-transmission allostery algorithms to identify potential allosteric networks within the protein system. An allosteric network was revealed across the ternary complex, passing from the G α protein coupling interface through the A_{2A}R TM3, TM7 and ECL2. In the Wacker, et al. manuscript reporting the first LSD-bound serotonin receptor the authors performed insightful mutagenesis studies on the 5-HT_{2A}R (L229A) and 5-HT_{2B}R (L209A), focusing on a leucine residue in the ECL2.⁴³⁶ Their data indicate the 5-HT_{2R} ECL2 plays an important role for ligand binding kinetics and agonist potency (**Table 1**). Comparing the wild-type 5-HT_{2A}R to the mutant L229A 5-HT_{2A}R, potency was observed to diminish for

5-HT and lysergamide (LSA) in a Gq-dependent Ca^{2+} efflux assay, whereas potency was reduced for 5-HT, LSD, LSA and ergotamine in a Gq-independent, β -arrestin recruitment assay, indicating some divergent influence on signaling pathways. Additionally, across agonists the effects on signaling pathways were variable when the ECL2 contained a mutated residue, providing evidence that ECL2 alterations impact signaling in a ligand-dependent manner. Thus, recalling the EAS theory for 5-HT₂R PAM mechanism, a 5-HT_{2A}R or 5-HT_{2C}R PAM that interacts with TM3, TM7 and ECL2, influences the efficacy of the receptor signaling complex via an allosteric network, and selectively modulates 5-HT-mediated signaling should elevate the signaling profile of 5-HT, specifically increasing the efficacy of the Gq-dependent signaling pathway.

Table 5.1 Mutations in the ECL2 alter functional response to 5-HT_{2A}R agonists

	WT 5-HT _{2A} R				L229A 5-HT _{2A} R				
	Ca ²⁺		β -Arrestin2		Ca ²⁺		β -Arrestin2		
	pEC ₅₀ ± SEM	E _{max} ± SEM	pEC ₅₀ ± SEM	E _{max} ± SEM	pEC ₅₀ ± SEM	E _{max} ± SEM	pEC ₅₀ ± SEM	E _{max} ± SEM	
5-HT	9.25 ± .11	100	6.89 ± .07	100	5-HT	7.85 ± .19	100	8.84 ± .03	100
LSD	8.45 ± .09	86 ± 4	9.35 ± .11	60 ± 4	LSD	8.37 ± .07	75 ± 5	8.00 ± .10	42 ± 9
LSA	7.79 ± .12	82 ± 3	7.29 ± .12	47 ± 4	LSA	7.18 ± .11	62 ± 6	6.37 ± .16	50 ± 8
ERG	8.32 ± .15	84 ± 3	8.60 ± .19	75 ± 4	ERG	7.99 ± .12	83 ± 3	7.84 ± .11	93 ± 7

Experimental data from Wacker, et al., *Cell* 2017, 168, 3, 377-389 (Supplemental Information). The wild-type 5-HT_{2A}R functionality is compared to the L229A mutant 5-HT_{2A}R in the presence of 5-HT, lysergic acid diethylamide (LSD), lysergamide (LSA) and ergotamine (ERG). Statistics were performed between WT and L229A conditions using a Welch's unpaired *t* test, *n*=3, via GraphPad: Red+Bold = statistically significant difference between the WT value and L229A value for the same compound/assay.

7. LIMITATIONS AND IMPLICATIONS OF THE 5-HT₂R PAM EAS MECHANISM

Importantly, although the proposed EAS mechanism described herein is supported by various findings across the GPCR pharmacology field, it remains speculative and theoretical. From this initial proposition, much future work can be accomplished to directly

support or invalidate this theory and is as follows. Mathematical modeling of the 5-HT₂R PAM mechanism can be accomplished by applying operational models of allosteric modulation to quantitatively derive PAM influence on 5-HT affinity and 5-HT₂R efficacy.^{440, 442} A particular weakness in this theory is that it relies on the assumption that the 5-HT+PAM-5-HT₂R complex conformation must have an increased signaling efficacy and that this conformation is a low-abundance conformer below 5-HT saturation concentrations due to probabilistic reasoning. Isotopic labeling NMR-based studies similar to those described in Huang, et al. could determine if the introduction of the PAM shifts the active-state peaks to show a new stabilized conformation.⁴⁴³ Alternatively, a possibility that the typical 5-HT active-state conformer is simply more abundant due to PAM stabilization was theoretically ruled out due to the influence this mechanism would have on lower concentrations of 5-HT (potency shift). By employing a GTP exchange assay, whereby the receptor activation is measured by the amount of radiolabeled, non-hydrolysable GTP bound to the activated G protein, one could gain a better resolution of the efficiency of the coupling and nucleotide exchange functionality presented by the EAS receptor conformer. This assay may be one method to compare 5-HT+PAM and 5-HT alone conditions in their capacity to facilitate receptor signaling. Based on the EAS mechanism proposed herein, the expectation would be an observable increase in radiolabeled GTP sequestration by the activated G proteins in the 5-HT+PAM condition, indicating enhanced efficiency in G protein coupling to 5-HT₂Rs and its subsequent functionality. Computational simulations may also be of use to understand free energy states of the PAM+5-HT 5-HT₂R complex, but simulation time would necessarily be very high due to the kinetics of GPCR activation and the presence of two ligands. Functionally, cell-based assays to measure multiple signaling pathways would be informative and could provide support for the role of ECL2 in 5-HT₂Rs. Additionally, site-directed mutagenesis studies on the ECL2 and other residues within the ABS could be employed to potentially validate the PAM binding site. Difficulties with this approach arise in the interpretation of

the data, since modeling suggests 5-HT utilizes several of the ABS residues as a MBS upon receptor entry. An ECL2 mutation alone was shown to alter 5-HT potency at the 5-HT_{2A}R (L229A) and 5-HT_{2B}R (L209A) by Wacker et al., thus caution should be used in scanning mutagenesis studies with a PAM.⁴³⁶ Lastly, the 5-HT_{2R} PAMs may stabilize other agonist-induced conformations. Ergotamine and LSD should be unable to occupy the receptor along with any of our currently designed PAMs due to molecular modeling information. However, lorcaserin or WAY163909 are small enough and are situated in a similar position as 5-HT, leaving open the possibility that PAM potentiation of these agonists is possible. Indeed, *in vivo* behavioral evidence shows that 5-HT_{2C}R PAMs can potentiate a WAY163909 dose in rats.^{381, 405} Further experiments with diverse agonists, *in vitro* and *in vivo*, could provide valuable information on probe dependence, functional selectivity, and the putative ABS. These studies and many others are certainly worth the pursuit to fully appreciate the 5-HT_{2R} PAM mechanism and there are likely much better solutions to these limitations that will be suggested.

CONCLUDING REMARKS

While this body of work provides the reader a comprehensive understanding of allosteric modulation and its pharmacological utility in targeting serotonin 5-HT₂ receptors (5-HT₂Rs), there are necessary omissions present due to the topical focus of this dissertation as well as the date of publication of the first four chapters, as they are written herein as they appear in print. These omissions I would like to briefly discuss and follow with general concluding remarks.

Allosteric modulation of G protein-coupled receptors (GPCRs) can be viewed as a rich subfield of pharmacology and medicinal chemistry and is consequently accompanied by a wealth of both experimental and theoretical literature. Topics such as mathematical models for receptor activation and the observed and theoretical benefits of allosteric modulation beyond receptor selectivity are briefly discussed in the preceding chapters, and I have published on this topic elsewhere.³⁸³ However, in light of new research on 5-HT₂Rs it is appropriate to highlight certain topics that may prove instrumental for future therapeutics. Lysergic acid diethylamide (LSD) once played a pivotal role in the description and characterization of the 5-HT_{2A}R, and now LSD and other psychedelic compounds are rejuvenating drug discovery efforts aimed at depression, post-traumatic stress disorder, anxiety, pain, inflammation, neurodegeneration, and other conditions.^{432, 447-449} As these molecules are agonists of the 5-HT_{2A}R, it is necessary to mention the potential applicability of 5-HT_{2A}R positive allosteric modulators (PAMs) in these conditions. The characteristic spatial and temporal modulatory facet of PAMs, for example only modulating the signaling of the 5-HT_{2A}R when and where 5-HT is released or present, could be a defining benefit in a drug's therapeutic profile by potentially reducing receptor desensitization and working within endogenous homeostatic mechanisms. This same benefit applies in the allosteric modulation of the 5-HT_{2C}R, whereby maintaining important neuronal signaling patterns PAMs can be employed in ways that traditional agonists

cannot. Additionally, as researchers begin to understand functional selectivity (i.e., biased signaling) more fully, it is conceivable that allosteric modulators can be employed to bias the signaling of endogenous ligands. For example, inflammation and the repair of tissues typically coincide, however if the characteristic inflammatory effects of asthma can be isolated to a particular signaling pathway then 5-HT activation can be biased away from the pathological response. Indeed, such suggestions have been made for biased 5-HT_{2A}R agonists for treating inflammation.⁴⁵⁰ The case can be made for non-hallucinogenic enhancement of 5-HT_{2A}R function in the same manner, but more work needs to be done on this front. Thus, the benefit of spatial and temporal control of receptor function, in addition to modulating functional selectivity, will be of great importance for future 5-HT_{2R}-targeted therapeutics.

Another important update to provide to the proceeding sections, especially chapter 2, is the market status of the 5-HT_{2C}R agonist lorcaserin, tradename Belviq. Although patient numbers were limited due to strict prescribing conditions around diabetes and obesity, lorcaserin was referred to as a hallmark of the 5-HT_{2C}Rs therapeutic potential.^{42, 264, 314-316, 339, 354} Recently the FDA reviewed phase IV clinical trial data and concluded that there was an increased risk of cancer in the treatment arm of the trial and recommended the suspension of lorcaserin prescribing.^{355, 451} This was subsequently followed by a request for withdrawal from the market, leaving the clinical space entirely void of a 5-HT_{2C}R agonist or PAM therapeutic.⁴⁵² With this occurrence and other considerations, it is the author's perspective that novel 5-HT_{2C}R and 5-HT_{2A}R agonist development will be fraught with numerous regulatory and off-target effect hurdles on the path towards reaching FDA-approval. The development of PAMs for the 5-HT_{2C}R and 5-HT_{2A}R could circumvent some of these issues by achieving unparalleled receptor selectivity and reducing adverse effect incidences.

Currently, the field is in the early stages of discovering and developing allosteric modulators for GPCRs and in the coming years these ligands will become more attractive

in applications where fine-tuning receptor function is paramount. A primary conclusion from this work is that GPCRs are characterized by sensitive allosteric networks throughout their domains and that these networks can be leveraged by small molecules to shift the potency and/or efficacy of orthosteric ligands. Additionally, a small molecule allosteric modulator must access an amenable binding pocket that contains residues able to transmit allosteric effects. These binding sites have been found in structurally and topologically diverse regions of GPCRs, highlighting the vast potential for modes of modulation, chemical diversity and ultimately ligand discovery. Our team has discovered novel allosteric modulators with activity at the 5-HT_{2C}R, 5-HT_{2A}R, and 5-HT_{2B}R indicating a similar allosteric binding pocket is present among the 5-HT₂Rs. With structure-activity relationship data and molecular modeling it is hypothesized that the 5-HT_{2C}R allosteric binding pocket lies within the transmembrane helix bundle near the extracellular portions of the receptor. This proposed site is supported by other studies that have shown an appropriate binding pocket space and modulation potential in the domains and residues surrounding the allosteric binding site. Finally, a theoretical mechanism for the observed positive allosteric modulation displayed by our 5-HT₂R PAMs is discussed in chapter five and termed the enhanced activation state (EAS). Taken together this dissertation is a thorough examination of the concepts in and application of 5-HT₂R allosteric modulation by small molecules.

References

1. Wold, E. A.; Chen, J.; Cunningham, K. A.; Zhou, J. Allosteric Modulation of Class A GPCRs: Targets, Agents, and Emerging Concepts. *J. Med. Chem.* **2019**, *62*, 88-127.
2. Wang, L.; Martin, B.; Brenneman, R.; Luttrell, L. M.; Maudsley, S. Allosteric Modulators of G Protein-Coupled Receptors: Future Therapeutics for Complex Physiological Disorders. *J. Pharmacol. Exp. Ther.* **2009**, *331*, 340-348.
3. Rask-Andersen, M.; Almén, M. S.; Schiöth, H. B. Trends in the exploitation of novel drug targets. *Nat. Rev. Drug Discov.* **2011**, *10*, 579-590.
4. Hauser, A. S.; Attwood, M. M.; Rask-Andersen, M.; Schiöth, H. B.; Gloriam, D. E. Trends in GPCR drug discovery: new agents, targets and indications. *Nat. Rev. Drug Discov.* **2017**, *16*, 829-842.
5. Wacker, D.; Stevens, R. C.; Roth, B. L. How Ligands Illuminate GPCR Molecular Pharmacology. *Cell* **2017**, *170*, 414-427.
6. Melancon, B. J.; Hopkins, C. R.; Wood, M. R.; Emmitte, K. A.; Niswender, C. M.; Christopoulos, A.; Conn, P. J.; Lindsley, C. W. Allosteric Modulation of Seven Transmembrane Spanning Receptors: Theory, Practice, and Opportunities for Central Nervous System Drug Discovery. *J. Med. Chem.* **2012**, *55*, 1445-1464.
7. Edgar, J.; Rochdi, B.; Marc, G.; Klaus, S. The 7 TM G-Protein-Coupled Receptor Target Family. *ChemMedChem* **2006**, *1*, 760-782.
8. Wootten, D.; Christopoulos, A.; Sexton, P. M. Emerging paradigms in GPCR allostery: implications for drug discovery. *Nat. Rev. Drug Discov.* **2013**, *12*, 630-644.
9. Changeux, J.-P.; Christopoulos, A. Allosteric Modulation as a Unifying Mechanism for Receptor Function and Regulation. *Cell* **2016**, *166*, 1084-1102.
10. van der Westhuizen, E. T.; Valant, C.; Sexton, P. M.; Christopoulos, A. Endogenous Allosteric Modulators of G Protein-Coupled Receptors. *J. Pharmacol. Exp. Ther.* **2015**, *353*, 246-260.
11. Foster, D. J.; Conn, P. J. Allosteric Modulation of GPCRs: New Insights and Potential Utility for Treatment of Schizophrenia and Other CNS Disorders. *Neuron* **2017**, *94*, 431-446.

12. Kenakin, T. P. Biased signalling and allosteric machines: new vistas and challenges for drug discovery. *Br. J. Pharmacol.* **2011**, *165*, 1659-1669.
13. Lee, Y.; Basith, S.; Choi, S. Recent Advances in Structure-Based Drug Design Targeting Class A G Protein-Coupled Receptors Utilizing Crystal Structures and Computational Simulations. *J. Med. Chem.* **2018**, *61*, 1-46.
14. Foord, S. M.; Bonner, T. I.; Neubig, R. R.; Rosser, E. M.; Pin, J.-P.; Davenport, A. P.; Spedding, M.; Harmar, A. J. International Union of Pharmacology. XLVI. G Protein-Coupled Receptor List. *Pharmacol. Rev.* **2005**, *57*, 279.
15. Fredriksson, R.; Lagerström, M. C.; Lundin, L.-G.; Schiöth, H. B. The G-Protein-Coupled Receptors in the Human Genome Form Five Main Families. Phylogenetic Analysis, Paralogue Groups, and Fingerprints. *Mol. Pharmacol.* **2003**, *63*, 1256-1272.
16. Roth, B. L.; Kroeze, W. K. Integrated Approaches for Genome-wide Interrogation of the Druggable Non-olfactory G Protein-coupled Receptor Superfamily. *J. Biol. Chem.* **2015**, *290*, 19471-19477.
17. Furness, S. G. B.; Liang, Y.-L.; Nowell, C. J.; Halls, M. L.; Wookey, P. J.; Dal Maso, E.; Inoue, A.; Christopoulos, A.; Wootten, D.; Sexton, P. M. Ligand-Dependent Modulation of G Protein Conformation Alters Drug Efficacy. *Cell* **2016**, *167*, 739-749.
18. Lu, S.; Zhang, J. Small Molecule Allosteric Modulators of G-Protein-Coupled Receptors: Drug-Target Interactions. *J. Med. Chem.* [Online early access]. DOI: 10.1021/acs.jmedchem.7b01844. Publication Date (Web): February 19, 2018.
19. Kruse, A. C.; Ring, A. M.; Manglik, A.; Hu, J.; Hu, K.; Eitel, K.; Hubner, H.; Pardon, E.; Valant, C.; Sexton, P. M.; Christopoulos, A.; Felder, C. C.; Gmeiner, P.; Steyaert, J.; Weis, W. I.; Garcia, K. C.; Wess, J.; Kobilka, B. K. Activation and allosteric modulation of a muscarinic acetylcholine receptor. *Nature* **2013**, *504*, 101-106.
20. Lu, J.; Byrne, N.; Wang, J.; Bricogne, G.; Brown, F. K.; Chobanian, H. R.; Colletti, S. L.; Di Salvo, J.; Thomas-Fowlkes, B.; Guo, Y.; Hall, D. L.; Hadix, J.; Hastings, N. B.; Hermes, J. D.; Ho, T.; Howard, A. D.; Josien, H.; Kornienko, M.; Lumb, K. J.; Miller, M. W.; Patel, S. B.; Pio, B.; Plummer, C. W.; Sherborne, B. S.; Sheth, P.; Souza, S.; Tummala, S.; Vonnrhein, C.; Webb, M.; Allen, S. J.; Johnston, J. M.; Weinglass, A. B.; Sharma, S.; Soisson, S. M. Structural basis for the cooperative allosteric activation of the free fatty acid receptor GPR40. *Nat. Struct. Mol. Biol.* **2017**, *24*, 570-577.
21. Liu, X.; Ahn, S.; Kahsai, A. W.; Meng, K. C.; Latorraca, N. R.; Pani, B.; Venkatakrisnan, A. J.; Masoudi, A.; Weis, W. I.; Dror, R. O.; Chen, X.; Lefkowitz,

- R. J.; Kobilka, B. K. Mechanism of intracellular allosteric β_2 AR antagonist revealed by X-ray crystal structure. *Nature* **2017**, *548*, 480-484.
22. Conn, P. J.; Lindsley, C. W.; Meiler, J.; Niswender, C. M. Opportunities and challenges in the discovery of allosteric modulators of GPCRs for treating CNS disorders. *Nat. Rev. Drug Discov.* **2014**, *13*, 692-708.
 23. Gregory, K. J.; Sexton, P. M.; Christopoulos, A. Overview of Receptor Allostereism. *Current Protocols in Pharmacology* **2010**, *51*, 1-34.
 24. Leach, K.; Sexton, P. M.; Christopoulos, A. Allosteric GPCR modulators: taking advantage of permissive receptor pharmacology. *Trends Pharmacol. Sci.* **2007**, *28*, 382-389.
 25. May, L. T.; Leach, K.; Sexton, P. M.; Christopoulos, A. Allosteric Modulation of G Protein-Coupled Receptors. *Annu. Rev. Pharmacol. Toxicol.* **2007**, *47*, 1-51.
 26. Tan, Q.; Zhu, Y.; Li, J.; Chen, Z.; Han, G. W.; Kufareva, I.; Li, T.; Ma, L.; Fenalti, G.; Li, J.; Zhang, W.; Xie, X.; Yang, H.; Jiang, H.; Cherezov, V.; Liu, H.; Stevens, R. C.; Zhao, Q.; Wu, B. Structure of the CCR5 chemokine receptor-HIV entry inhibitor maraviroc complex. *Science* **2013**, *341*, 1387-1390.
 27. Zheng, Y.; Qin, L.; Zacarias, N. V.; de Vries, H.; Han, G. W.; Gustavsson, M.; Dabros, M.; Zhao, C.; Cherney, R. J.; Carter, P.; Stamos, D.; Abagyan, R.; Cherezov, V.; Stevens, R. C.; Jzerman, A. P.; Heitman, L. H.; Tebben, A.; Kufareva, I.; Handel, T. M. Structure of CC chemokine receptor 2 with orthosteric and allosteric antagonists. *Nature* **2016**, *540*, 458-461.
 28. Oswald, C.; Rappas, M.; Kean, J.; Doré, A. S.; Errey, J. C.; Bennett, K.; Deflorian, F.; Christopher, J. A.; Jazayeri, A.; Mason, J. S.; Congreve, M.; Cooke, R. M.; Marshall, F. H. Intracellular allosteric antagonism of the CCR9 receptor. *Nature* **2016**, *540*, 462-465.
 29. Srivastava, A.; Yano, J.; Hirozane, Y.; Kefala, G.; Gruswitz, F.; Snell, G.; Lane, W.; Ivetac, A.; Aertgeerts, K.; Nguyen, J.; Jennings, A.; Okada, K. High-resolution structure of the human GPR40 receptor bound to allosteric agonist TAK-875. *Nature* **2014**, *513*, 124-127.
 30. Zhang, D.; Gao, Z.-G.; Zhang, K.; Kiselev, E.; Crane, S.; Wang, J.; Paoletta, S.; Yi, C.; Ma, L.; Zhang, W.; Han, G. W.; Liu, H.; Cherezov, V.; Katritch, V.; Jiang, H.; Stevens, R. C.; Jacobson, K. A.; Zhao, Q.; Wu, B. Two disparate ligand-binding sites in the human P2Y₁ receptor. *Nature* **2015**, *520*, 317-321.
 31. Cheng, R. K. Y.; Fiez-Vandal, C.; Schlenker, O.; Edman, K.; Aggeler, B.; Brown, D. G.; Brown, G. A.; Cooke, R. M.; Dumelin, C. E.; Dore, A. S.; Geschwindner, S.; Grebner, C.; Hermansson, N. O.; Jazayeri, A.; Johansson, P.; Leong, L.; Prihandoko,

- R.; Rappas, M.; Soutter, H.; Snijder, A.; Sundstrom, L.; Tehan, B.; Thornton, P.; Troast, D.; Wiggin, G.; Zhukov, A.; Marshall, F. H.; Dekker, N. Structural insight into allosteric modulation of protease-activated receptor 2. *Nature* **2017**, *545*, 112-115.
32. van Westen, G. J. P.; Gaulton, A.; Overington, J. P. Chemical, Target, and Bioactive Properties of Allosteric Modulation. *PLOS Comput. Biol.* **2014**, *10*, 1-17.
 33. Bologna, Z.; Teoh, J.-p.; Bayoumi, A. S.; Tang, Y.; Kim, I.-m. Biased G Protein-Coupled Receptor Signaling: New Player in Modulating Physiology and Pathology. *Biomol. Ther.* **2017**, *25*, 12-25.
 34. Lane, J. R.; May, L. T.; Parton, R. G.; Sexton, P. M.; Christopoulos, A. A kinetic view of GPCR allostery and biased agonism. *Nat. Chem. Biol.* **2017**, *13*, 929-937.
 35. Wild, C.; Cunningham, K. A.; Zhou, J. Allosteric Modulation of G Protein-Coupled Receptors: An Emerging Approach of Drug Discovery. *Austin J Pharmacol Ther.* **2014**, *2*, 1101.
 36. Amarandi, R.-M.; Hjortø, G. M.; Rosenkilde, M. M.; Karlshøj, S. Chapter Eight- Probing Biased Signaling in Chemokine Receptors. In *Methods in Enzymology*, Handel, T. M., Ed. Academic Press: 2016; Vol. 570, pp 155-186.
 37. Steen, A.; Larsen, O.; Thiele, S.; Rosenkilde, M. M. Biased and G Protein-Independent Signaling of Chemokine Receptors. *Front Immunol.* **2014**, *5*, 1-11.
 38. Viola, A.; Luster, A. D. Chemokines and Their Receptors: Drug Targets in Immunity and Inflammation. *Annu. Rev. Pharmacol. Toxicol.* **2008**, *48*, 171-197.
 39. Seitz, P. K.; Bremer, N. M.; McGinnis, A. G.; Cunningham, K. A.; Watson, C. S. Quantitative changes in intracellular calcium and extracellular-regulated kinase activation measured in parallel in CHO cells stably expressing serotonin (5-HT) 5-HT_{2A} or 5-HT_{2C} receptors. *BMC Neurosci.* **2012**, *13*, 25-25.
 40. Leysen, J. E.; Pauwels, P. J. 5-HT₂ Receptors, Roles and Regulation. *Ann. N.Y. Acad. Sci.* **1990**, *600*, 183-193.
 41. Bubar, M. J.; Cunningham, K. A. Prospects for serotonin 5-HT_{2R} pharmacotherapy in psychostimulant abuse. In *Progress in Brain Research*, Di Giovanni, G.; Di Matteo, V.; Esposito, E., Eds. Elsevier: 2008; Vol. 172, pp 319-346.
 42. Smith, S. R.; Prosser, W. A.; Donahue, D. J.; Morgan, M. E.; Anderson, C. M.; Shanahan, W. R. Lorcaserin (APD356), a Selective 5-HT_{2C} Agonist, Reduces Body Weight in Obese Men and Women. *Obesity* **2009**, *17*, 494-503.

43. Garcia-Carceles, J.; Decara, J. M.; Vazquez-Villa, H.; Rodriguez, R.; Codesido, E.; Cruces, J.; Brea, J.; Loza, M. I.; Alen, F.; Botta, J.; McCormick, P. J.; Ballesteros, J. A.; Benhamu, B.; Rodriguez de Fonseca, F.; Lopez-Rodriguez, M. L. A Positive Allosteric Modulator of the Serotonin 5-HT_{2C} Receptor for Obesity. *J. Med. Chem.* **2017**, *60*, 9575-9584.
44. Wild, C. T.; Miszkief, J. M.; Wold, E. A.; Soto, C. A.; Ding, C.; Hartley, R. M.; White, M. A.; Anastasio, N. C.; Cunningham, K. A.; Zhou, J. Design, Synthesis, and Characterization of 4-Undecylpiperidine-2-Carboxamides as Positive Allosteric Modulators of the Serotonin (5-HT) 5-HT_{2C} Receptor. In *J. Med. Chem. [Online early access]*. DOI: 10.1021/acs.jmedchem.8b00401. Publication Date (Web): April 5, 2018., ed.
45. Im, W. B.; Chio, C. L.; Alberts, G. L.; Dinh, D. M. Positive Allosteric Modulator of the Human 5-HT_{2C} Receptor. *Mol. Pharmacol.* **2003**, *64*, 78-84.
46. Ding, C.; Bremer, N. M.; Smith, T. D.; Seitz, P. K.; Anastasio, N. C.; Cunningham, K. A.; Zhou, J. Exploration of Synthetic Approaches and Pharmacological Evaluation of PNU-69176E and its Stereoisomer as 5-HT_{2C} Receptor Allosteric Modulators. *ACS Chem. Neurosci.* **2012**, *3*, 538-545.
47. Peng, Y.; McCorvy, J. D.; Harpsøe, K.; Lansu, K.; Yuan, S.; Popov, P.; Qu, L.; Pu, M.; Che, T.; Nikolajsen, L. F.; Huang, X.-P.; Wu, Y.; Shen, L.; Bjørn-Yoshimoto, W. E.; Ding, K.; Wacker, D.; Han, G. W.; Cheng, J.; Katritch, V.; Jensen, A. A.; Hanson, M. A.; Zhao, S.; Gloriam, D. E.; Roth, B. L.; Stevens, R. C.; Liu, Z.-J. 5-HT_{2C} Receptor Structures Reveal the Structural Basis of GPCR Polypharmacology. *Cell* **2018**, *172*, 719-730.
48. Bennett, T. A.; Montesinos, P.; Moscardo, F.; Martinez-Cuadron, D.; Martinez, J.; Sierra, J.; García, R.; de Oteyza, J. P.; Fernandez, P.; Serrano, J.; Fernandez, A.; Herrera, P.; Gonzalez, A.; Bethancourt, C.; Rodriguez-Macias, G.; Alonso, A.; Vera, J. A.; Navas, B.; Lavilla, E.; Lopez, J. A.; Jimenez, S.; Simiele, A.; Vidriales, B.; Gonzalez, B. J.; Burgaleta, C.; Hernandez Rivas, J. A.; Mascuñano, R. C.; Bautista, G.; Perez Simon, J. A.; Fuente, A. d. I.; Rayón, C.; Troconiz, I. F.; Janda, A.; Bosanquet, A. G.; Hernandez-Campo, P.; Primo, D.; Lopez, R.; Liebana, B.; Rojas, J. L.; Gorrochategui, J.; Sanz, M. A.; Ballesteros, J. Pharmacological Profiles of Acute Myeloid Leukemia Treatments in Patient Samples by Automated Flow Cytometry: A Bridge to Individualized Medicine. *Clinical Lymphoma Myeloma and Leukemia* **2014**, *14*, 305-318.
49. Tobin, A. B.; Butcher, A. J.; Kong, K. C. Location, location, location...site-specific GPCR phosphorylation offers a mechanism for cell-type-specific signalling. *Trends Pharmacol. Sci.* **2008**, *29*, 413-420.
50. Chakir, K.; Xiang, Y.; Yang, D.; Zhang, S.-J.; Cheng, H.; Kobilka, B. K.; Xiao, R.-P. The Third Intracellular Loop and the Carboxyl Terminus of β_2 -Adrenergic

- Receptor Confer Spontaneous Activity of the Receptor. *Mol. Pharmacol.* **2003**, *64*, 1048-1058.
51. Tobin, A. B. G-protein-coupled receptor phosphorylation: where, when and by whom. *Br. J. Pharmacol.* **2008**, *153*, 167-176.
 52. Lawson, Z.; Wheatley, M. The third extracellular loop of G-protein-coupled receptors: more than just a linker between two important transmembrane helices. *Biochem. Soc. Trans.* **2004**, *32*, 1048-1050.
 53. Anastasio, N. C.; Gilbertson, S. R.; Bubar, M. J.; Agarkov, A.; Stutz, S. J.; Jeng, Y.; Bremer, N. M.; Smith, T. D.; Fox, R. G.; Swinford, S. E.; Seitz, P. K.; Charendoff, M. N.; Craft, J. W., Jr.; Laezza, F. M.; Watson, C. S.; Briggs, J. M.; Cunningham, K. A. Peptide Inhibitors Disrupt the Serotonin 5-HT_{2C} Receptor Interaction with Phosphatase and Tensin Homolog to Allosterically Modulate Cellular Signaling and Behavior. *J. Neurosci.* **2013**, *33*, 1615-1630.
 54. Rasmussen, S. G. F.; Choi, H.-J.; Rosenbaum, D. M.; Kobilka, T. S.; Thian, F. S.; Edwards, P. C.; Burghammer, M.; Ratnala, V. R. P.; Sanishvili, R.; Fischetti, R. F.; Schertler, G. F. X.; Weis, W. I.; Kobilka, B. K. Crystal structure of the human β_2 adrenergic G-protein-coupled receptor. *Nature* **2007**, *450*, 383-387.
 55. Lefkowitz, R. J. Seven transmembrane receptors: something old, something new. *Acta Physiologica.* **2007**, *190*, 9-19.
 56. Brandt, D. R.; Asano, T.; Pedersen, S. E.; Ross, E. M. Reconstitution of catecholamine-stimulated guanosine triphosphatase activity. *Biochemistry* **1983**, *22*, 4357-4362.
 57. Cerione, R. A.; Codina, J.; Benovic, J. L.; Lefkowitz, R. J.; Birnbaumer, L.; Caron, M. G. Mammalian β_2 -adrenergic receptor: reconstitution of functional interactions between pure receptor and pure stimulatory nucleotide binding protein of the adenylate cyclase system. *Biochemistry* **1984**, *23*, 4519-4525.
 58. Ross, E.; Maguire, M.; Sturgill, T.; Biltonen, R.; Gilman, A. Relationship between the beta-adrenergic receptor and adenylate cyclase. *J. Biol. Chem.* **1977**, *252*, 5761-5775.
 59. De Lean, A.; Stadel, J.; Lefkowitz, R. A ternary complex model explains the agonist-specific binding properties of the adenylate cyclase-coupled beta-adrenergic receptor. *J. Biol. Chem.* **1980**, *255*, 7108-7117.
 60. Ahn, S.; Kahsai, A. W.; Pani, B.; Wang, Q. T.; Zhao, S.; Wall, A. L.; Strachan, R. T.; Staus, D. P.; Wingler, L. M.; Sun, L. D.; Sinnaeve, J.; Choi, M.; Cho, T.; Xu, T. T.; Hansen, G. M.; Burnett, M. B.; Lamerdin, J. E.; Bassoni, D. L.; Gavino, B. J.; Husemoen, G.; Olsen, E. K.; Franch, T.; Costanzi, S.; Chen, X.; Lefkowitz, R. J.

- Allosteric "beta-blocker" isolated from a DNA-encoded small molecule library. *Proc. Natl. Acad. Sci. U. S. A.* **2017**, *114*, 1708-1713.
61. Meng, K.; Shim, P.; Wang, Q.; Zhao, S.; Gu, T.; Kahsai, A. W.; Ahn, S.; Chen, X. Design, synthesis, and functional assessment of Cmpd-15 derivatives as negative allosteric modulators for the β_2 -adrenergic receptor. *Bioorg. Med. Chem.* **2018**, *26*, 2320-2330.
 62. Wood, M.; Ates, A.; Andre, V. M.; Michel, A.; Barnaby, R.; Gillard, M. In Vitro and In Vivo Identification of Novel Positive Allosteric Modulators of the Human Dopamine D₂ and D₃ Receptor. *Mol. Pharmacol.* **2016**, *89*, 303-312.
 63. Urs, N. M.; Peterson, S. M.; Caron, M. G. New Concepts in Dopamine D₂ Receptor Biased Signaling and Implications for Schizophrenia Therapy. *Biological Psychiatry* **2017**, *81*, 78-85.
 64. Kumar, V.; Bonifazi, A.; Ellenberger, M. P.; Keck, T. M.; Pommier, E.; Rais, R.; Slusher, B. S.; Gardner, E.; You, Z.-B.; Xi, Z.-X.; Newman, A. H. Highly Selective Dopamine D₃ Receptor (D₃R) Antagonists and Partial Agonists Based on Eticlopride and the D₃R Crystal Structure: New Leads for Opioid Dependence Treatment. *J. Med. Chem.* **2016**, *59*, 7634-7650.
 65. Cheng, M. H.; Garcia-Olivares, J.; Wasserman, S.; DiPietro, J.; Bahar, I. Allosteric modulation of human dopamine transporter activity under conditions promoting its dimerization. *J. Biol. Chem.* **2017**, *292*, 12471-12482.
 66. Marsango, S.; Caltabiano, G.; Jimenez-Roses, M.; Millan, M. J.; Padiani, J. D.; Ward, R. J.; Milligan, G. A Molecular Basis for Selective Antagonist Destabilization of Dopamine D₃ Receptor Quaternary Organization. *Sci. Rep.* **2017**, *7*, 2134.
 67. Niewiarowska-Sendo, A.; Polit, A.; Piwowar, M.; Tworzydło, M.; Kozik, A.; Guevara-Lora, I. Bradykinin B₂ and dopamine D₂ receptors form a functional dimer. *Biochim. Biophys. Acta* **2017**, *1864*, 1855-1866.
 68. Salmas, R. E.; Seeman, P.; Aksoydan, B.; Erol, I.; Kantarcioglu, I.; Stein, M.; Yurtsever, M.; Durdagi, S. Analysis of the Glutamate Agonist LY404,039 Binding to Nonstatic Dopamine Receptor D₂ Dimer Structures and Consensus Docking. *ACS Chem. Neurosci.* **2017**, *8*, 1404-1415.
 69. Carli, M.; Kolachalam, S.; Aringhieri, S.; Rossi, M.; Giovannini, L.; Maggio, R.; Scarselli, M. Dopamine D₂ Receptors Dimers: How can we Pharmacologically Target Them? *Curr. Neuropharmacol.* **2018**, *16*, 222-230.
 70. Kasai, R. S.; Ito, S. V.; Awane, R. M.; Fujiwara, T. K.; Kusumi, A. The Class-A GPCR Dopamine D₂ Receptor Forms Transient Dimers Stabilized by Agonists: Detection by Single-Molecule Tracking. *Cell Biochem. Biophys.* **2018**, *76*, 29-37.

71. Lai, C. Y.; Liu, Y. J.; Lai, H. L.; Chen, H. M.; Kuo, H. C.; Liao, Y. P.; Chern, Y. The D₂ Dopamine Receptor Interferes With the Protective Effect of the A_{2A} Adenosine Receptor on TDP-43 Mislocalization in Experimental Models of Motor Neuron Degeneration. *Front Neurosci.* **2018**, *12*, 187.
72. Verma, V.; Mann, A.; Costain, W.; Pontoriero, G.; Castellano, J. M.; Skoblenick, K.; Gupta, S. K.; Pristupa, Z.; Niznik, H. B.; Johnson, R. L.; Nair, V. D.; Mishra, R. K. Modulation of agonist binding to human dopamine receptor subtypes by L-prolyl-L-leucyl-glycinamide and a peptidomimetic analog. *J. Pharmacol. Exp. Ther.* **2005**, *315*, 1228-1236.
73. Fisher, A.; Mann, A.; Verma, V.; Thomas, N.; Mishra, R. K.; Johnson, R. L. Design and synthesis of photoaffinity-labeling ligands of the L-prolyl-L-leucylglycinamide binding site involved in the allosteric modulation of the dopamine receptor. *J. Med. Chem.* **2006**, *49*, 307-317.
74. Mann, A.; Verma, V.; Basu, D.; Skoblenick, K. J.; Beyaert, M. G.; Fisher, A.; Thomas, N.; Johnson, R. L.; Mishra, R. K. Specific binding of photoaffinity-labeling peptidomimetics of Pro-Leu-Gly-NH₂ to the dopamine D_{2L} receptor: evidence for the allosteric modulation of the dopamine receptor. *Eur. J Pharmacol.* **2010**, *641*, 96-101.
75. Ferreira da Costa, J.; Caamano, O.; Fernandez, F.; Garcia-Mera, X.; Sampaio-Dias, I. E.; Brea, J. M.; Cadavid, M. I. Synthesis and allosteric modulation of the dopamine receptor by peptide analogs of L-prolyl-L-leucyl-glycinamide (PLG) modified in the L-proline or L-proline and L-leucine scaffolds. *Eur. J. Med. Chem.* **2013**, *69*, 146-158.
76. Dyck, B.; Guest, K.; Sookram, C.; Basu, D.; Johnson, R.; Mishra, R. K. PAOPA, a potent analogue of Pro-Leu-glycinamide and allosteric modulator of the dopamine D₂ receptor, prevents NMDA receptor antagonist (MK-801)-induced deficits in social interaction in the rat: implications for the treatment of negative symptoms in schizophrenia. *Schizophr. Res.* **2011**, *125*, 88-92.
77. Beyaert, M. G.; Daya, R. P.; Dyck, B. A.; Johnson, R. L.; Mishra, R. K. PAOPA, a potent dopamine D₂ receptor allosteric modulator, prevents and reverses behavioral and biochemical abnormalities in an amphetamine-sensitized preclinical animal model of schizophrenia. *Eur. Neuropsychopharmacol.* **2013**, *23*, 253-262.
78. Tan, M. L.; Basu, D.; Kwiecien, J. M.; Johnson, R. L.; Mishra, R. K. Preclinical pharmacokinetic and toxicological evaluation of MIF-1 peptidomimetic, PAOPA: examining the pharmacology of a selective dopamine D₂ receptor allosteric modulator for the treatment of schizophrenia. *Peptides* **2013**, *42*, 89-96.

79. Bhagwanth, S.; Mishra, R. K.; Johnson, R. L. Development of peptidomimetic ligands of Pro-Leu-Gly-NH₂ as allosteric modulators of the dopamine D₂ receptor. *Beilstein J. Org. Chem.* **2013**, *9*, 204-214.
80. Raghavan, B.; Skoblenick, K. J.; Bhagwanth, S.; Argintaru, N.; Mishra, R. K.; Johnson, R. L. Allosteric modulation of the dopamine D₂ receptor by Pro-Leu-Gly-NH₂ peptidomimetics constrained in either a polyproline II helix or a type II beta-turn conformation. *J. Med. Chem.* **2009**, *52*, 2043-2051.
81. Bhagwanth, S.; Mishra, S.; Daya, R.; Mah, J.; Mishra, R. K.; Johnson, R. L. Transformation of Pro-Leu-Gly-NH₂ peptidomimetic positive allosteric modulators of the dopamine D₂ receptor into negative modulators. *ACS Chem. Neurosci.* **2012**, *3*, 274-284.
82. Silvano, E.; Millan, M. J.; Mannoury la Cour, C.; Han, Y.; Duan, L.; Griffin, S. A.; Luedtke, R. R.; Aloisi, G.; Rossi, M.; Zazzeroni, F.; Javitch, J. A.; Maggio, R. The tetrahydroisoquinoline derivative SB269,652 is an allosteric antagonist at dopamine D₃ and D₂ receptors. *Mol. Pharmacol.* **2010**, *78*, 925-934.
83. Rossi, M.; Fasciani, I.; Marampon, F.; Maggio, R.; Scarselli, M. The First Negative Allosteric Modulator for Dopamine D₂ and D₃ Receptors, SB269652 May Lead to a New Generation of Antipsychotic Drugs. *Mol. Pharmacol.* **2017**, *91*, 586-594.
84. Shonberg, J.; Draper-Joyce, C.; Mistry, S. N.; Christopoulos, A.; Scammells, P. J.; Lane, J. R.; Capuano, B. Structure-activity study of *N*-((*trans*)-4-(2-(7-cyano-3,4-dihydroisoquinolin-2(*1H*)-yl)ethyl)cyclohexyl)-*1H*-indole-2-carboxamide (SB269652), a bitopic ligand that acts as a negative allosteric modulator of the dopamine D₂ receptor. *J. Med. Chem.* **2015**, *58*, 5287-5307.
85. Conn, P. J.; Christopoulos, A.; Lindsley, C. W. Allosteric Modulators of GPCRs: a Novel Approach for the Treatment of CNS Disorders. *Nat. Rev. Drug Discov.* **2009**, *8*, 41-54.
86. Wess, J.; Eglén, R. M.; Gautam, D. Muscarinic acetylcholine receptors: mutant mice provide new insights for drug development. *Nat. Rev. Drug. Discov.* **2007**, *6*, 721-733.
87. Bock, A.; Schrage, R.; Mohr, K. Allosteric modulators targeting CNS muscarinic receptors. *Neuropharmacology* **2017**, *17*, 1-11.
88. Ma, L.; Seager, M. A.; Wittmann, M.; Jacobson, M.; Bickel, D.; Burno, M.; Jones, K.; Graufelds, V. K.; Xu, G.; Pearson, M.; McCampbell, A.; Gaspar, R.; Shughrue, P.; Danziger, A.; Regan, C.; Flick, R.; Pascarella, D.; Garson, S.; Doran, S.; Kretsoulas, C.; Veng, L.; Lindsley, C. W.; Shipe, W.; Kuduk, S.; Sur, C.; Kinney, G.; Seabrook, G. R.; Ray, W. J. Selective activation of the M₁ muscarinic

- acetylcholine receptor achieved by allosteric potentiation. *Proc. Natl. Acad. Sci. U. S. A.* **2009**, *106*, 15950-15955.
89. Yang, F. V.; Shipe, W. D.; Bunda, J. L.; Nolt, M. B.; Wisnoski, D. D.; Zhao, Z.; Barrow, J. C.; Ray, W. J.; Ma, L.; Wittmann, M.; Seager, M. A.; Koeplinger, K. A.; Hartman, G. D.; Lindsley, C. W. Parallel synthesis of *N*-biaryl quinolone carboxylic acids as selective M₁ positive allosteric modulators. *Bioorg. Med. Chem. Lett.* **2010**, *20*, 531-536.
 90. Mistry, S. N.; Valant, C.; Sexton, P. M.; Capuano, B.; Christopoulos, A.; Scammells, P. J. Synthesis and pharmacological profiling of analogues of benzyl quinolone carboxylic acid (BQCA) as allosteric modulators of the M₁ muscarinic receptor. *J. Med. Chem.* **2013**, *56*, 5151-5172.
 91. Kuduk, S. D.; Di Marco, C. N.; Cofre, V.; Ray, W. J.; Ma, L.; Wittmann, M.; Seager, M. A.; Koeplinger, K. A.; Thompson, C. D.; Hartman, G. D.; Bilodeau, M. T. Fused heterocyclic M₁ positive allosteric modulators. *Bioorg. Med. Chem. Lett.* **2011**, *21*, 2769-2772.
 92. Abdul-Ridha, A.; Lane, J. R.; Mistry, S. N.; Lopez, L.; Sexton, P. M.; Scammells, P. J.; Christopoulos, A.; Canals, M. Mechanistic insights into allosteric structure-function relationships at the M₁ muscarinic acetylcholine receptor. *J. Biol. Chem.* **2014**, *289*, 33701-33711.
 93. Kuduk, S. D.; Beshore, D. C.; Ng Di, M. C.; Greshock, T. J. Aryl methyl benzoquinazolinone M₁ receptor positive allosteric modulators. WO2010059773, 5/27/2010, 2010.
 94. Mistry, S. N.; Jorg, M.; Lim, H.; Vinh, N. B.; Sexton, P. M.; Capuano, B.; Christopoulos, A.; Lane, J. R.; Scammells, P. J. 4-Phenylpyridin-2-one Derivatives: A Novel Class of Positive Allosteric Modulator of the M₁ Muscarinic Acetylcholine Receptor. *J. Med. Chem.* **2016**, *59*, 388-409.
 95. Mistry, S. N.; Lim, H.; Jorg, M.; Capuano, B.; Christopoulos, A.; Lane, J. R.; Scammells, P. J. Novel Fused Arylpyrimidinone Based Allosteric Modulators of the M₁ Muscarinic Acetylcholine Receptor. *ACS Chem. Neurosci.* **2016**, *7*, 647-661.
 96. Han, C.; Chatterjee, A.; Noetzel, M. J.; Panarese, J. D.; Smith, E.; Chase, P.; Hodder, P.; Niswender, C.; Conn, P. J.; Lindsley, C. W.; Stauffer, S. R. Discovery and SAR of muscarinic receptor subtype 1 (M₁) allosteric activators from a molecular libraries high throughput screen. Part 1: 2,5-dibenzyl-2*H*-pyrazolo[4,3-*c*]quinolin-3(5*H*)-ones as positive allosteric modulators. *Bioorg. Med. Chem. Lett.* **2015**, *25*, 384-388.
 97. Kuduk, S. D.; Chang, R. K.; Di Marco, C. N.; Ray, W. J.; Ma, L.; Wittmann, M.; Seager, M. A.; Koeplinger, K. A.; Thompson, C. D.; Hartman, G. D.; Bilodeau, M.

- T. Quinolizidinone carboxylic acids as CNS penetrant, selective m1 allosteric muscarinic receptor modulators. *ACS Med. Chem. Lett.* **2010**, *1*, 263-267.
98. Kuduk, S. D.; Chang, R. K.; Di Marco, C. N.; Pitts, D. R.; Greshock, T. J.; Ma, L.; Wittmann, M.; Seager, M. A.; Koeplinger, K. A.; Thompson, C. D.; Hartman, G. D.; Bilodeau, M. T.; Ray, W. J. Discovery of a selective allosteric M₁ receptor modulator with suitable development properties based on a quinolizidinone carboxylic acid scaffold. *J. Med. Chem.* **2011**, *54*, 4773-4780.
99. Kuduk, S. D.; Chang, R. K.; Greshock, T. J.; Ray, W. J.; Ma, L.; Wittmann, M.; Seager, M. A.; Koeplinger, K. A.; Thompson, C. D.; Hartman, G. D.; Bilodeau, M. T. Identification of amides as carboxylic Acid surrogates for quinolizidinone-based M₁ positive allosteric modulators. *ACS Med. Chem. Lett.* **2012**, *3*, 1070-1074.
100. Kuduk, S. D.; Di Marco, C. N.; Saffold, J. R.; Ray, W. J.; Ma, L.; Wittmann, M.; Koeplinger, K. A.; Thompson, C. D.; Hartman, G. D.; Bilodeau, M. T.; Beshore, D. C. Identification of a methoxynaphthalene scaffold as a core replacement in quinolizidinone amide M₁ positive allosteric modulators. *Bioorg. Med. Chem. Lett.* **2014**, *24*, 1417-1420.
101. Reid, P. R.; Bridges, T. M.; Sheffler, D. J.; Cho, H. P.; Lewis, L. M.; Days, E.; Daniels, J. S.; Jones, C. K.; Niswender, C. M.; Weaver, C. D.; Conn, P. J.; Lindsley, C. W.; Wood, M. R. Discovery and optimization of a novel, selective and brain penetrant M₁ positive allosteric modulator (PAM): the development of ML169, an MLPCN probe. *Bioorg. Med. Chem. Lett.* **2011**, *21*, 2697-2701.
102. Tarr, J. C.; Turlington, M. L.; Reid, P. R.; Utley, T. J.; Sheffler, D. J.; Cho, H. P.; Klar, R.; Pancani, T.; Klein, M. T.; Bridges, T. M.; Morrison, R. D.; Blobaum, A. L.; Xiang, Z.; Daniels, J. S.; Niswender, C. M.; Conn, P. J.; Wood, M. R.; Lindsley, C. W. Targeting selective activation of M₁ for the treatment of Alzheimer's disease: further chemical optimization and pharmacological characterization of the M₁ positive allosteric modulator ML169. *ACS Chem. Neurosci.* **2012**, *3*, 884-895.
103. Ballard, T. M.; Flohr, A.; Groebke-Zbinden, K.; Pinard, E.; Rychmans, T.; Schaffhauser, H. Preparation of pyrrolopyridine and pyrazolopyridine derivatives as muscarinic M₁ receptor modulators. WO15028483, 03/05/2015.
104. Payne, A.; Castro-Pineiro, J. L.; Birch, L. M.; Khan, A.; Braunton, A. J.; Kitulagoda, J. E.; Soejima, M. Preparation of 4-azaindole derivatives as muscarinic M₁ receptor modulators for treatment of cognitive deficits. WO15049574, 04/02/2015.
105. Ballard, T. M.; Groebke-Zbinden, K.; Pinard, E.; Rychmans, T.; Schaffhauser, H. Preparation of indole and indazole derivatives as muscarinic M₁ receptor pos. allosteric modulators. WO15044072, 04/02/2015.

106. Davoren, J. E.; O'Neil, S. V.; Anderson, D. P.; Brodney, M. A.; Chenard, L.; Dlugolenski, K.; Edgerton, J. R.; Green, M.; Garnsey, M.; Grimwood, S.; Harris, A. R.; Kauffman, G. W.; LaChapelle, E.; Lazzaro, J. T.; Lee, C. W.; Lotarski, S. M.; Nason, D. M.; Obach, R. S.; Reinhart, V.; Salomon-Ferrer, R.; Steyn, S. J.; Webb, D.; Yan, J.; Zhang, L. Design and optimization of selective azaindole amide M₁ positive allosteric modulators. *Bioorg. Med. Chem. Lett.* **2016**, *26*, 650-655.
107. Rook, J. M.; Abe, M.; Cho, H. P.; Nance, K. D.; Luscombe, V. B.; Adams, J. J.; Dickerson, J. W.; Remke, D. H.; Garcia-Barrantes, P. M.; Engers, D. W.; Engers, J. L.; Chang, S.; Foster, J. J.; Blobaum, A. L.; Niswender, C. M.; Jones, C. K.; Conn, P. J.; Lindsley, C. W. Diverse Effects on M₁ Signaling and Adverse Effect Liability within a Series of M₁ Ago-PAMs. *ACS Chem. Neurosci.* **2017**, *8*, 866-883.
108. Bridges, T. M.; Phillip Kennedy, J.; Noetzel, M. J.; Breininger, M. L.; Gentry, P. R.; Conn, P. J.; Lindsley, C. W. Chemical lead optimization of a pan Gq mAChR M₁, M₃, M₅ positive allosteric modulator (PAM) lead. Part II: development of a potent and highly selective M₁ PAM. *Bioorg. Med. Chem. Lett.* **2010**, *20*, 1972-1975.
109. Melancon, B. J.; Poslusney, M. S.; Gentry, P. R.; Tarr, J. C.; Sheffler, D. J.; Mattmann, M. E.; Bridges, T. M.; Utley, T. J.; Daniels, J. S.; Niswender, C. M.; Conn, P. J.; Lindsley, C. W.; Wood, M. R. Isatin replacements applied to the highly selective, muscarinic M₁ PAM ML137: continued optimization of an MLPCN probe molecule. *Bioorg. Med. Chem. Lett.* **2013**, *23*, 412-416.
110. Ghoshal, A.; Rook, J. M.; Dickerson, J. W.; Roop, G. N.; Morrison, R. D.; Jalan-Sakrikar, N.; Lamsal, A.; Noetzel, M. J.; Poslusney, M. S.; Wood, M. R.; Melancon, B. J.; Stauffer, S. R.; Xiang, Z.; Daniels, J. S.; Niswender, C. M.; Jones, C. K.; Lindsley, C. W.; Conn, P. J. Potentiation of M₁ Muscarinic Receptor Reverses Plasticity Deficits and Negative and Cognitive Symptoms in a Schizophrenia Mouse Model. *Neuropsychopharmacology* **2016**, *41*, 598-610.
111. Davoren, J. E.; Garnsey, M.; Pettersen, B.; Brodney, M. A.; Edgerton, J. R.; Fortin, J. P.; Grimwood, S.; Harris, A. R.; Jenkinson, S.; Kenakin, T.; Lazzaro, J. T.; Lee, C. W.; Lotarski, S. M.; Nottebaum, L.; O'Neil, S. V.; Popiolek, M.; Ramsey, S.; Steyn, S. J.; Thorn, C. A.; Zhang, L.; Webb, D. Design and Synthesis of gamma- and delta-Lactam M₁ Positive Allosteric Modulators (PAMs): Convulsion and Cholinergic Toxicity of an M₁-Selective PAM with Weak Agonist Activity. *J. Med. Chem.* **2017**, *60*, 6649-6663.
112. Flohr, A.; Hutter, R.; Mueller, B.; Bohnert, C.; Pellisson, M.; Schaffhauser, H. Discovery of the first low-shift positive allosteric modulators for the muscarinic M₁ receptor. *Bioorg. Med. Chem. Lett.* **2017**, *27*, 5415-5419.
113. Gentry, P. R.; Bridges, T. M.; Lamsal, A.; Vinson, P. N.; Smith, E.; Chase, P.; Hodder, P. S.; Engers, J. L.; Niswender, C. M.; Daniels, J. S.; Conn, P. J.; Wood, M.

- R.; Lindsley, C. W. Discovery of ML326: The first sub-micromolar, selective M₅ PAM. *Bioorg. Med. Chem. Lett.* **2013**, *23*, 2996-3000.
114. Marlo, J. E.; Niswender, C. M.; Days, E. L.; Bridges, T. M.; Xiang, Y.; Rodriguez, A. L.; Shirey, J. K.; Brady, A. E.; Nalywajko, T.; Luo, Q.; Austin, C. A.; Williams, M. B.; Kim, K.; Williams, R.; Orton, D.; Brown, H. A.; Lindsley, C. W.; Weaver, C. D.; Conn, P. J. Discovery and characterization of novel allosteric potentiators of M₁ muscarinic receptors reveals multiple modes of activity. *Mol. Pharmacol.* **2009**, *75*, 577-588.
115. Bridges, T. M.; Marlo, J. E.; Niswender, C. M.; Jones, C. K.; Jadhav, S. B.; Gentry, P. R.; Plumley, H. C.; Weaver, C. D.; Conn, P. J.; Lindsley, C. W. Discovery of the first highly M₅-preferring muscarinic acetylcholine receptor ligand, an M₅ positive allosteric modulator derived from a series of 5-trifluoromethoxy N-benzyl isatins. *J. Med. Chem.* **2009**, *52*, 3445-3448.
116. Bridges, T. M.; Kennedy, J. P.; Hopkins, C. R.; Conn, P. J.; Lindsley, C. W. Heterobiaryl and heterobiaryl ether derived M₅ positive allosteric modulators. *Bioorg. Med. Chem. Lett.* **2010**, *20*, 5617-5622.
117. Bridges, T. M.; Kennedy, J. P.; Cho, H. P.; Breininger, M. L.; Gentry, P. R.; Hopkins, C. R.; Conn, P. J.; Lindsley, C. W. Chemical lead optimization of a pan G_q mAChR M₁, M₃, M₅ positive allosteric modulator (PAM) lead. Part I: Development of the first highly selective M₅ PAM. *Bioorg. Med. Chem. Lett.* **2010**, *20*, 558-562.
118. Gentry, P. R.; Kokubo, M.; Bridges, T. M.; Daniels, J. S.; Niswender, C. M.; Smith, E.; Chase, P.; Hodder, P. S.; Rosen, H.; Conn, P. J.; Engers, J.; Brewer, K. A.; Lindsley, C. W.; Wood, M. R. Development of the First CNS penetrant M₅ Positive Allosteric Modulator (PAM) Based on a Novel, non-Isatin Core. In *Probe Reports from the NIH Molecular Libraries Program*, National Center for Biotechnology Information (US): Bethesda (MD), 2010.
119. Gentry, P. R.; Kokubo, M.; Bridges, T. M.; Kett, N. R.; Harp, J. M.; Cho, H. P.; Smith, E.; Chase, P.; Hodder, P. S.; Niswender, C. M.; Daniels, J. S.; Conn, P. J.; Wood, M. R.; Lindsley, C. W. Discovery of the first M₅-selective and CNS penetrant negative allosteric modulator (NAM) of a muscarinic acetylcholine receptor: (S)-9b-(4-chlorophenyl)-1-(3,4-difluorobenzoyl)-2,3-dihydro-1H-imidazo[2,1-a]isoindol-5(9bH)-one (ML375). *J. Med. Chem.* **2013**, *56*, 9351-9355.
120. Kurata, H.; Gentry, P. R.; Kokubo, M.; Cho, H. P.; Bridges, T. M.; Niswender, C. M.; Byers, F. W.; Wood, M. R.; Daniels, J. S.; Conn, P. J.; Lindsley, C. W. Further optimization of the M₅ NAM MLPCN probe ML375: tactics and challenges. *Bioorg. Med. Chem. Lett.* **2015**, *25*, 690-694.

121. Lazareno, S.; Dolezal, V.; Popham, A.; Birdsall, N. J. Thiochrome enhances acetylcholine affinity at muscarinic M₄ receptors: receptor subtype selectivity via cooperativity rather than affinity. *Mol. Pharmacol.* **2004**, *65*, 257-266.
122. Chan, W. Y.; McKinzie, D. L.; Bose, S.; Mitchell, S. N.; Witkin, J. M.; Thompson, R. C.; Christopoulos, A.; Lazareno, S.; Birdsall, N. J.; Bymaster, F. P.; Felder, C. C. Allosteric modulation of the muscarinic M₄ receptor as an approach to treating schizophrenia. *Proc. Natl. Acad. Sci. U. S. A.* **2008**, *105*, 10978-10983.
123. Shirey, J. K.; Xiang, Z.; Orton, D.; Brady, A. E.; Johnson, K. A.; Williams, R.; Ayala, J. E.; Rodriguez, A. L.; Wess, J.; Weaver, D.; Niswender, C. M.; Conn, P. J. An allosteric potentiator of M₄ mAChR modulates hippocampal synaptic transmission. *Nat. Chem. Biol.* **2008**, *4*, 42-50.
124. Brady, A. E.; Jones, C. K.; Bridges, T. M.; Kennedy, J. P.; Thompson, A. D.; Heiman, J. U.; Breining, M. L.; Gentry, P. R.; Yin, H.; Jadhav, S. B.; Shirey, J. K.; Conn, P. J.; Lindsley, C. W. Centrally active allosteric potentiators of the M₄ muscarinic acetylcholine receptor reverse amphetamine-induced hyperlocomotor activity in rats. *J. Pharmacol. Exp. Ther.* **2008**, *327*, 941-953.
125. Kennedy, J. P.; Bridges, T. M.; Gentry, P. R.; Brogan, J. T.; Kane, A. S.; Jones, C. K.; Brady, A. E.; Shirey, J. K.; Conn, P. J.; Lindsley, C. W. Synthesis and structure-activity relationships of allosteric potentiators of the M₄ muscarinic acetylcholine receptor. *ChemMedChem* **2009**, *4*, 1600-1607.
126. Salovich, J. M.; Vinson, P. N.; Sheffler, D. J.; Lamsal, A.; Utley, T. J.; Blobaum, A. L.; Bridges, T. M.; Le, U.; Jones, C. K.; Wood, M. R.; Daniels, J. S.; Conn, P. J.; Niswender, C. M.; Lindsley, C. W.; Hopkins, C. R. Discovery of *N*-(4-methoxy-7-methylbenzo[d]thiazol-2-yl)isonicotinamide, ML293, as a novel, selective and brain penetrant positive allosteric modulator of the muscarinic 4 (M₄) receptor. *Bioorg. Med. Chem. Lett.* **2012**, *22*, 5084-5088.
127. Wood, M. R.; Noetzel, M. J.; Poslusney, M. S.; Melancon, B. J.; Tarr, J. C.; Lamsal, A.; Chang, S.; Luscombe, V. B.; Weiner, R. L.; Cho, H. P.; Bubser, M.; Jones, C. K.; Niswender, C. M.; Wood, M. W.; Engers, D. W.; Brandon, N. J.; Duggan, M. E.; Conn, P. J.; Bridges, T. M.; Lindsley, C. W. Challenges in the development of an M₄ PAM in vivo tool compound: The discovery of VU0467154 and unexpected DMPK profiles of close analogs. *Bioorg. Med. Chem. Lett.* **2017**, *27*, 171-175.
128. Bubser, M.; Bridges, T. M.; Dencker, D.; Gould, R. W.; Grannan, M.; Noetzel, M. J.; Lamsal, A.; Niswender, C. M.; Daniels, J. S.; Poslusney, M. S.; Melancon, B. J.; Tarr, J. C.; Byers, F. W.; Wess, J.; Duggan, M. E.; Dunlop, J.; Wood, M. W.; Brandon, N. J.; Wood, M. R.; Lindsley, C. W.; Conn, P. J.; Jones, C. K. Selective activation of M₄ muscarinic acetylcholine receptors reverses MK-801-induced behavioral impairments and enhances associative learning in rodents. *ACS Chem. Neurosci.* **2014**, *5*, 920-942.

129. Tarr, J. C.; Wood, M. R.; Noetzel, M. J.; Melancon, B. J.; Lamsal, A.; Luscombe, V. B.; Rodriguez, A. L.; Byers, F. W.; Chang, S.; Cho, H. P.; Engers, D. W.; Jones, C. K.; Niswender, C. M.; Wood, M. W.; Brandon, N. J.; Duggan, M. E.; Jeffrey Conn, P.; Bridges, T. M.; Lindsley, C. W. Challenges in the development of an M₄ PAM preclinical candidate: The discovery, SAR, and biological characterization of a series of azetidine-derived tertiary amides. *Bioorg. Med. Chem. Lett.* **2017**, *27*, 5179-5184.
130. Tarr, J. C.; Wood, M. R.; Noetzel, M. J.; Bertron, J. L.; Weiner, R. L.; Rodriguez, A. L.; Lamsal, A.; Byers, F. W.; Chang, S.; Cho, H. P.; Jones, C. K.; Niswender, C. M.; Wood, M. W.; Brandon, N. J.; Duggan, M. E.; Conn, P. J.; Bridges, T. M.; Lindsley, C. W. Challenges in the development of an M₄ PAM preclinical candidate: The discovery, SAR, and in vivo characterization of a series of 3-aminoazetidine-derived amides. *Bioorg. Med. Chem. Lett.* **2017**, *27*, 2990-2995.
131. Li, Q.; Chen, H.-F. Synergistic regulation mechanism of iperoxo and LY2119620 for muscarinic acetylcholine M₂ receptor. *RSC Advances* **2018**, *8*, 13067-13074.
132. Raasch, A.; Scharfenstein, O.; Trankle, C.; Holzgrabe, U.; Mohr, K. Elevation of ligand binding to muscarinic M₂ acetylcholine receptors by bis(ammonio)alkane-type allosteric modulators. *J. Med. Chem.* **2002**, *45*, 3809-3812.
133. Holzgrabe, U.; De Amici, M.; Mohr, K. Allosteric modulators and selective agonists of muscarinic receptors. *J. Mol. Neurosci.* **2006**, *30*, 165-168.
134. Moulton, B. C.; Fryer, A. D. Muscarinic receptor antagonists, from folklore to pharmacology; finding drugs that actually work in asthma and COPD. *Br. J. Pharmacol.* **2011**, *163*, 44-52.
135. Croy, C. H.; Schober, D. A.; Xiao, H.; Quets, A.; Christopoulos, A.; Felder, C. C. Characterization of the novel positive allosteric modulator, LY2119620, at the muscarinic M₂ and M₄ receptors. *Mol. Pharmacol.* **2014**, *86*, 106-115.
136. Miao, Y.; Goldfeld, D. A.; Moo, E. V.; Sexton, P. M.; Christopoulos, A.; McCammon, J. A.; Valant, C. Accelerated structure-based design of chemically diverse allosteric modulators of a muscarinic G protein-coupled receptor. *Proc. Natl. Acad. Sci. U. S. A.* **2016**, *113*, 5675-5684.
137. Korczynska, M.; Clark, M. J.; Valant, C.; Xu, J.; Moo, E. V.; Albold, S.; Weiss, D. R.; Torosyan, H.; Huang, W.; Kruse, A. C.; Lyda, B. R.; May, L. T.; Baltos, J. A.; Sexton, P. M.; Kobilka, B. K.; Christopoulos, A.; Shoichet, B. K.; Sunahara, R. K. Structure-based discovery of selective positive allosteric modulators of antagonists for the M₂ muscarinic acetylcholine receptor. *Proc. Natl. Acad. Sci. U. S. A.* **2018**, *115*, 2419-2428.
138. Saleh, N.; Hucke, O.; Kramer, G.; Schmidt, E.; Montel, F.; Lipinski, R.; Ferger, B.; Clark, T.; Hildebrand, P. W.; Tautermann, C. S. Multiple Binding Sites Contribute to

the Mechanism of Mixed Agonistic and Positive Allosteric Modulators of the Cannabinoid CB₁ Receptor. *Angew. Chem. Int. Ed.* **2018**, *57*, 2580-2585.

139. Di Marzo, V. CB₁ receptor antagonism: biological basis for metabolic effects. *Drug Discov. Today* **2008**, *13*, 1026-1041.
140. Navarro, G.; Morales, P.; Rodriguez-Cueto, C.; Fernandez-Ruiz, J.; Jagerovic, N.; Franco, R. Targeting Cannabinoid CB₂ Receptors in the Central Nervous System. Medicinal Chemistry Approaches with Focus on Neurodegenerative Disorders. *Front Neurosci.* **2016**, *10*, 406.
141. Martinez-Pinilla, E.; Varani, K.; Reyes-Resina, I.; Angelats, E.; Vincenzi, F.; Ferreiro-Vera, C.; Oyarzabal, J.; Canela, E. I.; Lanciego, J. L.; Nadal, X.; Navarro, G.; Borea, P. A.; Franco, R. Binding and Signaling Studies Disclose a Potential Allosteric Site for Cannabidiol in Cannabinoid CB₂ Receptors. *Front Pharmacol.* **2017**, *8*, 744.
142. Price, M. R.; Baillie, G. L.; Thomas, A.; Stevenson, L. A.; Easson, M.; Goodwin, R.; McLean, A.; McIntosh, L.; Goodwin, G.; Walker, G.; Westwood, P.; Marris, J.; Thomson, F.; Cowley, P.; Christopoulos, A.; Pertwee, R. G.; Ross, R. A. Allosteric modulation of the cannabinoid CB₁ receptor. *Mol. Pharmacol.* **2005**, *68*, 1484-1495.
143. Piscitelli, F.; Ligresti, A.; La Regina, G.; Coluccia, A.; Morera, L.; Allara, M.; Novellino, E.; Di Marzo, V.; Silvestri, R. Indole-2-carboxamides as allosteric modulators of the cannabinoid CB₁ receptor. *J. Med. Chem.* **2012**, *55*, 5627-5631.
144. Ahn, K. H.; Mahmoud, M. M.; Samala, S.; Lu, D.; Kendall, D. A. Profiling two indole-2-carboxamides for allosteric modulation of the CB₁ receptor. *J. Neurochem.* **2013**, *124*, 584-589.
145. Mahmoud, M. M.; Ali, H. I.; Ahn, K. H.; Damaraju, A.; Samala, S.; Pulipati, V. K.; Kolluru, S.; Kendall, D. A.; Lu, D. Structure-activity relationship study of indole-2-carboxamides identifies a potent allosteric modulator for the cannabinoid receptor 1 (CB₁). *J. Med. Chem.* **2013**, *56*, 7965-7975.
146. Khurana, L.; Ali, H. I.; Olszewska, T.; Ahn, K. H.; Damaraju, A.; Kendall, D. A.; Lu, D. Optimization of chemical functionalities of indole-2-carboxamides to improve allosteric parameters for the cannabinoid receptor 1 (CB₁). *J. Med. Chem.* **2014**, *57*, 3040-3052.
147. Nguyen, T.; German, N.; Decker, A. M.; Li, J. X.; Wiley, J. L.; Thomas, B. F.; Kenakin, T. P.; Zhang, Y. Structure-activity relationships of substituted *1H*-indole-2-carboxamides as CB₁ receptor allosteric modulators. *Bioorg. Med. Chem.* **2015**, *23*, 2195-2203.

148. Kulkarni, P. M.; Kulkarni, A. R.; Korde, A.; Tichkule, R. B.; Laprairie, R. B.; Denovan-Wright, E. M.; Zhou, H.; Janero, D. R.; Zvonok, N.; Makriyannis, A.; Cascio, M. G.; Pertwee, R. G.; Thakur, G. A. Novel Electrophilic and Photoaffinity Covalent Probes for Mapping the Cannabinoid 1 Receptor Allosteric Site(s). *J. Med. Chem.* **2016**, *59*, 44-60.
149. Qiao, C. J.; Ali, H. I.; Ahn, K. H.; Kolluru, S.; Kendall, D. A.; Lu, D. Synthesis and biological evaluation of indole-2-carboxamides bearing photoactivatable functionalities as novel allosteric modulators for the cannabinoid CB₁ receptor. *Eur. J. Med. Chem.* **2016**, *121*, 517-529.
150. Horswill, J. G.; Bali, U.; Shaaban, S.; Keily, J. F.; Jeevaratnam, P.; Babbs, A. J.; Reynet, C.; Wong Kai In, P. PSNCBAM-1, a novel allosteric antagonist at cannabinoid CB₁ receptors with hypophagic effects in rats. *Br. J. Pharmacol.* **2007**, *152*, 805-814.
151. Nguyen, T.; Li, J. X.; Thomas, B. F.; Wiley, J. L.; Kenakin, T. P.; Zhang, Y. Allosteric Modulation: An Alternate Approach Targeting the Cannabinoid CB₁ Receptor. *Med. Res. Rev.* **2017**, *37*, 441-474.
152. Baillie, G. L.; Horswill, J. G.; Anavi-Goffer, S.; Reggio, P. H.; Bolognini, D.; Abood, M. E.; McAllister, S.; Strange, P. G.; Stephens, G. J.; Pertwee, R. G.; Ross, R. A. CB₁ receptor allosteric modulators display both agonist and signaling pathway specificity. *Mol. Pharmacol.* **2013**, *83*, 322-338.
153. Khajehali, E.; Malone, D. T.; Glass, M.; Sexton, P. M.; Christopoulos, A.; Leach, K. Biased Agonism and Biased Allosteric Modulation at the CB₁ Cannabinoid Receptor. *Mol. Pharmacol.* **2015**, *88*, 368-379.
154. Khurana, L.; Fu, B. Q.; Duddupudi, A. L.; Liao, Y. H.; Immadi, S. S.; Kendall, D. A.; Lu, D. Pyrimidinyl Biphenylureas: Identification of New Lead Compounds as Allosteric Modulators of the Cannabinoid Receptor CB₁. *J. Med. Chem.* **2017**, *60*, 1089-1104.
155. Nguyen, T.; German, N.; Decker, A. M.; Langston, T. L.; Gamage, T. F.; Farquhar, C. E.; Li, J. X.; Wiley, J. L.; Thomas, B. F.; Zhang, Y. Novel Diarylurea Based Allosteric Modulators of the Cannabinoid CB₁ Receptor: Evaluation of Importance of 6-Pyrrolidinylpyridinyl Substitution. *J. Med. Chem.* **2017**, *60*, 7410-7424.
156. Bertini, S.; Chicca, A.; Gado, F.; Arena, C.; Nieri, D.; Digiaco, M.; Saccomanni, G.; Zhao, P.; Abood, M. E.; Macchia, M.; Gertsch, J.; Manera, C. Novel analogs of PSNCBAM-1 as allosteric modulators of cannabinoid CB₁ receptor. *Bioorg. Med. Chem.* **2017**, *25*, 6427-6434.

157. Priestley, R. S.; Nickolls, S. A.; Alexander, S. P.; Kendall, D. A. A potential role for cannabinoid receptors in the therapeutic action of fenofibrate. *FASEB J.* **2015**, *29*, 1446-1455.
158. Laprairie, R. B.; Bagher, A. M.; Kelly, M. E.; Denovan-Wright, E. M. Cannabidiol is a negative allosteric modulator of the cannabinoid CB₁ receptor. *Br. J. Pharmacol.* **2015**, *172*, 4790-4805.
159. Vallee, M.; Vitiello, S.; Bellocchio, L.; Hebert-Chatelain, E.; Monlezun, S.; Martin-Garcia, E.; Kasanetz, F.; Baillie, G. L.; Panin, F.; Cathala, A.; Roullot-Lacarriere, V.; Fabre, S.; Hurst, D. P.; Lynch, D. L.; Shore, D. M.; Deroche-Gamonet, V.; Spampinato, U.; Revest, J. M.; Maldonado, R.; Reggio, P. H.; Ross, R. A.; Marsicano, G.; Piazza, P. V. Pregnenolone can protect the brain from cannabis intoxication. *Science* **2014**, *343*, 94-98.
160. Laprairie, R. B.; Kulkarni, P. M.; Deschamps, J. R.; Kelly, M. E. M.; Janero, D. R.; Cascio, M. G.; Stevenson, L. A.; Pertwee, R. G.; Kenakin, T. P.; Denovan-Wright, E. M.; Thakur, G. A. Enantiospecific Allosteric Modulation of Cannabinoid 1 Receptor. *ACS Chem. Neurosci.* **2017**, *8*, 1188-1203.
161. Navarro, H. A.; Howard, J. L.; Pollard, G. T.; Carroll, F. I. Positive allosteric modulation of the human cannabinoid (CB) receptor by RTI-371, a selective inhibitor of the dopamine transporter. *Br. J. Pharmacol.* **2009**, *156*, 1178-1184.
162. Pamplona, F. A.; Ferreira, J.; Menezes de Lima, O., Jr.; Duarte, F. S.; Bento, A. F.; Forner, S.; Villarinho, J. G.; Bellocchio, L.; Wotjak, C. T.; Lerner, R.; Monory, K.; Lutz, B.; Canetti, C.; Matias, I.; Calixto, J. B.; Marsicano, G.; Guimaraes, M. Z.; Takahashi, R. N. Anti-inflammatory lipoxin A4 is an endogenous allosteric enhancer of CB₁ cannabinoid receptor. *Proc. Natl. Acad. Sci. U. S. A.* **2012**, *109*, 21134-21139.
163. Ganeshsingh A. Thakur, P. M. K. Allosteric modulators of CB₁ cannabinoid receptors. WO2013103967A1, 07/11/2013, 2013.
164. Ignatowska-Jankowska, B. M.; Baillie, G. L.; Kinsey, S.; Crowe, M.; Ghosh, S.; Owens, R. A.; Damaj, I. M.; Poklis, J.; Wiley, J. L.; Zanda, M.; Zanato, C.; Greig, I. R.; Lichtman, A. H.; Ross, R. A. A Cannabinoid CB₁ Receptor-Positive Allosteric Modulator Reduces Neuropathic Pain in the Mouse with No Psychoactive Effects. *Neuropsychopharmacology* **2015**, *40*, 2948-2959.
165. Straiker, A.; Mitjavila, J.; Yin, D.; Gibson, A.; Mackie, K. Aiming for allosterism: Evaluation of allosteric modulators of CB₁ in a neuronal model. *Pharmacol. Res.* **2015**, *99*, 370-376.
166. Mitjavila, J.; Yin, D.; Kulkarni, P. M.; Zanato, C.; Thakur, G. A.; Ross, R.; Greig, I.; Mackie, K.; Straiker, A. Enantiomer-specific positive allosteric modulation of CB₁ signaling in autaptic hippocampal neurons. *Pharmacol. Res.* **2018**, *129*, 475-481.

167. Milligan, G.; Shimpukade, B.; Ulven, T.; Hudson, B. D. Complex Pharmacology of Free Fatty Acid Receptors. *Chem. Rev.* **2017**, *117*, 67-110.
168. Tikhonova, I. G.; Sum, C. S.; Neumann, S.; Thomas, C. J.; Raaka, B. M.; Costanzi, S.; Gershengorn, M. C. Bidirectional, iterative approach to the structural delineation of the functional "chemoprint" in GPR40 for agonist recognition. *J. Med. Chem.* **2007**, *50*, 2981-2989.
169. Lin, D. C.; Guo, Q.; Luo, J.; Zhang, J.; Nguyen, K.; Chen, M.; Tran, T.; Dransfield, P. J.; Brown, S. P.; Houze, J.; Vimolratana, M.; Jiao, X. Y.; Wang, Y.; Birdsall, N. J.; Swaminath, G. Identification and pharmacological characterization of multiple allosteric binding sites on the free fatty acid 1 receptor. *Mol. Pharmacol.* **2012**, *82*, 843-859.
170. Milligan, G.; Shimpukade, B.; Ulven, T.; Hudson, B. D. Complex Pharmacology of Free Fatty Acid Receptors. *Chem. Rev.* **2017**, *117*, 67-110.
171. Yabuki, C.; Komatsu, H.; Tsujihata, Y.; Maeda, R.; Ito, R.; Matsuda-Nagasumi, K.; Sakuma, K.; Miyawaki, K.; Kikuchi, N.; Takeuchi, K.; Habata, Y.; Mori, M. A novel antidiabetic drug, fasiglifam/TAK-875, acts as an ago-allosteric modulator of FFAR1. *PLoS One* **2013**, *8*, 76280.
172. Bolognini, D.; Tobin, A. B.; Milligan, G.; Moss, C. E. The Pharmacology and Function of Receptors for Short-Chain Fatty Acids. *Mol. Pharmacol.* **2016**, *89*, 388-398.
173. Lee, T.; Schwandner, R.; Swaminath, G.; Weiszmann, J.; Cardozo, M.; Greenberg, J.; Jaeckel, P.; Ge, H.; Wang, Y.; Jiao, X.; Liu, J.; Kayser, F.; Tian, H.; Li, Y. Identification and functional characterization of allosteric agonists for the G protein-coupled receptor FFA2. *Mol. Pharmacol.* **2008**, *74*, 1599-1609.
174. Smith, N. J.; Ward, R. J.; Stoddart, L. A.; Hudson, B. D.; Kostenis, E.; Ulven, T.; Morris, J. C.; Trankle, C.; Tikhonova, I. G.; Adams, D. R.; Milligan, G. Extracellular loop 2 of the free fatty acid receptor 2 mediates allosterism of a phenylacetamide ago-allosteric modulator. *Mol. Pharmacol.* **2011**, *80*, 163-173.
175. Wang, Y.; Jiao, X.; Kayser, F.; Liu, J.; Wang, Z.; Wanska, M.; Greenberg, J.; Weiszmann, J.; Ge, H.; Tian, H.; Wong, S.; Schwandner, R.; Lee, T.; Li, Y. The first synthetic agonists of FFA2: Discovery and SAR of phenylacetamides as allosteric modulators. *Bioorg. Med. Chem. Lett.* **2010**, *20*, 493-498.
176. Bolognini, D.; Moss, C. E.; Nilsson, K.; Petersson, A. U.; Donnelly, I.; Sergeev, E.; Konig, G. M.; Kostenis, E.; Kurowska-Stolarska, M.; Miller, A.; Dekker, N.; Tobin, A. B.; Milligan, G. A Novel Allosteric Activator of Free Fatty Acid 2 Receptor Displays Unique G_i-functional Bias. *J. Biol. Chem.* **2016**, *291*, 18915-18931.

177. Leonard, J. N.; Chu, Z.; Bruce, M. A.; Boatman, P. D. GPR41 and modulators thereof for the treatment of insulin-related disorders. WO2006052566A3, 10/12/2006, 2006.
178. Hudson, B. D.; Christiansen, E.; Murdoch, H.; Jenkins, L.; Hansen, A. H.; Madsen, O.; Ulven, T.; Milligan, G. Complex pharmacology of novel allosteric free fatty acid 3 receptor ligands. *Mol. Pharmacol.* **2014**, *86*, 200-210.
179. Giovannoni, M. P.; Ciciani, G.; Cilibrizzi, A.; Crocetti, L.; Daniele, S.; Di Cesare Mannelli, L.; Ghelardini, C.; Giacomelli, C.; Guerrini, G.; Martini, C.; Trincavelli, M. L.; Vergelli, C. Further studies on pyrazolo[1',5':1,6]pyrimido[4,5-d]pyridazin-4(3H)-ones as potent and selective human A₁ adenosine receptor antagonists. *Eur. J. Med. Chem.* **2015**, *89*, 32-41.
180. Knight, A.; Hemmings, J. L.; Winfield, I.; Leuenberger, M.; Frattini, E.; Frenguelli, B. G.; Dowell, S. J.; Lochner, M.; Ladds, G. Discovery of Novel Adenosine Receptor Agonists That Exhibit Subtype Selectivity. *J. Med. Chem.* **2016**, *59*, 947-964.
181. van der Klein, P. A.; Kourounakis, A. P.; AP, I. J. Allosteric modulation of the adenosine A₁ receptor. Synthesis and biological evaluation of novel 2-amino-3-benzoylthiophenes as allosteric enhancers of agonist binding. *J. Med. Chem.* **1999**, *42*, 3629-3635.
182. Bruns, R. F.; Fergus, J. H. Allosteric enhancement of adenosine A₁ receptor binding and function by 2-amino-3-benzoylthiophenes. *Mol. Pharmacol.* **1990**, *38*, 939-949.
183. Bruns, R. F.; Fergus, J. H.; Coughenour, L. L.; Courtland, G. G.; Pugsley, T. A.; Dodd, J. H.; Tinney, F. J. Structure-activity relationships for enhancement of adenosine A₁ receptor binding by 2-amino-3-benzoylthiophenes. *Mol. Pharmacol.* **1990**, *38*, 950-958.
184. Baraldi, P. G.; Iaconinoto, M. A.; Moorman, A. R.; Carrion, M. D.; Cara, C. L.; Preti, D.; Lopez, O. C.; Fruttarolo, F.; Tabrizi, M. A.; Romagnoli, R. Allosteric enhancers for A₁ adenosine receptor. *Mini-Rev. Med. Chem.* **2007**, *7*, 559-569.
185. Childers, S. R.; Li, X.; Xiao, R.; Eisenach, J. C. Allosteric modulation of adenosine A₁ receptor coupling to G-proteins in brain. *J. Neurochem.* **2005**, *93*, 715-723.
186. Kimatrai-Salvador, M.; Baraldi, P. G.; Romagnoli, R. Allosteric modulation of A₁-adenosine receptor: a review. *Drug Discov. Today Technol.* **2013**, *10*, 285-296.
187. Ferguson, G. N.; Valant, C.; Horne, J.; Figler, H.; Flynn, B. L.; Linden, J.; Chalmers, D. K.; Sexton, P. M.; Christopoulos, A.; Scammells, P. J. 2-aminothienopyridazines as novel adenosine A₁ receptor allosteric modulators and antagonists. *J. Med. Chem.* **2008**, *51*, 6165-6172.

188. Romagnoli, R.; Baraldi, P. G.; AP, I. J.; Massink, A.; Cruz-Lopez, O.; Lopez-Cara, L. C.; Saponaro, G.; Preti, D.; Aghazadeh Tabrizi, M.; Baraldi, S.; Moorman, A. R.; Vincenzi, F.; Borea, P. A.; Varani, K. Synthesis and biological evaluation of novel allosteric enhancers of the A₁ adenosine receptor based on 2-amino-3-(4'-chlorobenzoyl)-4-substituted-5-arylethynyl thiophene. *J. Med. Chem.* **2014**, *57*, 7673-7686.
189. Romagnoli, R.; Baraldi, P. G.; Carrion, M. D.; Cara, C. L.; Cruz-Lopez, O.; Iaconinoto, M. A.; Preti, D.; Shryock, J. C.; Moorman, A. R.; Vincenzi, F.; Varani, K.; Andrea Borea, P. Synthesis and biological evaluation of 2-amino-3-(4-chlorobenzoyl)-4-[N-(substituted) piperazin-1-yl]thiophenes as potent allosteric enhancers of the A₁ adenosine receptor. *J. Med. Chem.* **2008**, *51*, 5875-5879.
190. Goblyos, A.; Ijzerman, A. P. Allosteric modulation of adenosine receptors. *Purinergic Signal.* **2009**, *5*, 51-61.
191. Valant, C.; Aurelio, L.; Devine, S. M.; Ashton, T. D.; White, J. M.; Sexton, P. M.; Christopoulos, A.; Scammells, P. J. Synthesis and characterization of novel 2-amino-3-benzoylthiophene derivatives as biased allosteric agonists and modulators of the adenosine A₁ receptor. *J. Med. Chem.* **2012**, *55*, 2367-2375.
192. Lutjens, H.; Zickgraf, A.; Figler, H.; Linden, J.; Olsson, R. A.; Scammells, P. J. 2-Amino-3-benzoylthiophene allosteric enhancers of A₁ adenosine agonist binding: new 3, 4-, and 5-modifications. *J. Med. Chem.* **2003**, *46*, 1870-1877.
193. Aurelio, L.; Figler, H.; Flynn, B. L.; Linden, J.; Scammells, P. J. 5-Substituted 2-aminothiophenes as A₁ adenosine receptor allosteric enhancers. *Bioorg. Med. Chem.* **2008**, *16*, 1319-1327.
194. Aurelio, L.; Valant, C.; Flynn, B. L.; Sexton, P. M.; Christopoulos, A.; Scammells, P. J. Allosteric modulators of the adenosine A₁ receptor: synthesis and pharmacological evaluation of 4-substituted 2-amino-3-benzoylthiophenes. *J. Med. Chem.* **2009**, *52*, 4543-4547.
195. Romagnoli, R.; Baraldi, P. G.; Carrion, M. D.; Cara, C. L.; Cruz-Lopez, O.; Salvador, M. K.; Preti, D.; Tabrizi, M. A.; Shryock, J. C.; Moorman, A. R.; Vincenzi, F.; Varani, K.; Borea, P. A. Structure-activity relationships of 2-amino-3-aryloyl-4-[(4-arylpiperazin-1-yl)methyl]thiophenes. Part 2: Probing the influence of diverse substituents at the phenyl of the arylpiperazine moiety on allosteric enhancer activity at the A₁ adenosine receptor. *Bioorg. Med. Chem.* **2012**, *20*, 996-1007.
196. Romagnoli, R.; Baraldi, P. G.; Carrion, M. D.; Cara, C. L.; Cruz-Lopez, O.; Salvador, M. K.; Preti, D.; Tabrizi, M. A.; Moorman, A. R.; Vincenzi, F.; Borea, P. A.; Varani, K. Synthesis and biological evaluation of 2-amino-3-(4-chlorobenzoyl)-4-[(4-arylpiperazin-1-yl)methyl]-5-substituted-thiophenes. effect of the 5-modification on

- allosteric enhancer activity at the A₁ adenosine receptor. *J. Med. Chem.* **2012**, *55*, 7719-7735.
197. Romagnoli, R.; Baraldi, P. G.; Carrion, M. D.; Cruz-Lopez, O.; Cara, C. L.; Saponaro, G.; Preti, D.; Tabrizi, M. A.; Baraldi, S.; Moorman, A. R.; Vincenzi, F.; Borea, P. A.; Varani, K. Synthesis and biological evaluation of novel 2-amino-3-aryl-4-neopentyl-5-substituted thiophene derivatives as allosteric enhancers of the A₁ adenosine receptor. *Bioorg. Med. Chem.* **2014**, *22*, 148-166.
198. Romagnoli, R.; Baraldi, P. G.; Lopez-Cara, C.; Cruz-Lopez, O.; Moorman, A. R.; Massink, A.; AP, I. J.; Vincenzi, F.; Borea, P. A.; Varani, K. Synthesis and biological evaluation of a new series of 2-amino-3-aryl thiophene derivatives as agonist allosteric modulators of the A₁ adenosine receptor. A position-dependent effect study. *Eur. J. Med. Chem.* **2015**, *101*, 185-204.
199. Gao, Z. G.; Gross, A. S.; Jacobson, K. A. Effects of the allosteric modulator SCH-202676 on adenosine and P₂Y receptors. *Life Sci.* **2004**, *74*, 3173-3180.
200. Gao, Z. G.; Ijzerman, A. P. Allosteric modulation of A_{2A} adenosine receptors by amiloride analogues and sodium ions. *Biochem. Pharmacol.* **2000**, *60*, 669-676.
201. Gao, Z. G.; Melman, N.; Erdmann, A.; Kim, S. G.; Muller, C. E.; AP, I. J.; Jacobson, K. A. Differential allosteric modulation by amiloride analogues of agonist and antagonist binding at A₁ and A₃ adenosine receptors. *Biochem. Pharmacol.* **2003**, *65*, 525-534.
202. Massink, A.; Louvel, J.; Adlere, I.; van Veen, C.; Huisman, B. J.; Dijksteel, G. S.; Guo, D.; Lenselink, E. B.; Buckley, B. J.; Matthews, H.; Ranson, M.; Kelso, M.; AP, I. J. 5'-Substituted Amiloride Derivatives as Allosteric Modulators Binding in the Sodium Ion Pocket of the Adenosine A_{2A} Receptor. *J. Med. Chem.* **2016**, *59*, 4769-4777.
203. Gutierrez-de-Teran, H.; Massink, A.; Rodriguez, D.; Liu, W.; Han, G. W.; Joseph, J. S.; Katritch, I.; Heitman, L. H.; Xia, L.; Ijzerman, A. P.; Cherezov, V.; Katritch, V.; Stevens, R. C. The role of a sodium ion binding site in the allosteric modulation of the A_{2A} adenosine G protein-coupled receptor. *Structure* **2013**, *21*, 2175-2185.
204. Taliani, S.; Trincavelli, M. L.; Cosimelli, B.; Laneri, S.; Severi, E.; Barresi, E.; Pugliesi, I.; Daniele, S.; Giacomelli, C.; Greco, G.; Novellino, E.; Martini, C.; Da Settimo, F. Modulation of A_{2B} adenosine receptor by 1-Benzyl-3-ketoindole derivatives. *Eur. J. Med. Chem.* **2013**, *69*, 331-337.
205. Trincavelli, M. L.; Giacomelli, C.; Daniele, S.; Taliani, S.; Cosimelli, B.; Laneri, S.; Severi, E.; Barresi, E.; Pugliesi, I.; Greco, G.; Novellino, E.; Da Settimo, F.; Martini, C. Allosteric modulators of human A_{2B} adenosine receptor. *Biochim. Biophys. Acta* **2014**, *1840*, 1194-1203.

206. Borea, P. A.; Varani, K.; Vincenzi, F.; Baraldi, P. G.; Tabrizi, M. A.; Merighi, S.; Gessi, S. The A₃ Adenosine Receptor: History and Perspectives. *Pharmacol. Rev.* **2015**, *67*, 74-102.
207. Goblyos, A.; Gao, Z. G.; Brussee, J.; Connestari, R.; Santiago, S. N.; Ye, K.; Ijzerman, A. P.; Jacobson, K. A. Structure-activity relationships of new *1H*-imidazo[4,5-*c*]quinolin-4-amine derivatives as allosteric enhancers of the A₃ adenosine receptor. *J. Med. Chem.* **2006**, *49*, 3354-3361.
208. Gao, Z. G.; Verzijl, D.; Zweemer, A.; Ye, K.; Goblyos, A.; Ijzerman, A. P.; Jacobson, K. A. Functionally biased modulation of A₃ adenosine receptor agonist efficacy and potency by imidazoquinolinamine allosteric enhancers. *Biochem. Pharmacol.* **2011**, *82*, 658-668.
209. Heitman, L. H.; Goblyos, A.; Zweemer, A. M.; Bakker, R.; Mulder-Krieger, T.; van Veldhoven, J. P.; de Vries, H.; Brussee, J.; Ijzerman, A. P. A series of 2,4-disubstituted quinolines as a new class of allosteric enhancers of the adenosine A₃ receptor. *J. Med. Chem.* **2009**, *52*, 926-931.
210. Van Poecke, S.; Barrett, M. O.; Santhosh Kumar, T.; Sinnaeve, D.; Martins, J. C.; Jacobson, K. A.; Kendall Harden, T.; Van Calenbergh, S. Synthesis and P2Y₂ receptor agonist activities of uridine 5'-phosphonate analogues. *Bioorg. Med. Chem. Lett.* **2012**, *20*, 2304-2315.
211. Yuan, S.; Chan, H. C.; Vogel, H.; Filipek, S.; Stevens, R. C.; Palczewski, K. The Molecular Mechanism of P2Y₁ Receptor Activation. *Angew. Chem. Int. Ed.* **2016**, *55*, 10331-10335.
212. Chao, H.; Turdi, H.; Herpin, T. F.; Roberge, J. Y.; Liu, Y.; Schnur, D. M.; Poss, M. A.; Rehfuss, R.; Hua, J.; Wu, Q.; Price, L. A.; Abell, L. M.; Schumacher, W. A.; Bostwick, J. S.; Steinbacher, T. E.; Stewart, A. B.; Ogletree, M. L.; Huang, C. S.; Chang, M.; Cacace, A. M.; Arcuri, M. J.; Celani, D.; Wexler, R. R.; Lawrence, R. M. Discovery of 2-(phenoxy)pyridine-3-phenylureas as small molecule P2Y₁ antagonists. *J. Med. Chem.* **2013**, *56*, 1704-1714.
213. Qiao, J. X.; Wang, T. C.; Ruel, R.; Thibeault, C.; L'Heureux, A.; Schumacher, W. A.; Spronk, S. A.; Hiebert, S.; Bouthillier, G.; Lloyd, J.; Pi, Z.; Schnur, D. M.; Abell, L. M.; Hua, J.; Price, L. A.; Liu, E.; Wu, Q.; Steinbacher, T. E.; Bostwick, J. S.; Chang, M.; Zheng, J.; Gao, Q.; Ma, B.; McDonnell, P. A.; Huang, C. S.; Rehfuss, R.; Wexler, R. R.; Lam, P. Y. S. Conformationally Constrained ortho-Anilino Diaryl Ureas: Discovery of 1-(2-(1'-Neopentylspiro[indoline-3,4'-piperidine]-1-yl)phenyl)-3-(4-(trifluoromethoxy)phenyl)urea, a Potent, Selective, and Bioavailable P2Y₁ Antagonist. *J. Med. Chem.* **2013**, *56*, 9275-9295.
214. Yang, W.; Wang, Y.; Lai, A.; Qiao, J. X.; Wang, T. C.; Hua, J.; Price, L. A.; Shen, H.; Chen, X.-q.; Wong, P.; Crain, E.; Watson, C.; Huang, C. S.; Seiffert, D. A.;

- Reh fuss, R.; Wexler, R. R.; Lam, P. Y. S. Discovery of 4-Aryl-7-Hydroxyindoline-Based P2Y₁ Antagonists as Novel Antiplatelet Agents. *J. Med. Chem.* **2014**, *57*, 6150-6164.
215. Gao, Z. G.; Jacobson, K. A. Distinct Signaling Patterns of Allosteric Antagonism at the P2Y₁ Receptor. *Mol. Pharmacol.* **2017**, *92*, 613-626.
216. Springthorpe, B.; Bailey, A.; Barton, P.; Birkinshaw, T. N.; Bonnert, R. V.; Brown, R. C.; Chapman, D.; Dixon, J.; Guile, S. D.; Humphries, R. G.; Hunt, S. F.; Ince, F.; Ingall, A. H.; Kirk, I. P.; Leeson, P. D.; Leff, P.; Lewis, R. J.; Martin, B. P.; McGinnity, D. F.; Mortimore, M. P.; Paine, S. W.; Pairaudeau, G.; Patel, A.; Rigby, A. J.; Riley, R. J.; Teobald, B. J.; Tomlinson, W.; Webborn, P. J. H.; Willis, P. A. From ATP to AZD6140: The discovery of an orally active reversible P2Y₁₂ receptor antagonist for the prevention of thrombosis. *Bioorg. Med. Chem. Lett.* **2007**, *17*, 6013-6018.
217. Lau, O. C.; Samarawickrama, C.; Skalicky, S. E. P2Y₂ receptor agonists for the treatment of dry eye disease: a review. *Clin. Ophthalmol.* **2014**, *8*, 327-334.
218. Sakuma, K.; Nakagawa, H.; Oikawa, T.; Noda, M.; Ikeda, S. Effects of 4(1*H*)-quinolinone derivative, a novel non-nucleotide allosteric purinergic P2Y₂ agonist, on cardiomyocytes in neonatal rats. *Sci. Rep.* **2017**, *7*, 6050.
219. Lau, O. C. F.; Samarawickrama, C.; Skalicky, S. E. P2Y₂ receptor agonists for the treatment of dry eye disease: a review. *Clin. Ophthalmol.* **2014**, *8*, 327-334.
220. Bachelierie, F.; Ben-Baruch, A.; Burkhardt, A. M.; Combadiere, C.; Farber, J. M.; Graham, G. J.; Horuk, R.; Sparre-Ulrich, A. H.; Locati, M.; Luster, A. D.; Mantovani, A.; Matsushima, K.; Murphy, P. M.; Nibbs, R.; Nomiya, H.; Power, C. A.; Proudfoot, A. E.; Rosenkilde, M. M.; Rot, A.; Sozzani, S.; Thelen, M.; Yoshie, O.; Zlotnik, A. Update on the extended family of chemokine receptors and introducing a new nomenclature for atypical chemokine receptors. *Pharmacol. Rev.* **2014**, *66*, 1-79.
221. Allegretti, M.; Cesta, M. C.; Locati, M. Allosteric Modulation of Chemoattractant Receptors. *Front Immunol.* **2016**, *7*, 170.
222. Thiele, S.; Malmgaard-Clausen, M.; Engel-Andreasen, J.; Steen, A.; Rummel, P. C.; Nielsen, M. C.; Gloriam, D. E.; Frimurer, T. M.; Ulven, T.; Rosenkilde, M. M. Modulation in selectivity and allosteric properties of small-molecule ligands for CC-chemokine receptors. *J. Med. Chem.* **2012**, *55*, 8164-8177.
223. Berger, E. A.; Murphy, P. M.; Farber, J. M. Chemokine receptors as HIV-1 coreceptors: roles in viral entry, tropism, and disease. *Annu. Rev. Immunol.* **1999**, *17*, 657-700.

224. Schwehm, C.; Kellam, B.; Garces, A. E.; Hill, S. J.; Kindon, N. D.; Bradshaw, T. D.; Li, J.; Macdonald, S. J.; Rowedder, J. E.; Stoddart, L. A.; Stocks, M. J. Design and Elaboration of a Tractable Tricyclic Scaffold To Synthesize Druglike Inhibitors of Dipeptidyl Peptidase-4 (DPP-4), Antagonists of the C-C Chemokine Receptor Type 5 (CCR5), and Highly Potent and Selective Phosphoinositol-3 Kinase delta (PI3Kdelta) Inhibitors. *J. Med. Chem.* **2017**, *60*, 1534-1554.
225. Maeda, K.; Das, D.; Nakata, H.; Mitsuya, H. CCR₅ inhibitors: emergence, success, and challenges. *Expert Opin. Emerg. Drugs* **2012**, *17*, 135-145.
226. Scholten, D. J.; Canals, M.; Maussang, D.; Roumen, L.; Smit, M. J.; Wijtmans, M.; de Graaf, C.; Vischer, H. F.; Leurs, R. Pharmacological modulation of chemokine receptor function. *Br. J. Pharmacol.* **2012**, *165*, 1617-1643.
227. Bertini, R.; Allegretti, M.; Bizzarri, C.; Moriconi, A.; Locati, M.; Zampella, G.; Cervellera, M. N.; Di Cioccio, V.; Cesta, M. C.; Galliera, E.; Martinez, F. O.; Di Bitondo, R.; Troiani, G.; Sabbatini, V.; D'Anniballe, G.; Anacardio, R.; Cutrin, J. C.; Cavalieri, B.; Mainiero, F.; Strippoli, R.; Villa, P.; Di Girolamo, M.; Martin, F.; Gentile, M.; Santoni, A.; Corda, D.; Poli, G.; Mantovani, A.; Ghezzi, P.; Colotta, F. Noncompetitive allosteric inhibitors of the inflammatory chemokine receptors CXCR1 and CXCR2: prevention of reperfusion injury. *Proc. Natl. Acad. Sci. U. S. A.* **2004**, *101*, 11791-11796.
228. Miller, E. J.; Jecs, E.; Truax, V. M.; Katzman, B. M.; Tahirovic, Y. A.; Wilson, R. J.; Kuo, K. M.; Kim, M. B.; Nguyen, H. H.; Saindane, M. T.; Zhao, H.; Wang, T.; Sum, C. S.; Cvijic, M. E.; Schroeder, G. M.; Wilson, L. J.; Liotta, D. C. Discovery of Tetrahydroisoquinoline-Containing CXCR4 Antagonists with Improved in Vitro ADMET Properties. *J. Med. Chem.* **2018**, *61*, 946-979.
229. Wendt, E.; Keshav, S. CCR9 antagonism: potential in the treatment of Inflammatory Bowel Disease. *Clin. Exp. Gastroenterol.* **2015**, *8*, 119-130.
230. O'Connor, T.; Borsig, L.; Heikenwalder, M. CCL2-CCR2 Signaling in Disease Pathogenesis. *Endocr Metab Immune Disord Drug Targets* **2015**, *15*, 105-118.
231. Procopiou, P. A.; Barrett, J. W.; Barton, N. P.; Begg, M.; Clapham, D.; Copley, R. C.; Ford, A. J.; Graves, R. H.; Hall, D. A.; Hancock, A. P.; Hill, A. P.; Hobbs, H.; Hodgson, S. T.; Jumeaux, C.; Lacroix, Y. M.; Miah, A. H.; Morriss, K. M.; Needham, D.; Sheriff, E. B.; Slack, R. J.; Smith, C. E.; Sollis, S. L.; Staton, H. Synthesis and structure-activity relationships of indazole arylsulfonamides as allosteric CC-chemokine receptor 4 (CCR4) antagonists. *J. Med. Chem.* **2013**, *56*, 1946-1960.
232. Ajram, L.; Begg, M.; Slack, R.; Cryan, J.; Hall, D.; Hodgson, S.; Ford, A.; Barnes, A.; Swieboda, D.; Mousnier, A.; Solari, R. Internalization of the chemokine receptor CCR4 can be evoked by orthosteric and allosteric receptor antagonists. *Eur. J. Pharmacol.* **2014**, *729*, 75-85.

233. Miah, A. H.; Copley, R. C.; O'Flynn, D.; Percy, J. M.; Procopiou, P. A. Lead identification and structure-activity relationships of heteroarylpyrazole arylsulfonamides as allosteric CC-chemokine receptor 4 (CCR4) antagonists. *Org. Biomol. Chem.* **2014**, *12*, 1779-1792.
234. Brox, R.; Milanos, L.; Saleh, N.; Baumeister, P.; Buschauer, A.; Hofmann, D.; Heinrich, M. R.; Clark, T.; Tschammer, N. Molecular Mechanisms of Biased and Probe-Dependent Signaling at CXC-Motif Chemokine Receptor CXCR3 Induced by Negative Allosteric Modulators. *Mol. Pharmacol.* **2018**, *93*, 309-322.
235. Admas, T. H.; Bernat, V.; Heinrich, M. R.; Tschammer, N. Development of Photoactivatable Allosteric Modulators for the Chemokine Receptor CXCR3. *ChemMedChem* **2016**, *11*, 575-584.
236. Bernat, V.; Brox, R.; Heinrich, M. R.; Auberson, Y. P.; Tschammer, N. Ligand-Biased and Probe-Dependent Modulation of Chemokine Receptor CXCR3 Signaling by Negative Allosteric Modulators. *ChemMedChem* **2015**, *10*, 566-574.
237. Neelakantan, H.; Holliday, E. D.; Fox, R. G.; Stutz, S. J.; Comer, S. D.; Haney, M.; Anastasio, N. C.; Moeller, F. G.; Cunningham, K. A. Lorcaserin Suppresses Oxycodone Self-Administration and Relapse Vulnerability in Rats. *ACS Chem. Neurosci.* **2017**, *8*, 1065-1073.
238. Remesic, M.; Hruby, V. J.; Porreca, F.; Lee, Y. S. Recent Advances in the Realm of Allosteric Modulators for Opioid Receptors for Future Therapeutics. *ACS Chem. Neurosci.* **2017**, *8*, 1147-1158.
239. Kathmann, M.; Flau, K.; Redmer, A.; Trankle, C.; Schlicker, E. Cannabidiol is an allosteric modulator at μ - and δ -opioid receptors. *Naunyn Schmiedeberg's Arch Pharmacol.* **2006**, *372*, 354-361.
240. Rothman, R. B.; Murphy, D. L.; Xu, H.; Godin, J. A.; Dersch, C. M.; Partilla, J. S.; Tidgewell, K.; Schmidt, M.; Prisinzano, T. E. Salvinorin A: allosteric interactions at the μ -opioid receptor. *J. Pharmacol. Exp. Ther.* **2007**, *320*, 801-810.
241. Burford, N. T.; Clark, M. J.; Wehrman, T. S.; Gerritz, S. W.; Banks, M.; O'Connell, J.; Traynor, J. R.; Alt, A. Discovery of positive allosteric modulators and silent allosteric modulators of the μ -opioid receptor. *Proc. Natl. Acad. Sci. U. S. A.* **2013**, *110*, 10830-10835.
242. Burford, N. T.; Traynor, J. R.; Alt, A. Positive allosteric modulators of the μ -opioid receptor: a novel approach for future pain medications. *Br. J. Pharmacol.* **2015**, *172*, 277-286.
243. Ohbuchi, K.; Miyagi, C.; Suzuki, Y.; Mizuhara, Y.; Mizuno, K.; Omiya, Y.; Yamamoto, M.; Warabi, E.; Sudo, Y.; Yokoyama, A.; Miyano, K.; Hirokawa, T.;

- Uezono, Y. Ignavine: a novel allosteric modulator of the μ opioid receptor. *Sci. Rep.* **2016**, *6*, 31748.
244. Livingston, K. E.; Stanczyk, M. A.; Burford, N. T.; Alt, A.; Canals, M.; Traynor, J. R. Pharmacologic Evidence for a Putative Conserved Allosteric Site on Opioid Receptors. *Mol. Pharmacol.* **2018**, *93*, 157-167.
245. Zvejniece, L.; Vavers, E.; Svalbe, B.; Vilskersts, R.; Domracheva, I.; Vorona, M.; Veinberg, G.; Misane, I.; Stonans, I.; Kalvinsh, I.; Dambrova, M. The cognition-enhancing activity of E₁R, a novel positive allosteric modulator of sigma-1 receptors. *Br. J. Pharmacol.* **2014**, *171*, 761-771.
246. Sakurai, T.; Ogawa, K.; Ishihara, Y.; Kasai, S.; Nakayama, M. The MCH1 receptor, an anti-obesity target, is allosterically inhibited by 8-methylquinoline derivatives possessing subnanomolar binding and long residence times. *Br. J. Pharmacol.* **2014**, *171*, 1287-1298.
247. Sliwoski, G.; Schubert, M.; Stichel, J.; Weaver, D.; Beck-Sickinger, A. G.; Meiler, J. Discovery of Small-Molecule Modulators of the Human Y4 Receptor. *PLoS One* **2016**, *11*, 1-13.
248. Schubert, M.; Stichel, J.; Du, Y.; Tough, I. R.; Sliwoski, G.; Meiler, J.; Cox, H. M.; Weaver, C. D.; Beck-Sickinger, A. G. Identification and Characterization of the First Selective Y4 Receptor Positive Allosteric Modulator. *J. Med. Chem.* **2017**, *60*, 7605-7612.
249. Maillet, E. L.; Pellegrini, N.; Valant, C.; Bucher, B.; Hibert, M.; Bourguignon, J. J.; Galzi, J. L. A novel, conformation-specific allosteric inhibitor of the tachykinin NK2 receptor (NK2R) with functionally selective properties. *FASEB J.* **2007**, *21*, 2124-2134.
250. Valant, C.; Maillet, E.; Bourguignon, J. J.; Bucher, B.; Utard, V.; Galzi, J. L.; Hibert, M. Allosteric functional switch of neurokinin A-mediated signaling at the neurokinin NK2 receptor: structural exploration. *J. Med. Chem.* **2009**, *52*, 5999-6011.
251. Wood, M. R.; Hopkins, C. R.; Brogan, J. T.; Conn, P. J.; Lindsley, C. W. "Molecular Switches" on mGluR Allosteric Ligands That Modulate Modes of Pharmacology. *Biochemistry* **2011**, *50*, 2403-2410.
252. Rook, J. M.; Noetzel, M. J.; Pouliot, W. A.; Bridges, T. M.; Vinson, P. N.; Cho, H. P.; Zhou, Y.; Gogliotti, R. D.; Manka, J. T.; Gregory, K. J.; Stauffer, S. R.; Dudek, F. E.; Xiang, Z.; Niswender, C. M.; Daniels, J. S.; Jones, C. K.; Lindsley, C. W.; Conn, P. J. Unique Signaling Profiles of Positive Allosteric Modulators of Metabotropic Glutamate Receptor Subtype 5 Determine Differences in In Vivo Activity. *Biological Psychiatry* **2013**, *73*, 501-509.

253. Congreve, M.; Oswald, C.; Marshall, F. H. Applying Structure-Based Drug Design Approaches to Allosteric Modulators of GPCRs. *Trends Pharmacol. Sci.* **2017**, *38*, 837-847.
254. Dror, R. O.; Green, H. F.; Valant, C.; Borhani, D. W.; Valcourt, J. R.; Pan, A. C.; Arlow, D. H.; Canals, M.; Lane, J. R.; Rahmani, R.; Baell, J. B.; Sexton, P. M.; Christopoulos, A.; Shaw, D. E. Structural basis for modulation of a G-protein-coupled receptor by allosteric drugs. *Nature* **2013**, *503*, 295-299.
255. Basith, S.; Cui, M.; Macalino, S. J. Y.; Park, J.; Clavio, N. A. B.; Kang, S.; Choi, S. Exploring G Protein-Coupled Receptors (GPCRs) Ligand Space via Cheminformatics Approaches: Impact on Rational Drug Design. *Front Pharmacol.* **2018**, *9*, 128.
256. Miao, Y.; Goldfeld, D. A.; Moo, E. V.; Sexton, P. M.; Christopoulos, A.; McCammon, J. A.; Valant, C. Accelerated structure-based design of chemically diverse allosteric modulators of a muscarinic G protein-coupled receptor. *Proc. Natl. Acad. Sci.* **2016**, *113*, 5675-5684.
257. Lambert Nevin, A.; Javitch Jonathan, A. CrossTalk opposing view: Weighing the evidence for class A GPCR dimers, the jury is still out. *J. Physiol.* **2014**, *592*, 2443-2445.
258. Bouvier, M.; Hébert Terence, E. CrossTalk proposal: Weighing the evidence for Class A GPCR dimers, the evidence favours dimers. *J. Physiol.* **2014**, *592*, 2439-2441.
259. Meral, D.; Provasi, D.; Prada-Gracia, D.; Möller, J.; Marino, K.; Lohse, M. J.; Filizola, M. Molecular details of dimerization kinetics reveal negligible populations of transient μ -opioid receptor homodimers at physiological concentrations. *Sci. Rep.* **2018**, *8*, 7705.
260. Pin, J.-P.; Bettler, B. Organization and functions of mGlu and GABA_B receptor complexes. *Nature* **2016**, *540*, 60-68.
261. Gurevich, V. V.; Gurevich, E. V. GPCRs and Signal Transducers: Interaction Stoichiometry. *Trends Pharmacol. Sci.* [Online early access]. DOI: 10.1016/j.tips.2018.04.002.
262. Jin, J.; Momboisse, F.; Boncompain, G.; Koensgen, F.; Zhou, Z.; Cordeiro, N.; Arenzana-Seisdedos, F.; Perez, F.; Lagane, B.; Kellenberger, E.; Brelot, A. CCR5 adopts three homodimeric conformations that control cell surface delivery. *Sci. Signal.* **2018**, *11*, 2869.
263. Stoeber, M.; Jullié, D.; Lobingier, B. T.; Laeremans, T.; Steyaert, J.; Schiller, P. W.; Manglik, A.; von Zastrow, M. A Genetically Encoded Biosensor Reveals Location Bias of Opioid Drug Action. *Neuron* [Online early access]. DOI: 10.1016/j.neuron.2018.04.021.

264. Wold, E. A.; Wild, C. T.; Cunningham, K. A.; Zhou, J. Targeting the 5-HT_{2C} Receptor in Biological Context and the Current State of 5-HT_{2C} Receptor Ligand Development. *Curr. Top. Med. Chem.* **2019**, *19*, 1381-1398.
265. Hauser, A. S.; Attwood, M. M.; Rask-Andersen, M.; Schiöth, H. B.; Gloriam, D. E. Trends in GPCR Drug Discovery: New Agents, Targets and Indications. *Nat. Rev. Drug Discov.* **2017**, *16*, 829-842.
266. Wild, C.; Cunningham, K. A.; Zhou, J. Allosteric Modulation of G Protein-Coupled Receptors: An Emerging Approach of Drug Discovery. *Austin J. Pharmacol. Ther.* **2014**, *2*, 1-8.
267. Hannon, J.; Hoyer, D. Molecular Biology of 5-HT Receptors. *Behav. Brain Res.* **2008**, *195*, 198-213.
268. The serotonin receptors. In *From molecular pharmacology to human therapeutics*, Roth, B. L., Ed. Humana Press: Totoaw, New Jersey, 2006.
269. Peng, Y.; McCorvy, J. D.; Harpsoe, K.; Lansu, K.; Yuan, S.; Popov, P.; Qu, L.; Pu, M.; Che, T.; Nikolajsen, L. F.; Huang, X. P.; Wu, Y.; Shen, L.; Bjorn-Yoshimoto, W. E.; Ding, K.; Wacker, D.; Han, G. W.; Cheng, J.; Katritch, V.; Jensen, A. A.; Hanson, M. A.; Zhao, S.; Gloriam, D. E.; Roth, B. L.; Stevens, R. C.; Liu, Z. J. 5-HT_{2C} Receptor Structures Reveal the Structural Basis of GPCR Polypharmacology. *Cell* **2018**, *172*, 719-730 e714.
270. Heifetz, A.; Storer, R. I.; McMurray, G.; James, T.; Morao, I.; Aldeghi, M.; Bodkin, M. J.; Biggin, P. C. Application of an integrated GPCR SAR-modeling platform to explain the activation selectivity of human 5-HT_{2C} over 5-HT_{2B}. *ACS Chem. Biol.* **2016**, *11*, 1372-1382.
271. Raymond, J. R.; Mukhin, Y. V.; Gelasco, A.; Turner, J.; Collinsworth, G.; Gettys, T. W.; Grewal, J. S.; Garnovskaya, M. N. Multiplicity of mechanisms of serotonin receptor signal transduction. *Pharmacol. Ther.* **2001**, *92*, 179-212.
272. Millan, M. J.; Marin, P.; Bockaert, J.; Mannoury la Cour, C. Signaling at G-protein-coupled serotonin receptors: recent advances and future research directions. *Trends Pharmacol. Sci.* **2008**, *29*, 454-464.
273. Seitz, P. K.; Bremer, N. M.; McGinnis, A. G.; Cunningham, K. A.; Watson, C. S. Quantitative Changes in Intracellular Calcium and Extracellular-regulated Kinase Activation Measured in Parallel in CHO Cells Stably Expressing Serotonin (5-HT) 5-HT_{2A} or 5-HT_{2C} Receptors. *BMC Neurosci.* **2012**, *13*, 25.
274. Roth, B. L.; Willins, D. L.; Kristiansen, K.; Kroeze, W. K. 5-Hydroxytryptamine 2-Family Receptors (5-Hydroxytryptamine 2A , 5-Hydroxytryptamine 2B , 5-

- Hydroxytryptamine 2C): Where Structure Meets Function. *Pharmacol. Ther.* **1998**, 79, 231-257.
275. Burke, J. E.; Dennis, E. A. Phospholipase A2 structure/function, mechanism, and signaling. *J. Lipid Res.* **2009**, 50 Suppl, S237-242.
276. Berg, K. A.; Maayani, S.; Goldfarb, J.; Scaramellini, C.; Leff, P.; Clarke, W. P. Effector pathway-dependent relative efficacy at serotonin type 2A and 2C receptors: evidence for agonist-directed trafficking of receptor stimulus. *Mol. Pharmacol.* **1998**, 54, 94-104.
277. Werry, T. D.; Stewart, G. D.; Crouch, M. F.; Watts, A.; Sexton, P. M.; Christopoulos, A. Pharmacology of 5HT(2C) Receptor-mediated ERK1/2 Phosphorylation: Agonist-specific Activation Pathways and the Impact of RNA Editing. *Biochem. Pharmacol.* **2008**, 76, 1276-1287.
278. Werry, T. D.; Gregory, K. J.; Sexton, P. M.; Christopoulos, A. Characterization of Serotonin 5-HT_{2C} Receptor Signaling to Extracellular Signal-regulated Kinases 1 and 2. *J. Neurochem.* **2005**, 93, 1603-1615.
279. Lauffer, L.; Glas, E.; Gudermann, T.; Breit, A. Endogenous 5-HT_{2C} Receptors Phosphorylate the cAMP Response Element Binding Protein via Protein Kinase C-promoted Activation of Extracellular-regulated Kinases-1/2 in Hypothalamic mHypA-2/10 Cells. *J. Pharmacol. Exp. Ther.* **2016**, 358, 39-49.
280. O'Neil, R. T.; Emeson, R. B. Quantitative analysis of 5HT(2C) receptor RNA editing patterns in psychiatric disorders. *Neurobiol. Dis.* **2012**, 45, 8-13.
281. Marion, S.; Weiner, D. M.; Caron, M. G. RNA editing induces variation in desensitization and trafficking of 5-hydroxytryptamine 2c receptor isoforms. *J. Biol. Chem.* **2004**, 279, 2945-2954.
282. Werry, T. D.; Loiacono, R.; Sexton, P. M.; Christopoulos, A. RNA editing of the serotonin 5HT_{2C} receptor and its effects on cell signalling, pharmacology and brain function. *Pharmacol. Ther.* **2008**, 119, 7-23.
283. Schaub, M.; Keller, W. RNA editing by adenosine deaminases generates RNA and protein diversity. *Biochimie* **2002**, 84, 791-803.
284. Chen, C. X.; Cho, D. S.; Wang, Q.; Lai, F.; Carter, K. C.; Nishikura, K. A third member of the RNA-specific adenosine deaminase gene family, ADAR3, contains both single- and double-stranded RNA binding domains. *RNA* **2000**, 6, 755-767.
285. Valente, L.; Nishikura, K. ADAR gene family and A-to-I RNA editing: diverse roles in posttranscriptional gene regulation. In *Progress in Nucleic Acid Research and Molecular Biology*, Academic Press: 2005; Vol. 79, pp 299-338.

286. Herrick-Davis, K.; Grinde, E.; Niswender, C. M. Serotonin 5-HT_{2C} receptor RNA editing alters receptor basal activity: implications for serotonergic signal transduction. *J. Neurochem.* **1999**, *73*, 1711-1717.
287. Berg, K. A.; Cropper, J. D.; Niswender, C. M.; Sanders-Bush, E.; Emeson, R. B.; Clarke, W. P. RNA-editing of the 5-HT(2C) receptor alters agonist-receptor-effector coupling specificity. *Br. J. Pharmacol.* **2001**, *134*, 386-392.
288. Maydanovych, O.; Beal, P. A. Breaking the central dogma by RNA editing. *Chem. Rev.* **2006**, *106*, 3397-3411.
289. Herrick-Davis, K.; Grinde, E.; Lindsley, T.; Teitler, M.; Mancina, F.; Cowan, A.; Mazurkiewicz, J. E. Native serotonin 5-HT_{2C} receptors are expressed as homodimers on the apical surface of choroid plexus epithelial cells. *Mol. Pharmacol.* **2015**, *87*, 660-673.
290. Herrick-Davis, K. F., Dinah T. 5-HT_{2C} receptor dimerization. In *5-HT_{2C} receptors in the pathophysiology of CNS disease*, Giuseppe Di Giovanni, E. E., Vincenzo Di Matteo, Ed. Blackwell Science Inc: British Journal of Clinical Pharmacology, 2011; Vol. 72, pp 129-155.
291. Schellekens, H.; van Oeffelen, W. E.; Dinan, T. G.; Cryan, J. F. Promiscuous dimerization of the growth hormone secretagogue receptor (GHS-R1a) attenuates ghrelin-mediated signaling. *J. Biol. Chem.* **2013**, *288*, 181-191.
292. Felsing, D. E.; Anastasio, N. C.; Miszkiel, J. M.; Gilbertson, S. R.; Allen, J. A.; Cunningham, K. A. Biophysical validation of serotonin 5-HT_{2A} and 5-HT_{2C} receptor interaction. *PLoS One* **2018**, *13*, e0203137.
293. Price, A. E.; Sholler, D. J.; Stutz, S. J.; Anastasio, N. C.; Cunningham, K. A. Endogenous serotonin 5-HT_{2A} and 5-HT_{2C} receptors associate in the medial prefrontal cortex. *ACS Chem. Neurosci.* **2019**.
294. Kamal, M.; Gbahou, F.; Guillaume, J. L.; Daulat, A. M.; Benleulmi-Chaachoua, A.; Luka, M.; Chen, P.; Kalbasi Anaraki, D.; Baroncini, M.; Mannoury la Cour, C.; Millan, M. J.; Prevot, V.; Delagrangé, P.; Jockers, R. Convergence of melatonin and serotonin (5-HT) signaling at MT₂/5-HT_{2C} receptor heteromers. *J. Biol. Chem.* **2015**, *290*, 11537-11546.
295. Moutkine, I.; Quentin, E.; Guiard, B. P.; Maroteaux, L.; Doly, S. Heterodimers of serotonin receptor subtypes 2 are driven by 5-HT_{2C} protomers. *J. Biol. Chem.* **2017**, *292*, 6352-6368.
296. Bigford, G. E.; Chaudhry, N. S.; Keane, R. W.; Holohean, A. M. 5-Hydroxytryptamine 5HT_{2C} receptors form a protein complex with N-methyl-D-

- aspartate GluN2A subunits and activate phosphorylation of Src protein to modulate motoneuronal depolarization. *J. Biol. Chem.* **2012**, 287, 11049-11059.
297. Bohn, L. M.; Schmid, C. L. Serotonin Receptor Signaling and Regulation via Beta-arrestins. *Crit. Rev. Biochem. Mol. Biol.* **2010**, 45, 555-566.
298. Howell, L. L.; Cunningham, K. A. Serotonin 5-HT₂ Receptor Interactions with Dopamine Function: Implications for Therapeutics in Cocaine Use Disorder. *Pharmacol. Rev.* **2015**, 67, 176-197.
299. Anastasio, N. C.; Stutz, S. J.; Fink, L. H.; Swinford-Jackson, S. E.; Sears, R. M.; DiLeone, R. J.; Rice, K. C.; Moeller, F. G.; Cunningham, K. A. Serotonin (5-HT) 5-HT_{2A} Receptor (5-HT_{2AR}):5-HT_{2CR} Imbalance in Medial Prefrontal Cortex Associates with Motor Impulsivity. *ACS Chem. Neurosci.* **2015**, 6, 1248-1258.
300. Prisco, S.; Pagannone, S.; Esposito, E. Serotonin-dopamine interaction in the rat ventral tegmental area: an electrophysiological study in vivo. *J. Pharmacol. Exp. Ther.* **1994**, 271, 83-90.
301. Di Giovanni, G.; Di Matteo, V.; La Grutta, V.; Esposito, E. m-Chlorophenylpiperazine excites non-dopaminergic neurons in the rat substantia nigra and ventral tegmental area by activating serotonin-2C receptors. *Neuroscience* **2001**, 103, 111-116.
302. Theile, J. W.; Morikawa, H.; Gonzales, R. A.; Morrisett, R. A. Role of 5-Hydroxytryptamine_{2C} Receptors in Ca²⁺-dependent Ethanol Potentiation of GABA Release onto Ventral Tegmental Area Dopamine Neurons. *J. Pharmacol. Exp. Ther.* **2009**, 329, 625-633.
303. Kasper, J. M.; Booth, R. G.; Peris, J. Serotonin-2C receptor agonists decrease potassium-stimulated GABA release in the nucleus accumbens. *Synapse* **2015**, 69, 78-85.
304. Di Giovanni, G.; De Deurwaerdere, P.; Di Mascio, M.; Di Matteo, V.; Esposito, E.; Spampinato, U. Selective blockade of serotonin-2C/2B receptors enhances mesolimbic and mesostriatal dopaminergic function: a combined in vivo electrophysiological and microdialysis study. *Neuroscience* **1999**, 91, 587-597.
305. Gobert, A.; Rivet, J.-M.; Lejeune, F.; Newman-Tancredi, A.; Adhumeau-Auclair, A.; Nicolas, J.-P.; Cistarelli, L.; Melon, C.; Millan, M. J. Serotonin_{2C} Receptors Tonicly Suppress the Activity of Mesocortical Dopaminergic and Adrenergic, but not Serotonergic, Pathways: A Combined Dialysis and Electrophysiological Analysis in the Rat. *Synapse* **2000**, 36, 205-221.

306. Bubar, M. J.; Stutz, S. J.; Cunningham, K. A. 5-HT_{2C} Receptors Localize to Dopamine and GABA Neurons in the Rat Mesoaccumbens Pathway. *PLoS One* **2011**, *6*, e20508.
307. Bubar, M. J.; Cunningham, K. A. Distribution of Serotonin 5-HT_{2C} Receptors in the Ventral Tegmental Area. *Neuroscience* **2007**, *146*, 286-297.
308. Xu, P.; He, Y.; Cao, X.; Valencia-Torres, L.; Yan, X.; Saito, K.; Wang, C.; Yang, Y.; Hinton, A., Jr.; Zhu, L.; Shu, G.; Myers, M. G., Jr.; Wu, Q.; Tong, Q.; Heisler, L. K.; Xu, Y. Activation of Serotonin 2C Receptors in Dopamine Neurons Inhibits Binge-like Eating in Mice. *Biol. Psychiatry* **2017**, *81*, 737-747.
309. Santana, N.; Artigas, F. Expression of serotonin_{2C} receptors in pyramidal and GABAergic neurons of rat prefrontal cortex: a comparison with striatum. *Cereb. Cortex* **2017**, *27*, 3125-3139.
310. Liu, S.; Bubar, M. J.; Lanfranco, M. F.; Hillman, G. R.; Cunningham, K. A. Serotonin_{2C} Receptor Localization in GABA Neurons of the Rat Medial Prefrontal Cortex: Implications for Understanding the Neurobiology of Addiction. *Neuroscience* **2007**, *146*, 1677-1688.
311. Anastasio, N. C.; Stutz, S. J.; Fox, R. G.; Sears, R. M.; Emeson, R. B.; DiLeone, R. J.; O'Neil, R. T.; Fink, L. H.; Li, D.; Green, T. A.; Moeller, F. G.; Cunningham, K. A. Functional Status of the Serotonin 5-HT_{2C} Receptor (5-HT_{2CR}) Drives Interlocked Phenotypes that Precipitate Relapse-like Behaviors in Cocaine Dependence. *Neuropsychopharmacology* **2014**, *39*, 370-382.
312. Bubar, M.; Cunningham, K. Serotonin 5-HT_{2A} and 5-HT_{2C} Receptors as Potential Targets for Modulation of Psychostimulant Use and Dependence. *Curr. Top. Med. Chem.* **2006**, *6*, 1971-1985.
313. Cunningham, K. A.; Anastasio, N. C.; Fox, R. G.; Stutz, S. J.; Bubar, M. J.; Swinford, S. E.; Watson, C. S.; Gilbertson, S. R.; Rice, K. C.; Rosenzweig-Lipson, S.; Moeller, F. G. Synergism Between a Serotonin 5-HT_{2A} Receptor (5-HT_{2AR}) Antagonist and 5-HT_{2CR} Agonist Suggests New Pharmacotherapeutics for Cocaine Addiction. *ACS Chem. Neurosci.* **2013**, *4*, 110-121.
314. Thomsen, W. J.; Grottick, A. J.; Menzaghi, F.; Reyes-Saldana, H.; Espitia, S.; Yuskin, D.; Whelan, K.; Martin, M.; Morgan, M.; Chen, W.; Al-Shamma, H.; Smith, B.; Chalmers, D.; Behan, D. Lorcaserin, a Novel Selective Human 5-Hydroxytryptamine_{2C} Agonist: In Vitro and In Vivo Pharmacological Characterization. *J. Pharmacol. Exp. Ther.* **2008**, *325*, 577-587.
315. Hoy, S. M. Lorcaserin: a Review of its Use in Chronic Weight Management. *Drugs* **2013**, *73*, 463-473.

316. Harvey-Lewis, C.; Li, Z.; Higgins, G. A.; Fletcher, P. J. The 5-HT_{2C} Receptor Agonist Lorcaserin Reduces Cocaine Self-administration, Reinstatement of Cocaine-seeking and Cocaine Induced Locomotor Activity. *Neuropharmacology* **2016**, 101, 237-245.
317. Di Giovanni, G.; De Deurwaerdere, P. New Therapeutic Opportunities for 5-HT_{2C} Receptor Ligands in Neuropsychiatric Disorders. *Pharmacol. Ther.* **2016**, 157, 125-162.
318. Higgins, G. A.; Fletcher, P. J. Therapeutic Potential of 5-HT_{2C} Receptor Agonists for Addictive Disorders. *ACS Chem. Neurosci.* **2015**, 6, 1071-1088.
319. Tecott, L. H.; Sun, L. M.; Akana, S. F.; Strack, A. M.; Lowenstein, D. H.; Dallman, M. F.; Julius, D. Eating Disorder and Epilepsy in Mice Lacking 5-HT_{2c} Serotonin Receptors. *Nature* **1995**, 374, 542-546.
320. Nonogaki, K.; Ohba, Y.; Sumii, M.; Oka, Y. Serotonin systems upregulate the expression of hypothalamic NUCB2 via 5-HT_{2C} receptors and induce anorexia via a leptin-independent pathway in mice. *Biochem. Biophys. Res. Commun.* **2008**, 372, 186-190.
321. Wirshing, D. A.; Wirshing, W. C.; Kysar, L.; Berisford, M. A.; Goldstein, D.; Pashdag, J.; Mintz, J.; Marder, S. R. Novel antipsychotics: comparison of weight gain liabilities. *J. Clin. Psychiatry* **1999**, 60, 358-363.
322. Kirk, S. L.; Glazebrook, J.; Grayson, B.; Neill, J. C.; Reynolds, G. P. Olanzapine-induced Weight Gain in the Rat: Role of 5-HT_{2C} and Histamine H₁ Receptors. *Psychopharmacology (Berl.)* **2009**, 207, 119-125.
323. Ge, T.; Zhang, Z.; Lv, J.; Song, Y.; Fan, J.; Liu, W.; Wang, X.; Hall, F. S.; Li, B.; Cui, R. The role of 5-HT_{2c} receptor on corticosterone-mediated food intake. *J. Biochem. Mol. Toxicol.* **2017**, 31.
324. Halford, J. C.; Lawton, C. L.; Blundell, J. E. The 5-HT₂ Receptor Agonist MK-212 Reduces Food Intake and Increases Resting but Prevents the Behavioural Satiety Sequence. *Pharmacol. Biochem. Behav.* **1997**, 56, 41-46.
325. Wacker, D. A.; Miller, K. J. Agonists of the Serotonin 5-HT_{2C} Receptor: Preclinical and Clinical Progression in Multiple Diseases. *Curr. Opin. Drug Discov. Devel.* **2008**, 11, 438-445.
326. Dunlop, J.; Sabb, A. L.; Mazandarani, H.; Zhang, J.; Kalgaonker, S.; Shukhina, E.; Sukoff, S.; Vogel, R. L.; Stack, G.; Schechter, L.; Harrison, B. L.; Rosenzweig-Lipson, S. WAY-163909 [(7bR, 10aR)-1,2,3,4,8,9,10,10a-Octahydro-7bH-cyclopenta-[b][1,4]diazepino[6,7,1hi]indole], a Novel 5-Hydroxytryptamine 2C

- Receptor-selective Agonist with Anorectic Activity. *J. Pharmacol. Exp. Ther.* **2005**, 313, 862-869.
327. Voigt, J. P.; Fink, H. Serotonin Controlling Feeding and Satiety. *Behav. Brain Res.* **2015**, 277, 14-31.
328. Gautron, L.; Elmquist, J. K.; Williams, K. W. Neural control of energy balance: translating circuits to therapies. *Cell* **2015**, 161, 133-145.
329. Smith, S. R.; Prosser, W. A.; Donahue, D. J.; Morgan, M. E.; Anderson, C. M.; Shanahan, W. R.; Group, A. P. D. S. Lorcaserin (APD356), a Selective 5-HT(2C) Agonist, Reduces Body Weight in Obese Men and Women. *Obesity* **2009**, 17, 494-503.
330. Bubar, M. J.; Cunningham, K. A. Prospects for Serotonin 5-HT_{2R} Pharmacotherapy in Psychostimulant Abuse. *Prog. Brain Res.* **2008**, 172, 319-346.
331. Moeller, F. G.; Cunningham, K. A. Innovative Therapeutic Intervention for Opioid Use Disorder. *Neuropsychopharmacology* **2018**, 43, 220-221.
332. Swinford-Jackson, S. E.; Anastasio, N. C.; Fox, R. G.; Stutz, S. J.; Cunningham, K. A. Incubation of Cocaine Cue Reactivity Associates with Neuroadaptations in the Cortical Serotonin (5-HT) 5-HT_{2C} Receptor (5-HT_{2CR}) System. *Neuroscience* **2016**, 324, 50-61.
333. Cunningham, K. A.; Fox, R. G.; Anastasio, N. C.; Bubar, M. J.; Stutz, S. J.; Moeller, F. G.; Gilbertson, S. R.; Rosenzweig-Lipson, S. Selective Serotonin 5-HT(2C) Receptor Activation Suppresses the Reinforcing Efficacy of Cocaine and Sucrose but Differentially Affects the Incentive-salience Value of Cocaine- vs. Sucrose-associated Cues. *Neuropharmacology* **2011**, 61, 513-523.
334. Grottick, A. J.; Fletcher, P. J.; Higgins, G. A. Studies to Investigate the Role of 5-HT(2C) Receptors on Cocaine- and Food-maintained Behavior. *J. Pharmacol. Exp. Ther.* **2000**, 295, 1183-1191.
335. Manvich, D. F.; Kimmel, H. L.; Cooper, D. A.; Howell, L. L. The Serotonin 2C Receptor Antagonist SB 242084 Exhibits Abuse-related Effects Typical of Stimulants in Squirrel Monkeys. *J. Pharmacol. Exp. Ther.* **2012**, 342, 761-769.
336. Manvich, D. F.; Kimmel, H. L.; Howell, L. L. Effects of Serotonin 2C Receptor Agonists on the Behavioral and Neurochemical Effects of Cocaine in Squirrel Monkeys. *J. Pharmacol. Exp. Ther.* **2012**, 341, 424-434.
337. Pelloux, Y.; Dilleen, R.; Economidou, D.; Theobald, D.; Everitt, B. J. Reduced Forebrain Serotonin Transmission is Causally Involved in the Development of Compulsive Cocaine Seeking in Rats. *Neuropsychopharmacology* **2012**, 37, 2505.

338. Fletcher, P. Differential Effects of the 5-HT_{2A} Receptor Antagonist M100,907 and the 5-HT_{2C} Receptor Antagonist SB242,084 on Cocaine-induced Locomotor Activity, Cocaine Self-administration and Cocaine-induced Reinstatement of Responding. *Neuropsychopharmacology* **2002**, 27, 576-586.
339. Shanahan, W. R.; Rose, J. E.; Glicklich, A.; Stubbe, S.; Sanchez-Kam, M. Lorcaserin for Smoking Cessation and Associated Weight Gain: a Randomized 12-week Clinical Trial. *Nicotine Tob. Res.* **2017**, 19, 944-951.
340. Farr, O. M.; Upadhyay, J.; Gavrieli, A.; Camp, M.; Spyrou, N.; Kaye, H.; Mathew, H.; Vamvini, M.; Koniaris, A.; Kilim, H.; Srnka, A.; Migdal, A.; Mantzoros, C. S. Lorcaserin Administration Decreases Activation of Brain Centers in Response to Food Cues and These Emotion- and Salience-related Changes Correlate with Weight Loss Effects: a 4-Week-long Randomized, Placebo-controlled, Double-blind Clinical Trial. *Diabetes* **2016**, 65, 2943-2953.
341. Cunningham, K. A.; Anastasio, N. C. Serotonin at the Nexus of Impulsivity and Cue Reactivity in Cocaine Addiction. *Neuropharmacology* **2014**, 76 Pt B, 460-478.
342. Moeller, F. G.; Barratt, E. S.; Dougherty, D. M.; Schmitz, J. M.; Swann, A. C. Psychiatric Aspects of Impulsivity. *Am. J. Psychiatry* **2001**, 158, 1783-1793.
343. Liu, S.; Lane, S. D.; Schmitz, J. M.; Waters, A. J.; Cunningham, K. A.; Moeller, F. G. Relationship Between Attentional Bias to Cocaine-related Stimuli and Impulsivity in Cocaine-dependent Subjects. *Am. J. Drug Alcohol Abuse* **2011**, 37, 117-122.
344. Leung, D.; Staiger, P. K.; Hayden, M.; Lum, J. A.; Hall, K.; Manning, V.; Verdejo-Garcia, A. Meta-analysis of the Relationship Between Impulsivity and Substance-related Cognitive Biases. *Drug Alcohol Depend.* **2017**, 172, 21-33.
345. Fletcher, P. J.; Tampakeras, M.; Sinyard, J.; Higgins, G. A. Opposing Effects of 5-HT_{2A} and 5-HT_{2C} Receptor Antagonists in the Rat and Mouse on Premature Responding in the Five-choice Serial Reaction Time Test. *Psychopharmacology (Berl.)* **2007**, 195, 223-234.
346. Winstanley, C. A.; Theobald, D. E.; Dalley, J. W.; Glennon, J. C.; Robbins, T. W. 5-HT_{2A} and 5-HT_{2C} Receptor Antagonists have Opposing Effects on a Measure of Impulsivity: Interactions with Global 5-HT Depletion. *Psychopharmacology (Berl.)* **2004**, 176, 376-385.
347. Pennanen, L.; van der Hart, M.; Yu, L.; Tecott, L. H. Impact of Serotonin (5-HT)_{2C} Receptors on Executive Control Processes. *Neuropsychopharmacology* **2013**, 38, 957-967.
348. Besson, M.; Pelloux, Y.; Dilleen, R.; Theobald, D. E.; Lyon, A.; Belin-Rauscent, A.; Robbins, T. W.; Dalley, J. W.; Everitt, B. J.; Belin, D. Cocaine Modulation of

- Frontostriatal Expression of Zif268, D2, and 5-HT_{2c} Receptors in High and Low Impulsive Rats. *Neuropsychopharmacology* **2013**, 38, 1963-1973.
349. Anastasio, N. C.; Liu, S.; Maili, L.; Swinford, S. E.; Lane, S. D.; Fox, R. G.; Hamon, S. C.; Nielsen, D. A.; Cunningham, K. A.; Moeller, F. G. Variation Within the Serotonin (5-HT) 5-HT_{2C} Receptor System Aligns with Vulnerability to Cocaine Cue Reactivity. *Transl. Psychiatry* **2014**, 4, e369.
350. Everitt, B. J.; Robbins, T. W. Drug Addiction: Updating Actions to Habits to Compulsions Ten Years On. *Annu. Rev. Psychol.* **2016**, 67, 23-50.
351. Nichols, D. E. Hallucinogens. *Pharmacol. Ther.* **2004**, 101, 131-181.
352. Fitzgerald, L. W.; Burn, T. C.; Brown, B. S.; Patterson, J. P.; Corjay, M. H.; Valentine, P. A.; Sun, J. H.; Link, J. R.; Abbaszade, I.; Hollis, J. M.; Largent, B. L.; Hartig, P. R.; Hollis, G. F.; Meunier, P. C.; Robichaud, A. J.; Robertson, D. W. Possible Role of Valvular Serotonin 5-HT_{2B} Receptors in the Cardiopathy Associated with Fenfluramine. *Mol. Pharmacol.* **2000**, 57, 75-81.
353. Connolly, H. M.; Crary, J. L.; McGoon, M. D.; Hensrud, D. D.; Edwards, B. S.; Edwards, W. D.; Schaff, H. V. Valvular Heart Disease Associated with Fenfluramine-phentermine. *N. Engl. J. Med.* **1997**, 337, 581-588.
354. Shram, M. J.; Schoedel, K. A.; Bartlett, C.; Shazer, R. L.; Anderson, C. M.; Sellers, E. M. Evaluation of the Abuse Potential of Lorcaserin, a Serotonin 2C (5-HT_{2C}) Receptor Agonist, in Recreational Polydrug Users. *Clin. Pharmacol. Ther.* **2011**, 89, 683-692.
355. Greenway, F. L.; Shanahan, W.; Fain, R.; Ma, T.; Rubino, D. Safety and Tolerability Review of Lorcaserin in Clinical Trials. *Clin. Obes.* **2016**, 6, 285-295.
356. Kalgutkar, A. S.; Dalvie, D. K.; Aubrecht, J.; Smith, E. B.; Coffing, S. L.; Cheung, J. R.; Vage, C.; Lame, M. E.; Chiang, P.; McClure, K. F.; Maurer, T. S.; Coelho, R. V., Jr.; Soliman, V. F.; Schildknecht, K. Genotoxicity of 2-(3-Chlorobenzoyloxy)-6-(piperazinyl)pyrazine, a Novel 5-Hydroxytryptamine_{2c} Receptor Agonist for the Treatment of Obesity: Role of Metabolic Activation. *Drug Metab. Dispos.* **2007**, 35, 848-858.
357. Kelly, C. R.; Sharif, N. A. Pharmacological evidence for a functional serotonin-2B receptor in a human uterine smooth muscle cell line. *J. Pharmacol. Exp. Ther.* **2006**, 317, 1254-1261.
358. Bos, M.; Jenck, F.; Martin, J. R.; Moreau, J. L.; Sleight, A. J.; Wichmann, J.; Widmer, U. Novel Agonists of 5HT_{2C} Receptors. Synthesis and Biological Evaluation of Substituted 2-(Indol-1-yl)-1-methylethylamines and 2-(Indeno[1,2-b]pyrrol-1-yl)-1-

- methylethylamines. Improved Therapeutics for Obsessive Compulsive Disorder. *J. Med. Chem.* **1997**, 40, 2762-2769.
359. Kimura, Y.; Hatanaka, K.; Naitou, Y.; Maeno, K.; Shimada, I.; Koakutsu, A.; Wanibuchi, F.; Yamaguchi, T. Pharmacological profile of YM348, a novel, potent and orally active 5-HT_{2C} receptor agonist. *Eur. J. Pharmacol.* **2004**, 483, 37-43.
360. Fitzgerald, L. W.; Burn, T. C.; Brown, B. S.; Patterson, J. P.; Corjay, M. H.; Valentine, P. A.; Sun, J.-H.; Link, J. R.; Abbaszade, I.; Hollis, J. M.; Largent, B. L.; Hartig, P. R.; Hollis, G. F.; Meunier, P. C.; Robichaud, A. J.; Robertson, D. W. Possible role of valvular serotonin 5-HT_{2B} receptors in the cardiopathy with fenfluramine. *Mol. Pharmacol.* **2000**, 57, 75-81.
361. Cheng, J.; Giguere, P. M.; Onajole, O. K.; Lv, W.; Gaisin, A.; Gunosewoyo, H.; Schmerberg, C. M.; Pogorelov, V. M.; Rodriguiz, R. M.; Vistoli, G.; Wetsel, W. C.; Roth, B. L.; Kozikowski, A. P. Optimization of 2-phenylcyclopropylmethylamines as selective serotonin 2C receptor agonists and their evaluation as potential antipsychotic agents. *J. Med. Chem.* **2015**, 58, 1992-2002.
362. Cheng, J.; Giguere, P. M.; Schmerberg, C. M.; Pogorelov, V. M.; Rodriguiz, R. M.; Huang, X. P.; Zhu, H.; McCorvy, J. D.; Wetsel, W. C.; Roth, B. L.; Kozikowski, A. P. Further Advances in Optimizing (2-Phenylcyclopropyl)methylamines as Novel Serotonin 2C Agonists: Effects on Hyperlocomotion, Prepulse Inhibition, and Cognition Models. *J. Med. Chem.* **2016**, 59, 578-591.
363. Zhang, G.; Cheng, J.; McCorvy, J. D.; Lorello, P. J.; Caldarone, B. J.; Roth, B. L.; Kozikowski, A. P. Discovery of N-substituted (2-phenylcyclopropyl)methylamines as functionally selective serotonin 2C receptor agonists for potential use as antipsychotic medications. *J. Med. Chem.* **2017**, 60, 6273-6288.
364. Siuciak, J. A.; Chapin, D. S.; McCarthy, S. A.; Guanowsky, V.; Brown, J.; Chiang, P.; Marala, R.; Patterson, T.; Seymour, P. A.; Swick, A.; Iredale, P. A. CP-809,101, a selective 5-HT_{2C} agonist, shows activity in animal models of antipsychotic activity. *Neuropharmacology* **2007**, 52, 279-290.
365. Fevig, J. M.; Feng, J.; Rossi, K. A.; Miller, K. J.; Wu, G.; Hung, C. P.; Ung, T.; Malmstrom, S. E.; Zhang, G.; Keim, W. J.; Cullen, M. J.; Rohrbach, K. W.; Qu, Q.; Gan, J.; Pelleymounter, M. A.; Robl, J. A. Synthesis and SAR of 2,3,3a,4-tetrahydro-1H-pyrrolo[3,4-c]isoquinolin-5(9bH)-ones as 5-HT_{2C} receptor agonists. *Bioorg. Med. Chem. Lett.* **2013**, 23, 330-335.
366. Zhao, G.; Kwon, C.; Bisaha, S. N.; Stein, P. D.; Rossi, K. A.; Cao, X.; Ung, T.; Wu, G.; Hung, C. P.; Malmstrom, S. E.; Zhang, G.; Qu, Q.; Gan, J.; Keim, W. J.; Cullen, M. J.; Rohrbach, K. W.; Devenny, J.; Pelleymounter, M. A.; Miller, K. J.; Robl, J. A. Synthesis and SAR of potent and selective tetrahydropyrazinoisoquinolinone 5-HT_{2C} receptor agonists. *Bioorg. Med. Chem. Lett.* **2013**, 23, 3914-3919.

367. Dunlop, J.; Watts, S. W.; Barrett, J. E.; Coupet, J.; Harrison, B.; Mazandarani, H.; Nawoschik, S.; Pangalos, M. N.; Ramamoorthy, S.; Schechter, L.; Smith, D.; Stack, G.; Zhang, J.; Zhang, G.; Rosenzweig-Lipson, S. Characterization of Vabicaserin (SCA-136), a Selective 5-Hydroxytryptamine 2C Receptor Agonist. *J. Pharmacol. Exp. Ther.* **2011**, *337*, 673-680.
368. Rouquet, G.; Moore, D. E.; Spain, M.; Allwood, D. M.; Battilocchio, C.; Blakemore, D. C.; Fish, P. V.; Jenkinson, S.; Jessiman, A. S.; Ley, S. V.; McMurray, G.; Storer, R. I. Design, synthesis, and evaluation of tetrasubstituted pyridines as potent 5-HT_{2C} receptor agonists. *ACS Med. Chem. Lett.* **2015**, *6*, 329-333.
369. Storer, R. I.; Brennan, P. E.; Brown, A. D.; Bungay, P. J.; Conlon, K. M.; Corbett, M. S.; DePianta, R. P.; Fish, P. V.; Heifetz, A.; Ho, D. K.; Jessiman, A. S.; McMurray, G.; de Oliveira, C. A.; Roberts, L. R.; Root, J. A.; Shanmugasundaram, V.; Shapiro, M. J.; Skerten, M.; Westbrook, D.; Wheeler, S.; Whitlock, G. A.; Wright, J. Multiparameter Optimization in CNS Drug Discovery: Design of Pyrimido[4,5-d]azepines as Potent 5-Hydroxytryptamine 2C (5-HT_{2C}) Receptor Agonists with Exquisite Functional Selectivity over 5-HT_{2A} and 5-HT_{2B} Receptors. *J. Med. Chem.* **2014**, *57*, 5258-5269.
370. Tye, H.; Mueller, S. G.; Prestle, J.; Scheuerer, S.; Schindler, M.; Nosse, B.; Prevost, N.; Brown, C. J.; Heifetz, A.; Moeller, C.; Pedret-Dunn, A.; Whittaker, M. Novel 6,7,8,9-tetrahydro-5H-1,4,7,10a-tetraaza-cyclohepta[f]indene analogues as potent and selective 5-HT_{2C} agonists for the treatment of metabolic disorders. *Bioorg. Med. Chem. Lett.* **2011**, *21*, 34-37.
371. Carpenter, J.; Wang, Y.; Wu, G.; Feng, J.; Ye, X. Y.; Morales, C. L.; Broekema, M.; Rossi, K. A.; Miller, K. J.; Murphy, B. J.; Wu, G.; Malmstrom, S. E.; Azzara, A. V.; Sher, P. M.; Fevig, J. M.; Alt, A.; Bertekap, R. L., Jr.; Cullen, M. J.; Harper, T. M.; Foster, K.; Luk, E.; Xiang, Q.; Grubb, M. F.; Robl, J. A.; Wacker, D. A. Utilization of an Active Site Mutant Receptor for the Identification of Potent and Selective Atypical 5-HT_{2C} Receptor Agonists. *J. Med. Chem.* **2017**, *60*, 6166-6190.
372. Felsing, D. E.; Canal, C. E.; Booth, R. G. Ligand-Directed Serotonin 5-HT_{2C} Receptor Desensitization and Sensitization. *Eur. J. Pharmacol.* **2019**, *848*, 131-139.
373. Menniti, F. S.; Lindsley, C. W.; Conn, P. J.; Pandit, J.; Zagouras, P.; Volkman, R. A. Allosteric modulators for the treatment of schizophrenia: targeting glutamatergic networks. *Curr. Top. Med. Chem.* **2013**, *13*, 26-54.
374. Christopoulos, A. Allosteric Binding Sites on Cell-surface Receptors: Novel Targets for Drug Discovery. *Nat. Rev. Drug Discov.* **2002**, *1*, 198-210.
375. Gregory, K. J.; Sexton, P. M.; Christopoulos, A. Overview of Receptor Allosterism. *Curr. Protoc. Pharmacol.* **2010**, Chapter 1, Unit 1 21.

376. Melancon, B. J.; Hopkins, C. R.; Wood, M. R.; Emmitte, K. A.; Niswender, C. M.; Christopoulos, A.; Conn, P. J.; Lindsley, C. W. Allosteric Modulation of Seven Transmembrane Spanning Receptors: Theory, Practice, and Opportunities for Central Nervous System Drug Discovery. *J. Med. Chem.* **2012**, *55*, 1445-1464.
377. Wootten, D.; Christopoulos, A.; Sexton, P. M. Emerging Paradigms in GPCR Allostery: Implications for Drug Discovery. *Nat. Rev. Drug Discov.* **2013**, *12*, 630-644.
378. Schlag, B. D.; Lou, Z.; Fennell, M.; Dunlop, J. Ligand dependency of 5-hydroxytryptamine 2C receptor internalization. *J. Pharmacol. Exp. Ther.* **2004**, *310*, 865-870.
379. Kenakin, T. P. 7TM receptor allostery: putting numbers to shapeshifting proteins. *Trends Pharmacol. Sci.* **2009**, *30*, 460-469.
380. Christopoulos, A. Advances in G Protein-Coupled Receptor Allostery: From Function to Structure. *Mol. Pharmacol.* **2014**, *86*, 463-478.
381. Wild, C. T.; Miszkief, J. M.; Wold, E. A.; Soto, C. A.; Ding, C.; Hartley, R. M.; White, M. A.; Anastasio, N. C.; Cunningham, K. A.; Zhou, J. Design, Synthesis, and Characterization of 4-Undecylpiperidine-2-carboxamides as Positive Allosteric Modulators of the Serotonin (5-HT) 5-HT_{2C} Receptor. *J. Med. Chem.* **2019**, *62*, 288-305.
382. Zhou, J.; Cunningham, K. A. Positive-allosteric modulation of the 5-HT_{2C} receptor: implications for neuropsychopharmacology and neurotherapeutics. *Neuropsychopharmacology* **2019**, *44*, 230-231.
383. Wold, E. A.; Zhou, J. GPCR Allosteric Modulators: Mechanistic Advantages and Therapeutic Applications. *Curr. Top. Med. Chem.* **2018**, *18*, 2002-2006.
384. Dror, R. O.; Green, H. F.; Valant, C.; Borhani, D. W.; Valcourt, J. R.; Pan, A. C.; Arlow, D. H.; Canals, M.; Lane, J. R.; Rahmani, R.; Baell, J. B.; Sexton, P. M.; Christopoulos, A.; Shaw, D. E. Structural Basis for Modulation of a G-Protein-Coupled Receptor by Allosteric Drugs. *Nature* **2013**, *503*, 295-299.
385. Bridges, T. M.; Lindsley, C. W. G-Protein-Coupled Receptors: From Classical Modes of Modulation to Allosteric Mechanisms. *ACS Chem. Biol.* **2008**, *3*, 530-541.
386. Lindsley, C. W.; Emmitte, K. A.; Hopkins, C. R.; Bridges, T. M.; Gregory, K. J.; Niswender, C. M.; Conn, P. J. Practical Strategies and Concepts in GPCR Allosteric Modulator Discovery: Recent Advances with Metabotropic Glutamate Receptors. *Chem. Rev.* **2016**, *116*, 6707-6741.

387. Merkler, D. J.; Merkler, K. A.; Stern, W.; Fleming, F. F. Fatty acid amide biosynthesis: a possible new role for peptidylglycine A-amidating enzyme and acyl-coenzyme A:glycine N-acyltransferase. *Arch. Biochem. Biophys.* **1996**, 330, 430-434.
388. Conn, P. J.; Lindsley, C. W.; Meiler, J.; Niswender, C. M. Opportunities and Challenges in the Discovery of Allosteric Modulators of GPCRs for Treating CNS Disorders. *Nat. Rev. Drug Discov.* **2014**, 13, 692-708.
389. Spizek, J.; Novotna, J.; Rezanka, T. Lincosamides: Chemical Structure, Biosynthesis, Mechanism of Action, Resistance, and Applications. *Adv. Appl. Microbiol.* **2004**, 56, 121-154.
390. Sugiura, T.; Kondo, S.; Kodaka, T.; Tonegawa, T.; Nakane, S.; Yamashita, A.; Ishima, Y.; Waku, K. Enzymatic synthesis of oleamide (cis-9, 10-octadecenoamide), an endogenous sleep-inducing lipid, by rat brain microsomes. *Biochem. Mol. Biol. Int.* **1996**, 40, 931-938.
391. Boger, D. L.; Sato, H.; Lerner, A. E.; Austin, B. J.; Patterson, J. E.; Patricelli, M. P.; Cravatt, B. F. Trifluoromethyl ketone inhibitors of fatty acid amide hydrolase: a probe of structural and conformational features contributing to inhibition. *Bioorg. Med. Chem. Lett.* **1999**, 9, 265-270.
392. Fedorova, I.; Hashimoto, A.; Fecik, R. A.; Hedrick, M. P.; Hanus, L. O.; Boger, D. L.; Rice, K. C.; Basile, A. S. Behavioral evidence for the interaction of oleamide with multiple neurotransmitter systems. *J. Pharmacol. Exp. Ther.* **2001**, 299, 332-342.
393. Soria-Gomez, E.; Marquez-Diosdado, M. I.; Montes-Rodriguez, C. J.; Estrada-Gonzalez, V.; Prospero-Garcia, O. Oleamide administered into the nucleus accumbens shell regulates feeding behaviour via CB1 and 5-HT2C receptors. *Int. J. Neuropsychopharmacol.* **2010**, 13, 1247-1254.
394. Boger, D. L.; Patterson, J. E.; Jin, Q. Structural requirements for 5-HT2A and 5-HT1A serotonin receptor potentiation by the biologically active lipid oleamide. *Proc. Natl. Acad. Sci. U. S. A.* **1998**, 95, 4102-4107.
395. Huidobro-Toro, J. P.; Harris, R. A. Brain lipids that induce sleep are novel modulators of 5-hydroxytryptamine receptors. *Proc. Natl. Acad. Sci. U. S. A.* **1996**, 93, 8078-8082.
396. Thomas, E. A.; Carson, M. J.; Neal, M. J.; Sutcliffe, J. G. Unique allosteric regulation of 5-hydroxytryptamine receptor-mediated signal transduction by oleamide. *Proc. Natl. Acad. Sci. U. S. A.* **1997**, 94, 14115-14119.
397. Hedlund, P. B.; Carson, M. J.; Sutcliffe, J. G.; Thomas, E. A. Allosteric regulation by oleamide of the binding properties of 5-hydroxytryptamine₇ receptors. *Biochem. Pharmacol.* **1999**, 58, 1807-1813.

398. Cheer, J. F.; Cadogan, A. K.; Marsden, C. A.; Fone, K. C.; Kendall, D. A. Modification of 5-HT₂ receptor mediated behaviour in the rat by oleamide and the role of cannabinoid receptors. *Neuropharmacology* **1999**, 38, 533-541.
399. Mikitsh, J. L.; Chacko, A. M. Pathways for Small Molecule Delivery to the Central Nervous System Across the Blood-Brain Barrier. *Perspect. Medicin. Chem.* **2014**, 6, 11-24.
400. Marona-Lewicka, D.; Nichols, D. E. Complex stimulus properties of LSD: a drug discrimination study with alpha 2-adrenoceptor agonists and antagonists. *Psychopharmacology (Berl.)* **1995**, 120, 384-391.
401. Kleven, M. S.; Assie, M. B.; Koek, W. Pharmacological characterization of in vivo properties of putative mixed 5-HT_{1A} agonist/5-HT_(2A/2C) antagonist anxiolytics. II. Drug discrimination and behavioral observation studies in rats. *J. Pharmacol. Exp. Ther.* **1997**, 282, 747-759.
402. Mohler, E. G.; Franklin, S. R.; Rueter, L. E. Discriminative-stimulus effects of NS9283, a nicotinic alpha4beta2* positive allosteric modulator, in nicotine-discriminating rats. *Psychopharmacology (Berl.)* **2014**, 231, 67-74.
403. Singh, K.; Sona, C.; Ojha, V.; Singh, M.; Mishra, A.; Kumar, A.; Siddiqi, M. I.; Tripathi, R. P.; Yadav, P. N. Identification of Dual Role of Piperazine-linked Phenyl Cyclopropyl Methanone as Positive Allosteric Modulator of 5-HT_{2C} and Negative Allosteric Modulator of 5-HT_{2B} Receptors. *Eur. J. Med. Chem.* **2019**, 164, 499-516.
404. Ward, R. J.; Padiani, J. D.; Godin, A. G.; Milligan, G. Regulation of oligomeric organization of the serotonin 5-hydroxytryptamine 2C (5-HT_{2C}) receptor observed by spatial intensity distribution analysis. *J. Biol. Chem.* **2015**, 290, 12844-12857.
405. Wold, E. A.; Garcia, E. J.; Wild, C. T.; Miszkiel, J. M.; Soto, C. A.; Chen, J.; Pazdrak, K.; Fox, R. G.; Anastasio, N. C.; Cunningham, K. A.; Zhou, J. Discovery of 4-Phenylpiperidine-2-Carboxamide Analogues as Serotonin 5-HT_{2C} Receptor-Positive Allosteric Modulators with Enhanced Drug-like Properties. *Journal of Medicinal Chemistry* **2020**, 63, 7529-7544.
406. Zhou, J.; Cunningham, K. A. Positive Allosteric Modulation of the 5-HT_{2C} Receptor: Implications for Neuropsychopharmacology and Neurotherapeutics. *Neuropsychopharmacology* **2019**, 44, 230-231.
407. Ge, T.; Zhang, Z.; Lv, J.; Song, Y.; Fan, J.; Liu, W.; Wang, X.; Hall, F. S.; Li, B.; Cui, R. The Role of 5-HT_{2c} Receptor on Corticosterone-mediated Food Intake. *J. Biochem. Mol. Toxicol.* **2017**, 31, DOI: 10.1002/jbt.21890.
408. Manivet, P.; Schneider, B.; Smith, J. C.; Choi, D. S.; Maroteaux, L.; Kellermann, O.; Launay, J. M. The Serotonin Binding Site of Human and Murine 5-HT_{2B} Receptors:

- Molecular Modeling and Site-Directed Mutagenesis. *J. Biol. Chem.* **2002**, 277, 17170-17178.
409. Song, K.; Liu, X.; Huang, W.; Lu, S.; Shen, Q.; Zhang, L.; Zhang, J. Improved Method for the Identification and Validation of Allosteric Sites. *J. Chem. Inf. Model.* **2017**, 57, 2358-2363.
410. Banerjee, P.; Eckert, A. O.; Schrey, A. K.; Preissner, R. ProTox-II: A Webserver for the Prediction of Toxicity of Chemicals. *Nucleic Acids Res.* **2018**, 46, W257-W263.
411. Wager, T. T.; Hou, X.; Verhoest, P. R.; Villalobos, A. Moving Beyond Rules: The Development of a Central Nervous System Multiparameter Optimization (CNS MPO) Approach to Enable Alignment of Druglike Properties. *ACS Chem. Neurosci.* **2010**, 1, 435-449.
412. Shaffer, C. L. Defining Neuropharmacokinetic Parameters in CNS Drug Discovery to Determine Cross-Species Pharmacologic Exposure-Response Relationships. In *Annual Reports in Medicinal Chemistry*, Macor, J. E., Ed. Academic Press: 2010; Vol. 45, pp 55-70.
413. Soto, C. A.; Du, H. C.; Fox, R. G.; Yang, T.; Hooson, J.; Anastasio, N. C.; Gilbertson, S. R.; Cunningham, K. A. In Vivo and In Vitro Analyses of Novel Peptidomimetic Disruptors for the Serotonin 5-HT_{2C} Receptor Interaction With Phosphatase and Tensin Homolog. *Front. Pharmacol.* **2019**, 10, 907.
414. Colpaert, F. C. Drug Discrimination in Neurobiology. *Pharmacol. Biochem. Behav.* **1999**, 64, 337-345.
415. Colpaert, F. C. Drug Discrimination: Methods of Manipulation, Measurement, and Analysis. In *Methods of Assessing the Reinforcing Properties of Abused Drugs*, Bozarth, M. A., Ed. Springer New York: New York, NY, 1987; pp 341-372.
416. Colpaert, F. C.; Janssen, P. A. Agonist and Antagonist Effects of Prototype Opiate Drugs in Rats Discriminating Fentanyl from Saline: Characteristics of Partial Generalization. *J. Pharmacol. Exp. Ther.* **1984**, 230, 193-199.
417. Negus, S. S.; Banks, M. L. Pharmacokinetic-Pharmacodynamic (PKPD) Analysis with Drug Discrimination. *Curr. Top. Behav. Neurosci.* **2018**, 39, 245-259.
418. McCreary, A. C.; Filip, M.; Cunningham, K. A. Discriminative Stimulus Properties of (+/-)-Fenfluramine: the Role of 5-HT₂ Receptor Subtypes. *Behav. Neurosci.* **2003**, 117, 212-221.
419. Callahan, P. M.; Cunningham, K. A. Involvement of 5-HT_{2C} Receptors in Mediating the Discriminative Stimulus Properties of m-Chlorophenylpiperazine (mCPP). *Eur. J. Pharmacol.* **1994**, 257, 27-38.

420. Frankel, P. S.; Cunningham, K. A. m-Chlorophenylpiperazine (mCPP) Modulates the Discriminative Stimulus Effects of Cocaine Through Actions at the 5-HT_{2C} Receptor. *Behav. Neurosci.* **2004**, 118, 157-162.
421. Glennon, R. A.; Young, R. Drug Discrimination and Development of Novel Agents and Pharmacological Tools. In *Drug Discrimination: Applications to Medicinal Chemistry and Drug Discovery*, Glennon, R. A.; Young, R., Eds. John Wiley and Sons: Hoboken, NJ: 2011; pp 217-238.
422. Mathis, D. A.; Emmett-Oglesby, M. W. Quantal vs. graded generalization in drug discrimination: measuring a graded response. **1990**.
423. Kennett, G. A.; Wood, M. D.; Bright, F.; Trail, B.; Riley, G.; Holland, V.; Avenell, K. Y.; Stean, T.; Upton, N.; Bromidge, S.; Forbes, I. T.; Brown, A. M.; Middlemiss, D. N.; Blackburn, T. P. SB 242084, a Selective and Brain Penetrant 5-HT_{2C} Receptor Antagonist. *Neuropharmacology* **1997**, 36, 609-620.
424. Fronik, P.; Gaiser, B. I.; Sejer Pedersen, D. Bitopic Ligands and Metastable Binding Sites: Opportunities for G Protein-Coupled Receptor (GPCR) Medicinal Chemistry. *J. Med. Chem.* **2017**, 60, 4126-4134.
425. Gaiser, B. I.; Danielsen, M.; Marcher-Rørsted, E.; Røpke Jørgensen, K.; Wróbel, T. M.; Frykman, M.; Johansson, H.; Bräuner-Osborne, H.; Gloriam, D. E.; Mathiesen, J. M.; Sejer Pedersen, D. Probing the Existence of a Metastable Binding Site at the β 2-Adrenergic Receptor with Homobivalent Bitopic Ligands. *J. Med. Chem.* **2019**, 62, 7806-7839.
426. Dror, R. O.; Pan, A. C.; Arlow, D. H.; Borhani, D. W.; Maragakis, P.; Shan, Y.; Xu, H.; Shaw, D. E. Pathway and Mechanism of Drug Binding to G-Protein-Coupled Receptors. *Proc. Nat. Acad. Sci.* **2011**, 108, 13118-13123.
427. Filip, M.; Bubar, M. J.; Cunningham, K. A. Contribution of Serotonin (5-HT) 5-HT₂ Receptor Subtypes to the Discriminative Stimulus Effects of Cocaine in Rats. *Psychopharmacology* **2006**, 183, 482-489.
428. Besnard, J.; Ruda, G. F.; Setola, V.; Abecassis, K.; Rodriguiz, R. M.; Huang, X.-P.; Norval, S.; Sassano, M. F.; Shin, A. I.; Webster, L. A.; Simeons, F. R. C.; Stojanovski, L.; Prat, A.; Seidah, N. G.; Constam, D. B.; Bickerton, G. R.; Read, K. D.; Wetsel, W. C.; Gilbert, I. H.; Roth, B. L.; Hopkins, A. L. Automated design of ligands to polypharmacological profiles. *Nature* **2012**, 492, 215-220.
429. Park, P. S.-H.; Lodowski, D. T.; Palczewski, K. Activation of G Protein-Coupled Receptors: Beyond Two-State Models and Tertiary Conformational Changes. *Annual Review of Pharmacology and Toxicology* **2008**, 48, 107-141.

430. Neubig, R. R. Membrane organization in G-protein mechanisms. *The FASEB Journal* **1994**, 8, 939-946.
431. Rebois, R. V.; Hébert, T. E. Protein Complexes Involved in Heptahelical Receptor-Mediated Signal Transduction. *Receptors and Channels* **2003**, 9, 169-194.
432. Kim, K.; Che, T.; Panova, O.; DiBerto, J. F.; Lyu, J.; Krumm, B. E.; Wacker, D.; Robertson, M. J.; Seven, A. B.; Nichols, D. E.; Shoichet, B. K.; Skiniotis, G.; Roth, B. L. Structure of a Hallucinogen-Activated Gq-Coupled 5-HT_{2A} Serotonin Receptor. *Cell* **2020**, 182, 1574-1588.e1519.
433. Wacker, D.; Wang, C.; Katritch, V.; Han, G. W.; Huang, X.-P.; Vardy, E.; McCorvy, J. D.; Jiang, Y.; Chu, M.; Siu, F. Y.; Liu, W.; Xu, H. E.; Cherezov, V.; Roth, B. L.; Stevens, R. C. Structural Features for Functional Selectivity at Serotonin Receptors. *Science* **2013**, 340, 615-619.
434. McCorvy, J. D.; Wacker, D.; Wang, S.; Agegnehu, B.; Liu, J.; Lansu, K.; Tribo, A. R.; Olsen, R. H. J.; Che, T.; Jin, J.; Roth, B. L. Structural determinants of 5-HT_{2B} receptor activation and biased agonism. *Nature Structural & Molecular Biology* **2018**, 25, 787-796.
435. Kimura, K. T.; Asada, H.; Inoue, A.; Kadji, F. M. N.; Im, D.; Mori, C.; Arakawa, T.; Hirata, K.; Nomura, Y.; Nomura, N.; Aoki, J.; Iwata, S.; Shimamura, T. Structures of the 5-HT_{2A} receptor in complex with the antipsychotics risperidone and zotepine. *Nature Structural & Molecular Biology* **2019**, 26, 121-128.
436. Wacker, D.; Wang, S.; McCorvy, J. D.; Betz, R. M.; Venkatakrishnan, A. J.; Levit, A.; Lansu, K.; Schools, Z. L.; Che, T.; Nichols, D. E.; Shoichet, B. K.; Dror, R. O.; Roth, B. L. Crystal Structure of an LSD-Bound Human Serotonin Receptor. *Cell* **2017**, 168, 377-389.e312.
437. Violin, J. D.; Lefkowitz, R. J. β -Arrestin-biased ligands at seven-transmembrane receptors. *Trends in Pharmacological Sciences* **2007**, 28, 416-422.
438. Allen, J. A.; Yost, J. M.; Setola, V.; Chen, X.; Sassano, M. F.; Chen, M.; Peterson, S.; Yadav, P. N.; Huang, X.-p.; Feng, B.; Jensen, N. H.; Che, X.; Bai, X.; Frye, S. V.; Wetsel, W. C.; Caron, M. G.; Javitch, J. A.; Roth, B. L.; Jin, J. Discovery of β -Arrestin-Biased Dopamine D₂ Ligands for Probing Signal Transduction Pathways Essential for Antipsychotic Efficacy. *Proceedings of the National Academy of Sciences* **2011**, 108, 18488-18493.
439. Manglik, A.; Lin, H.; Aryal, D. K.; McCorvy, J. D.; Dengler, D.; Corder, G.; Levit, A.; Kling, R. C.; Bernat, V.; Hübner, H.; Huang, X.-P.; Sassano, M. F.; Giguère, P. M.; Löber, S.; Da, D.; Scherrer, G.; Kobilka, B. K.; Gmeiner, P.; Roth, B. L.; Shoichet, B. K. Structure-based discovery of opioid analgesics with reduced side effects. *Nature* **2016**, 537, 185-190.

440. Christopoulos, A.; Kenakin, T. G Protein-Coupled Receptor Allosterism and Complexing. *Pharmacological Reviews* **2002**, 54, 323.
441. Christopoulos, A.; Mitchelson, F. Application of an allosteric ternary complex model to the technique of pharmacological resultant analysis. *J Pharm Pharmacol* **1997**, 49, 781-786.
442. Jakubík, J.; Randáková, A.; Chetverikov, N.; El-Fakahany, E. E.; Doležal, V. The operational model of allosteric modulation of pharmacological agonism. *Scientific Reports* **2020**, 10, 14421.
443. Huang, S. K.; Pandey, A.; Tran, D. P.; Villanueva, N. L.; Kitao, A.; Sunahara, R. K.; Sljoka, A.; Prosser, R. S. Delineating the conformational landscape of the adenosine A_{2A} receptor during G protein coupling. *Cell* **2021**, 184, 1884-1894.e1814.
444. Uprety, R.; Che, T.; Zaidi, S. A.; Grinnell, S. G.; Varga, B. R.; Faouzi, A.; Slocum, S. T.; Allaoa, A.; Varadi, A.; Nelson, M.; Bernhard, S. M.; Kulko, E.; Le Rouzic, V.; Eans, S. O.; Simons, C. A.; Hunkele, A.; Subrath, J.; Pan, Y. X.; Javitch, J. A.; McLaughlin, J. P.; Roth, B. L.; Pasternak, G. W.; Katritch, V.; Majumdar, S. Controlling opioid receptor functional selectivity by targeting distinct subpockets of the orthosteric site. *eLife* **2021**, 10, e56519.
445. Mokrosiński, J.; Frimurer, T. M.; Sivertsen, B.; Schwartz, T. W.; Holst, B. Modulation of Constitutive Activity and Signaling Bias of the Ghrelin Receptor by Conformational Constraint in the Second Extracellular Loop*. *Journal of Biological Chemistry* **2012**, 287, 33488-33502.
446. Peters, B. L.; Deng, J.; Ferguson, A. L. Free energy calculations of the functional selectivity of 5-HT_{2B} G protein-coupled receptor. *PLoS One* **2020**, 15, e0243313.
447. Cunningham, K. A.; Callahan, P. M.; Appel, J. B. Differentiation Between the Stimulus Effects of 1-5-Hydroxytryptophan and LSD. *Eur. J. Pharmacol.* **1985**, 108, 179-186.
448. Nutt, D. Psychedelic Drugs - A New Era in Psychiatry? *Dialogues in clinical neuroscience* **2019**, 21, 139-147.
449. Carhart-Harris, R.; Giribaldi, B.; Watts, R.; Baker-Jones, M.; Murphy-Beiner, A.; Murphy, R.; Martell, J.; Blemings, A.; Erritzoe, D.; Nutt, D. J. Trial of Psilocybin versus Escitalopram for Depression. *New England Journal of Medicine* **2021**, 384, 1402-1411.
450. Flanagan, T. W.; Nichols, C. D. Psychedelics as Anti-Inflammatory Agents. *International Review of Psychiatry* **2018**, 30, 363-375.

451. Safety Clinical Trial Shows Possible Increased Risk of Cancer with Weight-loss Medicine Belviq, Belviq XR (Lorcaserin). In U.S. Food and Drug Administration: Drug Safety and Availability, 2020.
452. FDA Requests the Withdrawal of the Weight-loss Drug Belviq, Belviq XR (Lorcaserin) from the Market. In U.S. Food and Drug Administration: Drug Safety and Availability, 2020.

Vita

Eric A. Wold received his Bachelor of Science degree from the University of Houston where he studied Biotechnology and Biology. During his undergraduate studies he assisted in research projects ranging from microbial bioprocessing to developing biopolymer materials, each characterized by exploring the interface between biology and chemistry. For his Doctor of Philosophy degree, Eric joined Dr. Jia Zhou's group at the University of Texas Medical Branch to learn medicinal chemistry and apply chemical tools towards understanding serotonin receptor biology. He was awarded a National Institutes of Health National Research Service Award (NRSA) F31 fellowship to discover small molecule serotonin 2C receptor (5-HT_{2C}R) allosteric modulators as potential Substance Use Disorder therapeutics. Eric became proficient using computational methods to identify prospective 5-HT_{2C}R and 5-HT_{2A}R allosteric small molecule binding sites and has worked with a multidisciplinary team led by Drs. Kathryn Cunningham and Jia Zhou to position select preclinical candidates for future therapeutic development. He is an author on 22 peer-reviewed publications, given three invited talks and six oral presentations at national meetings, for which he has received numerous travel awards including a NIDA Director's travel award, and has been fortunate to receive multiple other scholarships and awards. Apart from scientific endeavors, Eric served in the student government at UTMB, including one year as executive vice president, served on an oversight board for student health and counseling, and has participated in curriculum design initiatives for the graduate school. Eric supervised students during rotations and summer projects and co-authored a medical school Problem-Based Learning case study. In his final year in the graduate program he was among 15 fellows selected by the Yale Innovation to Impact program to participate in entrepreneurship training for translating laboratory discoveries into therapies for substance use disorders. He plans to use these cumulative experiences to discover new therapeutics in the future.

Permanent address: 2116 Church St. Apt. 2A, Galveston, TX 77550

This dissertation was typed by Eric A. Wold.